629.13
G79r
no.1888-
1898
Inc.

Digitized by the Internet Archive
in 2023 with funding from
University of Illinois Urbana-Champaign

https://archive.org/details/reportsmemoranda1888aero

TG29.13
G79r
no.1888

LIBRARY
UNIVERSITY OF ILLINOIS
URBANA

Engng.

R. & M. No. 1888
(4207)

AIR MINISTRY

AERONAUTICAL RESEARCH COMMITTEE
REPORTS AND MEMORANDA

# Methods for Calculating the Frequencies of Overtones

*By*

W. J. DUNCAN, D.Sc., A.M.I.Mech.E., F.R.Ae.S.,
Wakefield Professor of Aeronautics at University College, Hull,
and
D. D. LINDSAY, B.A.

*Crown Copyright Reserved*

LONDON: HIS MAJESTY'S STATIONERY OFFICE
Price 3*s.* 0*d.* net

Hawn

# AERODYNAMIC SYMBOLS

## 1. GENERAL

| | |
|---|---|
| $m$ | Mass |
| $t$ | Time |
| V | Resultant linear velocity |
| $\Omega$ | Resultant angular velocity |
| $\rho$ | Density, $\sigma$ relative density |
| $\nu$ | Kinematic coefficient of viscosity |
| R | Reynolds number, $R = lV/\nu$ (where $l$ is a suitable linear dimension) |

Normal temperature and pressure for aeronautical work are 15° C and 760 mm.

For air under these conditions $\left\{\begin{array}{l}\rho = 0{\cdot}002378 \text{ slug/cu. ft.} \\ \nu = 1{\cdot}59 \times 10^{-4} \text{ sq. ft./sec.}\end{array}\right.$

The slug is taken to be 32·2 lb.-mass.

| | |
|---|---|
| $\alpha$ | Angle of incidence |
| $e$ | Angle of downwash |
| S | Area |
| $b$ | Span |
| $c$ | Chord |
| A | Aspect ratio, $A = b^2/S$ |
| L | Lift, with coefficient $C_L = L/\frac{1}{2}\rho V^2 S$ |
| D | Drag, with coefficient $C_D = D/\frac{1}{2}\rho V^2 S$ |
| $\gamma$ | Gliding angle, $\tan\gamma = D/L$ |
| L | Rolling moment, with coefficient $C_l = L/\frac{1}{2}\rho V^2 bS$ |
| M | Pitching moment, with coefficient $C_m = M/\frac{1}{2}\rho V^2 cS$ |
| N | Yawing moment, with coefficient $C_n = N/\frac{1}{2}\rho V^2 bS$ |

## 2. AIRSCREWS

| | |
|---|---|
| $n$ | Revolutions per second |
| D | Diameter |
| J | $V/nD$ |
| P | Power |
| T | Thrust, with coefficient $k_T = T/\rho n^2 D^4$ |
| Q | Torque, with coefficient $k_Q = Q/\rho n^2 D^5$ |
| $\eta$ | Efficiency, $\eta = TV/P = Jk_T/2\pi k_Q$ |

629.13
G79r
no.1888
LIBRARY
UNIVERSITY OF ILLINOIS
URBANA

# Methods for Calculating the Frequencies of Overtones

*By*

W. J. Duncan, D.Sc., A.M.I.Mech.E., F.R.Ae.S.,
Wakefield Professor of Aeronautics at University College, Hull,
and
D. D. Lindsay, B.A.

*Reports and Memoranda No.* 1888
*19th September,* 1939

*Summary.*—Three methods of obtaining the frequencies of the overtone vibrations of elastic bodies are described. The first consists in the direct application of the Rayleigh or Galerkin methods. Experience shows that in order to obtain a good approximation to the frequency of the $r^{th}$ overtone it is necessary to use $(r + 2)$ independent displacement functions or degrees of freedom, and the labour becomes heavy when $r$ exceeds 1. This labour may be reduced by supplementing the Rayleigh or Galerkin methods by the matrix solution given in §3 of the text. However, a method depending on an application of the orthogonal properties of the modes is developed which allows the overtone frequencies to be obtained with satisfactory accuracy when only two degrees of freedom are used (§4). It is also shown that overtone frequencies can be obtained by a modification of the well known iterative process. The ordinary iterative method fails to yield the overtones on account of the phenomenon of regression to the fundamental (*see* §5), but this difficulty is avoided by making use of the orthogonal properties of the modes, and without any assumptions regarding the positions of the nodes. The various methods are illustrated by worked examples.

CONTENTS

| | | Page |
|---|---|---|
| §1. | Introduction | 2 |
| §2. | Direct Use of the Rayleigh or Galerkin Methods | 3 |
| 2.1. | General | 3 |
| 2.2. | Examples | 4 |
| | (1) Flexural Oscillations of a Uniform Cantilever | 4 |
| | (2) Torsional Oscillations of a Parabolic Cantilever | 5 |
| 2.3. | Conclusions | 6 |
| §3. | Matrix Solution of the Equations obtained by the Rayleigh or Galerkin Methods | 6 |
| 3.1. | General | 6 |
| 3.2. | Example. Torsional Oscillations of a Parabolic Cantilever | 7 |
| §4. | Method Depending on the Orthogonal Properties of the Modes | 9 |
| 4.1. | Nature of the Orthogonal Properties | 9 |
| 4.2. | Outline of the Method | 9 |
| 4.3. | Examples | 10 |
| | (1) Flexural Oscillations of a Uniform Cantilever | 10 |
| | (2) Flexural Oscillations of a Parabolic Cantilever | 12 |
| | (3) Flexural Oscillations of a Conical Cantilever | 13 |
| | (4) Torsional Oscillations of a Uniform Cantilever | 14 |
| | (5) Torsional Oscillations of a Parabolic Cantilever | 15 |
| §5. | Direct Iterative Solution | 15 |
| 5.1. | General | 15 |
| 5.2. | The Process of Derivation | 16 |
| 5.3. | Examples | 17 |
| | (1) Fundamental Torsional Mode of Parabolic Cantilever | 17 |
| | (2) Regression to the Fundamental | 18 |
| | (3) First Torsional Overtone of a Parabolic Cantilever | 18 |
| Appendix.—The Choice of Displacement Functions for Cantilever Beams | | 19 |
| List of References | | 20 |

§1. *Introduction.*—There is no difficulty of principle in obtaining the frequencies of the overtone vibrations of elastic bodies by means of the well known Rayleigh-Ritz and Galerkin methods. However, it is necessary according to experience to use not less than $(r + 2)$ independent displacement functions when it is desired to obtain the frequency of the $r^{th}$ overtone with satisfactory accuracy. The labour entailed in solving $(r + 2)$ simultaneous equations containing a frequency parameter (characteristic number) by the ordinary methods when $r$ exceeds 1 is excessive, and it is therefore desirable to find some method or device by which the labour may be reduced. One such device consists in solving the set of equations yielded by the Rayleigh or Galerkin methods by the application of the iterative matrix solution already given elsewhere [4, 5], and an example of this is given in §3. The advantage of the matrix process becomes more pronounced as the number of equations in the set increases, but the method cannot be used until the rules for the basic arithmetical operations with matrices have been mastered ; these are in fact simple and can easily be learned by those having no knowledge of the mathematical theory of matrices. However, it was thought desirable to formulate an easy process for obtaining overtone frequencies without recourse to matrices, and this has been done by making use of the orthogonal properties of the modes.

A displacement of an elastic body which is consistent with the conditions of support, but otherwise quite arbitrary, can be analysed into a set of displacements each of which is a natural mode of vibration of the body with an amplitude appropriate to the particular assumed displacement. But the amplitude of a selected mode of vibration will be zero when the assumed displacement renders a certain integral containing the displacement function of the selected mode zero, and when this is so the assumed displacement is said to be orthogonal to the selected mode. Suppose now that it is desired to find the first overtone frequency, the fundamental having already been found with sufficient accuracy (and it is important to observe that this can usually be done without excessive labour). Select a pair of independent displacement functions which are both orthogonal to the known fundamental mode, and employ these in the ordinary Rayleigh or Galerkin processes. The result will be a *quadratic* equation for the frequency parameter, and the lower of its roots will be an approximation to the value of the parameter for the first overtone, for no linear combination of the assumed displacement functions can contain the fundamental mode. The foregoing is a general description of a method which is explained in detail in §4, where the extension of the process to obtain the higher overtones is also given. It should be added that the restriction to the use of two orthogonal displacement functions is non-essential, but all the examples hitherto tested show that two independent functions are sufficient for obtaining the first and second overtones.

A well known method for obtaining the fundamental frequency is that in which an arbitrary displacement is adopted, the inertia forces deduced from this and then taken as a static load system to yield a second or derived displacement for the body. The process is repeated with the derived displacement substituted for that first used, and continued until the type of displacement is sensibly constant ; this is the fundamental mode of displacement and the frequency can be calculated. This iterative solution fails for the overtones because of the phenomenon of *regression to the fundamental* (*see* §5), but a successful modification of it which makes use of the orthogonal properties of the modes has been devised, and is illustrated in §5.

The choice of the basic set of displacement functions is a matter of great importance, and the form of the functions depends on the nature of the body at its boundaries. For example, in the case of a cantilever beam the section at the tip may be finite, or the beam may taper down to zero at the tip in a variety of different ways (for instance the tip may be rounded or pointed). The geometrical conditions to be satisfied by the displacement functions will in general be different in these cases, and this question is investigated in the Appendix, where suitable functions for various types of cantilever are given for the cases of flexural and torsional motion.

It must be pointed out that it is useless to employ any refined process for calculating frequencies unless an adequate standard of numerical accuracy is maintained in the computations. The

numerical accuracy in the illustrative examples included in this paper is for the most part higher than would usually be considered necessary, but it was desired to obtain really precise comparisons of the several methods used, and reliable checks against known solutions.

All the examples given in the paper refer to the oscillations of cantilever beams. The methods described are, however, applicable to elastic bodies in general.

§2. *Direct Use of the Rayleigh or Galerkin Methods.*—2.1. *General.*—Galerkin's method has been described and illustrated in R. & M. 1798[1], and it has been shown in R. & M. 1848[2] that this method necessarily yields results which are identical with those given by the application of Rayleigh's principle in all problems concerning the free oscillations of elastic bodies. It is therefore unnecessary here to give more than a very brief summary of these two standard methods, and to state the equations to which they lead for the cases of the flexural and torsional oscillations of beams.

The first step in the solution of a problem, whichever method is used, is to write down a sequence of functions, say $Y_1$, $Y_2$, $Y_3$, etc., which satisfy all the end conditions or boundary conditions of the problem. The actual displacement is then assumed to be

$$y = q_1 Y_1 + q_2 Y_2 + \text{etc.}, \quad .. \quad .. \quad .. \quad .. \quad .. \quad .. \quad (2.1.1)$$

where the quantities $q$ are constants whose ratios are to be determined. The functions Y are conveniently polynomials of rising degree, or trigonometric functions of rising periodicity. Functions suitable for the treatment of a number of oscillation problems are given in the Appendix.

In the Galerkin process the differential equation (or equations) of the particular problem is multiplied in succession by a set of functions which are usually the functions $Y_1$, $Y_2$, etc., themselves,* and then integrated over the entire oscillating body. This yields a set of linear homogeneous equations in the coefficients $q$, and their eliminant is an algebraic equation for the frequency of oscillation.

In the application of the Rayleigh principle the equation of energy is used to express the square of the frequency in any pure mode as a function of the coefficients $q$. In accordance with the principle the frequency is stationary for small variations of the coefficients $q$ from their true values. Hence the equation of energy can be differentiated with respect to each $q$ in turn, while the frequency is treated as constant. In this way a set of linear homogeneous equations in the coefficients $q$ is obtained, and it can be demonstrated (as in R. & M. 1848) that these are actually identical with the equations yielded by the Galerkin method, provided that the displacement functions Y are the same for both methods.

Suppose that a beam has flexural rigidity EI and mass per unit length $m$, where in general these will both be functions of the co-ordinate $x$ measured along the axis of the beam. Then Rayleigh's principle leads to a set of equations typified by

$$\int \mathrm{EI} \frac{d^2y}{dx^2} \frac{d^2\mathrm{Y}_r}{dx^2} dx - \omega^2 \int my\mathrm{Y}_r dx = 0$$

$$(r = 1, 2, \text{etc.}), \quad .. \quad .. \quad (2.1.2)$$

where $\omega$ is $2\pi$ times the frequency of flexural oscillation, and the integrals extend over the whole beam. Since $y$ is given by (2.1.1), the last equation is linear and homogeneous in the coefficients $q$, which may properly be regarded as the Lagrangian generalised co-ordinates of the beam. The corresponding typical equation given by the Galerkin method is

$$\int \mathrm{Y}_r \frac{d^2}{dx^2}\left( \mathrm{EI} \frac{d^2y}{dx^2} \right) dx - \omega^2 \int my\mathrm{Y}_r dx = 0, \quad .. \quad .. \quad .. \quad (2.1.3)$$

but this can be shown to be identical with (2.1.2) by integration by parts and use of the end conditions.†

* Rules for the choice of the multipliers are given in R. & M. 1848.

† It is assumed that the ends of the beam are free, simply supported or rigidly built in.

Next, for the case of torsional oscillation of a beam, let the angular displacement be $\theta$, and assume that

$$\theta = q_1\Theta_1 + q_2\Theta_2 + \text{etc.}, \quad .. \quad .. \quad .. \quad .. \quad .. \quad .. \quad (2.1.4)$$

where $\Theta_1$, $\Theta_2$, etc., satisfy the end conditions. Then if C is the torsional stiffness of unit length of the beam, and J is the polar moment of inertia of unit length about an axis through the centroid of the section, the typical Rayleigh equation is

$$\int \mathrm{C}\frac{d\theta}{dx}\frac{d\Theta_r}{dx}dx - \omega^2\int \mathrm{J}\theta\Theta_r dx = 0$$

$$(r = 1, 2, \text{etc.}). \quad .. \quad .. \quad (2.1.5)$$

The corresponding Galerkin equation is

$$\int \Theta_r \frac{d}{dx}\left(\mathrm{C}\frac{d\theta}{dx}\right)dx - \omega^2\int \mathrm{J}\theta\Theta_r dx = 0, \quad .. \quad .. \quad .. \quad (2.1.6)$$

and the identity of (2.1.5) and (2.1.6) can be established by integration by parts.

2.2. *Examples of the Direct Use of the Rayleigh and Galerkin Methods.*—A few examples will be given in order to show the degree of accuracy of the fundamental and lower overtone frequencies obtained by the use of varying numbers of independent functions (degrees of freedom) in the Rayleigh and Galerkin methods.

*Example* 1. *Flexural Oscillations of a Uniform Cantilever.*—The problem will be treated by use of the functions

$$\mathrm{Y}_r = \frac{1}{6}(r+2)(r+3)\xi^{r+1} - \frac{1}{3}r(r+3)\xi^{r+2} + \frac{1}{6}r(r+1)\xi^{r+3}, \quad .. \quad (2.2.1)$$

where $\xi = x/l$, and $l$ is the overhang. This set of functions is suitable for the treatment of the oscillations of any cantilever beam which does not taper to zero thickness at the tip (*see* the Appendix). When the flexural displacement is assumed to be given by

$$y = q_1\mathrm{Y}_1 + q_2\mathrm{Y}_2 + q_3\mathrm{Y}_3, \quad .. \quad .. \quad .. \quad .. \quad .. \quad .. \quad (2.2.2)$$

the equations (2.1.2) or (2.1.3) reduce to (compare §10 of R. & M. 1798)

$$q_1\left(\frac{16}{5} - \frac{104}{405}\alpha\right) + q_2\left(\frac{8}{3} - \frac{1304}{5670}\alpha\right) + q_3\left(\frac{16}{17} - \frac{2159}{10395}\alpha\right) = 0, \quad .. \quad .. \quad (2.2.3)$$

$$q_1\left(\frac{8}{3} - \frac{1304}{5670}\alpha\right) + q_2\left(\frac{80}{21} - \frac{1304}{6237}\alpha\right) + q_3\left(\frac{30}{7} - \frac{227}{1188}\alpha\right) = 0, \quad .. \quad .. \quad (2.2.4)$$

$$q_1\left(\frac{16}{7} - \frac{2159}{10395}\alpha\right) + q_2\left(\frac{30}{7} - \frac{227}{1188}\alpha\right) + q_3\left(\frac{40}{7} - \frac{227}{1287}\alpha\right) = 0, \quad .. \quad .. \quad (2.2.5)$$

where

$$\alpha = \frac{m\omega^2 l^4}{\mathrm{EI}}, \quad .. \quad .. \quad .. \quad .. \quad .. \quad .. \quad .. \quad .. \quad (2.2.6)$$

$m$ = mass per unit length,

$\omega = 2\pi$ times frequency,

EI = flexural rigidity.

The eliminant of (2.2.3) – (2.2.5) is exactly

$$851\alpha^3 - 4{,}159{,}518\alpha^2 + 1{,}865{,}239{,}200\alpha - 22{,}424{,}688{,}000 = 0, \quad .. \quad (2.2.7)$$

of which the roots are

$$\alpha_1 = \quad 12{\cdot}362367,$$

$$\alpha_2 = \quad 485{\cdot}56,$$

$$\alpha_3 = 4{,}389{\cdot}88.$$

In the following table these results, together with those obtained by the use of $Y_1$ and $Y_2$ and of $Y_1$ only, are compared with exact values of $\alpha$, which are the fourth powers of the roots of

$$1 + \cosh m \cos m = 0 \quad .. \quad .. \quad .. \quad .. \quad .. \quad .. \quad (2.2.8)$$

TABLE 1

*Values of Non-Dimensional Frequency Parameter for the Flexural Oscillations of a Uniform Cantilever*

| | | Root ($\alpha$) | | |
|---|---|---|---|---|
| | | Fundamental | First Overtone | Second Overtone |
| Value obtained by Rayleigh or Galerkin method with displacement functions as stated. | $Y_1$ | 12·46 | — | — |
| | $Y_1$ and $Y_2$ | 12·3625 | 515·86 | — |
| | $Y_1$, $Y_2$ and $Y_3$ | 12·362367 | 485·56 | 4389·88 |
| Exact value .. .. .. .. .. | | 12·3623* | 485·522 | 3806·55 |

* Last digit doubtful. The root of (2.2.8) is only known to six figures.

It will be seen that one function yields a fairly correct value for the fundamental, two functions give a very accurate fundamental and a rather inaccurate first overtone, while three functions lead to very accurate values for the fundamental and first overtone, but a very inaccurate second overtone.

*Example* 2. *Torsional Oscillations of a Parabolic Cantilever.*—The sections of the beam are all geometrically similar, and their linear dimensions are proportional to the square root of the distance from the tip. Hence both the torsional stiffness of unit length C and polar moment of inertia J are proportional to the square of the distance from the tip, so that

$$C = C_0(1 - \xi)^2 \quad .. \quad .. \quad .. \quad .. \quad .. \quad .. \quad .. \quad (2.2.9)$$

and

$$J = J_0(1 - \xi)^2 \quad .. \quad .. \quad .. \quad .. \quad .. \quad .. \quad .. \quad (2.2.10)$$

where $C_0$ and $J_0$ are the values of C and J respectively at the root, and $\xi$ is $x/l$ as usual. Accordingly the differential equation for the torsional displacement $\theta$ in any pure mode of oscillation is

$$\frac{d}{d\xi}\left[(1 - \xi)^2 \frac{d\theta}{d\xi}\right] + \alpha(1 - \xi)^2\theta = 0, \quad .. \quad .. \quad .. \quad .. \quad (2.2.11)$$

where

$$\alpha = \frac{\omega^2 J_0 l^2}{C_0}. \quad .. \quad .. \quad .. \quad .. \quad .. \quad .. \quad .. \quad (2.2.12)$$

The exact solution has been given by P. B. Walker[3] in terms of Bessel functions of order $\pm\frac{1}{2}$, but this can be more conveniently expressed as

$$\theta = \frac{a \sin \sqrt{\alpha}\,(1 - \xi)}{(1 - \xi)}. \quad .. \quad .. \quad .. \quad .. \quad .. \quad .. \quad (2.2.13)$$

The values of the non-dimensional frequency parameter $\alpha$ are $\pi^2$, $4\pi^2$, $9\pi^2$, . . . . $n^2\pi^2$ . . . .

In the approximate treatment of the problem by the Rayleigh or Galerkin methods it will be assumed that

$$\theta = q_1\Theta_1 + q_2\Theta_2 + q_3\Theta_3 \quad .. \quad .. \quad .. \quad .. \quad .. \quad .. \quad (2.2.14)$$

where† $$\Theta_r = (r + 1)\xi^r - r\xi^{r+1}. \quad .. \quad .. \quad .. \quad .. \quad .. \quad .. \quad (2.2.15)$$

Equations (2.1.5) or (2.1.6) become when reduced

$$q_1\left(\frac{4}{5} - \frac{8}{105}\alpha\right) + q_2\left(\frac{2}{5} - \frac{19}{420}\alpha\right) + q_3\left(\frac{8}{35} - \frac{1}{35}\alpha\right) = 0, \quad .. \quad .. \quad (2.2.16)$$

$$q_1\left(\frac{2}{5} - \frac{19}{420}\alpha\right) + q_2\left(\frac{12}{35} - \frac{19}{630}\alpha\right) + q_3\left(\frac{9}{35} - \frac{13}{630}\alpha\right) = 0, \quad .. \quad .. \quad (2.2.17)$$

$$q_1\left(\frac{8}{35} - \frac{1}{35}\alpha\right) + q_2\left(\frac{9}{35} - \frac{13}{630}\alpha\right) + q_3\left(\frac{8}{35} - \frac{52}{3465}\alpha\right) = 0 \ldots \quad .. \quad (2.2.18)$$

† See the Appendix.

The eliminant of these equations is exactly

$$2\alpha^3 - 327\alpha^2 + 12{,}060\alpha - 89{,}100 = 0, \quad .. \quad .. \quad .. \quad .. \quad (2.2.19)$$

of which the roots are 9·870019, 39·5742 and 114·056. A comparison of these with the true values of $\alpha$ for the fundamental and first two overtones is given in Table 2, which also contains the results obtained by the use of $\Theta_1$ only, and of $\Theta_1$ and $\Theta_2$.

TABLE 2

*Values of Non-Dimensional Frequency Parameter for the Torsional Oscillations of a Parabolic Cantilever*

| | | Root ($\alpha$) | | |
|---|---|---|---|---|
| | | Fundamental | First Overtone | Second Overtone |
| Value obtained by Rayleigh or Galerkin method with displacement functions as stated. | $\Theta_1$ | 10·5 | — | — |
| | $\Theta_1$ and $\Theta_2$ | 9·87076 | 46·069 | — |
| | $\Theta_1$, $\Theta_2$ and $\Theta_3$ | 9·870019 | 39·5742 | 114·056 |
| Exact value .. .. .. .. .. | | 9·869604 | 39·4784 | 88·8264 |

Again the rule holds that an accurate value for the $n^{th}$ root is obtained by the use of $(n + 1)$ functions. For instance, the error in the frequency* of the first overtone (second root) obtained with two functions or degrees of freedom is 8 per cent., but the error falls to 0·12 per cent. when three functions are used.

2.3. *Conclusions regarding the Direct Use of the Rayleigh and Galerkin Methods.*—The examples given above and many others show that when it is desired to obtain a closely correct approximation to the frequency in the $n^{th}$ mode† it is necessary and according to experience also sufficient‡ to use $(n + 1)$ distinct functions or degrees of freedom. Now the labour entailed in the computations increases very rapidly as the number of degrees of freedom rises, and it becomes of importance to devise means for reducing this labour. Two entirely different methods are described in §3 and §4. The second of these appears to be particularly effective and has the advantage that it involves no generally unfamiliar notation or process of computation.

§3. *Matrix Solution of the Equations obtained by the Rayleigh or Galerkin Methods.*‖ —3.1. *General.*—The Rayleigh and Galerkin methods lead to sets of linear homogeneous equations containing a characteristic number (non-dimensional frequency parameter), and a large part of the labour entailed in any particular problem is involved in the solution of these equations. A process for solving the equations without the laborious expansion of the Lagrangian determinant, and making use of the notation for matrices, has already been published[4, 5], and its application to the present problem will be briefly described.

The equations yielded by the direct application of the Galerkin and Rayleigh methods may be written

$$\left.\begin{aligned} (c_{11} - \alpha a_{11})q_1 + (c_{12} - \alpha a_{12})q_2 + \text{etc.} = 0 \\ (c_{21} - \alpha a_{21})q_1 + (c_{22} - \alpha a_{22})q_2 + \text{etc.} = 0 \\ \text{etc.} \end{aligned}\right\} \quad .. \quad .. \quad .. \quad (3.1.1)$$

This set of scalar equations can be represented by the single matrix equation

$$cq - \alpha aq = 0, \quad .. \quad .. \quad .. \quad (3.1.2)$$

* Note that the frequency is proportional to the square root of $\alpha$.

† The fundamental is the first mode, the first overtone is the second mode, and so on.

‡ Hitherto the methods have not been applied to modes higher than the third.

‖ Readers who are unacquainted with matrices may omit this section without detriment to their understanding of the rest of the paper.

where $c$ and $a$ are the square matrices formed from the elements $c_{ij}$ and $a_{ij}$ respectively, and $q$ is the column matrix or modal column formed with the elements $q$. When (3.1.2) is pre-multiplied by $c^{-1}$ it becomes

$$q - \alpha c^{-1} a q = 0,$$

or
$$Dq = \alpha^{-1} q, \quad .. \quad .. \quad .. \quad .. \quad .. \quad .. \quad .. \quad .. \quad (3.1.3)$$

where
$$D \equiv c^{-1} a \quad .. \quad .. \quad .. \quad .. \quad .. \quad .. \quad .. \quad .. \quad (3.1.4)$$

is the *dynamical matrix*. Equation (3.1.3) shows that $\alpha^{-1}$ is a *latent root* of the dynamical matrix, and $q$ is the associated modal column.

The matrix method of solution of (3.1.3) consists in taking an arbitrary column $z_0$ and repeatedly multiplying this by D to obtain in succession columns $z_1, z_2, \ldots z_n$. After a time the columns so obtained become proportional to one another and to the modal column for the fundamental root, and the fundamental root is then given by the ratio of an element of $z_n$ to the corresponding element of $z_{n+1}$. The higher or overtone roots are obtained in succession by using modified dynamical matrices possessing all the latent roots of D except the fundamental and other roots already found. This process will be illustrated in an example. It is fully explained in §§4.18 and 10.2 of Reference 5, and in Reference 4.

3.2. *Example of the Matrix Solution.*—The matrix method will be applied to the problem of the torsional oscillation of a parabolic cantilever, of which the direct solution is given in Example 2 of §2.2. The equations to be solved are (2.2.16)—(2.2.18), and these when multiplied throughout* by 13,860 to clear of fractions become

$$q_1 (11088 - 1056\alpha) + q_2 (5544 - 627\alpha) + q_3 (3168 - 396\alpha) = 0,$$
$$q_1 (5544 - 627\alpha) + q_2 (4752 - 418\alpha) + q_3 (3564 - 286\alpha) = 0,$$
$$q_1 (3168 - 396\alpha) + q_2 (3564 - 286\alpha) + q_3 (3168 - 208\alpha) = 0.$$

Hence
$$a = \begin{bmatrix} 1056 & 627 & 396 \\ 627 & 418 & 286 \\ 396 & 286 & 208 \end{bmatrix}$$

and
$$c = \begin{bmatrix} 11088 & 5544 & 3168 \\ 5544 & 4752 & 3564 \\ 3168 & 3564 & 3168 \end{bmatrix}$$

The reciprocal of the last† is found to be

$$c^{-1} = \begin{bmatrix} \frac{1}{2640} & \frac{-1}{990} & \frac{1}{1320} \\ \frac{-1}{990} & \frac{2}{495} & \frac{-7}{1980} \\ \frac{1}{1320} & \frac{-7}{1980} & \frac{7}{1980} \end{bmatrix}$$

Hence
$$D = c^{-1} a = \begin{bmatrix} \frac{1}{15} & \frac{23}{720} & \frac{37}{1980} \\ \frac{1}{15} & \frac{2}{45} & \frac{2}{99} \\ \frac{-1}{60} & \frac{1}{120} & \frac{4}{165} \end{bmatrix}$$

* The same multiplier must be used for all the equations. It can be shown that when different multipliers are used the dynamical matrix is unaltered, but errors are liable to arise in the calculation of the overtones since the matrices $a$ and $c$ are unsymmetrical and are not the true inertia and stiffness matrices (*see* Chap. 10 of Reference 5).

† For methods of calculating reciprocal matrices *see* Chap. 4 of Reference 5.

The iterative solution was begun with the quite arbitrarily chosen column having elements 0·9, 0·95, 1·0. After sixteen multiplications* by D a column is obtained with elements proportional to

$$\begin{matrix} 1{\cdot}0 \\ 1{\cdot}139151138 \\ -0{\cdot}093075413. \end{matrix}$$

When this is multiplied again by D the result is

$$0{\cdot}101316929 \begin{bmatrix} 1{\cdot}0 \\ 1{\cdot}139151138 \\ -0{\cdot}093075413 \end{bmatrix}.$$

Hence for the fundamental

$$\alpha = \frac{1}{0{\cdot}101316929} = 9{\cdot}870019$$

and the modal column is

$$\begin{matrix} 1{\cdot}0 \\ 1{\cdot}139151138 \\ -0{\cdot}093075413. \end{matrix}$$

The root agrees exactly with that obtained by direct solution (*see* § 2.2, Example 2).

When the fundamental is absent the numbers $q$ satisfy the equation

$$\varkappa_{11}q_1 + \varkappa_{21}q_2 + \varkappa_{31}q_3 = 0, \quad .. \quad .. \quad .. \quad .. \quad .. \quad .. \quad (3.2.1)$$

where the coefficients $\varkappa$ can be obtained as a row by repeated postmultiplication of an arbitrarily chosen row by D until proportionate rows are obtained, or with less labour as a column from the product $aq$, where $q$ is the modal column for the fundamental already obtained. In either of these ways it is found that

$$\begin{bmatrix} \varkappa_{11} & \varkappa_{21} & \varkappa_{31} \end{bmatrix} = \begin{bmatrix} 1{\cdot}0 & 0{\cdot}621064 & 0{\cdot}405239 \end{bmatrix},$$

where for convenience the first element has been made equal to unity by multiplying throughout by the appropriate factor. The modified dynamical matrix from which the fundamental has been eliminated is

$$\mathrm{D}_1 = \mathrm{D} - \begin{vmatrix} \frac{1}{15} \\ \frac{1}{15} \\ \frac{-1}{60} \end{vmatrix} \begin{bmatrix} 1{\cdot}0 & 0{\cdot}621064 & 0{\cdot}405239 \end{bmatrix}$$

$$= \begin{bmatrix} 0 & -0{\cdot}009459805 & -0{\cdot}0083290781 \\ 0 & +0{\cdot}003040195 & -0{\cdot}006813927 \\ 0 & +0{\cdot}018684395 & +0{\cdot}030996411 \end{bmatrix}.$$

Repeated multiplication of an arbitrary column by this matrix yields the first overtone root

$$\alpha = \frac{1}{0{\cdot}025269} = 39{\cdot}5742$$

in agreement with the direct solution, and the corresponding modal column is

$$\begin{matrix} 1{\cdot}0 \\ 1{\cdot}426740 \\ -4{\cdot}654280. \end{matrix}$$

* The modal column repeats to six figures after only eleven multiplications.

If in addition to the fundamental the first overtone is also absent, the numbers $q$ satisfy an additional relation

$$\varkappa_{12}q_1 + \varkappa_{22}q_2 + \varkappa_{32}q_3 = 0. \quad .. \quad .. \quad .. \quad .. \quad .. \quad .. \quad (3.2.2)$$

The coefficients $\varkappa$ can be obtained by repeated postmultiplication of an arbitrary row by $D_1$, or as the row $aq$, where $q$ is now the already obtained modal column for the first overtone. It is found that

$$\begin{bmatrix} \varkappa_{12} & \varkappa_{22} & \varkappa_{32} \end{bmatrix} = \begin{bmatrix} 1{\cdot}0 & -1{\cdot}002561 & -1{\cdot}526384 \end{bmatrix}.$$

When (3.2.1) and (3.2.2) are both satisfied it follows that

$$q_1 : q_2 : q_3 = 1 : -3{\cdot}565825 : 2{\cdot}997253.$$

These then are the ratios appropriate to the second overtone. Let D operate once on the column formed from these numbers. The ratio of corresponding elements in the original and derived columns is 114·056, which is therefore the second overtone root in accordance with the direct solution given in §2.2.

§ 4. *Method Depending on the Orthogonal Properties of the Modes.*—4.1. *Nature of the Orthogonal Properties.*—The displacements of any conservative dynamical system performing small oscillations in any pure mode possess certain orthogonal properties[5, 6], which are of the following general nature. The sum (or integral) taken over the whole system of the continued products of the corresponding displacements in two distinct pure modes and the appropriate inertia coefficient is zero, and there is a somewhat similar orthogonal property in which the inertia coefficient is replaced by a stiffness coefficient. In the present paper the examples are concerned with the flexural and torsional oscillations of beams or blades; accordingly the orthogonal properties will be explicitly stated for these cases.* First consider flexural motion, and suppose that $y_r$ and $y_s$ are the amplitudes of the displacement for any two *distinct* pure modes of oscillation, while $m$ is the mass per unit length of the beam (in general a function of $x$, the longitudinal co-ordinate). Then

$$\int m y_r y_s dx = 0, \quad .. \quad .. \quad .. \quad .. \quad .. \quad .. \quad .. \quad .. \quad (4.1.1)$$

and

$$\int \mathrm{EI} \frac{d^2y_r}{dx^2}\frac{d^2y_s}{dx^2}\,dx = 0, \quad .. \quad .. \quad .. \quad .. \quad .. \quad .. \quad .. \quad .. \quad (4.1.2)$$

where the integrals extend over the whole beam. For the case of torsional motion let the amplitudes in the distinct modes be $\theta_r$ and $\theta_s$, and let the polar moment of inertia of unit length of the beam and the local torsional stiffness of unit length be J and C respectively. Then the two orthogonal properties are represented by

$$\int \mathrm{J}\theta_r\theta_s dx = 0, \quad .. \quad .. \quad .. \quad .. \quad .. \quad .. \quad .. \quad .. \quad (4.1.3)$$

and

$$\int \mathrm{C} \frac{d\theta_r}{dx}\frac{d\theta_s}{dx}\,dx = 0. \quad .. \quad .. \quad .. \quad .. \quad .. \quad .. \quad .. \quad .. \quad (4.1.4)$$

For convenience the orthogonal property depending on the inertias (e.g. (4.1.1) and (4.1.3)) will be called the first orthogonal property, and that depending on the stiffnesses the second orthogonal property.

4.2. *Outline of the Method.*—The method is applicable to any body or system whose equations of motion are linear with constant coefficients, but for definiteness it will be explained in relation to the flexural oscillations of a beam. As in §2.1 let $\mathrm{Y}_1$, $\mathrm{Y}_2$, $\mathrm{Y}_3$, etc., be a sequence of functions satisfying the end conditions. The first step consists in finding the *fundamental* mode by the ordinary Rayleigh or Galerkin method (*see* §§2 and 3), on the assumption† that this mode is a linear combination of $\mathrm{Y}_1$ and $\mathrm{Y}_2$. Let the fundamental mode determined in this way be

$$y_1 = \mathrm{Y}_1 + b\mathrm{Y}_2. \quad .. \quad .. \quad .. \quad .. \quad .. \quad .. \quad .. \quad (4.2.1)$$

* The ends of the beam are supposed to be free, simply supported or rigidly built-in.

† Any number of degrees of freedom can be used when determining the fundamental and overtones. However, experience indicates that two degrees of freedom are sufficient unless very high accuracy is required. Throughout the explanation two degrees of freedom will be assumed, but the modifications in the method required for a greater number are obvious.

Then any possible mode of displacement $y$ from which the fundamental is entirely absent can be expressed linearly in terms of the first, second and higher overtone modes, and therefore by the orthogonal properties of the modes—

$$\int myy_1 dx = 0, \quad .. \quad .. \quad .. \quad .. \quad .. \quad .. \quad .. \quad (4.2.2)$$

and

$$\int \mathrm{EI} \frac{d^2y}{dx^2} \frac{d^2y_1}{dx^2} dx = 0. \quad .. \quad .. \quad .. \quad .. \quad .. \quad .. \quad .. \quad (4.2.3)$$

Equations (4.2.2.) and (4.2.3) express the first and second orthogonal properties respectively. Next, take the functions

$$\eta_{l1} = \mathrm{Y}_1 + g\mathrm{Y}_2, \quad .. \quad .. \quad .. \quad .. \quad .. \quad .. \quad (4.2.4)$$

and

$$\eta_{l2} = \mathrm{Y}_2 + h\mathrm{Y}_3, \quad .. \quad .. \quad .. \quad .. \quad .. \quad .. \quad (4.2.5)$$

and choose the constants $g$ and $h$ so that $\eta_{l1}$ and $\eta_{l2}$ are both orthogonal to the fundamental. Then the fundamental will be absent from any linear combination of $\eta_{l1}$ and $\eta_{l2}$, so that if $\eta_{l1}$ and $\eta_{l2}$ are used as displacement functions in the ordinary Rayleigh or Galerkin process, the *lower* root of the resulting frequency equation must correspond to the *first overtone* of the beam. The coefficients $g$ and $h$ are very easily found. It is entirely a matter of convenience which orthogonal property is used, but if it is, say, the first, then

$$\int m\eta_{l1} y_1 dx = 0,$$

and

$$\int m\eta_{l2} y_1 dx = 0.$$

Hence

$$\int m\mathrm{Y}_1 y_1 dx + g \int m\mathrm{Y}_2 y_1 dx = 0, \quad .. \quad .. \quad .. \quad .. \quad .. \quad .. \quad .. \quad (4.2.6)$$

and

$$\int m\mathrm{Y}_2 y_1 dx + h \int m\mathrm{Y}_3 y_1 dx = 0, \quad .. \quad .. \quad .. \quad .. \quad .. \quad .. \quad .. \quad (4.2.7)$$

from which $g$ and $h$ can be determined, since $y_1$, $\mathrm{Y}_1$, $\mathrm{Y}_2$ and $\mathrm{Y}_3$ are all known.

The foregoing process yields a good approximation to the first overtone frequency and mode. In order to obtain the second overtone frequency and mode the procedure is as follows.

Take the functions

$$\eta_{l3} = \mathrm{Y}_1 + j\mathrm{Y}_2 + k\mathrm{Y}_3 \quad .. \quad .. \quad .. \quad .. \quad .. \quad (4.2.8)$$

and

$$\eta_{l4} = \mathrm{Y}_2 + l\mathrm{Y}_3 + m\mathrm{Y}_4 \quad .. \quad .. \quad .. \quad .. \quad .. \quad (4.2.9)$$

and choose the constants $j$, $k$, $l$ and $m$ so that $\eta_{l3}$ and $\eta_{l4}$ are orthogonal to both the fundamental and first overtone modes as already found. These conditions lead to a pair of simultaneous linear equations for $j$ and $k$, and to a similar set in $l$ and $m$, which are readily solved. Finally $\eta_{l3}$ and $\eta_{l4}$ are used as displacement functions in the ordinary Rayleigh or Galerkin method, and the second overtone frequency is obtained as the lower root of the resulting frequency equation.

Evidently the method indicated above can be extended to find any desired overtone. At each stage only two displacement functions are used, and both of these are made orthogonal to all the lower modes already found. However, it must be remembered that the fundamental and lower overtone modes are only determined approximately, and there must be a tendency for the errors to accumulate as the order of the overtone rises. Hence it may be anticipated that it would be necessary to determine the fundamental and lower overtones with special accuracy if it were desired to investigate an overtone of high order. This might require the use of more than two degrees of freedom at each stage of the process, but even so the labour would be much less than that entailed in a direct attack on the problem.

A number of illustrative examples are given in §4.3.

4.3. *Examples of the Method Depending on the Orthogonal Properties of the Modes.—Example* 1. *Flexural Oscillations of a Uniform Cantilever.*—The first step is to obtain an approximation to the fundamental mode, which is assumed to be a linear combination of

$$\mathrm{Y}_1 = 2\xi^2 - \frac{4}{3}\xi^3 + \frac{1}{3}\xi^4,$$

and

$$\mathrm{Y}_2 = \frac{10}{3}\xi^3 - \frac{10}{3}\xi^4 + \xi^5.$$

The Rayleigh and Galerkin methods lead to the equations (compare Example 1 of §2.2)

$$q_1\left(\frac{16}{5}-\frac{104}{405}\alpha\right)+q_2\left(\frac{8}{3}-\frac{1304}{5670}\alpha\right)=0,$$

and

$$q_1\left(\frac{8}{3}-\frac{1304}{5670}\alpha\right)+q_2\left(\frac{20}{81}-\frac{1304}{6237}\alpha\right)=0.$$

The result of eliminating $q_1$ and $q_2$ is a quadratic equation in $\alpha$ of which the smaller root is 12·3625. When this value of $\alpha$ is substituted in either of the foregoing equations it is found that

$$\frac{q_2}{q_1}=0\cdot144100,$$

so that the fundamental mode is approximately

$$y_1=\mathrm{Y}_1+0\cdot144100\mathrm{Y}_2. \quad .. \quad .. \quad .. \quad .. \quad .. \quad .. \quad .. \quad (4.3.1)$$

The next step is to find the coefficients $g$ and $h$ which appear in the equations (4.2.4) and (4.2.5) defining the functions $\eta_1$ and $\eta_2$ which are orthogonal to the fundamental mode. If the *first* orthogonal property is used, then, since $m$ is here a constant, (4.2.6) yields

$$g=-\frac{\int \mathrm{Y}_1 y_1 dx}{\int \mathrm{Y}_2 y_1 dx}=-1\cdot114644,$$

while from (4.2.7)

$$h=-\frac{\int \mathrm{Y}_2 y_1 dx}{\int \mathrm{Y}_3 y_1 dx}=-1\cdot105769.$$

Hence

$$\begin{aligned}\eta_1&=\mathrm{Y}_1-1\cdot114644\mathrm{Y}_2\\&=2\xi^2-5\cdot048813\xi^3+4\cdot048813\xi^4-1\cdot114644\xi^5 \quad .. \quad .. \quad (4.3.2)\end{aligned}$$

and

$$\eta_2=3\cdot333333\xi^3-8\cdot862178\xi^4+7\cdot634614\xi^5-2\cdot211538\xi^6 \quad .. \quad (4.3.3)$$

When $\eta_1$ and $\eta_2$ are adopted as displacement functions the Rayleigh and Galerkin methods lead to the following quadratic equation for the frequency parameter

$$\alpha^2-4{,}861\cdot184\alpha+2{,}124{,}577=0.$$

The roots of this are 485·55 and 4,375·6, and the mode corresponding to the smaller root is

$$y_2=\eta_1+0\cdot661018\eta_2. \quad .. \quad .. \quad .. \quad .. \quad .. \quad .. \quad (4.3.4)$$

The approximation 485·55 to the first overtone root may be compared with the value 485·56 obtained by the use of three degrees of freedom (*see* §2.2, Example 1), and with the true root 485·522.

The results obtained when the *second* orthogonal property is used instead of the first are :—

$$\begin{aligned}g&=-1\cdot114644^*,\\h&=-1\cdot107579,\\\alpha&=485\cdot62 \text{ (or } 4340\cdot1),\\y_2&=\eta_1+0\cdot659083\eta_2.\end{aligned}$$

Since the differences from the former results are very small it is evidently immaterial which of the orthogonal properties is used. In the present case the labour is reduced by using the second property, and this will be adopted in working out the second overtone.

* It will be noted that this is identical with the result obtained from the first orthogonal property. The two properties will always yield identical results when the function made orthogonal to a mode is a linear combination of exactly the same displacement functions as those of which the mode itself is compounded ; for instance, here both the fundamental mode and $\eta_1$ are linear combinations of $\mathrm{Y}_1$ and $\mathrm{Y}_2$ only. Another illustration occurs in Example 4 below.

In order that $\eta_3$ shall be orthogonal to the fundamental mode and 1st overtone it is necessary that the following equations be satisfied

$$j + 0{\cdot}902870k + 1{\cdot}114643 = 0,$$
$$j + 1{\cdot}746696k - 0{\cdot}144100 = 0.$$

Hence $j = -2{\cdot}461462,$
and $k = 1{\cdot}491709.$
Similarly $l = -2{\cdot}440966,$
and $m = 1{\cdot}466118,$

when $\eta_4$ is orthogonal to the fundamental mode and 1st overtone. When $\eta_3$ and $\eta_4$ are used as displacement functions, the Rayleigh and Galerkin methods lead to a quadratic equation for $\alpha$ whose roots are 3,802·15 and 82,393. The true value of $\alpha$ for the second overtone is 3,806·55, to which the lower root of the quadratic is a close approximation.

*Example* 2. *Flexural Oscillations of a Parabolic Cantilever.*—The sections of the beam are geometrically similar and the linear dimensions are proportional to the square root of the distance measured from the tip. Let

$x$ = distance measured from root,
$l$ = overhang,
$\xi = x/l,$
$m$ = mass per unit length,
EI = flexural rigidity of the section,

and denote values measured at the root by addition of a zero suffix. Then clearly

$$m = m_0 (1 - \xi),$$
and $$\mathrm{EI} = \mathrm{EI}_0 (1 - \xi)^2.$$

The differential equation for the displacement in any pure mode is

$$\frac{d^2}{d\xi^2}\left[ (1 - \xi)^2 \frac{d^2y}{d\xi^2} \right] - \alpha (1 - \xi) y = 0, \quad .. \quad .. \quad .. \quad .. \quad (4.3.5)$$

where $$\alpha = \frac{m_0 \omega^2 l^4}{\mathrm{EI}_0}. \quad .. \quad .. \quad .. \quad .. \quad .. \quad .. \quad .. \quad .. \quad (4.3.6)$$

The end conditions are

$$y = \frac{dy}{d\xi} = 0 \text{ when } \xi = 0, \quad .. \quad .. \quad .. \quad .. \quad .. \quad .. \quad (4.3.7)$$

$$\mathrm{EI} \frac{d^2y}{d\xi^2} = \frac{d}{d\xi}\left( \mathrm{EI} \frac{d^2y}{d\xi^2} \right) = 0 \text{ when } \xi = 1. \quad .. \quad .. \quad .. \quad .. \quad .. \quad (4.3.8)$$

No exact solution of this problem has been obtained, but it follows from results given on p. 108 of Watson's "Bessel Functions"[7] that the solution is associated with a series of a generalised hypergeometric type ; in Watson's notation the series is

$${}_0\mathrm{F}_3\left( \frac{2}{3}, 1, \frac{2}{3}, \frac{z^3}{81} \right), \quad .. \quad .. \quad .. \quad .. \quad .. \quad .. \quad .. \quad (4.3.9)$$

where $$z = \sqrt[3]{\alpha}\,(1 - \xi). \quad .. \quad .. \quad .. \quad .. \quad .. \quad .. \quad .. \quad (4.3.10)$$

The series solution has been discussed by Morris[8], and his results when converted to the present notation give the following values of $\alpha$ for the fundamental and first overtone :—

$$39{\cdot}674,\ 514{\cdot}8.$$

The parabolic beam tapers to zero at the tip, and it follows from the discussion given in the Appendix that the conditions (4.3.8) reduce to $d^2y/d\xi^2 = 0$ when $\xi = 1$. Accordingly the displacement functions

$$\mathrm{Y}_r' = \tfrac{1}{2}(r + 2)\,\xi^{r+1} - \tfrac{1}{2} r \xi^{r+2} \quad .. \quad .. \quad .. \quad .. \quad .. \quad .. \quad (4.3.11)$$

are suitable for use in the Rayleigh and Galerkin methods. If the displacement is assumed to be given by

$$y = Y_1' + bY_2', \qquad \ldots\ldots\ldots\ldots\ldots\ldots\ldots \quad (4.3.12)$$

these methods lead to the equations

$$\left(\frac{9}{5} - \frac{7}{160}\alpha\right) + b\left(\frac{6}{5} - \frac{17}{504}\alpha\right) = 0, \qquad \ldots\ldots\ldots\ldots \quad (4.3.13)$$

$$\left(\frac{6}{5} - \frac{17}{504}\alpha\right) + b\left(\frac{48}{35} - \frac{17}{630}\alpha\right) = 0. \qquad \ldots\ldots\ldots\ldots \quad (4.3.14)$$

The quadratic eliminant reduces to

$$17\alpha^2 - 10{,}962\alpha + 408{,}240 = 0,$$

of which the roots are 39·684 and 605·14. The smaller root agrees well with Morris's result for the fundamental. On substitution of the smaller root in (4.3.13) or (4.3.14) it is found that $b = 0{\cdot}461$.

The displacement functions

$$\eta_1 = Y_1' + gY_2',$$

and

$$\eta_2 = Y_2' + hY_3'$$

are orthogonal to the fundamental mode already obtained (if the second orthogonal property is used) when $g = -1{\cdot}284$ and $h = -1{\cdot}264$. With the orthogonal displacement functions in use the Rayleigh and Galerkin methods lead to a quadratic equation for $\alpha$ whose roots are 513·0 and 1564·3. The smaller of these agrees closely with the value 514·8 obtained for the first overtone by Morris.

*Example* 3.—*Flexural Oscillations of a Conical Cantilever.*—The beam is in the form of a cone or pyramid tapering to a point at the tip. The sections are geometrically similar, and

$$m = m_0(1 - \xi)^2,$$

$$EI = EI_0(1 - \xi)^4.$$

Hence the differential equation for the displacement is

$$\frac{d^2}{d\xi^2}\left[(1 - \xi)^4 \frac{d^2y}{d\xi^2}\right] - \alpha(1 - \xi)^2 y = 0, \qquad \ldots\ldots\ldots\ldots \quad (4.3.15)$$

where $\alpha$ is defined in equation (4.3.6).

This problem was first discussed by Kirchhoff and later by several other writers, including Wrinch.[9] These authors succeeded in obtaining a solution in Bessel functions which it is not necessary to quote here.* The numerical results which will be compared with the approximations obtained by the present method are taken from the paper by Wrinch.

It is shown in the Appendix that for a beam of this type neither $d^2y/d\xi^2$ nor $d^3y/d\xi^3$ vanish at the tip. Hence the displacement functions

$$Y_r'' = \xi^{r+1} \qquad \ldots\ldots\ldots\ldots\ldots\ldots\ldots\ldots \quad (4.3.16)$$

may be adopted. Accordingly, assume that

$$y = \xi^2 + b\xi^3. \qquad \ldots\ldots\ldots\ldots\ldots\ldots\ldots\ldots \quad (4.3.17)$$

The Rayleigh and Galerkin methods lead to a quadratic equation for $\alpha$ (as defined in equation (4.3.6)) whose roots are 76·304 and 634·1, whereas according to Wrinch the value for the fundamental should be 76·042. Also the value of $b$ corresponding to the smaller root is 1·3526.

* On this point the reader may also consult Watson's " Bessel Functions ", p. 408, or Maclachlan's " Bessel Functions for Engineers ", p. 114.

It is found that the functions $\xi^2 - 1{\cdot}552584\xi^3$ and $\xi^3 - 1{\cdot}498569\xi^4$ are orthogonal (second property) to the fundamental mode already obtained. When these are used as displacement functions a quadratic equation for $\alpha$ results, of which the roots are $460{\cdot}4$ and $2656{\cdot}6$. The correct value of $\alpha$ for the first overtone is $447{\cdot}16$. Since $\alpha$ is proportional to the square of the frequency, the error in the first overtone frequency is about $1{\cdot}4$ per cent. The comparatively low accuracy in this example may be attributed to the fact that the displacement functions $Y_r''$ do not have to satisfy any condition at the tip, and are therefore less tightly conditioned than the displacement functions for Examples 1 and 2.

*Example* 4.—*Torsional Oscillations of a Uniform Cantilever.*—The differential equation for the displacement in a pure mode is

$$\frac{d^2\theta}{d\xi^2} + \alpha\theta = 0, \quad \ldots \quad \ldots \quad \ldots \quad \ldots \quad \ldots \quad \ldots \quad \ldots \quad \ldots \quad (4.3.18)$$

where $\alpha$ is defined in equation (2.2.12). The end conditions are

$$\theta = 0 \text{ when } \xi = 0,$$

$$\frac{d\theta}{d\xi} = 0 \text{ when } \xi = 1.$$

Hence (*see* the Appendix) the displacement functions

$$\Theta_r = (r+1)\xi^r - r\xi^{r+1} \quad \ldots \quad \ldots \quad \ldots \quad \ldots \quad \ldots \quad \ldots \quad (4.3.19)$$

are suitable for the treatment of the problem. When the functions $\Theta_1$ and $\Theta_2$ are used, the Rayleigh and Galerkin methods yield a quadratic equation for $\alpha$ whose roots are $2{\cdot}4680$ and $23{\cdot}5625$, whereas the correct values for the fundamental and first overtone are

$$\frac{\pi^2}{4} = 2{\cdot}4674 \text{ and } \frac{9\pi^2}{4} = 22{\cdot}207.$$

The corresponding approximation to the fundamental mode is $\theta = \Theta_1 + 0{\cdot}245279\Theta_2$. Displacement functions orthogonal to this are

$$\eta_{i1} = \Theta_1 - 1{\cdot}219632\Theta_2 \ (1^{st} \text{ or } 2^{nd} \text{ property}),$$

and

$$\eta_{i2} = \Theta_2 - 1{\cdot}189888\Theta_3 \ (1^{st} \text{ property}),$$

or

$$\eta_{i2} = \Theta_2 - 1{\cdot}182759\Theta_3 \ (2^{nd} \text{ property}).$$

When $\eta_{i1}$ and $\eta_{i2}$ corresponding to the first orthogonal property are used as displacement functions the results obtained are

$$\alpha = 22{\cdot}402 \text{ or } 69{\cdot}661$$
$$\text{Mode } \theta = \eta_{i1} + 0{\cdot}9255\ \eta_{i2}.$$

If $\eta_{i1}$ and $\eta_{i2}$ correspond to the second orthogonal property the results are

$$\alpha = 22{\cdot}397 \text{ or } 69{\cdot}158$$
$$\text{Mode } \theta = \eta_{i1} + 0{\cdot}9328\eta_{i2}.$$

The error in the first overtone frequency is about $0{\cdot}4$ per cent.

In order to obtain the value of $\alpha$ for the second overtone, displacement functions

$$\eta_{i3} = \Theta_1 + j\Theta_2 + k\Theta_3,$$

and

$$\eta_{i4} = \Theta_2 + l\Theta_3 + m\Theta_4.$$

both made orthogonal to the fundamental and to the first overtone mode (as obtained by use of the second orthogonal property) will be adopted. The equation for $\alpha$ obtained by use of these functions has the roots $63{\cdot}317$ and $136{\cdot}185$, whereas the correct value for the second overtone is $25\pi^2/4 = 61{\cdot}685$. Hence the error in the second overtone frequency is about $1{\cdot}2$ per cent.

*Example* 5. *Torsional Oscillations of a Parabolic Cantilever.*—The problem has already been treated by the direct method in Example 2 of §2.2, and the application of the matrix method to the direct solution has been given in §3.2. The differential equation is (2.2.11), and as shown in the Appendix the functions $\Theta_r$ as defined in equation (4.3.19) are applicable. When the displacement is assumed to be

$$\theta = \Theta_1 + b\Theta_2,$$

the results given by the direct application of the Rayleigh and Galerkin methods are

$$\alpha = 9{\cdot}87076 \text{ or } 46{\cdot}069$$

$$\text{Mode } \theta = \Theta_1 + 1{\cdot}03026\Theta_2.$$

The correct fundamental root is $\pi^2 = 9{\cdot}869604$, so that the error in the fundamental root is only $0{\cdot}005$ per cent. To obtain the first overtone functions $\eta_{l1}$ and $\eta_{l2}$ constructed as in Example 4 and made orthogonal to the fundamental mode according to the second property are adopted. The results obtained are

$$\alpha = 39{\cdot}568 \text{ or } 114{\cdot}196$$

$$\begin{aligned}\text{Mode } \theta &= \eta_{l1} + 3{\cdot}032527\eta_{l2} \\ &= \Theta_1 + 1{\cdot}423323\Theta_2 - 4{\cdot}628607\Theta_3 \\ &= 2\xi + 3{\cdot}269969\xi^2 - 21{\cdot}361074\xi^3 + 13{\cdot}885821\xi^4.\end{aligned}$$

Since the correct value of $\alpha$ for the first overtone is $4\pi^2 = 39{\cdot}478$, the error in the first overtone frequency is about $0{\cdot}12$ per cent. Lastly, when the second overtone is obtained by use of the displacement functions $\eta_{l3}$ and $\eta_{l4}$ as in Example 4 the results are

$$\alpha = 88{\cdot}880 \text{ or } 238{\cdot}958$$

$$\text{Mode } \theta = 2\xi + 5{\cdot}588\xi^2 - 71{\cdot}688\xi^3 + 128{\cdot}077\xi^4 - 62{\cdot}684\xi^5.$$

The true value of $\alpha$ for the second overtone is $9\pi^2 = 88{\cdot}826$, so that the error in the second overtone frequency is only about $0{\cdot}02$ per cent.

§ 5. *Direct Iterative Solution.*—5.1. *General.*—One of the oldest processes for obtaining the natural frequencies of vibration of elastic bodies may be called the direct iterative method.* According to this system a mode of oscillation, consistent with the conditions of support, is assumed, and from this the distribution of the inertia forces in a presumed sinusoidal motion having the same frequency at all points is calculated. The inertia forces are taken as a load system for the body, and the corresponding static deflexions are calculated from the known elastic properties of the body. These static deflexions are then taken as the assumed mode, and the process is repeated. In this way a sequence of modes is obtained, and these converge to a definite mode,† which is in fact the *fundamental* mode for the body. The fundamental frequency can then be calculated from the mode in the ordinary way, but it can also be found from the displacements in a pair of consecutive derived modes as explained below.

The process of iteration easily leads to the fundamental mode and frequency, but a serious difficulty arises when an attempt is made to derive any overtone mode and frequency in the same manner. If a mode closely approximating to a certain overtone mode be assumed, it is found that the successive derived modes *diverge* from the true overtone mode, and if the process be sufficiently continued they again converge upon the fundamental. This phenomenon will be described as *regression to the fundamental*, and an illustration of it is given below. It may be remarked that systems possessing only a finite number of degrees of freedom behave in exactly the same way, as can be proved by the theory of matrices [4, 5]. This proof can be extended to a continuous elastic body if it be regarded as a dynamical system possessing a very large number of degrees of freedom.

---

* The earliest reference to this method known to the writers is Vianello, Z.V.D.I., 1898, p. 1436.

† The mere amplitude does not converge, but the ratios of displacements converge.

Attempts have been made to evade the difficulty in obtaining the overtones by invoking the principle, inherent in Rayleigh's principle itself, that the frequency is stationary for small departures of the nodes from their true positions. Hohenemser[10] makes a preliminary estimate of the nodal positions by an approximate method, assumes the nodes fixed, and finds the fundamental frequency of the body so constrained. Hansen and Mesmer[11, 12] regard the nodal positions as known, and use a modification of the iterative method. For example, their procedure in finding the first overtone is as follows. Take an assumed mode having its node at the chosen position, apply the iterative process, and so obtain a derived mode which will in general not have the assumed node. This derived mode is combined linearly with the fundamental in such a proportion that the node is brought to the chosen position, and the frequency is found for this modified mode. The second overtone can similarly be found by combining the mode derived by iteration with proportions of the fundamental and first overtone so chosen as to bring the two nodes to the selected positions.

A modification of the iterative solution is now proposed which dispenses with all preliminary knowledge of the nodal positions. This modification makes use of the orthogonal properties of the modes (*see* §4.1), and is as follows. To find the first overtone assume an initial mode, which, in order to shorten the work, should be a guessed approximation to the first overtone mode.* The usual process of derivation is applied once or oftener to the assumed mode. The derived mode is then combined linearly with such a proportion of the fundamental that the result is orthogonal to the fundamental, and the frequency is calculated for the orthogonal mode. The whole process may be repeated until the calculated frequency becomes constant. The procedure in determining the second overtone is similar, but the derived mode is combined with proportions of the fundamental and first overtone, and made orthogonal to both of these. The extension to higher overtones is obvious.

5.2. *The Process of Derivation.*—First consider the torsional oscillations of a beam or blade of overhang $l$, and measure the co-ordinate $x$ along the blade with the origin at the root. Let

$$c(\xi) = \frac{C(\xi)}{C_0}, \quad .. \quad .. \quad .. \quad .. \quad .. \quad .. \quad .. \quad .. \quad (5.2.1)$$

$$j(\xi) = \frac{J(\xi)}{J_0}, \quad .. \quad .. \quad .. \quad .. \quad .. \quad .. \quad .. \quad .. \quad (5.2.2)$$

$$\alpha = \frac{\omega^2 J_0 l^2}{C_0}, \quad .. \quad .. \quad .. \quad .. \quad .. \quad .. \quad .. \quad .. \quad (5.2.3)$$

where $\xi = x/l$, $C(\xi)$ is the local torsional stiffness of unit length of the beam, $J(\xi)$ is the polar moment of inertia of unit length, and the zero suffix indicates a value measured at the root. Let the assumed initial mode be $\theta_1$ and the successive derived modes $\theta_2, \ldots \theta_{n-1}, \theta_n$. Define the function $f_{n-1}(\xi)$ by the equation

$$f_{n-1}(\xi) = \int_\xi^1 j(\xi)\theta_{n-1} d\xi. \quad .. \quad .. \quad .. \quad .. \quad .. \quad .. \quad .. \quad (5.2.4)$$

Then

$$\frac{d\theta_n}{d\xi} = \frac{f_{n-1}(\xi)}{c(\xi)} \quad .. \quad .. \quad .. \quad .. \quad .. \quad .. \quad .. \quad .. \quad (5.2.5)$$

and

$$\theta_n = \int_0^\xi \frac{d\theta_n}{d\xi} d\xi. \quad .. \quad .. \quad .. \quad .. \quad .. \quad .. \quad .. \quad .. \quad (5.2.6)$$

The last three equations define the process by which each mode is obtained from its predecessor. It should be noted that

$$f_{n-1}(1) = 0, \quad .. \quad .. \quad .. \quad .. \quad .. \quad .. \quad .. \quad .. \quad .. \quad (5.2.7)$$

and

$$\frac{df_{n-1}(\xi)}{d\xi} = -j(\xi)\theta_{n-1}. \quad .. \quad .. \quad .. \quad .. \quad .. \quad .. \quad .. \quad (5.2.8)$$

* A study of known solutions will enable the calculator to make a good choice of mode.

The approximation to $\alpha$ corresponding to the mode $\theta_n$ as given by the usual energy quotation is

$$\alpha_n = \frac{\int_0^1 c\,(\xi)\left(\frac{d\theta_n}{d\xi}\right)^2 d\xi}{\int_0^1 j\,(\xi)\,\theta_n^2\,d\xi} \qquad \text{(5.2.9)}$$

This can be put in a more convenient form. For by (5.2.5)

$$\int_0^1 c\,(\xi)\left(\frac{d\theta_n}{d\xi}\right)^2 d\xi = \int_0^1 \frac{d\theta_n}{d\xi}\, f_{n-1}\,(\xi)\,d\xi$$

$$= \Big[\,\theta_n f_{n-1}(\xi)\,\Big]_0^1 - \int_0^1 \theta_n\, \frac{df_{n-1}\,(\xi)}{d\xi}\, d\xi.$$

But $\theta_n$ vanishes when $\xi = 0$ and $f_{n-1}\,(1)$ is zero by (5.2.7). Hence

$$\int_0^1 c\,(\xi)\left(\frac{d\theta_n}{d\xi}\right)^2 d\xi = -\int_0^1 \theta_n \frac{df_{n-1}(\xi)}{d\xi}\, d\xi$$

$$= \int_0^1 j\,(\xi)\theta_{n-1}\,\theta_n\,d\xi \qquad \text{(5.2.10)}$$

by (5.2.8). Therefore (5.2.9) becomes

$$\alpha_n = \frac{\int_0^1 j\,(\xi)\;\theta_{n-1}\,\theta_n\,d\xi}{\int_0^1 j\,(\xi)\;\theta_n^2 d\xi} \qquad \text{(5.2.11)}$$

In the limit when $\theta_n$ is proportional to $\theta_{n-1}$ this shows that

$$\alpha = \frac{\theta_{n-1}}{\theta_n} \qquad \text{(5.2.12)}$$

The truth of (5.2.11) also follows from a general argument which shows that a similar formula, with $\theta$ representing the displacement and $j(\xi)$ the appropriate inertia coefficient, must hold in other cases. (For instance, in a flexural oscillation $\theta$ would be identified with the normal displacement $y$ and $j(\xi)$ with the mass per unit length divided by the value of this quantity at the root.) For the numerator of (5.2.9) is twice the elastic energy,* while the numerator of (5.2.11) is twice the work done by the load system whose intensity is $j(\xi)\;\theta_{n-1}$, and these are necessarily equal.†

The details of the process of derivation in the important case of the flexural oscillations of a beam deserve some comment. In the usual notation the inertia force per unit span is $my\omega^2$, but in the derivation of the modes the factor $\omega^2$ is omitted (compare the torsional case already discussed). From this loading the bending moment $M(x)$ is calculated in the ordinary way. The deflexion $y$ is then always expressible by *single* integrals. For a cantilever or other beam built in at the end $x = 0$ the formula is

$$y = \int_0^x (x - x')\,\frac{M(x')}{EI(x')}\,dx', \qquad \text{(5.2.13)}$$

while for a beam of span $l$ simply supported at the end $x = 0$.

$$y = \int_0^x (x - x')\,\frac{M(x')}{EI(x')}\,dx' - \frac{x}{l}\int_0^1 (l - x')\,\frac{M(x')}{EI(x')}\,dx'. \qquad \text{(5.2.14)}$$

5.3. *Examples of the Iterative Solution.—Example* 1.—*Fundamental Torsional Mode of a Parabolic Cantilever.*—The symbols have the same meanings as in Example 2 of §2.2. Take $\Theta_1$ (*see*

* The constant factor $C_0$ is extracted.

† This argument is indicated by Hohenemser[10].

equation (2.2.15)) as the first approximation $\theta_1$ to the mode. Since $j(\xi) = (1 - \xi)^2$ equation (5.2.4) yields

$$f_1(\xi) = \int_\xi^1 (1 - \xi)^2 \Theta_1 \, d\xi,$$
$$= \int_\xi^1 (1 - \xi)^2 (2\xi - \xi^2) \, d\xi,$$
$$= \frac{1}{15}(2 - 15\xi^2 + 25\xi^3 - 15\xi^4 + 3\xi^5),$$

and by (5.2.5)

$$\frac{d\theta_2}{d\xi} = \frac{f_1(\xi)}{c(\xi)} = \frac{f_1(\xi)}{(1 - \xi)^2},$$
$$= \frac{1}{15}(2 + 4\xi - 9\xi^2 + 3\xi^3).$$

Hence

$$\theta_2 = \int_0^\xi \frac{d\theta_2}{d\xi} \, d\xi,$$
$$= \frac{1}{60}(8\xi + 8\xi^2 - 12\xi^3 + 3\xi^4),$$

and by (5.2.11)

$$\alpha_2 = \frac{\int_0^1 (1 - \xi)^2 \theta_1 \theta_2 \, d\xi}{\int_0^1 (1 - \xi)^2 \theta_2^2 \, d\xi} = 9{\cdot}90.$$

The value of the frequency parameter corresponding to the mode $\theta_1$ is 10·5 (*see* Table 2 of §2.2), and the true value is 9·8696. The process has been carried one stage further, and all of the results are summarised as follows :—

| *Mode* | *Value of* $\alpha$ | *Error in frequency per cent.* |
|---|---|---|
| $\theta_1$ | 10·5 | 3 |
| $\theta_2$ | 9·90 | 0·15 |
| $\theta_3$ | 9·870 | 0·005 |

*Example* 2. *Regression to the Fundamental.*—The node for the first torsional overtone of the parabolic cantilever is at $\xi = 0{\cdot}5$.

The function

$$\theta_1 = \Theta_1 - 1{\cdot}5\Theta_2$$

vanishes when $\xi = 0{\cdot}5$ and yields $\alpha_1 = 44{\cdot}8$ as against the correct value 39·478 for the first overtone. Hence $\theta_1$ is a fair approximation to the first overtone. The values of $\alpha$ for $\theta_1$ and the successively derived modes are :—

$$\alpha_1 = 44{\cdot}8$$
$$\alpha_2 = 27{\cdot}2$$
$$\alpha_3 = 12{\cdot}2$$

It will be seen that $\alpha$ is already approaching the value 9·87 appropriate to the *fundamental* mode.

*Example* 3. *First Torsional Overtone Mode for the Parabolic Cantilever.*—In order to illustrate the convergence of $\alpha$ to the true value notwithstanding a bad choice of the initial mode this will be taken as

$$\theta_1 = \Theta_1 - \Theta_2 = 2\xi(1 - \xi)^2.$$

This has its node at the tip and yields $\alpha_1 = 21{\cdot}6$. The mode derived from $\theta_1$ by use of the formulae (5.2.4) to (5.2.6) is

$$\theta_2 = \frac{1}{30}(2\xi + 2\xi^2 - 8\xi^3 + 7\xi^4 - 2\xi^5).$$

The fundamental mode as derived in Example 1 (there called $\theta_3$) is

$$\theta_0 = \frac{1}{2520}(32\xi + 32\xi^2 - 24\xi^3 - 24\xi^4 + 18\xi^5 - 3\xi^6).$$

Take $\theta_2' = (\theta_2 + k_2\theta_0)$ and make this orthogonal to $\theta_0$.

Then

$$\int_0^1 (1-\xi)^2\theta_0\,(\theta_2 + k\theta_0)d\xi = 0,$$

so that

$$k_2 = -\frac{\int_0^1 (1-\xi)^2\theta_0\theta_2 d\xi}{\int_0^1 (1-\xi)^2\theta_0^2\, d\xi}$$

$$= -3{\cdot}743824.$$

The value of $\alpha$ obtained from the mode $\theta_2'$ by means of (5.2.9) is $40{\cdot}362$ (note that (5.2.11) cannot be used since $\theta_2'$ is not directly derived from $\theta_1$). The error in the frequency at this stage is $1{\cdot}1$ per cent.

The process of derivation defined by (5.2.4) to (5.2.6) is applied to $\theta_2'$ and yields a mode $\theta_3$. Then

$$\theta_3' = \theta_3 + k_3\theta_0$$

is made orthogonal to $\theta_0$, and the numerical value of $k_3$ is found to be $0{\cdot}000344$. The smallness of this shows that $\theta_3$ is almost free from admixture with the fundamental. Finally the mode $\theta_3'$ yields on application of (5.2.9) the value $39{\cdot}645$ for $\alpha$. The corresponding error in the frequency is $0{\cdot}2$ per cent.

In this example it probably would have been advantageous to apply the process of derivation again to $\theta_3$ before making the mode orthogonal to the fundamental. It may also be noted that it was found convenient to use Simpson's rule in working out the integrals concerned.

---

## APPENDIX

### *The Choice of Displacement Functions for Cantilever Beams*

*Flexural Oscillations.*—The differential equation to be satisfied is

$$\frac{d^2}{dz^2}\mathrm{EI}\frac{d^2y}{dz^2} = m\omega^2 y \qquad \ldots\ldots\ldots\ldots\ldots\ldots\ldots\ldots \quad (1)$$

For convenience measure $z$ from the tip, and suppose that

$$\left.\begin{aligned} \mathrm{EI} &= b(z)z^p \\ m &= c(z)z^q \\ \frac{d^2y}{dx^2} &= d(z)z^r \end{aligned}\right\} \qquad \ldots\ldots\ldots\ldots\ldots\ldots\ldots\ldots \quad (2)$$

where $b(0)$, $c(0)$ and $d(0)$ are neither zero nor infinite. Then the right hand side of (1) is proportional to $z^q$ when $z$ is small since $y$ does not vanish at the tip, whereas the left-hand side is proportional to $z^{p+r-2}$. Hence

$$p + r - 2 = q$$

or

$$r = q - p + 2 \qquad \ldots\ldots\ldots\ldots\ldots\ldots\ldots\ldots \quad (3)$$

*Flexure. Case* 1. *Beam not tapering to Zero at the Tip.*—Here $p = q = 0$. Hence (3) gives $r = 2$, so that near the tip

$$\frac{d^2y}{dz^2} = d(z)z^2,$$

and

$$\frac{d^3y}{dz^3} = 2zd(z) + z^2d'(z).$$

Therefore, $\frac{d^2y}{dx^2}$ and $\frac{d^3y}{dx^3}$ are both zero at the tip. At the root $y = \frac{dy}{dx} = 0$. The following functions satisfy the conditions

$$\mathrm{Y}_r = \frac{1}{6}(r+2)(r+3)\xi^{r+1} - \frac{1}{3}r(r+3)\xi^{r+2} + \frac{1}{6}r(r+1)\xi^{r+3}, \ldots\ldots\ldots \quad (4)$$

where $\xi = x/l$ and $l$ is the overhang, while $x$ is measured from the root as usual ($z = l - x$).

*Flexure. Case 2. Beam with Rounded Tip. Ratio of Depth to Breadth of Section neither Zero nor Infinite near Tip.*—Here $p = 2$ and $q = 1$. Hence by (3) $r = 1$, and

$$\frac{d^2y}{dz^2} = d(z)z, \frac{d^3y}{dz^3} = d(z) + d'(z)z.$$

It follows that $d^2y/dx^2$ vanishes at the tip, whereas $d^3y/dx^3$ is *not* zero there. With the same notation as before a suitable displacement function is

$$Y_r' = \tfrac{1}{2}(r+2)\xi^{r+1} - \tfrac{1}{2}r\xi^{r+2} \quad .. \quad .. \quad .. \quad .. \quad .. \quad .. \quad (5)$$

*Flexure. Case 3. Beam with Pointed Tip of Finite Angle.*—Here $p = 4$ and $q = 2$, and by (3) $r = 0$. Hence neither $d^2y/dx^2$ nor $d^3y/dx^3$ vanish at the tip. Consequently

$$Y_r'' = \xi^{r+1} \quad .. \quad .. \quad .. \quad .. \quad .. \quad .. \quad .. \quad .. \quad .. \quad (6)$$

is a suitable displacement function.

*Torsional Oscillations.*—The differential equation is

$$\frac{d}{dz}\left(C\frac{d\theta}{dz}\right) = -J\omega^2\theta. \quad .. \quad .. \quad .. \quad .. \quad .. \quad .. \quad .. \quad .. \quad (7)$$

Measure $z$ from the tip and let

$$\left.\begin{aligned} C &= c(z)z^p \\ J &= j(z)z^q \\ \frac{d\theta}{dz} &= t(z)z^r \end{aligned}\right\} \quad .. \quad .. \quad .. \quad .. \quad .. \quad .. \quad .. \quad .. \quad .. \quad (8)$$

where $c(0)$, $j(0)$ and $t(0)$ are neither zero nor infinite. Then the right-hand side of (7) contains $z^q$ while the left-hand side contains $z^{p+r-1}$. Hence

$$p + r - 1 = q$$

or

$$r = q - p + 1. \quad .. \quad .. \quad .. \quad .. \quad .. \quad .. \quad .. \quad .. \quad (9)$$

Now provided that the ratio of depth to breadth of the section remains finite near the tip C and J will vary with $z$ in the same manner, so that $p = q$. Hence by (9) $r = 1$, and $d\theta/dx$ vanishes at the tip, but $d^2\theta/dx^2$ does not vanish. It follows that the functions

$$\Theta_r = (r+1)\xi^r - r\xi^{r+1} \quad .. \quad .. \quad .. \quad .. \quad .. \quad .. \quad .. \quad (10)$$

are suitable to represent the torsional displacement.

The method used here to investigate the geometrical conditions at the tip of a cantilever was given in Appendices II and III of Reference 4.

---

## LIST OF REFERENCES


| *No.* | *Author.* | *Title.* |
|---|---|---|
| 1 | W. J. Duncan .. .. .. .. | Galerkin's Method in Mechanics and Differential Equations. R. & M. 1798, 1938. |
| 2 | W. J. Duncan .. .. .. .. | The Principles of the Galerkin Method. R. & M. 1848, 1939. |
| 3 | P. B. Walker .. .. .. .. | Simple Formulae for the Fundamental Natural Frequencies of Cantilevers. R. & M. 1831, 1938. |
| 4 | W. J. Duncan and A. R. Collar .. | A Method for the Solution of Oscillation Problems by Matrices. Phil. Mag., May 1934, p. 865. |
| 5 | R. A. Frazer, W. J. Duncan and A. R. Collar. | Elementary Matrices. Cambridge, 1938. |
| 6 | H. Lamb.. .. .. .. .. | Higher Mechanics. Cambridge. |
| 7 | G. N. Watson .. .. .. .. | Treatise on Bessel Functions. Cambridge. |
| 8 | J. Morris .. .. .. .. | Airscrew Blade Vibration. R. & M. 1835, 1939. |
| 9 | D. Wrinch .. .. .. .. | On the Lateral Vibrations of Bars of Conical Type. Proc. Roy. Soc., A., Vol. 101 (1922), p. 493. |
| 10 | K. Hohenemser .. .. .. | Beitrag zur Dynamik des elastischen Stabes mit Anwendung auf den Propeller. Z.F.M., 1932, p. 37. |
| 11 | M. Hansen and G. Mesmer .. .. | Luftschraubenschwingungen. Z.F.M., 1933, p. 298. |
| 12 | M. Hansen and G. Mesmer .. .. | Airscrew Oscillations. Aircraft Engineering, March 1935, p. 65. |


(53486) Wt. 4 500 1/41 Hw. G.377/1

## SYSTEM OF AXES

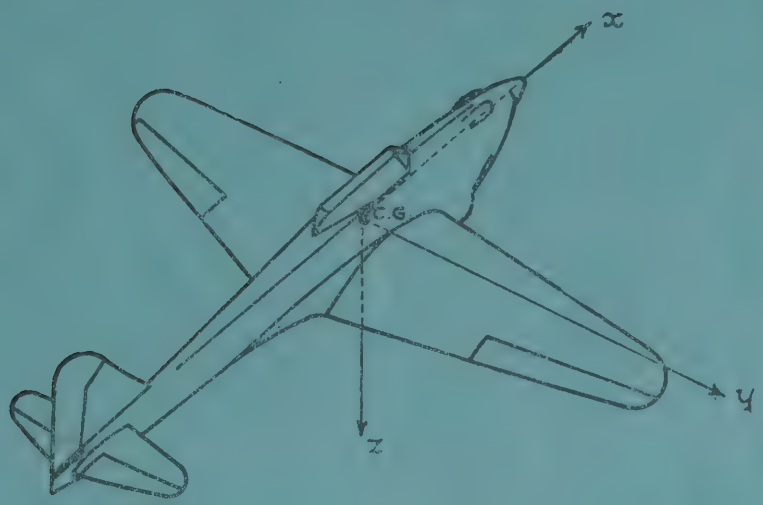


| Axes | Symbol Designation Positive direction | $x$ longitudinal forward | $y$ lateral starboard | $z$ normal downward |
|---|---|---|---|---|
| Force | Symbol | X | Y | Z |
| Moment | Symbol<br>Designation | L<br>rolling | M<br>pitching | N<br>yawing |
| Angle of Rotation | Symbol | $\phi$ | $\theta$ | $\psi$ |
| Velocity | Linear<br>Angular | $u$<br>$p$ | $v$<br>$q$ | $w$<br>$r$ |
| Moment of Inertia | | A | B | C |

Components of linear velocity and force are positive in the positive direction of the corresponding axis.

Components of angular velocity and moment are positive in the cyclic order $y$ to $z$ about the axis of $x$, $z$ to $x$ about the axis of $y$, and $x$ to $y$ about the axis of $z$.

The angular movement of a control surface (elevator or rudder) is governed by the same convention, the elevator angle being positive downwards and the rudder angle positive to port. The aileron angle is positive when the starboard aileron is down and the port aileron is up. A positive control angle normally gives rise to a negative moment about the corresponding axis.

The symbols for the control angles are :—

$\xi$ aileron angle
$\eta$ elevator angle
$\eta_T$ tail setting angle
$\zeta$ rudder angle

# Publications of the Aeronautical Research Committee

TECHNICAL REPORTS OF THE AERONAUTICAL RESEARCH COMMITTEE—

1933-34 Vol. I. Aerodynamics. £1 5*s*.
Vol. II. Structures, Engines, Instruments, etc. £1 10*s*.

1934-35 Vol. I. Aerodynamics. £2.
Vol. II. Seaplanes, Structures, Engines, Materials, etc. £2.

1935-36 Vol. I. Aerodynamics. £1 10*s*.
Vol. II. Structures, Flutter, Engines, Seaplanes, etc. £1 10*s*.

1936 Vol. I. Aerodynamics General, Performance, Airscrews, Flutter and Spinning. £2.
Vol. II. Stability and Control, Structures, Seaplanes, Engines, etc. £2 10*s*.

ANNUAL REPORTS OF THE AERONAUTICAL RESEARCH COMMITTEE—

1933-34 1*s*. 6*d*.
1934-35 1*s*. 6*d*.
April 1, 1935 to December 31, 1936. 4*s*.
1937 2*s*.

INDEX TO THE TECHNICAL REPORTS OF THE ADVISORY COMMITTEE ON AERONAUTICS—

1909-1919 Reports and Memoranda No. 1600. 8*s*.

NUMERICAL LISTS OF REPORTS AND MEMORANDA published between 1909 and 1936—

Reports and Memoranda Nos. 650 (9*d*.), 750 (6*d*.), 850 (1*d*.), 950 (4*d*.), 1050 (4*d*.), 1150 (4*d*.) (*Out of print*), 1250 (6*d*.) (*Out of print*), 1350 (6*d*.) (*Out of print*), 1450 (6*d*.), 1550 (6*d*.), 1650 (6*d*.), 1750 (1*s*. 3*d*.)

LIST OF PUBLICATIONS ON AERONAUTICS—

Aeronautical Research Committee Publications (classified under subjects). Post free on application.

*Prices are net and postage extra.*

## His Majesty's Stationery Office

London W.C.2 : York House, Kingsway

Edinburgh 2 : 120 George Street
Manchester 1 : 26 York Street
Cardiff : 1 St. Andrew's Crescent
Belfast : 80 Chichester Street

or through any bookseller.

S.O. Code No. 23-1888

Engrg.
LIBRARY
UNIVERSITY OF ILLINOIS
URBANA
Engineering Library
629.13
G79r
no.1889

R. & M. No. 1889
(4668)

AIR MINISTRY

AERONAUTICAL RESEARCH COMMITTEE
REPORTS AND MEMORANDA

# The Design of Wind Tunnel Fans

*By*

A. R. Collar, B. A., B. Sc.

*Crown Copyright Reserved*

LONDON: HIS MAJESTY'S STATIONERY OFFICE
Price 2*s.* 6*d.* net

Return this book on or before the
**Latest Date** stamped below.
Theft, mutilation, and underlining of books are reasons for disciplinary action and may result in dismissal from the University.
University of Illinois Library

MAY 20 1965
JUN 13 1965
JUL 17 1969
JUL 24 1969
AUG 21 1969
L161— O-1096

# SYMBOLS

1. [illegible]

sity
(where $l$ is a suitable linear dimension)
ure for aeronautical work are 15° C

02378 slug/cu. ft.
$9 \times 10^{-4}$ sq. ft./sec.
.-mass.

$/\frac{1}{2}\rho V^2S$
$D/\frac{1}{2}\rho V^2S$

| | |
|---|---|
| L | [illegible] cient $C_l = L/\frac{1}{2}\rho V^2bS$ |
| M | Pitching moment, with coefficient $C_m = M/\frac{1}{2}\rho V^2cS$ |
| N | Yawing moment, with coefficient $C_n = N/\frac{1}{2}\rho V^2bS$ |

2. AIRSCREWS

| | |
|---|---|
| $n$ | Revolutions per second |
| D | Diameter |
| J | $V/nD$ |
| P | Power |
| T | Thrust, with coefficient $k_T = T/\rho n^2D^4$ |
| Q | Torque, with coefficient $k_Q = Q/\rho n^2D^5$ |
| $\eta$ | Efficiency, $\eta = TV/P = Jk_T/2\pi k_Q$ |

LIBRARY
UNIVERSITY OF ILLINOIS
URBANA

# The Design of Wind Tunnel Fans

*By*

A. R. Collar, B. A., B. Sc.,
of the Aerodynamics Department, N.P.L.

*Reports and Memoranda No.* 1889
10*th August*, 1940

*Summary.*—The present report is one of a series dealing with N.P.L. methods for the design of return flow wind tunnels. Reports already issued deal with the design of the Compressed Air Tunnel[1] and Open Jet Tunnels,[2] with the design of corner cascades[3] and fan straighteners,[4] and with the improvement of velocity distribution by means of windmills[5] and gauzes.[6]

An explanation is now given of the method usually adopted in the design of fans for return flow tunnels; as an example of the method, the design of the fan for the N.P.L. non-turbulent tunnel is considered in detail. It is shown that for a wind tunnel a fan with blades of constant chord is advisable; and a formula is given by means of which a rapid estimate can be made of the variation in rotational speed of the fan corresponding to a variation in power factor at constant power.

1. *Power Factor.*—The power factor $\lambda$ of a wind tunnel is defined by the equation

$$\tfrac{1}{2}\rho AV^3\lambda = P, \quad \ldots \quad (1)$$

where P is the power input (ft.lb./sec.), $\rho$ the air density (slug/ft.$^3$), A the area of the working section (ft.$^2$) and V the wind speed in the working section (ft./sec.). The power factor is sometimes defined as the reciprocal of the quantity given by (1); but the form adopted here is in the nature of a drag coefficient, so that a low power factor corresponds to a low tunnel drag and, therefore, implies an efficient tunnel. It is, in fact, possible to obtain an estimate of the power factor and of the variation of power factor with wind speed by direct addition of the drags of the various internal surfaces of a tunnel at different Reynolds numbers; this has been done, for instance, by Wattendorf.[7,8]

For a new wind tunnel of conventional type, the power factor can usually be estimated with sufficient accuracy by comparison of the design with those of other similar tunnels for which the power factors are known. A return flow tunnel with a contraction ratio of about 4 and a closed working section for which A and V are respectively of the order of 100 ft.$^2$ and 200 ft./sec. will normally have a power factor in the neighbourhood of 0·25; power factors as low as 0·2 have been achieved in some tunnels which were designed to have the minimum possible internal drag. The provision of such features as a honeycomb and a settling length may raise the power factor to 0·3. If the tunnel has an open working section its power factor will usually lie between 0·35 and 0·45.

When the power factor of a new design has been assessed, equation (1) is used to obtain the wind speed resulting from a given power input, or the power input required to produce a given wind speed. It will be assumed in what follows that the power input P is fixed.

If the area of the fan disc is $A_0$ and the mean axial speed through the fan is $u$, then by continuity

$$A_0 u = AV, \quad \ldots \quad (2)$$

whence $u$ may be found. It should be remarked that in the evaluation of $A_0$, account should be taken of the area of the fan boss; for reasons given in § 4, the boss diameters of the fans of N.P.L. tunnels are usually 0·3 to 0·4 of the fan diameters.

Since uniformity of velocity in the working section is an essential in a wind tunnel, it is obviously advantageous to keep the axial speed across all sections as uniform as possible. In

# AERODYNAMIC SYMBOLS

## 1. GENERAL

| | |
|---|---|
| $m$ | Mass |
| $t$ | Time |
| V | Resultant linear velocity |
| $\Omega$ | Resultant angular velocity |
| $\rho$ | Density, $\sigma$ relative density |
| $\nu$ | Kinematic coefficient of viscosity |
| R | Reynolds number, $R = lV/\nu$ (where $l$ is a suitable linear dimension) |

Normal temperature and pressure for aeronautical work are 15° C and 760 mm.

For air under these conditions $\left\{\begin{array}{l}\rho = 0{\cdot}002378 \text{ slug/cu. ft.} \\ \nu = 1{\cdot}59 \times 10^{-4} \text{ sq. ft./sec.}\end{array}\right.$

The slug is taken to be 32·2 lb.-mass.

| | |
|---|---|
| $\alpha$ | Angle of incidence |
| $e$ | Angle of downwash |
| S | Area |
| $b$ | Span |
| $c$ | Chord |
| A | Aspect ratio, $A = b^2/S$ |
| L | Lift, with coefficient $C_L = L/\frac{1}{2}\rho V^2 S$ |
| D | Drag, with coefficient $C_D = D/\frac{1}{2}\rho V^2 S$ |
| $\gamma$ | Gliding angle, $\tan\gamma = D/L$ |
| L | Rolling moment, with coefficient $C_l = L/\frac{1}{2}\rho V^2 bS$ |
| M | Pitching moment, with coefficient $C_m = M/\frac{1}{2}\rho V^2 cS$ |
| N | Yawing moment, with coefficient $C_n = N/\frac{1}{2}\rho V^2 bS$ |

## 2. AIRSCREWS

| | |
|---|---|
| $n$ | Revolutions per second |
| D | Diameter |
| J | $V/nD$ |
| P | Power |
| T | Thrust, with coefficient $k_T = T/\rho n^2 D^4$ |
| Q | Torque, with coefficient $k_Q = Q/\rho n^2 D^5$ |
| $\eta$ | Efficiency, $\eta = TV/P = Jk_T/2\pi k_Q$ |

LIBRARY
UNIVERSITY OF ILLINOIS
URBANA

# The Design of Wind Tunnel Fans

*By*

A. R. Collar, B. A., B. Sc.,
of the Aerodynamics Department, N.P.L.

*Reports and Memoranda No.* 1889
10*th August,* 1940

*Summary.*—The present report is one of a series dealing with N.P.L. methods for the design of return flow wind tunnels. Reports already issued deal with the design of the Compressed Air Tunnel[1] and Open Jet Tunnels,[2] with the design of corner cascades[3] and fan straighteners,[4] and with the improvement of velocity distribution by means of windmills[5] and gauzes.[6]

An explanation is now given of the method usually adopted in the design of fans for return flow tunnels; as an example of the method, the design of the fan for the N.P.L. non-turbulent tunnel is considered in detail. It is shown that for a wind tunnel a fan with blades of constant chord is advisable; and a formula is given by means of which a rapid estimate can be made of the variation in rotational speed of the fan corresponding to a variation in power factor at constant power.

1. *Power Factor.*—The power factor $\lambda$ of a wind tunnel is defined by the equation

$$\tfrac{1}{2}\rho AV^3\lambda = P, \quad \ldots \quad (1)$$

where P is the power input (ft.lb./sec.), $\rho$ the air density (slug/ft.$^3$), A the area of the working section (ft.$^2$) and V the wind speed in the working section (ft./sec.). The power factor is sometimes defined as the reciprocal of the quantity given by (1); but the form adopted here is in the nature of a drag coefficient, so that a low power factor corresponds to a low tunnel drag and, therefore, implies an efficient tunnel. It is, in fact, possible to obtain an estimate of the power factor and of the variation of power factor with wind speed by direct addition of the drags of the various internal surfaces of a tunnel at different Reynolds numbers; this has been done, for instance, by Wattendorf.[7,8]

For a new wind tunnel of conventional type, the power factor can usually be estimated with sufficient accuracy by comparison of the design with those of other similar tunnels for which the power factors are known. A return flow tunnel with a contraction ratio of about 4 and a closed working section for which A and V are respectively of the order of 100 ft.$^2$ and 200 ft./sec. will normally have a power factor in the neighbourhood of 0·25; power factors as low as 0·2 have been achieved in some tunnels which were designed to have the minimum possible internal drag. The provision of such features as a honeycomb and a settling length may raise the power factor to 0·3. If the tunnel has an open working section its power factor will usually lie between 0·35 and 0·45.

When the power factor of a new design has been assessed, equation (1) is used to obtain the wind speed resulting from a given power input, or the power input required to produce a given wind speed. It will be assumed in what follows that the power input P is fixed.

If the area of the fan disc is $A_0$ and the mean axial speed through the fan is $u$, then by continuity

$$A_0 u = AV, \quad \ldots \quad (2)$$

whence $u$ may be found. It should be remarked that in the evaluation of $A_0$, account should be taken of the area of the fan boss; for reasons given in § 4, the boss diameters of the fans of N.P.L. tunnels are usually 0·3 to 0·4 of the fan diameters.

Since uniformity of velocity in the working section is an essential in a wind tunnel, it is obviously advantageous to keep the axial speed across all sections as uniform as possible. In

practice, the axial speed through the fan usually varies from point to point ; but the differences are not large, and in the absence of information on the distribution (as obtained for instance from experiments on a model of the tunnel) it is assumed to be constant in the design of the fan.

2. *Strip Theory Formulae.*—Corresponding values of $u$ and P for the tunnel are found as in § 1. To proceed to the fan design, the appropriate strip theory formulae are required. These are given in R. & M. 1293,[9] and may be written in the form

$$\frac{dT}{dr} = \tfrac{1}{2}\rho N c u^2 G \cot\phi, \quad \ldots\ldots\ldots\ldots\ldots\ldots\ldots\ldots \quad (3)$$

$$\frac{dQ}{dr} = \tfrac{1}{2}\rho N c u^2 H r \cot\phi, \quad \ldots\ldots\ldots\ldots\ldots\ldots\ldots\ldots \quad (4)$$

$$G = \frac{C_L}{\sin\phi} - \frac{C_D}{\cos\phi}, \quad \ldots\ldots\ldots\ldots\ldots\ldots\ldots\ldots \quad (5)$$

$$H = \frac{C_D}{\sin\phi} + \frac{C_L}{\cos\phi}, \quad \ldots\ldots\ldots\ldots\ldots\ldots\ldots\ldots \quad (6)$$

$$\tan\phi = \frac{u}{r\Omega(1-a_2)}, \quad \ldots\ldots\ldots\ldots\ldots\ldots\ldots\ldots \quad (7)$$

$$\frac{1}{1-a_2} = 1 + \frac{Nc}{8\pi r} H, \quad \ldots\ldots\ldots\ldots\ldots\ldots\ldots\ldots \quad (8)$$

$$\phi = \theta - \alpha, \quad \ldots\ldots\ldots\ldots\ldots\ldots\ldots\ldots \quad (9)$$

where $T$ = thrust,
$Q$ = torque,
$r$ = local radius,
$N$ = number of blades,
$c$ = local chord,
$C_L$ = local lift coefficient,
$C_D$ = local drag coefficient,
$\Omega$ = angular velocity of fan,
$a_2$ = rotational inflow factor,
$\theta$ = local blade angle,
$\alpha$ = local incidence.

The exact application of these formulae will be explained later. To make a preliminary fan design, the equations are simplified by omission of the drag coefficient (which is usually quite small) and of the rotational inflow factor. Moreover, since wind tunnel fans are seldom of high pitch, $u$ is small in comparison with $r\Omega$, and it is, therefore, possible to write

$$\tan\phi = \sin\phi = \phi = \frac{u}{r\Omega}, \quad \ldots\ldots\ldots\ldots\ldots\ldots\ldots\ldots \quad (10)$$

with $\cos\phi = 1$. Accordingly (3) and (4) reduce to

$$\frac{dT}{dr} = \tfrac{1}{2}\rho N c r^2 \Omega^2 C_L, \quad \ldots\ldots\ldots\ldots\ldots\ldots\ldots\ldots \quad (11)$$

$$\frac{dQ}{dr} = \tfrac{1}{2}\rho N c r^2 u \Omega C_L. \quad \ldots\ldots\ldots\ldots\ldots\ldots\ldots\ldots \quad (12)$$

It will be seen that, to the degree of approximation adopted, the torque power input $\Omega Q$ and the thrust power output $uT$ are equal. The formula (11) can evidently be written down at sight if it is assumed that the velocity of the blade element relative to the wind is the rotational velocity $r\Omega$. Actually, the rotational inflow factor decreases the velocity below $r\Omega$, while the axial velocity component increases it ; the corrections are usually of the same order of magnitude, so that (11) gives a sufficiently accurate representation of the thrust grading for preliminary design purposes.

3. *Preliminary Design Considerations.*—In order to maintain across the sections of the tunnel duct the constancy of total head which corresponds to uniformity of velocity in rectilinear flow, it is desirable that the pressure increment through the fan disc shall be constant, i.e., independent of radius. In practice it is sometimes found advantageous to increase the pressure slightly towards the outer radii, more particularly for open jet tunnels, since a considerable part of the energy loss in the tunnel takes place at the boundaries of the stream ; however, the departure from constancy is not great. If the pressure increment is $p$, then by (11)

$$p = \frac{1}{2\pi r}\frac{dT}{dr} = \frac{1}{4\pi}\ \rho N c r\ \Omega^2\ C_L,$$

or

$$\rho\ \Omega^2\ N c r C_L = 4\pi p. \qquad \ldots\ \ldots\ \ldots\ \ldots\ \ldots\ \ldots\ \ldots\ \ldots \quad (13)$$

If $p$ is to be independent of radius, it follows from (13) that $crC_L$ must be constant along the blades : a condition well-known in tunnel fan design. Also, to the present degree of approximation,

$$P = pA_0 u, \qquad \ldots\ \ldots\ \ldots\ \ldots\ \ldots\ \ldots\ \ldots\ \ldots \quad (14)$$

so that (13) becomes

$$\rho A_0 u\ \Omega^2\ N c r C_L = 4\pi P. \qquad \ldots\ \ldots\ \ldots\ \ldots\ \ldots\ \ldots\ \ldots\ \ldots \quad (15)$$

It remains to choose $\Omega$ and the local values of $Nc$ and $C_L$ to satisfy (15), in which the other quantities are known.

Now, for several reasons, it is usual to make $c$ constant along the blades. Thus, if the root chord is much smaller than the tip the stresses in the blade root may be too high ; moreover, a small root chord implies a lift coefficient which may be excessively high. On the other hand, if the root chord is large, blade root interference may appear. There is, however, a more important reason. Suppose the power factor achieved in a wind tunnel differs from the figure used in the fan design (the power factor will in any case vary slightly with wind speed) ; or alternatively, suppose that, by the addition of screens or a honeycomb, the power factor is materially altered from that applicable to the empty tunnel. This will be the case, for instance, in the non-turbulent tunnel at the N.P.L., in which the introduction of certain artificial turbulence screens may increase the power factor from 0·3 to 1·0 or even higher. Then the fan may, and in some cases certainly will, have to work under conditions different from those assumed in the design ; and the local lift coefficients will be different. If, for two conditions of working, the lift coefficients at radius $r$ are $C_L$ and $C_L + \delta C_L$, and if in both cases the pressure increment through the fan is constant, it follows from (13) that both $crC_L$ and $cr\delta C_L$ must be constant along the blades. Now for the linear portion of the lift curve it is possible to write

$$C_L = \frac{\partial C_L}{\partial \alpha}(\mu + \alpha), \qquad \ldots\ \ldots\ \ldots\ \ldots\ \ldots\ \ldots\ \ldots \quad (16)$$

where $-\mu$ is the no lift angle, and the slope of the lift curve is for all practical purposes the same at all radii. In view of (9) and (10), (16) becomes

$$C_L = \frac{\partial C_L}{\partial \alpha}\left(\mu + \theta - \frac{u}{r\Omega}\right), \qquad \ldots\ \ldots\ \ldots\ \ldots\ \ldots\ \ldots \quad (17)$$

and hence, for the second working condition,

$$\delta C_L = -\frac{1}{r}\frac{\partial C_L}{\partial \alpha}\delta\left(\frac{u}{\Omega}\right),$$

or

$$cr\delta C_L = -c\frac{\partial C_L}{\partial \alpha}\delta\left(\frac{u}{\Omega}\right) \ldots \qquad \ldots\ \ldots\ \ldots\ \ldots\ \ldots\ \ldots \quad (18)$$

Since $cr\delta C_L$ is to be independent of radius, it follows from (18) that $c$ must be constant along the blades.

Equation (15) may now be used to fix the values of $\Omega$ and N$c$. In the first place it is usual to choose $C_L = 0{\cdot}6$ at the tip radius $r = r_1$. A lower value of $C_L$ would lead to a fan of less efficiency; and it is an empirical fact (noted for instance in R. & M.1569[2]) that a value in excess of 0·7 is not usually attainable at the tip. In any case, the value chosen leads to sufficiently high values of $C_L$ at the root. Accordingly (13) gives

$$\Omega^2 \mathrm{N}c = \frac{4\pi \mathrm{P}}{0{\cdot}6\, r_1 \rho \mathrm{A}_0 u}. \qquad (19)$$

Either $\Omega$ or N$c$ may now be arbitrarily fixed, subject to the following limitations. If $\Omega$ is chosen too low, N$c$ will become large and blade root interference may result; moreover, the pitch of the fan will become high, while the motor design may present difficulties. On the other hand, if $\Omega$ is chosen to be large, the fan blades will be narrow even when N = 2, and the blade strength may be insufficient; in addition, the tip speed may be so high that noise and compressibility effects become serious. On the last account, it is usual to limit the tip speed to be not greater than half the speed of sound; and as a result of the other considerations, the permissible range of $\Omega$ is usually not great. When $\Omega$ has been fixed, N$c$ is given by (19). The number of blades N is to some extent arbitrary; it should not be too large, or the blades become unduly weak, while construction of the fan is complicated. For N.P.L. tunnels, N is usually chosen to be 2 or 4.

Since $c$ and $cr\mathrm{C_L}$ are constant along the blades, $r\mathrm{C_L}$ is constant and equal to the value at the tip. Again, since $r\mathrm{C_L}$ is constant, it follows from (17) that $r(\mu + \theta)$ is also constant along the blades.

4. *The Preliminary Design.*—So far, it has been shown how to determine preliminary values of $\Omega$, N, and $c$ for the fan. It has also been shown that $r\mathrm{C_L}$ is constant along the blades; hence, unless the boss diameter is fairly large, the blade roots will stall. For N.P.L. tunnels the fan boss diameter is usually chosen to lie between 0·3 and 0·4 of the fan diameter; efficient working of the root sections is thus obtained. Moreover, a boss of this size is generally large enough to allow the fan motor to be placed inside the boss fairing; the power unit is then very compact. The support of the boss fairing and motor on the fan straighteners is described in R. & M.1885.[4]

The blade sections used for N.P.L. fans are usually sections C, D, E and F of the family of airscrews, details of which are given in R. & M.829.[10] To suit the constant chord required for the present purpose, sections C, D and E have been slightly altered, while section F has relatively a much thinner trailing edge. The sections have flat undersurfaces, and are thus easy to construct. Details of the sections are given in Table 6 and Fig. 1. The lift and drag coefficients for infinite aspect ratio are given in Fig. 2 over a sufficiently wide range of incidence.

To complete the preliminary design, therefore, it is usual to take four equally spaced radii, the innermost just outside the boss and the outermost just inside the tip. The sections C, D, E, and F are assigned to these radii in the order of increasing radius. From the local value of $C_L$, the incidence $\alpha$ of the section is found from Fig. 2; and the blade angle is then given by (9) and (10) as

$$\theta = \alpha + \frac{u}{r\Omega}. \qquad (20)$$

5. *Strip Theory Calculations.*—A more accurate estimate of the performance of the preliminary design of fan found by the methods of § 4 is now obtained by the use of equations (3) to (9). To apply these equations a successive approximation process is used, which in practice converges very rapidly.

The values of $u$, $\Omega$, N, $c$ and $\theta$ obtained in the preliminary design are treated as fixed. The local Reynolds number R at which the blade sections operate is given approximately by $r\Omega c/\nu$, where $\nu$ is the kinematic viscosity; it is usually sufficiently accurate to take a mean value of R for the whole blade.

As a first approximation, put $C_D = 0$ and $\cos\phi = 1$ in equation (6), and use the local value of $C_L$ found in the preliminary design. The resulting first approximation $H = C_L$ is then used in (8) to find at each of the reference radii a first approximation to $1/(1 - a_2)$, which in turn is

used in (7) to give a first approximation to $\phi$. Equation (9) is next used to find $\alpha$, and thence, from the curves of Fig. 2, values of $C_L$ and $C_D$ at the appropriate Reynolds number are obtained. The values of $\phi$, $C_L$ and $C_D$ are then used in (6) to obtain a second approximation to H, which is inserted in (8) to obtain a second approximation to $1/(1 - a_2)$ ; and thence from (7) a second approximation to $\phi$ is found. The process of approximation is continued until $\phi$ repeats. In practice $\phi$ is computed to the nearest tenth of a degree, and usually it repeats to this order of accuracy after only two steps in the process of approximation.

When final values of $\phi$, $C_L$ and $C_D$ have been found, equations (5) and (6) are used to obtain values of H and G, which are inserted in equations (3) and (4) to give curves of thrust and torque grading. These curves are integrated graphically or by Simpson's rule to obtain the thrust and torque* ; and thence the torque power input, thrust power output, and fan efficiency are obtained.

There is generally a difference of anything up to about 6 per cent. between the power input $P_1$ obtained in this manner and the input P assumed in making the preliminary design ; there is therefore (since the axial speed is common to both methods) the same difference in power factor ; an error of this magnitude is usually within the limits of possible error in the estimation of the power factor. To reduce $P_1$ to P, both $u$ and $\Omega$ must be multiplied by $(P/P_1)^{1/3}$, which usually represents a change of only about 2 per cent. and is thus not serious. If, however, the error in the power factor is considered to be serious, the blade angles or chord of the fan may be altered (the approximate extent required is obvious from the calculations) and the strip theory calculations repeated.

Again, from the thrust grading, the distribution of the pressure increment $p$ with radius is found. If this is considered to be unsatisfactory, local alterations in blade angle can be made to improve it. The fan design is thus completed.

As a numerical example, the design of the fan for the N.P.L. non-turbulent tunnel is discussed in detail in § 8.

6. *General Remarks.*—In equation (20), two approximations are involved : the omission of the rotational inflow factor and the approximation $\tan \phi = \phi$. It so happens that for a blade of normal design the errors thus introduced, which are always of opposite sign, are of nearly equal magnitude, so that the value of $\phi$ given by $u/r\,\Omega$ is very nearly the same, for the whole length of the blade, as that obtained in the strip theory calculations.

It may be argued that the sections of the family of airscrews are not so efficient as other sections developed in recent years. However, the sections are quite good for the ranges of $C_L$ employed, and give tunnel fan efficiencies of the order of 90 per cent. ; since, in addition, the sections have such simple shapes, refinement seems hardly worth while.

A short explanation of the derivation of the curves of Fig. 2 may be given here. The lift and drag coefficients of the sections of the family of airscrews, corresponding to infinite aspect ratio, are tabulated in R. & M. 892[11] and R. & M. 1771[12] ; the first report relates to tests in an atmospheric tunnel, and the second to C.A.T. tests. The range of Reynolds number covered is from about $0{\cdot}1\times10^6$ to $6\times10^6$. The tests show that the scale effect on the lift coefficients in the working range (which for the most part is well below the stall) is not great. Accordingly, for design purposes it is sufficient to use the curves of Fig. 2 for values of R from about $0{\cdot}2\times10^6$ to $6\times10^6$. These curves are mean curves obtained from all the data of the two above reports ; but the incidences for section F have been changed by the addition of a constant factor to give the theoretical no-lift angle for the altered section used in the present report. This no-lift angle was found by means of Glauert's formula,[13] which gives sufficiently good agreement with the experimental no-lift angles of sections C, D and E.

The drag coefficient curves of Fig. 2 are also considered to be of ample accuracy for the purposes of tunnel fan design, though no great absolute accuracy can be attached to them. Examination of the experimental data for sections C, D and E showed that the drag coefficients corresponding to infinite aspect ratio decreased with increasing R in a manner which could be approximately represented by the equation

$$C_D + 0{\cdot}004 \log_{10} R = \text{constant}.$$

* For usual spacings of the sections, the formula given in Appendix II may be used to obtain the integrated values of thrust and torque.

Mean curves of variation of $C_D + 0{\cdot}004 \log_{10} (R \times 10^{-6})$ against $\alpha$, for the whole range of R covered by the experimental data, were therefore drawn ; these are the curves C, D and E of Fig. 2. The values of minimum drag coefficient thus obtained are only a little higher than those calculated by Squire and Young in R. & M. 1838[14] for modern aerofoil shapes with the transition point at the leading edge ; the rate of variation with $\log_{10}$ R in the neighbourhood of $R = 10^6$ is also in quite good agreement with the results of these writers. The curve shown in Fig. 2 for the modified section F used in the present report was estimated from the curves for the other sections, the difference being based on the results of R. & M. 1838.[14]

The stresses and deflections in the blades due to centrifugal force, thrust, and twisting moment are briefly discussed in Appendix I. A representative blade is examined ; and since the ratio of boss radius to tip radius, and the disposition of the sections along the blades, do not vary much in N.P.L. fans, the results for this representative blade can be used to obtain a rough estimate of the stresses and deflections to be expected in any other blade. If $\gamma$ is the density of the material of the blade and E is Young's modulus, it is shown that the maximum tensile stress, which occurs near the root, is given approximately by

$$\sigma_c + \sigma_b = 0{\cdot}25\,\gamma r_1^2\Omega^2 + 12{\cdot}5\,\rho r_1^2\Omega^2 (r_1/c)^2, \quad .. \quad .. \quad .. \quad .. \quad (21)$$

and that the extension due to centrifugal force and deflection due to thrust, measured at the tip, are respectively

$$e_c = 0{\cdot}11\,\gamma\,\Omega^2 r_1^3/E, \quad .. \quad .. \quad .. \quad .. \quad .. \quad .. \quad .. \quad (22)$$

$$e_b = 26\,\rho\Omega^2 r_1^3\,(r_1/c)^3/E. \quad .. \quad .. \quad .. \quad .. \quad .. \quad .. \quad .. \quad (23)$$

A rough estimate of the critical flutter speed of the blades of a new fan can be made on the basis of formulae given in R. & M. 1518,[15] which discusses the flutter of solid cylindrical blades in a uniform airstream.

7. *Variation of Rotational Speed with Power Factor.*—If the power input P is fixed, equations (1) and (2) show that $\lambda V^3$ and $\lambda u^3$ are constant. The variations in axial speed corresponding to small variations in $\lambda$ are thus not great. The speed obtained for a given power in a new wind tunnel is for this reason usually quite close to the anticipated figure. The rotational speed of the fan is usually also very close to the design figure, though the reason for this is not so immediately obvious.

The calculation of the variation of $\Omega$ with $\lambda$ by the exact strip theory equations is best effected indirectly. Any reasonable relative values of $u$ and $\Omega$ are assumed, and by the methods of § 5, the corresponding power input $P_1$ is calculated. The values of $u$ and $\Omega$ are then multiplied by $(P/P_1)^{1/3}$ to bring the power input to the fixed value P ; corresponding values of $\Omega$ and $\lambda$ are thus obtained. The calculations are repeated for other values of $u$ and $\Omega$, and a curve of variation of $\Omega$ with $\lambda$ can then be drawn.

For most practical purposes, however, it is sufficiently accurate, besides being simpler and more instructive, to use a formula derived from the approximate equations of § 3. Substitution from (17) in (15) for $C_L$ gives

$$\rho A_0 u \Omega^2 Nc \frac{\partial C_L}{\partial \alpha} \left\{ r(\mu + \theta) - \frac{u}{\Omega} \right\} = 4\pi P,$$

and substitution from (1) and (2) for $u$ in terms of P then yields a quadratic for $\Omega$ of which the solution is

$$\Omega = K_1 \lambda^{-1/3} \left\{ 1 + \sqrt{1 + K_2 \lambda} \right\}, \quad .. \quad .. \quad .. \quad .. \quad .. \quad (24)$$

where

$$K_1 = \frac{1}{2} \left( \frac{2P}{\rho A} \right)^{1/3} \frac{A}{A_0 r(\mu + \theta)},$$

$$K_2 = \frac{8\pi}{Nc} \frac{\partial \alpha}{\partial C_L} \left( \frac{A_0}{A} \right)^2 r(\mu + \theta).$$

The quantities $K_1$ and $K_2$ are constants since, as shown above, $c$ and $r(\mu + \theta)$ are constant along the blades. As $\lambda$ increases, the first factor in the expression (24) for $\Omega$ decreases while the second increases ; for the practical range of $\lambda$ the resulting variation in $\Omega$ is usually quite small.

By differentiation of (24), a very simple expression results which can be used directly to obtain the small variation $\delta\Omega$ corresponding to a small variation $\delta\lambda$. The equation obtained, after a little reduction, is

$$\frac{d\Omega}{d\lambda} = \frac{\Omega}{3\lambda}\left[\frac{\Omega r(\mu+\theta) - 2u}{2\Omega r(\mu+\theta) - u}\right]. \quad .. \quad .. \quad .. \quad .. \quad .. \quad (25)$$

Numerical examples of equations (24) and (25) are given in § 8.

8. *The Design of the Fan for the N.P.L. Non-Turbulent Tunnel.*—As an illustration of the methods described above, details will now be given of the fan design for the N.P.L. non-turbulent tunnel. The tunnel has a working section in the shape of a regular 16-sided polygon, the diameter of the inscribed circle being 7 ft. Accordingly,

$$A = 39{\cdot}0 \text{ ft.}^2 \quad .. \quad .. \quad .. \quad .. \quad .. \quad .. \quad .. \quad .. \quad (26)$$

The tunnel is unusually long ; the working section has a length of 45 ft. There follows a short expansion leading to the fan section ; there is then a long expanding cone, the diameter reached being 20 ft. A fine mesh honeycomb and a settling chamber about 30 ft. long are provided. The contraction ratio is about 8. Since the tunnel has so many unusual features, the estimate of power factor is comparatively rough. For the empty tunnel it may be as low as 0·3. When artificial turbulence screens are introduced, however, it is anticipated that the power factor may rise to 1·0 or even higher ; the fan will therefore have to work under widely varying conditions. It must evidently be designed to be unstalled at the highest power factor, and will then be further from the stall for the less resistant conditions.

The fan diameter is 8·5 ft., and the boss diameter 3·0 ft. ; a motor of 100 H.P. is installed in the boss fairing. Accordingly

$$A_0 = 49{\cdot}65 \text{ ft.}^2 \quad .. \quad .. \quad .. \quad .. \quad .. \quad .. \quad .. \quad .. \quad (27)$$

$$P = 5{\cdot}5 \times 10^4 \text{ ft. lb./sec.} \quad .. \quad .. \quad .. \quad .. \quad .. \quad .. \quad (28)$$

For a power factor of $\lambda = 1$, therefore, equations (1) and (2) give, with $\rho = 23{\cdot}8 \times 10^{-4}$ slug/ft.$^3$,

$$V = 105{\cdot}8 \text{ ft./sec.} \quad .. \quad .. \quad .. \quad .. \quad .. \quad .. \quad .. \quad (29)$$

$$u = 83{\cdot}1 \text{ ft./sec.} \quad .. \quad .. \quad .. \quad .. \quad .. \quad .. \quad .. \quad (30)$$

Hence from (19), since $r_1 = 4{\cdot}25$ ft.,

$$Nc\Omega^2 = 2{\cdot}76 \times 10^4 \text{ ft./sec.}^2 \quad .. \quad .. \quad .. \quad .. \quad .. \quad .. \quad (31)$$

It was decided that a rotational speed of about 1,000 r.p.m., giving a value of $\Omega$ just in excess of 100 rad./sec. and a fan tip speed of about 450 ft./sec., would be suitable. Hence the following figure was chosen

$$Nc = 2{\cdot}5 \text{ ft.}, \quad .. \quad .. \quad .. \quad .. \quad .. \quad .. \quad .. \quad .. \quad (32)$$

and therefore

$$\Omega = 105{\cdot}1 \text{ rad./sec.} \quad .. \quad .. \quad .. \quad .. \quad .. \quad .. \quad .. \quad (33)$$

The reference radii were chosen to be 1·75, 2·5, 3·25, and 4·0 ft., and the sections C, D, E and F were assigned to these radii, respectively. The lift coefficient at radius $r$ is given by

$$rC_L = 2{\cdot}55. \quad .. \quad .. \quad .. \quad .. \quad .. \quad .. \quad .. \quad .. \quad (34)$$

From the lift coefficient the local incidence $\alpha$ is found from the curves of Fig. 2 ; the blade angle is then given by (20), in which $u$ and $\Omega$ have the values given by (30) and (33). The results are summarised in Table 1.

TABLE 1

| $r$ (ft.) | Section | $C_L$ | $\alpha$ (deg.) | $\frac{u}{r\Omega}$ (rad.) | $\frac{u}{r\Omega}$ (deg.) | $\theta$ (deg.) |
|---|---|---|---|---|---|---|
| 1·75 | C | 1·458 | 10·0 | 0·452 | 25·9 | 35·9 |
| 2·5 | D | 1·020 | 4·8 | 0·316 | 18·1 | 22·9 |
| 3·25 | E | 0·785 | 3·2 | 0·243 | 13·9 | 17·1 |
| 4·0 | F | 0·638 | 2·6 | 0·198 | 11·3 | 13·9 |

The above is an illustration of the usual method for the preliminary design of a fan. In the case of the non-turbulent tunnel, however, the blade angles given by Table 1 were not finally adopted, since in view of the very long and narrow working section it was thought that the total head losses near the walls would be considerable. Accordingly, instead of keeping the pressure increment $p$ constant, it was decided to increase it linearly with radius. For constant chord, (13) shows that $rC_L$ must then increase linearly with radius also. The relation adopted was

$$rC_L = 1{\cdot}64 + 0{\cdot}28\,r, \quad \ldots \quad \ldots \quad \ldots \quad \ldots \quad \ldots \quad \ldots \quad \ldots \quad (35)$$

so that at section F, $p$ is roughly 30 per cent. greater than at section C. With the expression (35) for $rC_L$ and the values of $u$, $\Omega$, and $Nc$ given by (30), (33), and (32), the integral of the thrust power output found from (11) is 98·6 H.P., which is sufficiently accurate for the preliminary design.

The blade angles were, therefore, determined as in Table 2.

TABLE 2

| $r$ (ft.) | Section | $C_L$ | $\alpha$ (deg.) | $\phi$ (deg.) | $\theta$ (deg.) |
|---|---|---|---|---|---|
| 1·75 | C | 1·215 | 6·2 | 25·9 | 32·1 |
| 2·5 | D | 0·935 | 3·9 | 18·1 | 22·0 |
| 3·25 | E | 0·785 | 3·2 | 13·9 | 17·1 |
| 4·0 | F | 0·690 | 3·1 | 11·3 | 14·4 |

The preliminary design was then chosen to be a 2-bladed fan, of constant chord 15 in., and having the sections and blade angles given by Table 2.

A computation of the performance of this fan by the exact strip theory equations will now be carried out exactly as in § 3. A mean Reynolds number for the blades is $R = 3\times10^6$ approximately; accordingly the curves of Fig. 2 represent $C_D + 0{\cdot}0019$. Details of the process of successive approximation to $\phi$ are given in Table 3. It will be seen that, except for the innermost radius, the second approximation to $\phi$ repeats the first; and only one step further is required for the radius $r = 1{\cdot}75$ ft. It will be noticed that the final values of $\phi$ obtained in Table 3 are practically identical with those given in Table 2, which are found from the approximate equation (10) (see remarks in § 6).

The final values of $\phi$, $C_L$ and $C_D$ are used in Table 4 to obtain values of thrust and torque grading from equations (3) to (6). The pressure increment through the fan is

$$p = \frac{1}{4\pi}\,\rho N c u^2 \left(\frac{G\cot\phi}{r}\right), \quad \ldots \quad \ldots \quad \ldots \quad \ldots \quad \ldots \quad (36)$$

and from the last column of Table 4 it will be seen that $p$ increases steadily towards the outer radii. Integration of (3) and (4) using the values of $Hr\cot\phi$ and $G\cot\phi$ contained in Table 4 gives the torque power input and thrust power output respectively as

$$\Omega Q = 56{,}600 \text{ ft. lb./sec.} \quad \ldots \quad \ldots \quad \ldots \quad \ldots \quad \ldots \quad \ldots \quad (37)$$

$$= 102{\cdot}9 \text{ H.P.}$$

$$uT = 51{,}700 \text{ ft. lb./sec.} \quad \ldots \quad \ldots \quad \ldots \quad \ldots \quad \ldots \quad \ldots \quad (38)$$

The ratio of (38) to (37) gives the fan efficiency as

$$\eta = 0{\cdot}914. \quad .. \quad .. \quad .. \quad .. \quad .. \quad .. \quad .. \quad .. \quad (39)$$

TABLE 3

| $r$ | Section | $\theta$ | $\frac{Nc}{8\pi r}$ | $\frac{u}{r\Omega}$ | $C_L$ | $\frac{1}{1-a_2}$ | $\tan\phi$ | $\phi$ |
|---|---|---|---|---|---|---|---|---|
| 1·75 | C | 32·1 | 0·0569 | 0·452 | 1·215 | 1·069 | 0·483 | 25·8 |
| 2·5 | D | 22·0 | 0·0398 | 0·316 | 0·935 | 1·037 | 0·328 | 18·2 |
| 3·25 | E | 17·1 | 0·0306 | 0·243 | 0·785 | 1·024 | 0·249 | 14·0 |
| 4·0 | F | 14·4 | 0·0249 | 0·198 | 0·690 | 1·017 | 0·201 | 11·4 |

| $\sin\phi$ | $\cos\phi$ | $\alpha$ | $C_L$ | $C_D$ | H | $\frac{1}{1-a_2}$ | $\tan\phi$ | $\phi$ |
|---|---|---|---|---|---|---|---|---|
| 0·435 | 0·900 | 6·3 | 1·218 | 0·0196 | 1·398 | 1·079 | 0·487 | 26·0 |
| 0·312 | 0·950 | 3·8 | 0·925 | 0·0130 | 1·015 | 1·040 | 0·328 | 18·2 |
| 0·242 | 0·970 | 3·1 | 0·771 | 0·0108 | 0·840 | 1·026 | 0·249 | 14·0 |
| 0·198 | 0·980 | 3·0 | 0·682 | 0·0098 | 0·746 | 1·019 | 0·202 | 11·4 |

| $\sin\phi$ | $\cos\phi$ | $\alpha$ | $C_L$ | $C_D$ | H | $\frac{1}{1-a_2}$ | $\tan\phi$ | $\phi$ |
|---|---|---|---|---|---|---|---|---|
| 0·438 | 0·899 | 6·1 | 1·202 | 0·0192 | 1·381 | 1·079 | 0·487 | 26·0 |
| — | — | — | — | — | — | — | — | — |
| — | — | — | — | — | — | — | — | — |
| — | — | — | — | — | — | — | — | — |

TABLE 4

| $r$ | H | G | $Hr\cot\phi$ | $G\cot\phi$ | $\frac{G\cot\phi}{r}$ |
|---|---|---|---|---|---|
| 1·75 | 1·381 | 2·725 | 4·97 | 5·59 | 3·20 |
| 2·5 | 1·015 | 2·950 | 7·73 | 8·99 | 3·60 |
| 3·25 | 0·840 | 3·175 | 10·97 | 12·78 | 3·94 |
| 4·0 | 0·746 | 3·435 | 14·78 | 17·02 | 4·26 |

The value of V given by (29) was calculated on the assumption that $\lambda = 1$ and P = 100 H.P. Since the power is 102·9 H.P. it follows that $\lambda = 1{\cdot}029$. To reduce the power to 100 H.P., the speeds must all be divided by $\sqrt[3]{1{\cdot}029}$. The resulting value of $\Omega$ is

$$\Omega = 104{\cdot}1 \text{ rad./sec.}, \quad .. \quad .. \quad .. \quad .. \quad .. \quad .. \quad .. \quad (40)$$

the rotational speed being 995 r.p.m.

Calculations have also been made for this fan for conditions giving power factors of $\lambda = 0{\cdot}70$ and $\lambda = 0{\cdot}33$. The fan was considered to give a satisfactory performance throughout the probable range of operation ; accordingly, no alteration was made in the preliminary design.

The values of $\Omega$ corresponding to an input of 100 H.P. at the three power factors 1·03, 0·70 and 0·33 are plotted in Fig. 3 as isolated points. It will be seen that the variation in $\Omega$ is quite small. In Fig. 3 the approximate curve of $\Omega$ against $\lambda$ given by equation (24) is also drawn. To determine this curve, values of the slope of the lift curve and of $r(\mu + \theta)$ were required. In view of the altered distribution of $p$, $r(\mu + \theta)$ is not now independent of radius ; the variation is, however, slight, and an arithmetical mean

$$r(\mu + \theta) = 1{\cdot}213 \quad .. \quad .. \quad .. \quad .. \quad .. \quad .. \quad .. \quad .. \quad (41)$$

was obtained from Table 5, which also gives values of the slope of the lift curve, estimated from the incidence range $0 - 5°$. The mean value was taken to be

$$\frac{\partial C_L}{\partial \alpha} = 5{\cdot}60. \quad .. \quad .. \quad .. \quad .. \quad .. \quad .. \quad .. \quad .. \quad (42)$$

Equation (24) now becomes

$$\Omega = 34{\cdot}3\lambda^{-1/3}\left\{1 + \sqrt{1 + 3{\cdot}52\,\lambda}\right\}, \quad .. \quad .. \quad .. \quad .. \quad (43)$$

which is the curve of Fig. 3. The agreement between this curve and the three isolated points found from the exact strip theory equations is quite good.

TABLE 5

| $r$ | Section | $\mu$ (deg.) | $\theta$ (deg.) | $\mu+\theta$ (rad.) | $r(\mu+\theta)$ | $\partial C_L/\partial\alpha$ |
|---|---|---|---|---|---|---|
| 1·75 | C | 6·7 | 32·1 | 0·677 | 1·184 | 5·16 |
| 2·5 | D | 5·5 | 22·0 | 0·480 | 1·200 | 5·56 |
| 3·25 | E | 4·5 | 17·1 | 0·377 | 1·225 | 5·73 |
| 4·0 | F | 3·7 | 14·4 | 0·316 | 1·265 | 5·96 |

For comparison, Fig. 3 gives also the curve of variation of $u$ with $\lambda$. It is

$$u = 83{\cdot}1\,\lambda^{-1/3}, \quad .. \quad .. \quad .. \quad .. \quad .. \quad .. \quad .. \quad (44)$$

and it will be seen that the variation in $u$ is much greater than the variation in $\Omega$.

Through each of the three isolated points in Fig. 3 is drawn a short straight line having a slope given by (25). It is apparent that (25) gives a very good estimate of the rate of variation of $\Omega$ with $\lambda$. Fig. 3 shows that, for the extreme conditions of working of the non-turbulent tunnel, the variation in rotational speed of the fan for a power input of 100 H.P. is only from about 975 r.p.m. to 1,125 r.p.m.

The stresses in the fan may be estimated on the basis of the representative fan discussed in Appendix I, for which the stresses and deflections are given by equations (21), (22) and (23). For the fan discussed in the present paragraph

$$r_1/c = 3{\cdot}40, \quad .. \quad .. \quad .. \quad .. \quad .. \quad .. \quad .. \quad .. \quad (45)$$

while the maximum value of $\Omega$ will be about 120 rad./sec. (see Fig. 3) so that

$$\Omega r_1 = 510 \text{ ft./sec.} \quad .. \quad .. \quad .. \quad .. \quad .. \quad .. \quad .. \quad (46)$$

It was decided that the fan should be made of spruce, for which the density $\gamma$ and Young's modulus E are approximately

$$\gamma = 1{\cdot}0 \text{ slug/ft.}^3, \quad .. \quad .. \quad .. \quad .. \quad .. \quad .. \quad .. \quad (47)$$

$$E = 2{\cdot}4 \times 10^8 \text{ lb./ft.}^2 \quad .. \quad .. \quad .. \quad .. \quad .. \quad .. \quad (48)$$

Accordingly, equation (21) gives the maximum tensile stress as

$$\begin{aligned}\sigma_c + \sigma_b &= 6{\cdot}5 \times 10^4 + 8{\cdot}9 \times 10^4 \\ &= 15{\cdot}4 \times 10^4 \text{ lb./ft.}^2, \quad .. \quad .. \quad .. \quad .. \quad .. \quad .. \quad (49)\end{aligned}$$

which is about one-fifth of the elastic limit of spruce.

The extension due to the centrifugal force becomes

$$\begin{aligned}e_c &= 5{\cdot}1 \times 10^{-4} \text{ ft.} \\ &= 0{\cdot}006 \text{ in.}, \quad .. \quad .. \quad .. \quad .. \quad .. \quad .. \quad .. \quad .. \quad (50)\end{aligned}$$

approximately. Similarly, the tip deflection due to thrust is roughly

$$\begin{aligned}e_b &= 112 \times 10^{-4} \text{ ft.} \\ &= 0{\cdot}13 \text{ in.} \quad .. \quad .. \quad .. \quad .. \quad .. \quad .. \quad .. \quad .. \quad (51)\end{aligned}$$

## APPENDIX I

9. *Stresses and Deflections in the Blades of a Representative Fan.*—The stresses and strains occurring in an airscrew are discussed in some detail in R. & M.1274.[16] The main stresses may be classified under the following heads :—

(*a*) Tensile stress due to centrifugal force.
(*b*) Tensile and compressive stress resulting from the bending moment due to thrust.
(*c*) Shear stress due to thrust.
(*d*) Shear stress resulting from the untwisting effect of the centrifugal pull.
(*e*) Shear stress due to the twisting moment of the centrifugal forces.
(*f*) Shear stress due to aerodynamical twisting moment.

If the blades have any " hang-forward " or " hang-back " there will be a contribution to the bending moment from the centrifugal forces ; in the present discussion it will be assumed that the blade sections are so disposed that there is no such contribution.

The forces occurring in the blades of a fan obviously increase toward the root ; the thickness of the fan blades discussed in the present paper has been chosen to increase toward the root to minimise the resultant stresses. Consider a representative fan blade and regard it as being encastré at the root radius

$$r0 = 0{\cdot}4r_1, \qquad (52)$$

where $r_1$ is the tip radius ; and write

$$r = xr_1, \qquad (53)$$

where $r$ is the current radius. If in the representative fan, sections C, D, E and F are assigned to the points $x = 0{\cdot}475$, $0{\cdot}625$, $0{\cdot}775$ and $0{\cdot}925$ respectively, then to a close degree of approximation

$$\frac{t}{c} = \frac{0{\cdot}08}{x}, \qquad (54)$$

where $t$ is the maximum thickness of the section. Moreover, the sections are derivable from each other by orthogonal projection ; and the area of cross-section and moment of inertia about the neutral axis parallel to the chord are respectively

$$a = 0{\cdot}745ct,$$
$$\mathrm{I} = 0{\cdot}05ct^3,$$

which in view of (54) become

$$a = 59{\cdot}6 \times 10^{-3}\, c^2x^{-1}, \qquad (55)$$

$$\mathrm{I} = 25{\cdot}6 \times 10^{-6}\, c^4x^{-3}. \qquad (56)$$

The material of the blade will be assumed to be isotropic and of density $\gamma$. A caution should be added here that all densities must be expressed in the proper units ; if the unit of force is one pound weight and the unit of length one foot, then the density must be expressed in slugs/ft.$^3$ ; if, however, the inch is chosen as the unit of length, the unit of mass becomes 12 slugs, and the density must be expressed as the number of these units per cubic foot.

The centrifugal force on a slice of the blade of thickness $r_1dx$ is $\gamma ar_1^2\Omega^2xdx$ ; hence, in view of (55), the total tension at any radius $x$ is

$$\gamma r_1^2\Omega^2 \int_x^1 axdx = 59{\cdot}6 \times 10^{-3}\, c^2\gamma r_1^2\Omega^2(1 - x), \qquad (57)$$

and the stress, i.e., the tension per unit area, is therefore

$$\sigma_c = \gamma r_1^2\Omega^2x(1 - x). \qquad (58)$$

The maximum value of this stress occurs when $x = 0{\cdot}5$ and is of magnitude

$$\sigma_c = 0{\cdot}25\gamma r_1^2\Omega^2. \quad .. \quad .. \quad .. \quad .. \quad .. \quad .. \quad .. \quad (59)$$

The variation in the stress over the inner third of the blade is very slight; for the range $x = 0{\cdot}4$ to $x = 0{\cdot}6$ it can be assumed that the stress is given by (59).

If $e_c$ is the extension of the blade due to the centrifugal forces, then

$$\frac{1}{r_1}\frac{de_c}{dx} = \frac{\sigma_c}{E},$$

where E is Young's modulus for the material of the blade, and $\sigma_c$ is given by (58). The integral of this equation over the whole of the blade gives approximately

$$e_c = 0{\cdot}11\ \gamma r_1^3\Omega^2/E. \quad .. \quad .. \quad .. \quad .. \quad .. \quad .. \quad .. \quad (60)$$

In the determination of the bending stresses due to the thrust the assumption will be made that the blade angles are small and that the thrust is normal to the chord. The stresses are then probably not smaller than those occurring in an actual twisted blade.

Equation (11) gives the approximate value of the element of thrust at $x = \xi$ on each blade as

$$dT = \tfrac{1}{2}\rho c r_1^3\Omega^2 C_L\xi^2 d\xi, \quad .. \quad .. \quad .. \quad .. \quad .. \quad .. \quad .. \quad (61)$$

and the total bending moment at the point $x$, due to the elements of thrust external to $x$, is therefore

$$M = \tfrac{1}{2}\rho c r_1^4\Omega^2 \int_x^1 C_L\xi^2(\xi - x)d\xi. \quad .. \quad .. \quad .. \quad .. \quad .. \quad (62)$$

Now since $rC_L$ is constant along the blade, and $C_L = 0{\cdot}6$ at the tip, $C_L\xi = 0{\cdot}6$; hence (62) reduces to

$$M = 0{\cdot}05\ \rho\, c r_1^4\,\Omega^2\,(1 - x)^2\,(2 + x). \quad .. \quad .. \quad .. \quad .. \quad .. \quad (63)$$

Moreover, the neutral axis of the section is very approximately at $0{\cdot}5\,t$ from the chord; hence the maximum stress at the section is

$$\sigma_b = 0{\cdot}5\,tM/I,$$

which on substitution from (54), (56) and (63) gives

$$\sigma_b = 78{\cdot}1\ \rho\, r_1^2\Omega^2\left(\frac{r_1}{c}\right)^2 x^2\,(1 - x)^2\,(2 + x). \quad .. \quad .. \quad .. \quad (64)$$

This is itself a maximum for $x = 0{\cdot}525$; as for the case of the centrifugal stress, however, its value is practically constant over the inner third of the blade, and is of magnitude, approximately

$$\sigma_b = 12{\cdot}5\ \rho r_1^2\Omega^2\,(r_1/c)^2. \quad .. \quad .. \quad .. \quad .. \quad .. \quad .. \quad (65)$$

If $e_b$ is the total deflection of the blade tip due to bending, then

$$\frac{1}{r_1}\frac{de_b}{dx} = \frac{Mr_1\,(1 - x)}{EI},$$

which on substitution from (56) and (63) gives approximately

$$e_b = 26\ \frac{\rho\, r_1^2\Omega^2}{E}\left(\frac{r_1}{c}\right)^2. \quad .. \quad .. \quad .. \quad .. \quad .. \quad .. \quad .. \quad (66)$$

The stress given by (65) is tensile on the flat face of the blade and compressive on the curved face. Actually, the maximum compressive stress is probably a little greater than the maximum tensile stress, since the neutral axis is, in fact, rather nearer the flat face than is assumed above. However, the centrifugal tensile stress has to be added to the bending stress ; since the maximum stresses due to both causes occur over the inner third of the blade, it is sufficient in practice to say that the maximum stress is tensile and of magnitude

$$\sigma_c + \sigma_b = 0{\cdot}25\,\gamma r_1^2\Omega^2 + 12{\cdot}5\,\rho r_1^2\Omega^2\,(r_1/c)^2. \qquad (67)$$

In a similar manner it is readily shown that the shear stress due to the thrust is

$$\sigma_s = 0{\cdot}97\,\rho r_1^2\Omega^2\,(r_1/c), \qquad (68)$$

and the deflection due to shear is

$$e_s = 0{\cdot}45\,\frac{\rho r_1^3\Omega^2}{\mu}\left(\frac{r_1}{c}\right), \qquad (69)$$

where $\mu$ is the modulus of rigidity. As is usual for a loaded cantilever of slender form, however, these shearing actions are small in comparison with the bending actions.

As regards the torsional actions classified above under the headings (*d*) and (*e*), these involve the blade angle and rate of twist, and cannot profitably be discussed for the representative blade. They can be evaluated by the methods described in R. & M. 1274.[16] It may be remarked, however, that the twisting moments due to these two causes are of opposite sense : the direct centrifugal pull tends to untwist the blade, i.e., to increase the blade angles, while for normal blade angles the moment of the centrifugal forces tends to throw the blade sections into the plane of rotation, and thus to decrease the blade angles. For fans with relatively low tip speeds, such as are discussed in the present paper, the resultant moment is probably not great.

Finally, the aerodynamical twisting moment is in practice negligibly small. Values of the aerodynamical pitching moment coefficient for the sections of the family of airscrews, measured about the quarter-chord position, are given in R. & M. 1771.[12] For each section, the moment is almost independent of the value of $C_L$ ; it follows that the lift force acts at the quarter-chord point. These pitching moment coefficients are, as might be expected, very nearly proportional to the thickness-chord ratio of the section, and for the representative blade, they can in view of (54) be taken to be given by $-\,0{\cdot}05x^{-1}$. Now the centre of twist of the sections, estimated from the formulae of R. & M. 1444,[17] is at $0{\cdot}34\,c$ from the leading edge. Hence the total pitching moment coefficient, measured about this axis of twist, is for the section at radius $r_1 x$

$$C_m = C_L\,(0{\cdot}34 - 0{\cdot}25) - 0{\cdot}05x^{-1}.$$

But $xC_L$ has the constant value $0{\cdot}6$ along the blade ; hence

$$\begin{aligned} C_m &= 0{\cdot}054x^{-1} - 0{\cdot}05x^{-1} \\ &= 0{\cdot}004x^{-1}. \end{aligned} \qquad (70)$$

No accuracy can be attached to the numerical coefficient in (70) ; it can only be said that it is of this order. It is, however, so small that the resultant torsional moments are negligibly small. On the basis of equation (70), a blade of chord $c = 1$ ft., tip radius $r_1 = 5$ ft., and having a tip speed of 500 ft./sec., will be subjected to a total aerodynamical twisting moment, measured at the root, of only about $2{\cdot}5$ lb. ft.

To sum up, it may be said that in practice equations (66) and (67) provide useful criteria for the strength of a fan blade of the type discussed in the present paper. If the deflection given by (66) is unimportant and the stress given by (67) is well within the elastic limit of the material, then in practice the blade is of adequate strength.

## APPENDIX II

10. *A Formula for the Integration of the Thrust and Torque Grading Curves.*—The thrust and torque grading are each defined by four points, one at each reference section. In drawing a smooth curve through four typical points, and integrating graphically or by Simpson's rule from root to tip, an error of the order of $\pm 0{\cdot}5$ per cent. may be introduced; thus the error in efficiency may be $\pm$ 1 per cent. This error may be reduced by determining, for both thrust and torque grading, the cubic curve which passes through the four given points, and by analytical integration of this curve. When, as is nearly always the case, the distance from the root to section C is the same as the distance from section F to the tip, and when there is equal spacing $s$ between the four reference sections, the integral of the cubic curve is given by equation (71), which is an extension of Simpson's three-eighths rule. If the given ordinates are $y_1$, $y_2$, $y_3$ and $y_4$, and if the blade length $r_1 - r_0$ is $l$, then

$$\int_{r_0}^{r_1} y\,dr = \frac{l}{48}\left\{\left(\frac{l^2}{s^2} - 3\right)(y_1 + y_4) + \left(27 - \frac{l^2}{s^2}\right)(y_2 + y_3)\right\} \quad \ldots \quad (71)$$

---

## TABLE 6

*Details of Airscrew Blade Sections*

$\eta$ = fraction of chord from leading edge.
$R_l$ = leading edge radius.
$R_t$ = trailing edge radius.

| $\eta$ | Ordinate, as fraction of chord | | | |
|---|---|---|---|---|
| | C | D | E | F |
| 0 | 0·0212 | 0·0163 | 0·0130 | 0·0108.. |
| 0·05 | 0·1000 | 0·0768 | 0·0613 | 0·0512 |
| 0·1 | 0·1326 | 0·1018 | 0·0813 | 0·0679 |
| 0·2 | 0·1611 | 0·1237 | 0·0988 | 0·0825 |
| 0·3 | 0·1680 | 0·1290 | 0·1030 | 0·0860 |
| 0·4 | 0·1660 | 0·1275 | 0·1018 | 0·0850 |
| 0·5 | 0·1591 | 0·1222 | 0·0975 | 0·0814 |
| 0·6 | 0·1460 | 0·1121 | 0·0895 | 0·0747 |
| 0·7 | 0·1253 | 0·0962 | 0·0768 | 0·0642 |
| 0·8 | 0·0968 | 0·0743 | 0·0593 | 0·0495 |
| 0·9 | 0·0627 | 0·0481 | 0·0384 | 0·0321 |
| 1·0 | 0·0124 | 0·0095 | 0·0076 | 0·0064 |
| $R_l$ | 0·0212 | 0·0163 | 0·0130 | 0·0108 |
| $R_t$ | 0·0124 | 0·0095 | 0·0076 | 0·0064 |

## LIST OF REFERENCES


| *No.* | *Author.* | *Title.* |
|---|---|---|
| 1 | R. Jones and A. H. Bell .. .. | Experiments on Models of a Compressed Air Wind Tunnel. R. & M. 1355. |
| 2 | A. R. Collar .. .. .. .. | The N.P.L. Open Jet Wind Tunnel. R. & M. 1569. |
| 3 | A. R. Collar .. .. .. .. | Some Experiments with Cascades of Aerofoils. R. & M. 1768. |
| 4 | A. R. Collar .. .. .. .. | Cascade Theory and the Design of Fan Straighteners. R. & M. 1885. |
| 5 | A. R. Collar .. .. .. .. | The Use of a Freely Rotating Windmill to improve the Flow in a Wind Tunnel. R. & M. 1866. |
| 6 | A. R. Collar .. .. .. .. | The Effect of a Gauze on the Velocity Distribution in a Uniform Duct. R. & M. 1867. |
| 7 | F. L. Wattendorf .. .. .. | The Efficiency of Return Flow Wind Tunnels. Sci. Rep. Tsing Hua Univ., Ser. A, Vol. III. |
| 8 | F. L. Wattendorf, K. L. Feng and C. C. Chang. | The Energy Ratio of the Tsing Hua Wind Tunnel. Sci. Rep. Tsing Hua Univ., Ser. A, Vol. III. |
| 9 | C. N. H. Lock and A. R. Collar .. | Exploration of the Flow near the Screw Proposed for the N.P.L. Compressed Air Tunnel. R. & M. 1293. |
| 10 | A. Fage, C. N. H. Lock, R. G. Howard and H. Bateman. | Experiments with a Family of Airscrews, including the Effect of Tractor and Pusher Bodies. Part I. R. & M. 829. |
| 11 | C. N. H. Lock and H. Bateman .. | Experiments with a Family of Airscrews. Part III. R. & M. 892. |
| 12 | D. H. Williams, A. F. Brown and E. Smyth. | Tests of Four Airscrew Sections in the Compressed Air Tunnel. R. & M. 1771. |
| 13 | H. Glauert .. .. .. .. | Aerofoil and Airscrew Theory, p. 92. |
| 14 | H. B. Squire and A. D. Young .. | The Calculation of the Profile Drag of Aerofoils. R. & M. 1838. |
| 15 | W. J. Duncan and A. R. Collar .. | The Present Position of the Investigation of Airscrew Flutter. R. & M. 1518. |
| 16 | R. McK. Wood and W. G. A. Perring.. | Stresses and Strains in Airscrews, with Particular Reference to Twist. R. & M. 1274. |
| 17 | W. J. Duncan .. .. .. .. | The Torsion and Flexure of Cylinders and Tubes. R. & M. 1444. |

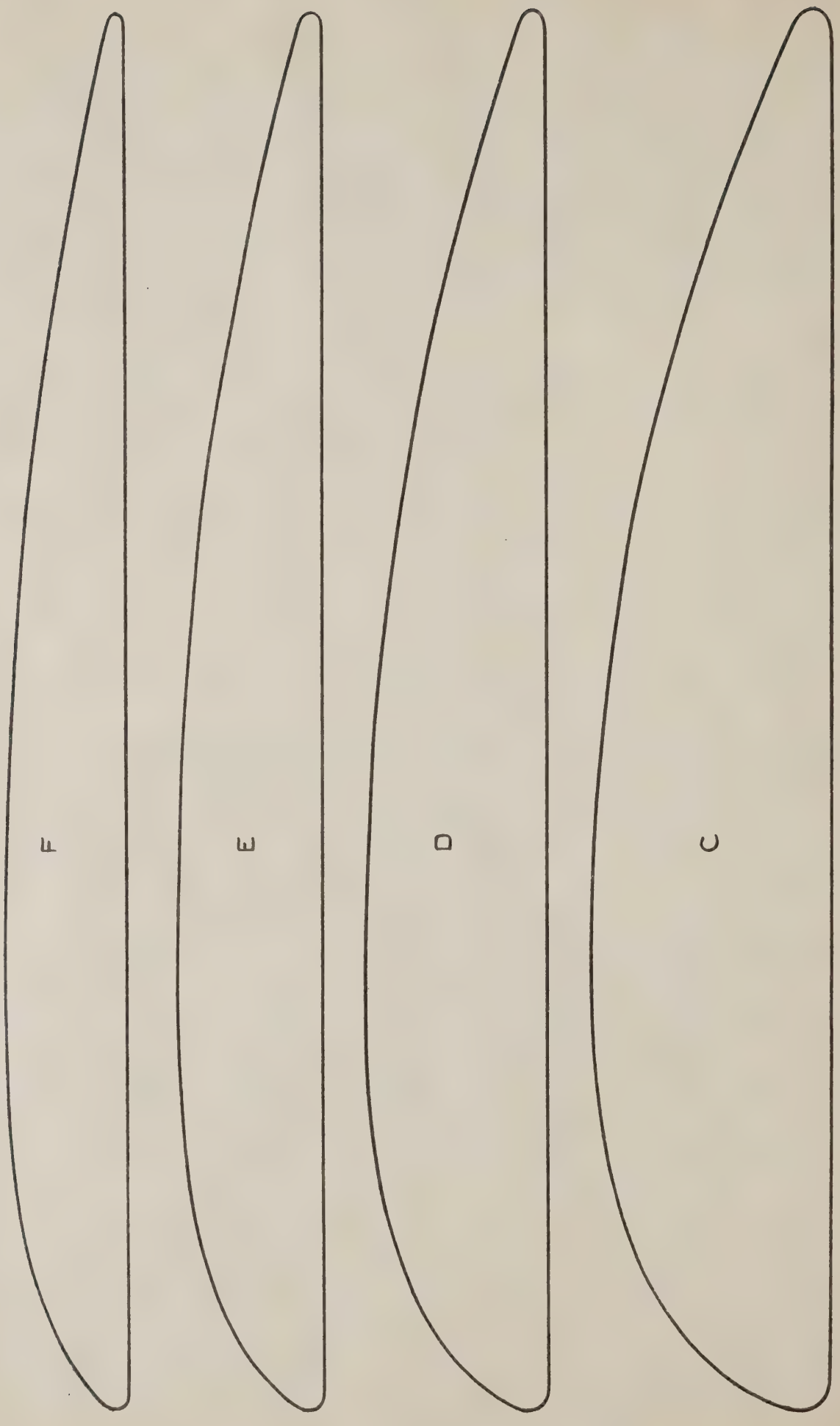


FIG. 1

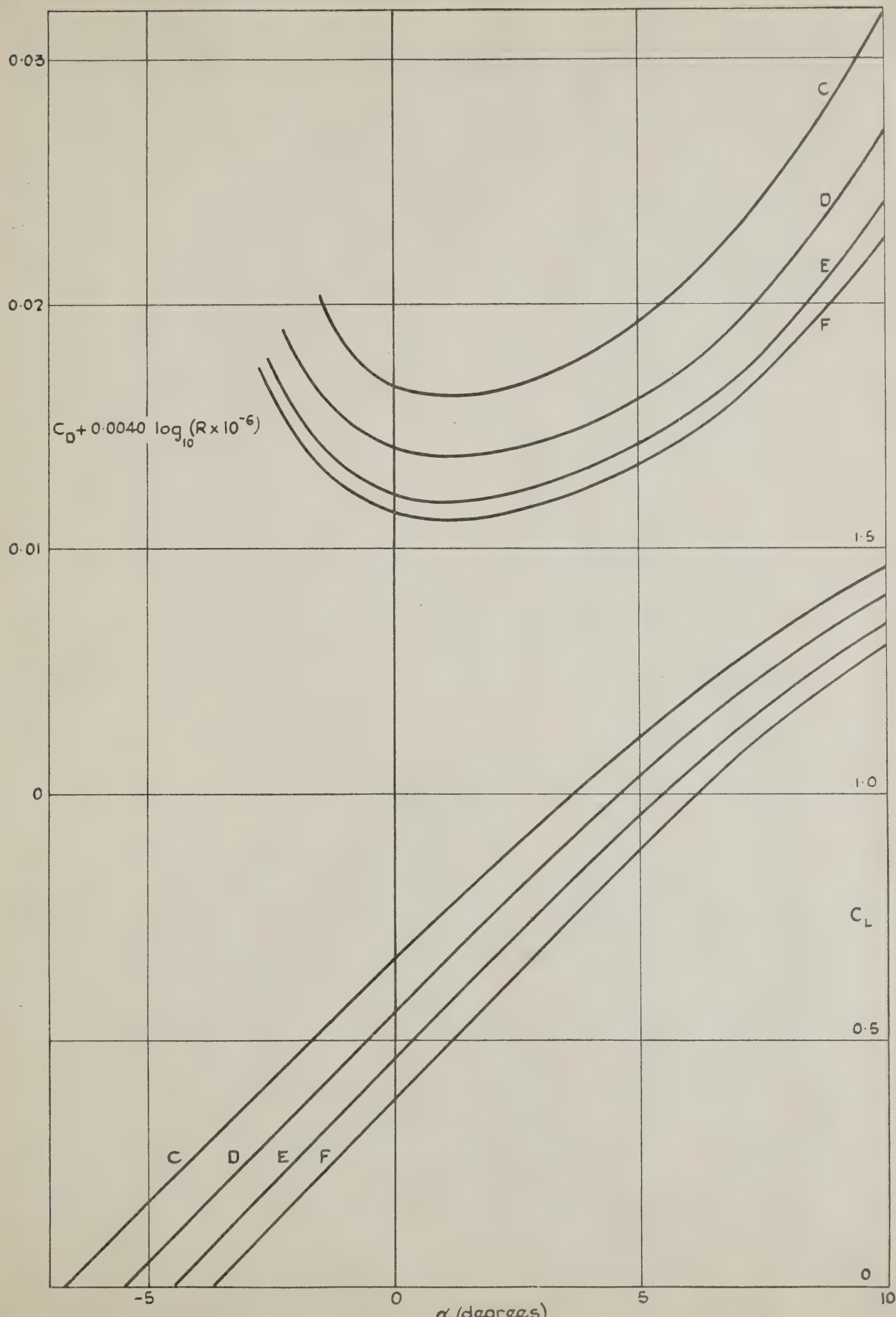
0·03
0·02
0·01
0
$C_D + 0{\cdot}0040 \log_{10}(R \times 10^{-6})$
C
D
E
F
1·5
1·0
0·5
0
$C_L$
C D E F
-5
0
5
10
α (degrees)

FIG. 2

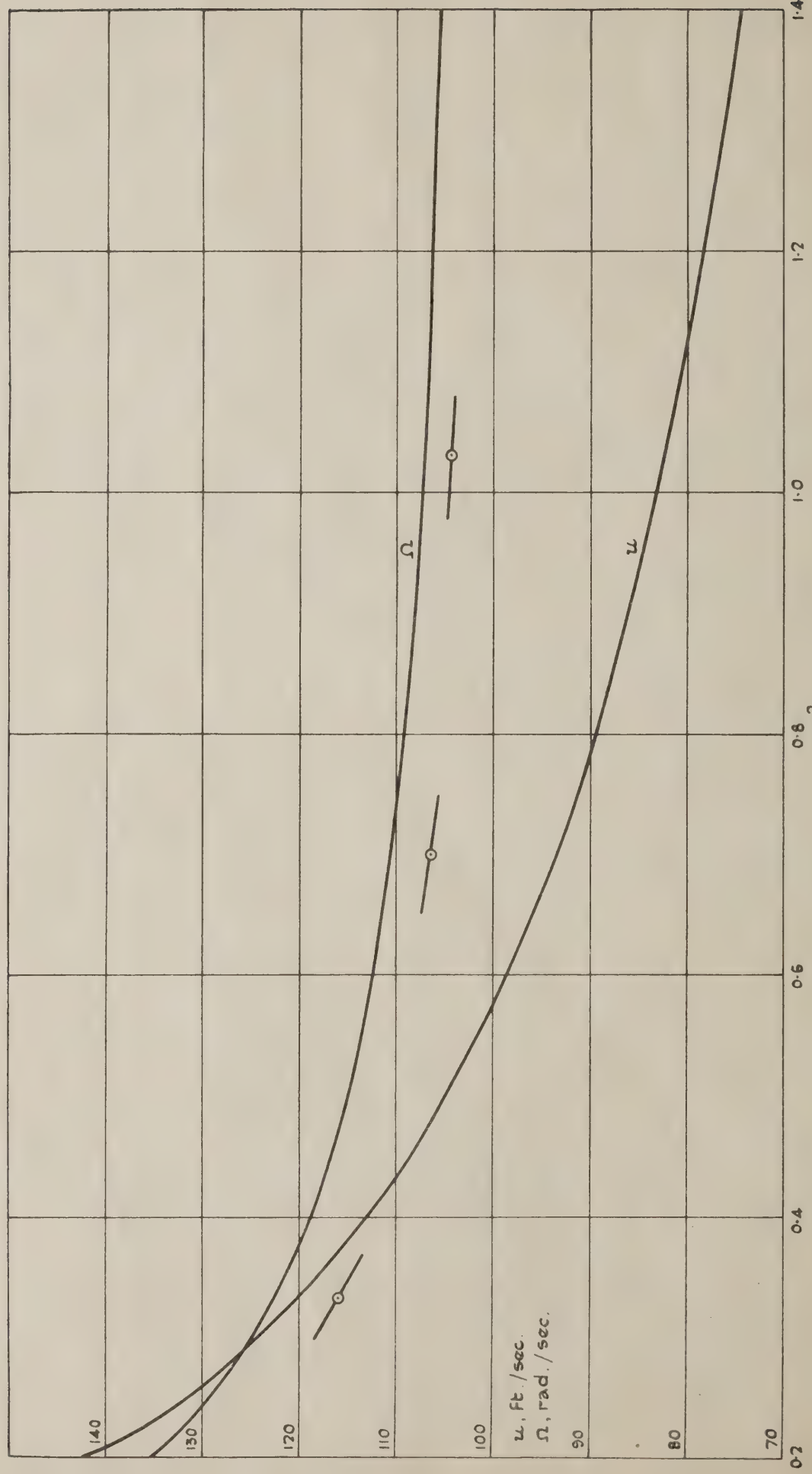


FIG. 3

(53487) Wt. 4 500 12 40 Hw. G.377/4

## SYSTEM OF AXES

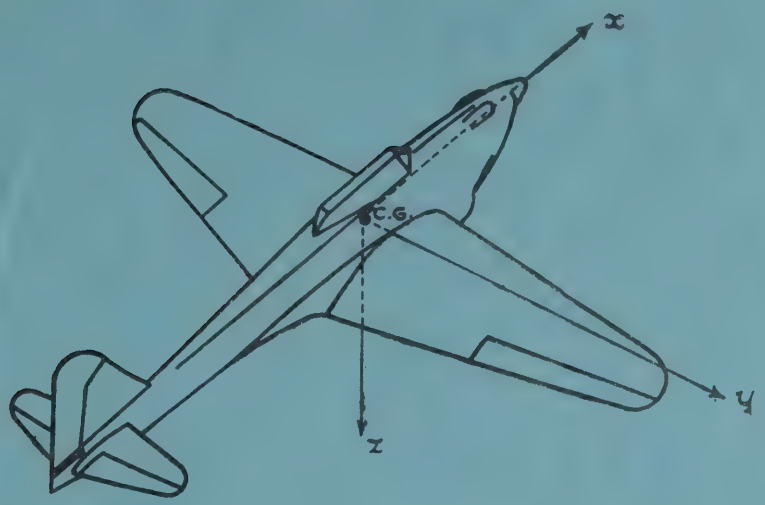


| Axes | Symbol Designation Positive direction | $x$ longitudinal forward | $y$ lateral starboard | $z$ normal downward |
|---|---|---|---|---|
| Force | Symbol | X | Y | Z |
| Moment | Symbol Designation | L rolling | M pitching | N yawing |
| Angle of Rotation | Symbol | $\phi$ | $\theta$ | $\psi$ |
| Velocity | Linear<br>Angular | $u$<br>$p$ | $v$<br>$q$ | $w$<br>$r$ |
| Moment of Inertia | | A | B | C |

Components of linear velocity and force are positive in the positive direction of the corresponding axis.

Components of angular velocity and moment are positive in the cyclic order $y$ to $z$ about the axis of $x$, $z$ to $x$ about the axis of $y$, and $x$ to $y$ about the axis of $z$.

The angular movement of a control surface (elevator or rudder) is governed by the same convention, the elevator angle being positive downwards and the rudder angle positive to port. The aileron angle is positive when the starboard aileron is down and the port aileron is up. A positive control angle normally gives rise to a negative moment about the corresponding axis.

The symbols for the control angles are :—

$\xi$ aileron angle
$\eta$ elevator angle
$\eta_T$ tail setting angle
$\zeta$ rudder angle

# Publications of the Aeronautical Research Committee

TECHNICAL REPORTS OF THE AERONAUTICAL RESEARCH COMMITTEE—

1933-34 Vol. I. Aerodynamics. £1 5*s*.
Vol. II. Structures, Engines, Instruments, etc. £1 10*s*.

1934-35 Vol. I. Aerodynamics. £2.
Vol. II. Seaplanes, Structures, Engines, Materials, etc. £2.

1935-36 Vol. I. Aerodynamics. £1 10*s*.
Vol. II. Structures, Flutter, Engines, Seaplanes, etc. £1 10*s*.

1936 Vol. I. Aerodynamics General, Performance, Airscrews, Flutter and Spinning. £2.
Vol. II. Stability and Control, Structures, Seaplanes, Engines, etc. £2 10*s*.

ANNUAL REPORTS OF THE AERONAUTICAL RESEARCH COMMITTEE—

1933-34 1*s*. 6*d*.
1934-35 1*s*. 6*d*.
April 1, 1935 to December 31, 1936. 4*s*.
1937 2*s*.

INDEX TO THE TECHNICAL REPORTS OF THE ADVISORY COMMITTEE ON AERONAUTICS—

1909-1919 Reports and Memoranda No. 1600. 8*s*.

NUMERICAL LISTS OF REPORTS AND MEMORANDA published between 1909 and 1936—

Reports and Memoranda Nos. 650 (9*d*.), 750 (6*d*.), 850 (1*d*.), 950 (4*d*.), 1050 (4*d*.), 1150 (4*d*.) (*Out of print*), 1250 (6*d*.) (*Out of print*), 1350 (6*d*.) (*Out of print*), 1450 (6*d*.), 1550 (6*d*.), 1650 (6*d*.), 1750 (1*s*. 3*d*.)

LIST OF PUBLICATIONS ON AERONAUTICS—

Aeronautical Research Committee Publications (classified under subjects). Post free on application.

*Prices are net and postage extra.*

## His Majesty's Stationery Office

London W.C.2 : York House, Kingsway

Edinburgh 2 : 120 George Street
Manchester 1 : 26 York Street
Cardiff : 1 St. Andrew's Crescent
Belfast : 80 Chichester Street

or through any bookseller.

S.O. Code No. 23-1889

629.13
G79r
no.1890

Engng

LIBRARY
UNIVERSITY OF ILLINOIS
URBANA

R. & M. No. 1890
(4341)
A.R.C. Technical Report

AIR MINISTRY

AERONAUTICAL RESEARCH COMMITTEE
REPORTS AND MEMORANDA

# Flow of an Ideal Fluid past a Cascade of Blades

*By*

W. MERCHANT, M.A., S.M.,
of Metropolitan-Vickers Electrical Co., Ltd.

---

COMMUNICATED BY PROFESSOR R.V. SOUTHWELL, F.R.S.

*Crown Copyright Reserved*

LONDON: HIS MAJESTY'S STATIONERY OFFICE
Price 1*s.* 6*d.* net

# AERODYNAMIC SYMBOLS

## 1. GENERAL

| | |
|---|---|
| $m$ | Mass |
| $t$ | Time |
| V | Resultant linear velocity |
| $\Omega$ | Resultant angular velocity |
| $\rho$ | Density, $\sigma$ relative density |
| $\nu$ | Kinematic coefficient of viscosity |
| R | Reynolds number, $R = lV/\nu$ (where $l$ is a suitable linear dimension) |

Normal temperature and pressure for aeronautical work are 15° C and 760 mm.

For air under these conditions $\begin{cases} \rho = 0{\cdot}002378 \text{ slug/cu. ft.} \\ \nu = 1{\cdot}59 \times 10^{-4} \text{ sq. ft./sec.} \end{cases}$

The slug is taken to be 32·2 lb.-mass.

| | |
|---|---|
| $\alpha$ | Angle of incidence |
| $e$ | Angle of downwash |
| S | Area |
| $b$ | Span |
| $c$ | Chord |
| A | Aspect ratio, $A = b^2/S$ |
| L | Lift, with coefficient $C_L = L/\frac{1}{2}\rho V^2 S$ |
| D | Drag, with coefficient $C_D = D/\frac{1}{2}\rho V^2 S$ |
| $\gamma$ | Gliding angle, $\tan\gamma = D/L$ |
| L | Rolling moment, with coefficient $C_l = L/\frac{1}{2}\rho V^2 bS$ |
| M | Pitching moment, with coefficient $C_m = M/\frac{1}{2}\rho V^2 cS$ |
| N | Yawing moment, with coefficient $C_n = N/\frac{1}{2}\rho V^2 bS$ |

## 2. AIRSCREWS

| | |
|---|---|
| $n$ | Revolutions per second |
| D | Diameter |
| J | $V/nD$ |
| P | Power |
| T | Thrust, with coefficient $k_T = T/\rho n^2 D^4$ |
| Q | Torque, with coefficient $k_Q = Q/\rho n^2 D^5$ |
| $\eta$ | Efficiency, $\eta = TV/P = Jk_T/2\pi k_Q$ |

LIBRARY
UNIVERSITY OF ILLINOIS
URBANA

# Flow of an Ideal Fluid past a Cascade of Blades

*By*

W. Merchant, M.A., S.M.,
of Metropolitan-Vickers Electrical Co., Ltd.

Communicated by Professor R. V. Southwell, F.R.S.

*Reports and Memoranda No.* 1890

*8th July*, 1940

*SUMMARY.*—This is a mathematical investigation into the flow of the ideal fluid of hydrodynamics past a cascade of blades. A complete solution is given for a cascade of straight blades set at any angle to the cascade axis and for any pitch chord ratio. Previous work on the subject is reviewed and compared with the results of this investigation.

Part I of this report contains an investigation of the general problem and a general relationship which must hold for all types of blades is found. Part II gives a complete solution for any cascade of straight blades at any angle to the cascade axis and any pitch chord ratio. There are also three appendices. The first contains an alternative proof of the general relationship due to Dr. D. M. Smith. This is based on somewhat simpler principles than that given in the main body of the report and is only omitted there because it is not in the main line of the reasoning. The second deals with the relation between the lift coefficient for an aerofoil in a cascade and that of an individual aerofoil. The last reviews previous work on the subject. For the symbols used in relation to a cascade, *see* Fig. 4.

*Part I. General Theory.*—The flow of an ideal fluid is governed by Laplace's equation

$$\nabla^2 V \equiv \frac{\partial^2 V}{\partial x^2} + \frac{\partial^2 V}{\partial y^2} = 0.$$

Both the velocity potential $\Phi$ and the stream function $\Psi$ obey this equation.

Consider any function of the complex variable

$$w = f(z) = \xi + i\eta,$$

where $z = x + iy$.

Then

$$\nabla^2 \xi = \nabla^2 \eta = 0.$$

Hence we can identify $\xi$ and $\eta$ with $\Phi$ and $\Psi$, and from any function of the complex variable can obtain a solution of some flow problem.

Let

$$w = \Phi + i\Psi.$$

Then

$$\frac{dw}{dz} = u - iv,$$

where

$$u = \frac{\partial \Phi}{\partial x} = \frac{\partial \Psi}{\partial y},$$

and

$$v = \frac{\partial \Phi}{\partial y} = -\frac{\partial \Psi}{\partial x},$$

and hence $u$ and $v$ give the components of the velocity of the motion parallel to the axes.

It is also useful to remember that the deflections of a uniformly stretched thin elastic sheet, under no loading but having applied boundary conditions, obey Laplace's equation. We thus can picture every flow problem as an elastic sheet problem and can equate contours with either flow lines or velocity potential lines as required.

Consider any flow problem of which there is a known solution and imagine that we have the $\Phi$, $\Psi$ lines drawn. These intersect orthogonally everywhere and if drawn for equal increments of $\Phi$ and $\Psi$ then if one element forms a curvilinear square all form curvilinear squares. In such a case we may specify the position of a point either by $x$, $y$ co-ordinates or by $\Phi$, $\Psi$ co-ordinates. We can also consider a plane in which $\Phi$ and $\Psi$ are ordinary Cartesian co-ordinates.

Consider any other flow in the $x$, $y$ plane with a potential function

$$w' = \Phi' + i\Psi'.$$

Then

$$\nabla^2\Phi' = \nabla^2\Psi' = 0.$$

Now to every small square in the $x$, $y$ plane corresponds a small square in the $\Phi$, $\Psi$ plane. Hence

$$0 = \frac{\partial^2\Phi'}{\partial\Phi^2} + \frac{\partial^2\Phi'}{\partial\Psi^2}$$

$$0 = \frac{\partial^2\Psi'}{\partial\Phi^2} + \frac{\partial^2\Psi'}{\partial\Psi^2}.$$

Therefore to every flow in the $x$, $y$ plane there is a corresponding flow in the $\Phi$, $\Psi$ plane. We can thus obtain corresponding flows by plotting the flow lines in the one plane on the other using the correspondence between the $x$, $y$ and the $\Phi$, $\Psi$ co-ordinates as a mapping function. This process is known as conformal transformation.

The particular method used in this report is as follows. For any cascade of blades there is a direction of flow for which there is no deviation of the fluid stream. Let the angle of inclination of this direction with the normal to the cascade axis be $\varphi$; this direction is called the direction of neutral flow, or more shortly the neutral direction. Suppose the flow net is known for this direction. It can be replotted in the $\Phi$, $\Psi$ plane as a simple square mesh. In this case the blades will transform into finite lengths of the $\Psi$ lines.

Now consider a series of laminas uniformly distributed along the $x$ axis, as in Fig. 1.

FIG. 1

Further consider the flow past them, with no circulation round the laminas, whose direction at infinity makes the same angle $\varphi$ with the normal to the cascade axis. Since there is no circulation round the blades there is no change in the direction of the velocity at infinity on both sides of the cascade; there is only a local distortion round the blades. This flow can also be replotted as a simple square mesh in the $\Phi$, $\Psi$ plane. The blades again transform into finite lengths of the $\Psi$ lines. If these lengths are the same in the two cases and we know other flows round the blades on the real axis, we can use the $\Phi$, $\Psi$ plane to transfer these flows to flows round the actual series of blades in the cascade.

As a partial problem we will therefore consider the general flow past straight blades uniformly distributed along the cascade axis.

Consider the flow represented by the equation

$$u - iv = \frac{dw}{dz} = \mathrm{U} + \frac{\mathrm{V}\sqrt{2}\sin\frac{1}{2}z}{\sqrt{r + \cos z}} + \frac{\mathrm{W}\sqrt{2}\cos\frac{1}{2}z}{\sqrt{r + \cos z}}, \quad (-1 \leqslant r \leqslant +1).$$

The first term represents a uniform flow parallel to the axis of $x$ and of velocity U. It obviously fits in with the boundary conditions for flow past blades on the cascade axis.

The second term is alternately real and imaginary for periods along the cascade axis as shown below in Fig. 2.

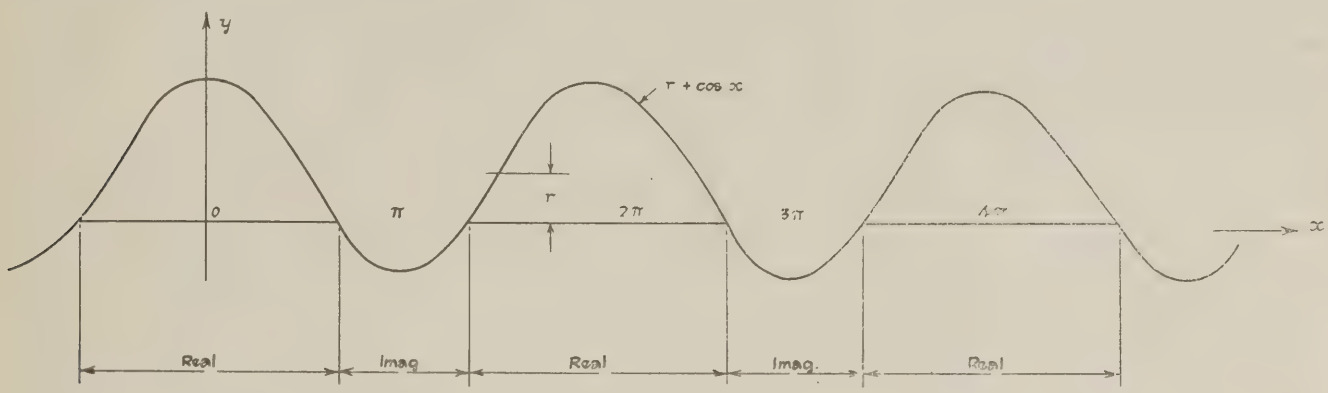


FIG. 2

Now a real term represents flow parallel to the $x$ axis and an imaginary term flow parallel to the $y$ axis. Therefore the flow is consistent with flow round blades along the real axis where the half length is given by $r + \cos x = 0$.

Through the centre of a gap, e.g. at $x = \pi$, we have for the flow due to the second term

$$u - iv = \frac{\mathrm{V}\sqrt{2}\sin\frac{1}{2}(\pi + iy)}{\sqrt{r + \cos(\pi + iy)}} = \frac{\mathrm{V}\sqrt{2}\cosh\frac{1}{2}y}{\sqrt{r - \cosh y}}$$

Now $\cosh y$ is always positive and greater than 1. Therefore the expression above is always purely imaginary ; and hence there is no flow across the line $x = \pi$.

Further

$$\underset{y \to \pm\infty}{Lt}(u - iv) = \frac{\mathrm{V}}{i}.$$

Therefore the velocity a large distance from the cascade is of constant value and parallel to the $y$ axis. Also there are no singularities apart from the real axis. Therefore the term represents the flow of a uniform stream normal to the cascade and of velocity V at infinity.

In similar manner the third term can be shown to represent the flow due to equal circulations round the blades corresponding to velocities at infinity of $\pm$W parallel to the $x$ axis.

We thus have the solution for the general flow past the cascade of blades.

For the flow with no circulation, W = 0 ; if this flow is at an angle $\varphi$ to the normal to the cascade we have $\tan\varphi = \mathrm{U}/\mathrm{V}$, and the stagnation points are given by

$$u = 0 = \mathrm{U} + \frac{\mathrm{V}\sqrt{2}\sin\frac{1}{2}x_1}{\sqrt{r + \cos x_1}},$$

whence

$$\tan^2 \varphi = \frac{1 - \cos x_1}{r + \cos x_1},$$

or

$$\cos x_1 = \cos^2\varphi - r \sin^2\varphi.$$

We thus know the point on the back face of the lamina which corresponds to the trailing edge of the blades.

Now Joukowski's hypothesis requires that for flow in any direction there shall be associated that amount of circulation which will keep the velocity at the trailing edge finite. Changing the problem to that of blades along the real axis this requires that the stagnation point should remain in the same place for other incident directions of flow than $\varphi$.

Consider a direction of flow, free from the circulation imposed by the blades, of $\theta$. If a circulation is added to this flow, the stagnation points are given by

$$u = 0 = \mathrm{U} + \frac{\mathrm{V}\sqrt{2}\sin \frac{1}{2}x_1}{\sqrt{r + \cos x_1}} + \frac{\mathrm{W}\sqrt{2}\cos \frac{1}{2}x_1}{\sqrt{r + \cos x_1}}$$

with

$$\tan \theta = \frac{\mathrm{U}}{\mathrm{V}}.$$

If these are the same points as for $\varphi$ with no circulation,

$$\cos x_1 = \cos^2\varphi - r \sin^2\varphi,$$

or

$$\tan \varphi = -\frac{\sqrt{2}\ \sin\ \frac{1}{2}x_1}{\sqrt{r + \cos x_1}},$$

Hence

$$0 = \tan \theta - \tan \varphi + \frac{\mathrm{W}}{\mathrm{V}} \frac{\sqrt{2}\cos\ \frac{1}{2}x_1,}{\sqrt{r + \cos x_1}}.$$

and it therefore follows that

$$\frac{\mathrm{V}}{\mathrm{W}} (\tan \theta - \tan \varphi) = \sqrt{1 + \frac{(1 - r)}{(1 + r)} \sec^2\varphi}.$$

Now

$$\tan \alpha = \frac{\mathrm{U} + \mathrm{W}}{\mathrm{V}},$$

$$\tan \beta = \frac{\mathrm{U} - \mathrm{W}}{\mathrm{V}},$$

$$\tan \theta = \frac{\mathrm{U}}{\mathrm{V}}.$$

Therefore

$$\frac{\tan \alpha + \tan \beta - 2 \tan \varphi}{\tan \alpha - \tan \beta} = \sqrt{1 + \frac{(1 - r)}{(1 + r)} \sec^2\varphi}.$$

Put

$$y = \sqrt{1 + \left(\frac{1 - r}{1 + r}\right) \sec^2\varphi} - 1$$

$$= \sqrt{\frac{1 + \cos x_1}{r + \cos x_1}} - 1$$

Then

$$\tan \beta = \frac{y \tan \alpha + 2 \tan \varphi}{y + 2},$$

which is the general relationship mentioned in the summary to this report.

We thus see that the general problem of flow past a cascade of blades resolves itself into two partial problems. The first is to determine the neutral direction for the cascade. The second to determine the length of the transformed laminas along the cascade axis.

*Part II. Complete Solution for Cascade of Straight Blades at any Angle to the Axis and any Pitch Chord Ratio.*—Here $\varphi$ is known being the angle the blades make with the normal to the cascade axis.

We can determine $r$ as follows—When we replot the flow in the $\Phi$, $\Psi$ plane the length of the laminas is equal to the change in $\Phi$ between the stagnation points. The width of the gap is the change in $\Psi$ between each lamina. From Fig. 3 it is now evident that the change in $\Phi$ is

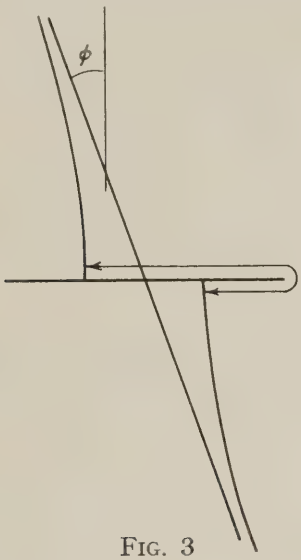


FIG. 3

$$c = \int_{x_1}^{\cos^{-1}(-r)} u \, dx + \int_{x_1}^{-\cos^{-1}(-r)} u \, dx,$$

where $x_1$ is a stagnation point. Also,

$$u = V\left[\tan \varphi + \frac{\sqrt{2} \sin \frac{1}{2}x}{\sqrt{r + \cos x}}\right].$$

The integrals can be readily evaluated by means of the substitution

$$\cos \tfrac{1}{2}x = \sqrt{\frac{1 - r}{2}} \sec \lambda,$$

the result being

$$c = V\left[-2 \tan \varphi \, x_1 + 4 \log\left(\sqrt{\frac{1 + \cos x_1}{1 - r}} + \sqrt{\frac{r + \cos x_1}{1 - r}}\right)\right],$$

or, in terms of the parameter $y$ of Part I,

$$c = 4V\left[\tan \varphi \tan^{-1}\left(\frac{\tan \varphi}{1 + y}\right) + \frac{1}{2} \log \frac{y + 2}{y}\right].$$

Also

$$s \cos \varphi = \int_0^{2\pi} V \, dx = 2\pi V.$$

Therefore

$$\frac{s}{c} = \frac{\frac{\pi}{2} \sec \varphi}{\tan \varphi \tan^{-1}\left(\frac{\tan \varphi}{1 + y}\right) + \frac{1}{2} \log\left(\frac{y + 2}{y}\right)}$$

which completes the solution for the straight blades. A graph of $y$ against $s/c$ for $\varphi = 0, \pi/4$ is appended (Fig. 5).

In conclusion the writer would like to express his thanks to Messrs. Metropolitan Vickers Electrical Co., Ltd., for permission to publish this paper.

## APPENDIX I

*Alternative Proof of General Relationship*

By Dr. D. M. Smith

Consider flow of a perfect fluid, of uniform velocity at $y = +\infty$ and at $y = -\infty$, past a cascade of uniform blades arranged along the $x$ axis. The most general possible type of uniform flow is compounded of the following velocities at $y = \pm\infty$:

(1) $-$ V in $y$ direction.

(2) U in $x$ direction.

(3) $+$ W at $y = +\infty$, and $-$ W at $y = -\infty$, in $x$ direction, due to a certain circulation round each blade.

The resultant approaching velocity makes angle $\alpha$ with $y$ direction, where $\tan\alpha = \frac{U + W}{V}$: similarly for leaving angle $\beta$, $\tan\beta = \frac{U - W}{V}$.

Now consider the local velocity at any point P on the boundary of one blade. This local velocity may be written

$$c = Uu + Vv + Ww,$$

where $u$, $v$, $w$ are constant for any given point on a given blade at a given setting; and the condition that P should be a stagnation point is that the values of U, V and W should be such that

$$Uu + Vv + Ww = 0.$$

The direction of the flow without circulation which makes P a stagnation point is given by

$$\tan\varphi = -\frac{v}{u}.$$

The condition $Vv + Uu + Ww = 0$ is equivalent to

$$\frac{v}{u} + \frac{U}{V} + \frac{W}{V}\frac{w}{u} = 0$$

or

$$\frac{v}{u} + \frac{1}{2}\left(1 + \frac{w}{u}\right)\frac{W + U}{V} + \frac{1}{2}\left(1 - \frac{w}{u}\right)\frac{U - W}{V} = 0.$$

or

$$-\tan\varphi + \frac{1}{2}\left(1 + \frac{w}{u}\right)\tan\alpha + \frac{1}{2}\left(1 - \frac{w}{u}\right)\tan\beta = 0.$$

These relations still hold good if P is a sharp trailing edge, because although $u$, $v$, $w$ become infinite their ratios remain finite; hence the last relation is true if P is the sharp trailing edge of a cascade of blades the circulation round which is in accordance with Joukowski's hypothesis.

The last relation is equivalent to

$$\tan\beta = \frac{y\tan\alpha + 2\tan\varphi,}{y + 2}$$

where

$$-y = 1 + \frac{w}{u}.$$

## APPENDIX II

*Effect on Lift Coefficient of Interference due to being in a Cascade*

Specify everything in terms of $V_\infty$ and $\theta$; we have

$$U = V_\infty \sin\theta,$$
$$V = V_\infty \cos\theta,$$
$$\tan\alpha = \frac{W + V_\infty \sin\theta}{V_\infty \cos\theta},$$
$$\tan\beta = \frac{-W + V_\infty \sin\theta}{V_\infty \cos\theta},$$
$$\tan\beta = \frac{y\tan\alpha + 2\tan\varphi}{y+2}.$$

Hence

$$W = \frac{V_\infty \cos\theta(\tan\theta - \tan\varphi)}{(y+1)};$$

Let the circulation per blade be $\Gamma$. Then

$$\Gamma = 2Ws$$
$$= \frac{2s\,V_\infty \sin(\theta-\varphi)}{\cos\varphi\,(y+1)};$$

therefore $\Gamma$ varies as the velocity normal to the blades. The lift per blade, per unit length, is given by

$$L = \tfrac{1}{2}C_L c\rho V_\infty^2$$
$$= \rho V_\infty \Gamma$$
$$C_L = \frac{2\Gamma}{cV_\infty} = \frac{4s}{c}\,\frac{\sin(\theta-\varphi)}{\cos\varphi\,(y+1)},$$

where for straight blades

$$\frac{s}{c} = \frac{\frac{\pi}{2}\sec\varphi}{\tan\varphi\tan^{-1}\left(\frac{\tan\varphi}{1+y}\right) + \frac{1}{2}\log\left(\frac{y+2}{y}\right)}.$$

To find the value for an individual blade we have to take the limit as $\frac{s}{c}\to\infty$, i.e. as $y\to\infty$. Now

$$\underset{y\to\infty}{\mathrm{Lt}}\,(y+1)\log\left(\frac{y+2}{y}\right) = \mathrm{Lt}\,\frac{\frac{y}{y+2}\,\frac{-2}{y^2}}{\frac{-1}{(y+1)^2}} = 2.$$

Also

$$\underset{y\to\infty}{\mathrm{Lt}}\,(y+1)\tan^{-1}\left(\frac{\tan\varphi}{1+y}\right) = \mathrm{Lt}\,\frac{\frac{1}{1+\left(\frac{\tan\varphi}{y}\right)^2}\,\frac{-\tan\varphi}{y^2}}{-\frac{1}{y^2}} = \tan\varphi.$$

Therefore for a single straight aerofoil

$$C_L = \frac{4\sin(\theta-\varphi)\,\frac{1}{2}\pi\sec\varphi}{\cos\varphi\,(\tan^2\varphi+1)} = 2\pi\sin(\theta-\varphi),$$

which agrees with previous published results.

Write $C_{LC}$ for the lift coefficient of the aerofoil in the cascade. Then

$$\frac{C_{LC}}{C_L} = \frac{2s}{\pi c} \frac{1}{(y+1)\cos\varphi},$$

where

$$\frac{s}{c} = \frac{\frac{\pi}{2}\sec\varphi}{\tan\varphi \tan^{-1}\left(\frac{\tan\varphi}{1+y}\right) + \frac{1}{2}\log\left(\frac{y+2}{y}\right)}.$$

Graphs are given of $\frac{C_{LC}}{C_L}$ for $\varphi = 0, \frac{\pi}{4}, \frac{\pi}{2}$ (Fig. 6).

## APPENDIX III

*Brief Review of Previous Theory and Bibliography*

The problem has been under consideration for about thirty years.

*Kutta* in 1911 obtained a solution for a set of straight blades normal to the cascade axis.

*Grammel* in 1917 obtained a solution for a set of approximately straight blades at any angle to the axis. For $\varphi = 0, \pi/2$ the blades are straight and for $\varphi = 0$ agree with Kutta.

*Glauert and McKinnon Wood*, 1918–20, realised the interference due to the blades being in a series should be applied to airscrew theory and did apparently the first tests on blades in a cascade to obtain modified lift coefficients for use in airscrew theory.

*Konig*, 1922, solved the problem in *mathematical* terms in a manner which would do for any shape of blade. The mathematics are very intractable and no subsequent use seems to have been made of his method. He gives figures for straight blades at $\pi/4$ to the axis which agree with those of this paper.

*Numachi*, 1929, calculated out the Grammel Formula as being the best available means of predicting the interference of blades in a series. His values for $\varphi = 0, \pi/2$ agree with those of this paper. They do not agree for $\varphi = \pi/4$, but are of the same order. This is due to the Grammel blades not being straight for $\varphi = \pi/4$.

*Betz*, 1931, gave a method of successive approximation to pass from an isolated aerofoil with all its properties known to an equivalent aerofoil in a cascade. The method is intended to be used for thin slightly curved aerofoils and needs considerable labour.

*Pistolesi*, 1937, gave a valid method for blades which are a small variation of straight lines normal to the axis. The method is an extension of that of Birnbaum-Glauert for single aerofoils. He applied the same method to small variations from oblique lines, but the mathematics become very complicated. He obtained Grammel's formula, but for thick blades of an undetermined thickness. This made him think that the curved blades Grammel obtains should be reflected about their axes.

*Braun*, 1932, gave a formula for the effect of varying $s/c$ and $\alpha$ and backs the formula from Christiani's experimental work. He stated that the theory would be published elsewhere. The formula does not agree in form with the general relationship given in this report.

## BIBLIOGRAPHY


1. A. Betz. Diagramme zur Berechnung von Flugelreihen. Ing. Archiv., Vol. 2, 1931, p. 359.
2. R. McK. Wood and H. Glauert. Preliminary Investigation of Multiplane Interference applied to Propeller Theory. Tech. Report, Advisory Committee for Aeronautics, 1918–19, No. 620.
3. Wood, Bradfield and Barker. Multiplane Interference applied to Airscrew Theory. R. & M. 639, September, 1919.
4. E. Braun. Zur Gittertheorie der Propeller rader. Escher Wyss Mitt, Vol. 5, p. 64, 1932.
5. Fukusaburo Numachi. Aerofoil Theory of Propeller Turbines and Propeller Pumps with Special Reference to the Effects of Blade Interference upon the Lift and Cavitation. Tech. Reports, Tokyo Imperial University, Vol. 8, No. 3, 1929.
6. Konig. Potentialstromung durch Gitter. Z.A.M.M., Vol. 2, p. 422, 1922.
7. E. Pistolesi. Flugelgitter. L'Aerotecnica, 17 (1937), S.484.
8. A. Betz. Tragfugel und hydraulische Maschinen. Handbuch der Physik. Bd.VII, S.272, Berlin, 1927.
9. Grammel. Die Hydrodynamische Grundlagen des Fluges, 1917.

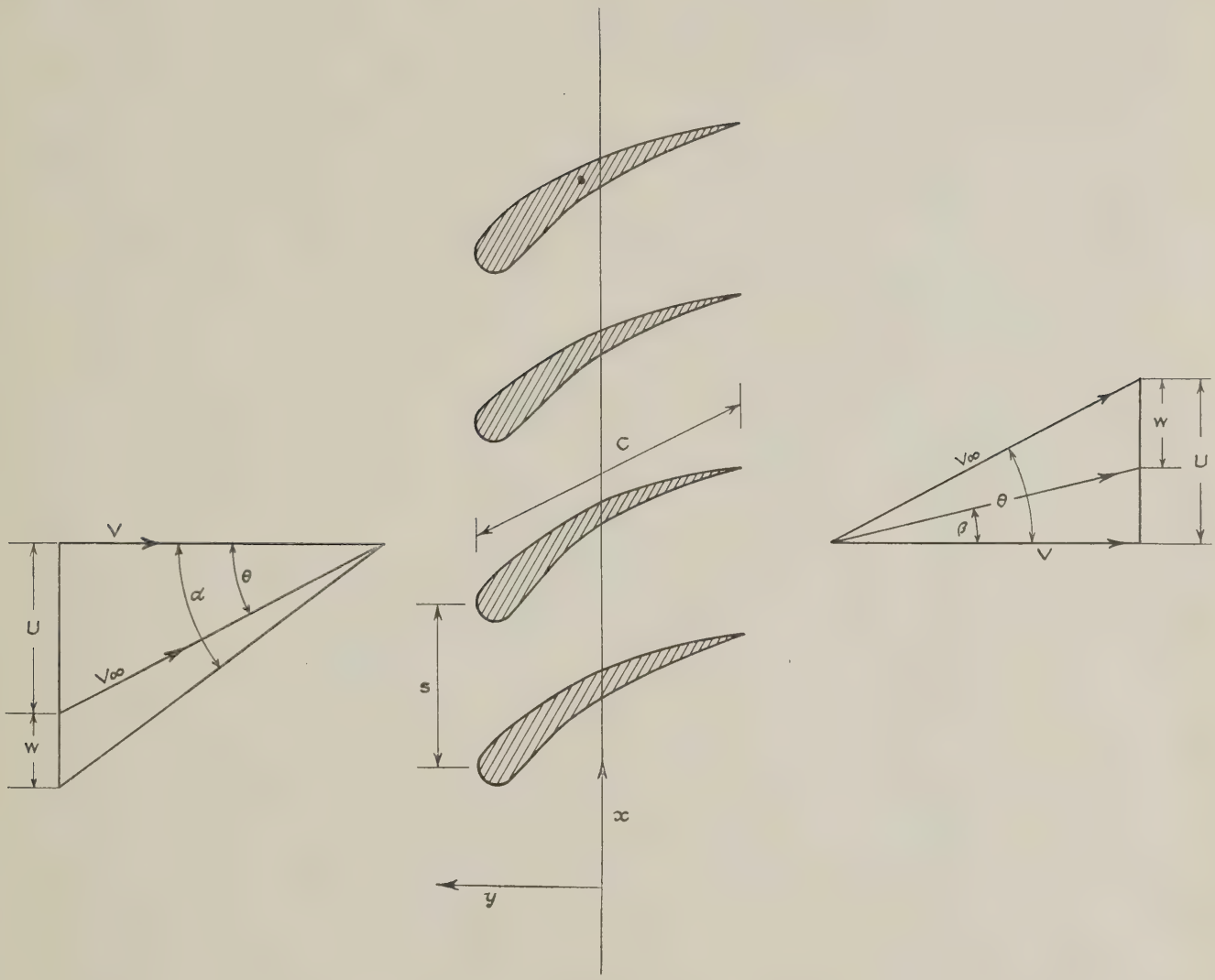


FIG. 4

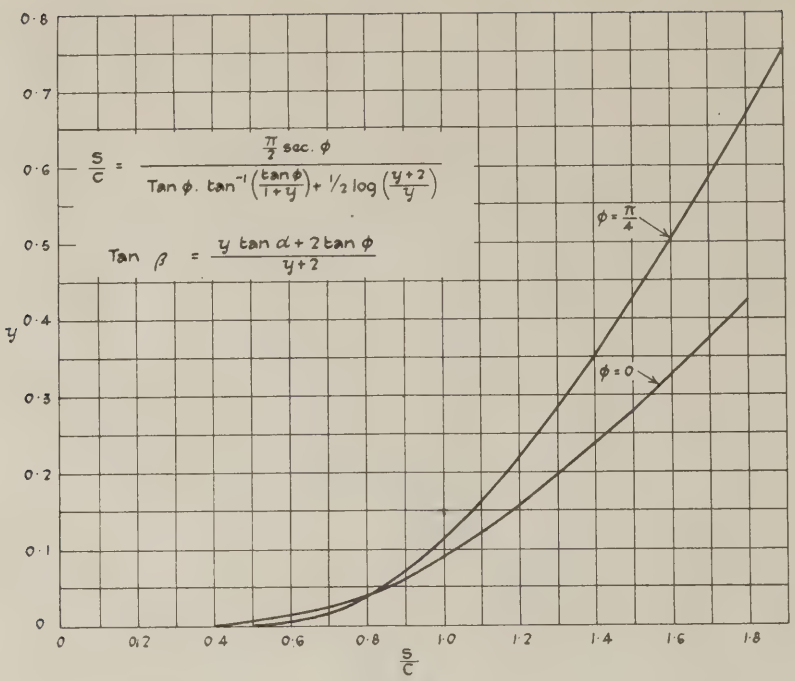


FIG. 5

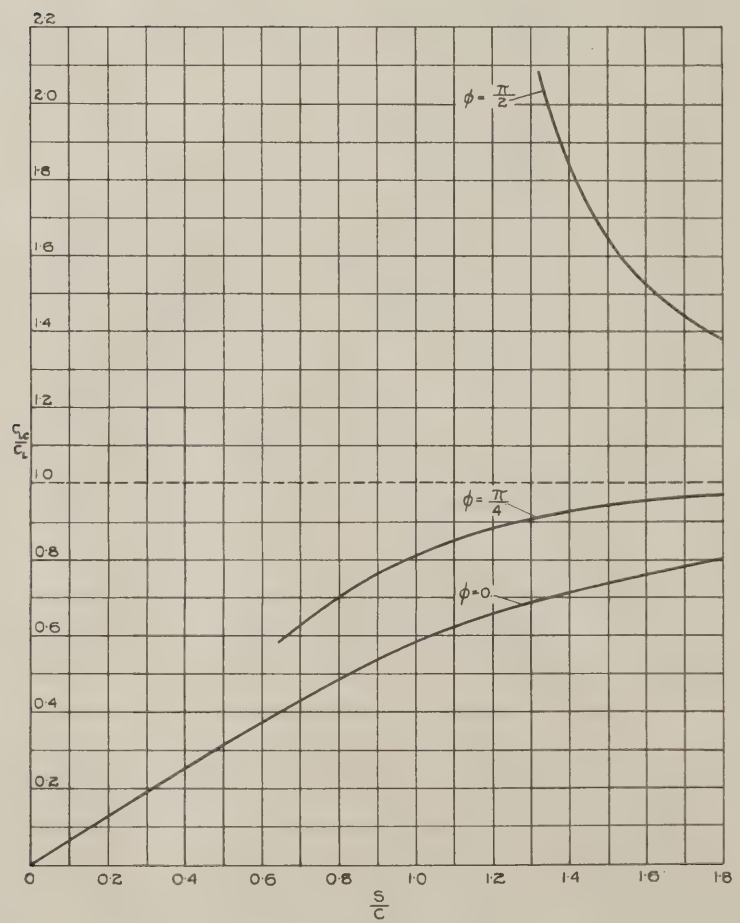


FIG. 6

(53685) Wt. 4 500 2/41 Hw. G.371

## SYSTEM OF AXES

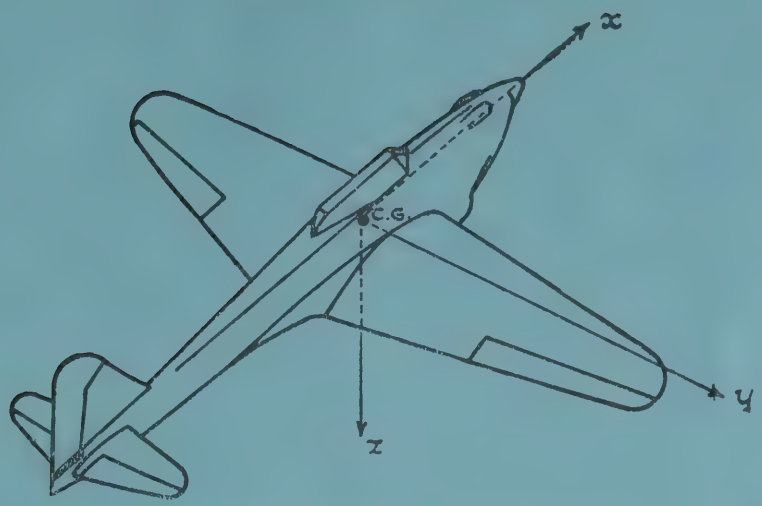


| Axes | Symbol Designation Positive direction | $x$ longitudinal forward | $y$ lateral starboard | $z$ normal downward |
|---|---|---|---|---|
| Force | Symbol | X | Y | Z |
| Moment | Symbol<br>Designation | L<br>rolling | M<br>pitching | N<br>yawing |
| Angle of Rotation | Symbol | $\phi$ | $\theta$ | $\psi$ |
| Velocity | Linear<br>Angular | $u$<br>$p$ | $v$<br>$q$ | $w$<br>$r$ |
| Moment of Inertia | | A | B | C |

Components of linear velocity and force are positive in the positive direction of the corresponding axis.

Components of angular velocity and moment are positive in the cyclic order $y$ to $z$ about the axis of $x$, $z$ to $x$ about the axis of $y$, and $x$ to $y$ about the axis of $z$.

The angular movement of a control surface (elevator or rudder) is governed by the same convention, the elevator angle being positive downwards and the rudder angle positive to port. The aileron angle is positive when the starboard aileron is down and the port aileron is up. A positive control angle normally gives rise to a negative moment about the corresponding axis.

The symbols for the control angles are :—

- $\xi$ aileron angle
- $\eta$ elevator angle
- $\eta_T$ tail setting angle
- $\zeta$ rudder angle

# Publications of the Aeronautical Research Committee

TECHNICAL REPORTS OF THE AERONAUTICAL RESEARCH COMMITTEE—

1933-34 Vol. I. Aerodynamics. £1 5*s*.
Vol. II. Structures, Engines, Instruments, etc. £1 10*s*.

1934-35 Vol. I. Aerodynamics. £2.
Vol. II. Seaplanes, Structures, Engines, Materials, etc. £2.

1935-36 Vol. I. Aerodynamics. £1 10*s*.
Vol. II. Structures, Flutter, Engines, Seaplanes, etc. £1 10*s*.

1936 Vol. I. Aerodynamics General, Performance, Airscrews, Flutter and Spinning. £2.
Vol. II. Stability and Control, Structures, Seaplanes, Engines, etc. £2 10*s*.

ANNUAL REPORTS OF THE AERONAUTICAL RESEARCH COMMITTEE—

1933-34 1*s*. 6*d*.
1934-35 1*s*. 6*d*.
April 1, 1935 to December 31, 1936. 4*s*.
1937 2*s*.

INDEX TO THE TECHNICAL REPORTS OF THE ADVISORY COMMITTEE ON AERONAUTICS—

1909-1919 Reports and Memoranda No. 1600. 8*s*.

NUMERICAL LISTS OF REPORTS AND MEMORANDA published between 1909 and 1936—

Reports and Memoranda Nos. 650 (9*d*.), 750 (6*d*.), 850 (1*d*.), 950 (4*d*.), 1050 (4*d*.), 1150 (4*d*.) (*Out of print*), 1250 (6*d*.) (*Out of print*), 1350 (6*d*.) (*Out of print*), 1450 (6*d*.), 1550 (6*d*.), 1650 (6*d*.), 1750 (1*s*. 3*d*.)

LIST OF PUBLICATIONS ON AERONAUTICS—

Aeronautical Research Committee Publications (classified under subjects). Post free on application.

*Prices are net and postage extra.*

## His Majesty's Stationery Office

London W.C.2 : York House, Kingsway
Edinburgh 2 : 120 George Street
Manchester 1 : 26 York Street
Cardiff : 1 St. Andrew's Crescent
Belfast : 80 Chichester Street
or through any bookseller.

S.O. Code No. 23-1890

LIBRARY
UNIVERSITY OF ILLINOIS
URBANA

R. & M. No. 1891
(4906)

629.13
G79r
no.1891

MINISTRY OF AIRCRAFT PRODUCTION

AERONAUTICAL RESEARCH COMMITTEE
REPORTS AND MEMORANDA

# Physical Properties of the Standard Atmosphere

*By*
R. C. PANKHURST, A.R.C.S., B.Sc.
AND
J. F. C. CONN, B.Sc., M.I.N.A.
of the Aerodynamics Department, N.P.L.

*Crown Copyright Reserved*

LONDON: HIS MAJESTY'S STATIONERY OFFICE
Price 9*d.* net

# AERODYNAMIC SYMBOLS

## 1. GENERAL

| | |
|---|---|
| $m$ | Mass |
| $t$ | Time |
| V | Resultant linear velocity |
| $\Omega$ | Resultant angular velocity |
| $\rho$ | Density, $\sigma$ relative density |
| $\nu$ | Kinematic coefficient of viscosity |
| R | Reynolds number, $R = lV/\nu$ (where $l$ is a suitable linear dimension) |

Normal temperature and pressure for aeronautical work are 15° C and 760 mm.

For air under these conditions $\begin{cases} \rho = 0{\cdot}002378 \text{ slug/cu. ft.} \\ \nu = 1{\cdot}56 \times 10^{-4} \text{ ft.}^2\text{/sec.} \end{cases}$

The slug is taken to be 32·2 lb.-mass.

| | |
|---|---|
| $\alpha$ | Angle of incidence |
| $e$ | Angle of downwash |
| S | Area |
| $b$ | Span |
| $c$ | Chord |
| A | Aspect ratio, $A = b^2/S$ |
| L | Lift, with coefficient $C_L = L/\frac{1}{2}\rho V^2 S$ |
| D | Drag, with coefficient $C_D = D/\frac{1}{2}\rho V^2 S$ |
| $\gamma$ | Gliding angle, $\tan\gamma = D/L$ |
| L | Rolling moment, with coefficient $C_l = L/\frac{1}{2}\rho V^2 bS$ |
| M | Pitching moment, with coefficient $C_m = M/\frac{1}{2}\rho V^2 cS$ |
| N | Yawing moment, with coefficient $C_n = N/\frac{1}{2}\rho V^2 bS$ |

## 2. AIRSCREWS

| | |
|---|---|
| $n$ | Revolutions per second |
| D | Diameter |
| J | $V/nD$ |
| P | Power |
| T | Thrust, with coefficient $k_T = T/\rho n^2 D^4$ |
| Q | Torque, with coefficient $k_Q = Q/\rho n^2 D^5$ |
| $\eta$ | Efficiency, $\eta = TV/P = Jk_T/2\pi k_Q$ |

29.13
G79
1891

# Physical Properties of the Standard Atmosphere

*By*

R. C. Pankhurst, A.R.C.S., B.Sc.

and

J. F. C. Conn, B.Sc., M.I.N.A.

of the Aerodynamics Department, N.P.L.

*Reports and Memoranda No.* 1891

*9th January*, 1941

APR 27 1942

*Summary.*—The accompanying tables and figures give those properties of the Standard Atmosphere which are required for the prediction and analysis of aircraft performance.

*Definition of Standard Atmosphere.*—In order to compare observations obtained in flight tests it is necessary to convert them to standard atmospheric conditions. In this connection an International Standard Atmosphere has been defined in the Official Bulletin of the International Commission on Air Navigation[1] and reproduced in Air Publication 1275[2]. The relevant portions of the definition may be summarised as follows :—

(*a*) *Temperature.*—The temperature is taken as 15°C. at sea level, with a constant rate of fall with height of 6·5° per km. up to 11 km. (the lower limit of the stratosphere) beyond which it remains constant at − 56·5°C.

(*b*) *Pressure.*—The pressure at sea level is that corresponding to a barometric height of 760 mm. of mercury at 0° C. with $g = 980{\cdot}62$ cm. per sec. per sec. The variation of pressure with height is given by the following formulae, which may be deduced from the gas law $p = \rho RT$ together with the relation $dp/dz = -\rho g$.

$$\frac{p_z}{p_0} = \left(\frac{288 - 6{\cdot}5\,z}{288}\right)^{5{\cdot}256} \qquad \text{for } z < 11 \quad .. \quad .. \quad .. \quad .. \quad .. \quad (1)$$

$$\text{and } \log_{10}\frac{p_{11}}{p_z} = \frac{z - 11}{14{\cdot}6} \qquad \text{for } z > 11, \quad .. \quad .. \quad .. \quad .. \quad .. \quad (2)$$

$z$ being the height in km.

(*c*) *Density.*—The density is 1·2257 kg. per cu. m. at sea level and varies according to the formulae

$$\frac{\rho_z}{\rho_0} = \left(\frac{288 - 6{\cdot}5\,z}{288}\right)^{4{\cdot}256} \qquad \text{for } z < 11 \quad .. \quad .. \quad .. \quad .. \quad .. \quad (3)$$

$$\text{and } \log_{10}\frac{\rho_{11}}{\rho_z} = \frac{z - 11}{14{\cdot}6} \qquad \text{for } z > 11. \quad .. \quad .. \quad .. \quad .. \quad .. \quad (4)$$

*Conversion to British Units.*—As the equivalent values in British units (column 3 of Table 1) are very close to round numbers, it was agreed between the Royal Aircraft Establishment and the National Physical Laboratory (May, 1925) that the rounded values of column 4 should be used in evaluating the temperature and pressure as functions of height ; the corresponding values agreed upon for pressures in inches of mercury were used as the basis of the calculations of the data of Table 2.

TABLE 1

| | | | |
|---|---|---|---|
| Rate of fall of temperature .. | 6·5° per km. | 1·9812° per 1,000 ft. | 1·98° per 1,000 ft. |
| Stratosphere (Eqns. (2) and (4)) .. | −56·5°C. at 11 km.<br>14·6 km. | −56·458°C. at 36,089·3 ft.<br>47,900·3 ft. | −56·5°C. at 36,090 ft.<br>47,900 ft. |

For the present work the further conversions involved were

980·62 cm. per sec. per sec. ($= g$) = 32·1726 ft. per sec. per sec.
760 mm. of mercury ($= p_0$) = 2116·21 lb. per sq. ft.
1·2257 kg.. per cu. m. ($= \rho_0$) = 0·00237835 slug per cu. ft.

These were calculated using the following relations* between the fundamental units :

1 kg. = 2·204622 lb.
1 m. = 39·37011 in.

The density of mercury was taken as 13·5951 gm. per cu. cm. at 0°C.

The velocity of sound at sea level was taken as the theoretical value

$$\sqrt{\gamma p/\rho} = 1{,}117 \text{ ft. per sec.},$$

where $\gamma$, the ratio of the specific heats, was taken as 1·403 (International Critical Tables)[3].

*Viscosity.*—The coefficient of viscosity ($\mu$) or kinematic viscosity ($\nu$) is required for calculating Reynolds number. For this purpose the variation of $\mu$ with temperature (T degrees Absolute) was assumed to follow Sutherland's formula

$$\mu = A \frac{T^{3/2}}{T+B},$$

the values used for A and B being those given by Goldstein[4], namely

A = 3·059 × $10^{-8}$ slug per ft. sec.
B = 114 degrees.

The experimental data used in deriving these values were obtained from the International Critical Tables[5] ; although the calculated values are quoted to four significant figures there may be some inaccuracy in the absolute value of the last figure, but it is considered that this uncertainty may be no more than the probable error of the available experimental data and in any case will have little practical effect on Reynolds number.

*Acknowledgement.*—The authors thank Mr. F. A. Gould of the Metrology Department, N.P.L. for helpful discussion of various points involved in the work.

## REFERENCES

1. International Commission on Air Navigation. Official Bulletin No. 7, p. 34, Dec. 1924.
2. Instrument Manual, Section IV, Chapter 1, Appendix II. Air Publication 1275, **1**, 1940.
3. International Critical Tables **5**, 81, 1929.
4. S. Goldstein. Private Communication.
5. International Critical Tables **5**, 2, 1929.

* The above relations received legal sanction by Order in Council of May, 1898 (Statutory Rules and Orders, 1898, No. 411).

# TABLE 2

## *Properties of the Standard Atmosphere*

List of symbols: $h$ = height; $t$ = temperature; $a$ = velocity of sound; $p$ = pressure; $\varrho$ = density; $\sigma$ = density relative to sea level; $\mu$ = coefficient of viscosity; $\nu$ = coefficient of kinematic viscosity

The suffix $(\ )_0$ refers to sea level ($h = 0$)

| $h$ ft. | $t$ °C. | $\frac{a}{a_0}$ | $a$ ft./sec. | $a$ m.p.h. | $\frac{p}{p_0}$ | $p$ lb./sq. ft. | $p$ millibars | $\sigma = \frac{\varrho}{\varrho_0}$ | $\varrho$ slug/cu. ft. | $\sigma^{\frac{1}{2}}$ | $\mu \times 10^7$ slug/ft. sec. | $\nu \times 10^4$ ft.²/sec. |
|---|---|---|---|---|---|---|---|---|---|---|---|---|
| 0 | 15·00 | 1·0000 | 1117 | 761·6 | 1·0000 | 2116·2 | 1013·2 | 1·0000 | 0·002378 | 1·0000 | 3·719 | 1·564 |
| 1,000 | 13·02 | 0·9966 | 1113 | 759·0 | 0·9644 | 2040·9 | 977·1 | 0·9711 | 0·002310 | 0·9854 | 3·699 | 1·602 |
| 2,000 | 11·04 | 0·9931 | 1109 | 756·3 | 0·9298 | 1967·7 | 942·1 | 0·9428 | 0·002242 | 0·9710 | 3·679 | 1·641 |
| 3,000 | 9·06 | 0·9896 | 1105 | 753·7 | 0·8963 | 1896·7 | 908·1 | 0·9152 | 0·002177 | 0·9566 | 3·659 | 1·681 |
| 4,000 | 7·08 | 0·9862 | 1102 | 751·0 | 0·8637 | 1827·7 | 875·1 | 0·8881 | 0·002112 | 0·9424 | 3·639 | 1·723 |
| 5,000 | 5·10 | 0·9827 | 1098 | 748·4 | 0·8321 | 1760·8 | 843·0 | 0·8617 | 0·002049 | 0·9283 | 3·618 | 1·766 |
| 6,000 | 3·12 | 0·9792 | 1094 | 745·7 | 0·8014 | 1696·0 | 812·0 | 0·8359 | 0·001988 | 0·9143 | 3·598 | 1·810 |
| 7,000 | + 1·14 | 0·9756 | 1090 | 743·0 | 0·7717 | 1633·0 | 781·8 | 0·8107 | 0·001928 | 0·9004 | 3·577 | 1·855 |
| 8,000 | − 0·84 | 0·9721 | 1086 | 740·4 | 0·7428 | 1571·9 | 752·6 | 0·7860 | 0·001869 | 0·8866 | 3·557 | 1·903 |
| 9,000 | − 2·82 | 0·9686 | 1082 | 737·7 | 0·7148 | 1512·8 | 724·3 | 0·7620 | 0·001812 | 0·8729 | 3·536 | 1·951 |
| 10,000 | − 4·80 | 0·9650 | 1078 | 734·9 | 0·6877 | 1455·4 | 696·8 | 0·7385 | 0·001756 | 0·8594 | 3·515 | 2·002 |
| 11,000 | − 6·78 | 0·9614 | 1074 | 732·2 | 0·6614 | 1399·8 | 670·2 | 0·7156 | 0·001702 | 0·8459 | 3·495 | 2·054 |
| 12,000 | − 8·76 | 0·9579 | 1070 | 729·5 | 0·6360 | 1345·9 | 644·4 | 0·6932 | 0·001649 | 0·8326 | 3·474 | 2·107 |
| 13,000 | −10·74 | 0·9543 | 1066 | 726·8 | 0·6113 | 1293·7 | 619·4 | 0·6714 | 0·001597 | 0·8194 | 3·453 | 2·163 |
| 14,000 | −12·72 | 0·9507 | 1062 | 724·0 | 0·5875 | 1243·2 | 595·2 | 0·6500 | 0·001546 | 0·8063 | 3·432 | 2·220 |
| 15,000 | −14·70 | 0·9470 | 1058 | 721·2 | 0·5644 | 1194·3 | 571·8 | 0·6292 | 0·001497 | 0·7933 | 3·411 | 2·280 |
| 16,000 | −16·68 | 0·9434 | 1054 | 718·5 | 0·5420 | 1147·0 | 549·1 | 0·6090 | 0·001448 | 0·7804 | 3·390 | 2·341 |
| 17,000 | −18·66 | 0·9397 | 1050 | 715·7 | 0·5203 | 1101·1 | 527·2 | 0·5892 | 0·001401 | 0·7676 | 3·369 | 2·404 |
| 18,000 | −20·64 | 0·9361 | 1046 | 712·9 | 0·4994 | 1056·9 | 506·0 | 0·5699 | 0·001355 | 0·7549 | 3·347 | 2·470 |
| 19,000 | −22·62 | 0·9324 | 1041 | 710·1 | 0·4792 | 1014·0 | 485·5 | 0·5511 | 0·001311 | 0·7424 | 3·326 | 2·538 |
| 20,000 | −24·60 | 0·9287 | 1037 | 707·3 | 0·4596 | 972·6 | 465·6 | 0·5328 | 0·001267 | 0·7299 | 3·305 | 2·608 |
| 21,000 | −26·58 | 0·9250 | 1033 | 704·5 | 0·4406 | 932·5 | 446·4 | 0·5150 | 0·001225 | 0·7176 | 3·283 | 2·681 |
| 22,000 | −28·56 | 0·9213 | 1029 | 701·6 | 0·4223 | 893·8 | 427·9 | 0·4976 | 0·001183 | 0·7054 | 3·262 | 2·757 |
| 23,000 | −30·54 | 0·9175 | 1025 | 698·8 | 0·4047 | 856·4 | 410·0 | 0·4807 | 0·001143 | 0·6933 | 3·240 | 2·834 |
| 24,000 | −32·52 | 0·9138 | 1021 | 695·9 | 0·3876 | 820·3 | 392·7 | 0·4642 | 0·001104 | 0·6813 | 3·218 | 2·915 |
| 25,000 | −34·50 | 0·9100 | 1017 | 693·1 | 0·3711 | 785·3 | 376·0 | 0·4481 | 0·001066 | 0·6694 | 3·196 | 2·999 |
| 26,000 | −36·48 | 0·9062 | 1012 | 690·2 | 0·3552 | 751·7 | 359·9 | 0·4325 | 0·001029 | 0·6576 | 3·174 | 3·087 |
| 27,000 | −38·46 | 0·9024 | 1008 | 687·3 | 0·3399 | 719·2 | 344·3 | 0·4173 | 0·000993 | 0·6460 | 3·153 | 3·177 |
| 28,000 | −40·44 | 0·8986 | 1004 | 684·4 | 0·3251 | 687·9 | 329·3 | 0·4025 | 0·000957 | 0·6345 | 3·130 | 3·270 |
| 29,000 | −42·42 | 0·8948 | 999 | 681·5 | 0·3108 | 657·6 | 314·9 | 0·3882 | 0·000923 | 0·6230 | 3·108 | 3·367 |
| 30,000 | −44·40 | 0·8909 | 995 | 678·5 | 0·2970 | 628·5 | 300·9 | 0·3741 | 0·000890 | 0·6116 | 3·086 | 3·469 |
| 31,000 | −46·38 | 0·8871 | 991 | 675·6 | 0·2837 | 600·4 | 287·5 | 0·3606 | 0·000858 | 0·6005 | 3·064 | 3·573 |
| 32,000 | −48·36 | 0·8832 | 987 | 672·6 | 0·2709 | 573·3 | 274·5 | 0·3473 | 0·000826 | 0·5894 | 3·041 | 3·682 |
| 33,000 | −50·34 | 0·8793 | 982 | 669·7 | 0·2586 | 547·3 | 262·0 | 0·3345 | 0·000796 | 0·5784 | 3·019 | 3·795 |
| 34,000 | −52·32 | 0·8754 | 978 | 666·7 | 0·2467 | 522·2 | 250·0 | 0·3220 | 0·000766 | 0·5675 | 2·997 | 3·913 |
| 35,000 | −54·30 | 0·8714 | 973 | 663·7 | 0·2353 | 498·0 | 238·4 | 0·3099 | 0·000737 | 0·5567 | 2·974 | 4·036 |
| 36,000 | −56·28 | 0·8675 | 969 | 660·7 | 0·2244 | 474·8 | 227·3 | 0·2981 | 0·000709 | 0·5460 | 2·951 | 4·159 |
| 36,090 | −56·5 | 0·8670 | 968 | 660·3 | 0·2234 | 472·7 | 226·3 | 0·2972 | 0·000707 | 0·5451 | 2·948 | 4·172 |
| 36,090 | −56·5 | 0·8670 | 968 | 660·3 | 0·2234 | 472·7 | 226·3 | 0·2972 | 0·0007068 | 0·5451 | 2·948 | 4·172 |
| 37,000 | −56·5 | 0·8670 | 968 | 660·3 | 0·2138 | 452·5 | 216·7 | 0·2845 | 0·0006766 | 0·5334 | 2·948 | 4·358 |
| 38,000 | −56·5 | 0·8670 | 968 | 660·3 | 0·2038 | 431·2 | 206·5 | 0·2711 | 0·0006448 | 0·5207 | 2·948 | 4·573 |
| 39,000 | −56·5 | 0·8670 | 968 | 660·3 | 0·1942 | 411·0 | 196·8 | 0·2584 | 0·0006145 | 0·5083 | 2·948 | 4·799 |
| 40,000 | −56·5 | 0·8670 | 968 | 660·3 | 0·1851 | 391·8 | 187·6 | 0·2463 | 0·0005857 | 0·4963 | 2·948 | 5·034 |
| 41,000 | −56·5 | 0·8670 | 968 | 660·3 | 0·1764 | 373·4 | 178·8 | 0·2347 | 0·0005582 | 0·4845 | 2·948 | 5·282 |
| 42,000 | −56·5 | 0·8670 | 968 | 660·3 | 0·1681 | 355·8 | 170·4 | 0·2237 | 0·0005320 | 0·4730 | 2·948 | 5·542 |
| 43,000 | −56·5 | 0·8670 | 968 | 660·3 | 0·1603 | 339·1 | 162·4 | 0·2132 | 0·0005071 | 0·4617 | 2·948 | 5·815 |
| 44,000 | −56·5 | 0·8670 | 968 | 660·3 | 0·1527 | 323·2 | 154·8 | 0·2032 | 0·0004833 | 0·4508 | 2·948 | 6·102 |
| 45,000 | −56·5 | 0·8670 | 968 | 660·3 | 0·1456 | 308·0 | 147·5 | 0·1936 | 0·0004605 | 0·4400 | 2·948 | 6·403 |
| 46,000 | −56·5 | 0·8670 | 968 | 660·3 | 0·1387 | 293·6 | 140·6 | 0·1846 | 0·0004390 | 0·4296 | 2·948 | 6·718 |
| 47,000 | −56·5 | 0·8670 | 968 | 660·3 | 0·1322 | 279·8 | 134·0 | 0·1759 | 0·0004184 | 0·4194 | 2·948 | 7·049 |
| 48,000 | −56·5 | 0·8670 | 968 | 660·3 | 0·1260 | 266·6 | 127·7 | 0·1676 | 0·0003987 | 0·4094 | 2·948 | 7·396 |
| 49,000 | −56·5 | 0·8670 | 968 | 660·3 | 0·1201 | 254·1 | 121·7 | 0·1598 | 0·0003800 | 0·3997 | 2·948 | 7·761 |
| 50,000 | −56·5 | 0·8670 | 968 | 660·3 | 0·1145 | 242·2 | 116·0 | 0·1523 | 0·0003622 | 0·3902 | 2·948 | 8·141 |

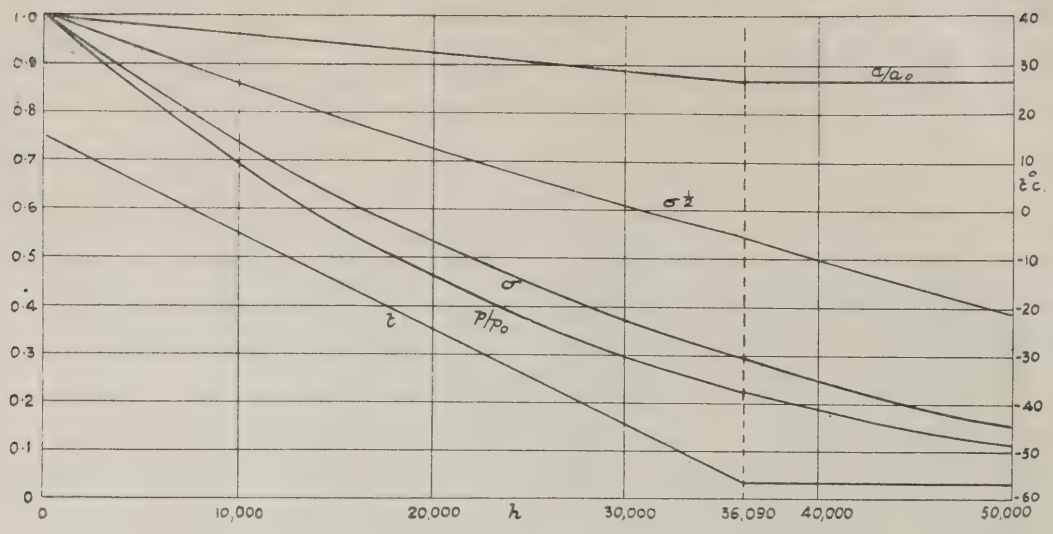


FIG. 1.—Properties of standard atmosphere.

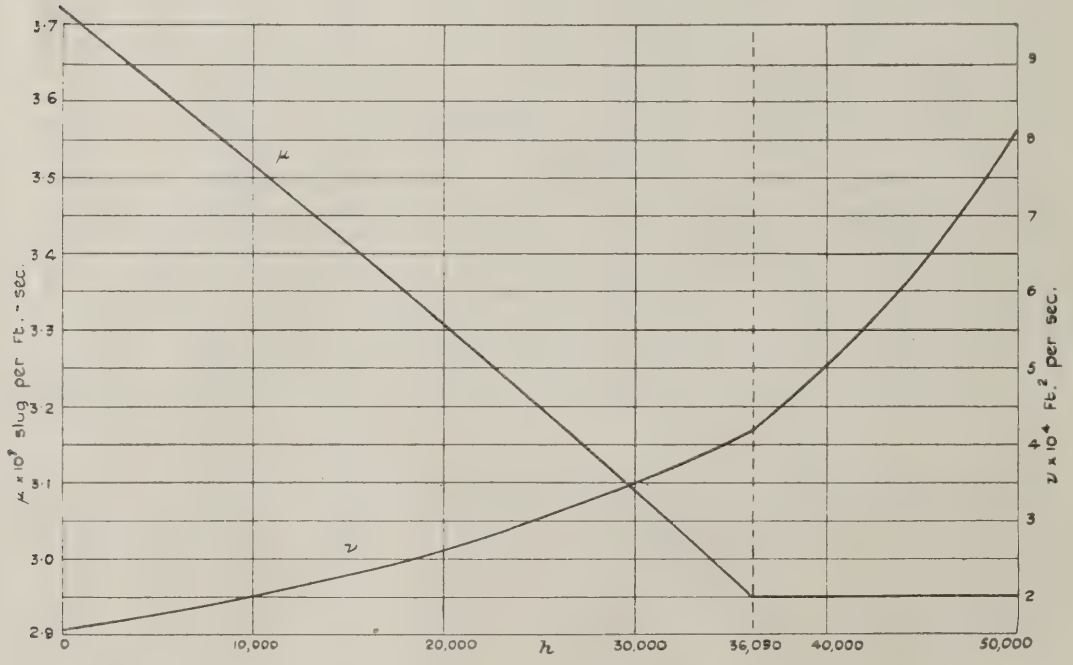


FIG. 2.—Variation of viscosity with height.

(55239) Wt. 500 6/41 Hw. G. 377 1

## SYSTEM OF AXES

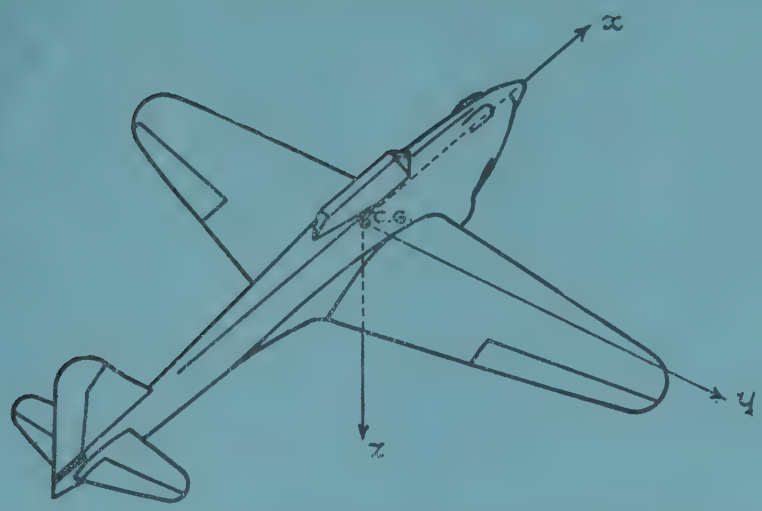


| Axes | Symbol Designation Positive direction | $x$ longitudinal forward | $y$ lateral starboard | $z$ normal downward |
|---|---|---|---|---|
| Force | Symbol | X | Y | Z |
| Moment | Symbol<br>Designation | L<br>rolling | M<br>pitching | N<br>yawing |
| Angle of Rotation | Symbol | $\phi$ | $\theta$ | $\psi$ |
| Velocity | Linear<br>Angular | $u$<br>$p$ | $v$<br>$q$ | $w$<br>$r$ |
| Moment of Inertia | | A | B | C |

Components of linear velocity and force are positive in the positive direction of the corresponding axis.

Components of angular velocity and moment are positive in the cyclic order $y$ to $z$ about the axis of $x$, $z$ to $x$ about the axis of $y$, and $x$ to $y$ about the axis of $z$.

The angular movement of a control surface (elevator or rudder) is governed by the same convention, the elevator angle being positive downwards and the rudder angle positive to port. The aileron angle is positive when the starboard aileron is down and the port aileron is up. A positive control angle normally gives rise to a negative moment about the corresponding axis.

The symbols for the control angles are :—

- $\xi$ aileron angle
- $\eta$ elevator angle
- $\eta_T$ tail setting angle
- $\zeta$ rudder angle

# Publications of the Aeronautical Research Committee

TECHNICAL REPORTS OF THE AERONAUTICAL RESEARCH COMMITTEE—

1933-34 Vol. I. Aerodynamics. £1 5s.
Vol. II. Structures, Engines, Instruments, etc. £1 10s.

1934-35 Vol. I. Aerodynamics. £2.
Vol. II. Seaplanes, Structures, Engines, Materials, etc. £2.

1935-36 Vol. I. Aerodynamics. £1 10s.
Vol. II. Structures, Flutter, Engines, Seaplanes, etc. £1 10s.

1936 Vol. I. Aerodynamics General, Performance, Airscrews, Flutter and Spinning. £2.
Vol. II. Stability and Control, Structures, Seaplanes, Engines, etc. £2 10s.

ANNUAL REPORTS OF THE AERONAUTICAL RESEARCH COMMITTEE—

1933-34 1s. 6d.
1934-35 1s. 6d.
April 1, 1935 to December 31, 1936. 4s.
1937 2s.

INDEX TO THE TECHNICAL REPORTS OF THE ADVISORY COMMITTEE ON AERONAUTICS—

1909-1919 Reports and Memoranda No. 1600. 8s.

NUMERICAL LISTS OF REPORTS AND MEMORANDA published between 1909 and 1936—

Reports and Memoranda Nos. 650 (9d.), 750 (6d.), 850 (1d.), 950 (4d.), 1050 (4d.), 1150 (4d.) (*Out of print*), 1250 (6d.) (*Out of print*), 1350 (6d.) (*Out of print*), 1450 (6d.), 1550 (6d.), 1650 (6d.), 1750 (1s. 3d.)

LIST OF PUBLICATIONS ON AERONAUTICS—

Aeronautical Research Committee Publications (classified under subjects). Post free on application.

*Prices are net and postage extra.*

## His Majesty's Stationery Office

London W.C.2 : York House, Kingsway
Edinburgh 2 : 120 George Street
Manchester 2 : 39-41 King Street
Cardiff : 1 St. Andrew's Crescent
Belfast : 80 Chichester Street
or through any bookseller.

S.O. Code No. 23-1891

LIBRARY
UNIVERSITY OF ILLINOIS
URBANA

629.13
G79r
no. 1892

R. & M. No. 1892
(4734)
A.R.C. Technical Report

MINISTRY OF AIRCRAFT PRODUCTION

AERONAUTICAL RESEARCH COMMITTEE
REPORTS AND MEMORANDA

# Drag of Circular Cylinders in Flight

*By*

A. V. Stephens, M.A.

*Crown Copyright Reserved*

LONDON : HIS MAJESTY'S STATIONERY OFFICE
Price 2*s.* 0*d.* net

# AERODYNAMIC SYMBOLS

## 1. GENERAL

$m$ Mass

$t$ Time

V Resultant linear velocity

$\Omega$ Resultant angular velocity

$\rho$ Density, $\sigma$ relative density

$\nu$ Kinematic coefficient of viscosity

R Reynolds number, $R = lV/\nu$ (where $l$ is a suitable linear dimension)

Normal temperature and pressure for aeronautical work are 15° C and 760 mm.

For air under these conditions $\begin{cases} \rho = 0{\cdot}002378 \text{ slug/cu. ft.} \\ \nu = 1{\cdot}56 \times 10^{-4} \text{ ft.}^2\text{/sec.} \end{cases}$

The slug is taken to be 32·2 lb.-mass.

$\alpha$ Angle of incidence

$\epsilon$ Angle of downwash

S Area

$b$ Span

$c$ Chord

A Aspect ratio, $A = b^2/S$

L Lift, with coefficient $C_L = L/\frac{1}{2}\rho V^2 S$

D Drag, with coefficient $C_D = D/\frac{1}{2}\rho V^2 S$

$\gamma$ Gliding angle, $\tan\gamma = D/L$

L Rolling moment, with coefficient $C_l = L/\frac{1}{2}\rho V^2 bS$

M Pitching moment, with coefficient $C_m = M/\frac{1}{2}\rho V^2 cS$

N Yawing moment, with coefficient $C_n = N/\frac{1}{2}\rho V^2 bS$

## 2. AIRSCREWS

$n$ Revolutions per second

D Diameter

J $V/nD$

P Power

T Thrust, with coefficient $k_T = T/\rho n^2 D^4$

Q Torque, with coefficient $k_Q = Q/\rho n^2 D^5$

$\eta$ Efficiency, $\eta = TV/P = Jk_T/2\pi k_Q$

# Drag of Circular Cylinders in Flight

*By*

A. V. Stephens, M.A.

Communicated by the Director of Scientific Research, Ministry of Aircraft Production.

*Reports and Memoranda No.* 1892

*9th October*, 1940*

*Summary—Reasons for enquiry.*—Measurements of the drag of a circular cylinder in flight were required.

*Range of investigation.*—Measurements of the drag of smooth cylinders 2 in. and 3 in. in diameter of effective length 5 ft., were made made over a speed range of 100 to 200 m.p.h. in non-turbulent air. The effects of roughening the surface were investigated.

*Conclusions.*—The sharp fall in the drag coefficient characteristic of circular cylinders occurred at approximately the same Reynolds number in flight as had previously been found in low turbulence wind tunnels. Roughening the cylinder caused this fall to occur at a lower Reynolds number, but the lowest drag coefficient then reached was greater than that of the smooth cylinder.

The following values for the greatest drag per ft. run of smooth and rough cylinders at indicated speeds up to 250 m.p.h. at 15,000 ft. illustrate the magnitude of these effects.

| Diameter, in. | Drag per ft. run, lb. | |
|---|---|---|
| | Smooth. | Rough. |
| 1 | 14·0 | 14·0 |
| 1½ | 21·0 | 12·7 |
| 2 | 24·0 | 12·7 |
| 2½ | 19·0 | 16·0 |
| 3 | 14·7 | 19·2 |

The roughness which produced the above results was such as to show the greatest reduction in drag. On a cylinder 2 in. in diameter it consisted of sharp particles of abrasive approximately 0·001 in. high. It should be emphasised that the above results apply only to cylinders in non-turbulent air.

*Introduction.*—Much data has been collected on the drag of circular cylinders in wind tunnels [1, 2]. In all tests the drag coefficient is found to maintain a steady value of approximately 1·2 up to a certain Reynolds number and then to fall progressively to a much lower value. The lower the turbulence and the smoother the cylinder the higher does this Reynolds number become. It is now well established[3] that no turbulence of an intensity and scale likely to promote transition is to be found in the free atmosphere. It therefore seemed possible that the sudden fall in the drag coefficient might be delayed to a considerably higher Reynolds number than had been found in these experiments, in the case of a cylinder carried on an aeroplane. In fact on the basis of the wind tunnel data it was found impossible to predict the drag of a particular cylinder some 2 in. in diameter attached to a high performance aeroplane without a possible error of even 100 per cent. A simple experiment was therefore conducted in flight to provide further data.

* R.A.E. Report, May, 1940.

*Method of experiment.*—A steel tube 7 ft. long and 2 in. in diameter was mounted so as to project vertically out of the gun turret of a Blenheim aeroplane for a distance of 5 ft. It was thus well clear of the slipstreams. The tube was rigidly attached to the gun mounting and arrangements were made to determine its resistance by measuring the deflection of the tube itself at a point 18 in. from the fixed end.

For this purpose an Ames dial was mounted on a stanchion based upon a stout steel plate welded to the bottom of the cylinder. This arrangement is shown in Fig. 1. The apparatus was calibrated on the ground by applying known loads to the centre of the protruding part of the cylinder and noting the corresponding deflections. The drag of the cylinder in flight could then be obtained by reading the Ames dial. Strictly speaking this method involved the assumption that the resultant drag occurred at the centre of the exposed cylinder. This could not be guaranteed because the air velocity along the cylinder was probably not exactly constant. There was also a probability of end effect. In point of fact neither of these uncertainties vitiated the experiments, because the cylinder tested was of the same general proportions as that to which it was proposed to apply the results. It should be noted that the deflection of the cylinder was taken at a point relatively near the fixed end so that the deflection was in effect a measure of the torque, due to the resultant wind force on the cylinder, about an axis through the fixed end of the cylinder. Beam theory shows that even if the resultant force occurred at a point 6 in. above the centre of the protruding part of the cylinder the Ames dial would indicate its torque about the end of the cylinder correct to $1\frac{1}{2}$ per cent. The use of this crude and convenient method of measurement was justified by the results obtained. The maximum and minimum drag coefficients of a smooth cylinder agreed reasonably well with the results of previous measurements in wind tunnels, so there was no reason to doubt the intermediate values which were of primary interest in the present tests.

The inclination of the cylinder to the vertical in horizontal flight ranged from 1° at an indicated speed of 220 m.p.h. to $7\frac{1}{2}$° at 100 m.p.h. Due to downwash effects it is probable that the cylinder was approximately perpendicular to the local air stream at all speeds. Owing to the inclination of the cylinder to the vertical, small corrections were made to the measured drag to allow for the component of the weight of the cylinder in this direction.

The local velocity at a point 1 ft. in front of the centre of the exposed part of the cylinder was measured by means of a swivelling pitot-static head attached to the cylinder itself during one flight. Having established the relation between local indicated speed and ordinary A.S.I. reading all drag measurements were made by reference to the latter, with the swivelling pitot removed.

The Reynolds number was calculated on the basis of the local speed at the cylinder. Air density and viscosity were obtained from readings of aneroid and air thermometer. The range of Reynolds number covered by the experiments was extended by fitting a cylinder 3 in. in diameter for the outer five feet of the 2-in. cylinder for some of the tests.

*Results—Smooth cylinder.*—Data obtained on the drag of smooth cylinders is given in Fig. 2. It will be seen that the nature of the surface was varied during the tests. For the first flights with the 2-in. cylinder the steel was simply polished with fine emery paper and left bare. When it became apparent that the results were highly sensitive to the nature of the surface the tests were repeated with the 3-in. cylinder in a very smooth condition. The surface was filled and given a number of coats of cellulose paint in accordance with modern practice for high-grade coachwork. A high polish resulted and every confidence could be felt that the cylinder was then aerodynamically smooth. All the results were probably affected to some extent by vibration of the cylinder. This was most noticeable on the larger cylinder at the lower speeds. In drawing a curve through these points the results for the 2-in. cylinder have therefore been given more weight than those for the 3-in. cylinder at Reynolds numbers around $3 \times 10^5$. The curve has also been drawn through the set of points giving the higher drag for the 2-in. cylinder, as it is considered that the cylinder must have been smoother on this occasion than for the previous flight.

It had been repolished between the two flights to remove traces of rust. The results of experiments in the C.A.T. by Mr. E. F. Relf are given for comparison, and in order to provide a basis for extrapolating the flight results to higher Reynolds numbers than were covered by the test.

*Drag of rough cylinder.*—During the tests it was noticed that the drag of the 2-in. cylinder was greatly reduced when flying through cloud. It was therefore decided to make tests of artificially roughened cylinders to see whether practical use could be made of this phenomenon. As is usual in experiments of this nature difficulty was experienced in specifying the nature of the surfaces tested. The present tests were mainly exploratory and the surfaces will therefore be related merely to the processes by which they were produced.

1. *Extreme roughness.*—The cylinder was sprinkled with fine sand while the paint was still wet and then re-sprayed with paint. The resulting surface resembled a coarse sand paper.

2. *Moderate roughness.*—The cylinder was sprayed while wet with a fine silicon abrasive. The surface was examined with a microscope and found to consist of closely packed sharp cornered particles averaging perhaps 0·001 in. interspersed with isolated particles of 0·003 in. to 0·005 in.

3. *Slight roughness.*—The surface was prepared as for (2) but rubbed down with fine sand paper. This removed the larger isolated particles, leaving the equivalent of a very fine emery paper.

4. *Stove enamelled.*—The cylinder was polished with emery and given one coat of glossy stove enamel. Under the microscope some of the scratches due to polishing appeared and the surface was found to be composed of " orange peel " markings.

The curves of drag coefficient against Reynolds number are plotted in Fig. 3 for the surface in these four conditions. The curve for smooth cylinders from Fig. 2 is given for purposes of comparison. It will be seen that roughening has two distinct effects, both of which increase progressively with the degree of roughness over the range covered. Firstly, the fall in drag coefficient occurs at lower Reynolds numbers and, secondly, the drag coefficient reached after the critical change becomes progressively increased. Even though the degree of roughness of the cylinders tested has not been precisely defined, the curves taken together give a good idea of the lowest drag coefficient that can be obtained by roughening at any Reynolds number between $2\times10^5$ and $5\times10^5$.

*Application of results.*—Some consideration is required to apply the results obtained to design a cylinder giving the least drag in a practical case. It will be readily seen that over limited ranges of Reynolds number the drag of a cylinder can be reduced—

(*a*) by increasing the diameter,

(*b*) by roughening the surface.

Both these expedients will, however, increase the drag at Reynolds numbers outside these ranges. The maximum effects obtainable by either method are large and seem to warrant investigation. In approaching the problem it will be assumed that it is the greatest drag which can be encountered under any probable circumstances of flight which will be of primary concern to the designer. This greatest drag will not necessarily occur at the greatest indicated speed to be reached.

*Effect of diameter on maximum drag of cylinder up to a particular speed.*—In Figures 4 (*a*) and 4 (*b*) curves are given for the actual drag per foot run of smooth cylinders of diameter 1 in. to 3 in. at indicated speeds up to 350 m.p.h. Values are computed for sea level and an altitude of 15,000 ft. These curves are based entirely on the single experimental curve of Fig. 2 but present the results in a form more suitable for the present purpose. From these curves it is possible to read off the greatest drag reached up to a given speed at a given altitude. Values of greatest drag have been plotted against diameter in Fig. 5 for indicated speeds up to 250, 300 and 350 m.p.h.

The possibilities of reducing the drag of existing cylinders by increasing the diameter can be easily assessed from this diagram. It should, however, be stressed that these results apply only to very smooth cylindrical sections in an airstream free from turbulence. For a cylinder in a slipstream it would probably not be advantageous to increase the diameter.

*Effect of roughness on drag of cylinder.*—From the curves of Fig. 3 it appears that the surface designated as " slight roughness " gives the greatest reduction of drag obtainable by roughening at a Reynolds number of $3\times10^5$. At this Reynolds number the drag of a smooth cylinder is reduced by 52 per cent. and some reduction is obtained between $1{\cdot}6\times10^5$ and $3{\cdot}9\times10^5$. On the other hand at $4{\cdot}5\times10^5$ the drag is increased by 80 per cent. by this degree of roughness. In order to simplify the problem this roughness will be adopted for purposes of computation. It should be remembered that in applying the results to cylinders of size different from the test cylinder the scale of the roughness should be considered to be increased in proportion to the diameter of the cylinder.

Taking the curve for slight roughness in Fig. 3, values of the actual drag of cylinders of various diameters have been computed for indicated speeds up to 350 m.p.h. and altitudes of 0 ft. and 15,000 ft. In all cases it was found that the curves of drag against speed did not reach maxima at any point in the speed range. In consequence the greatest drag encountered up to a given speed is merely the drag at that speed. The values of the actual drags per foot run at indicated speeds of 250, 300 and 350 m.p.h. have been plotted against cylinder diameter in Fig. 6 (*a*) and 6 (*b*), for comparison with the corresponding curves from Fig. 5. These figures indicate the advantage that can be obtained by " roughening slightly " if the diameter of the cylinder and the maximum indicated speed are known. The curves also set limits to the maximum drag that may be expected for ordinary commercial finishes.

---

## REFERENCES


| *No.* | *Author.* | *Title, etc.* |
|---|---|---|
| 1. | A. Fage and J. H. Warsap .. .. | The effects of turbulence and surface roughness on the drag of a circular cylinder. R. & M. No. 1283. October, 1929. |
| 2. | A. Fage .. .. .. .. | Drag of circular cylinders and spheres. R. & M. No. 1370. May, 1940. |
| 3. | A. V. Stephens and A. A. Hall .. | Hot wires in flight. Proceedings of Fifth International Congress for Applied Mechanics. September, 1938. |

FIG. 1.

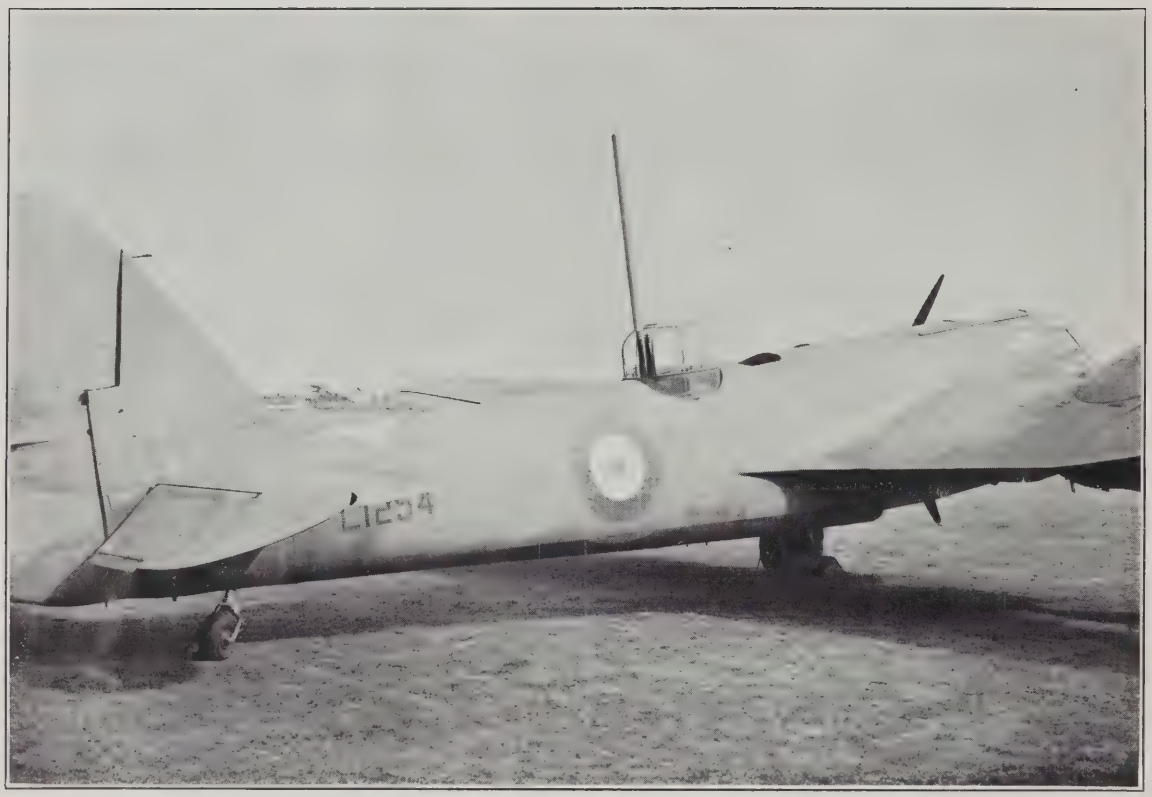

FIG. 1A.

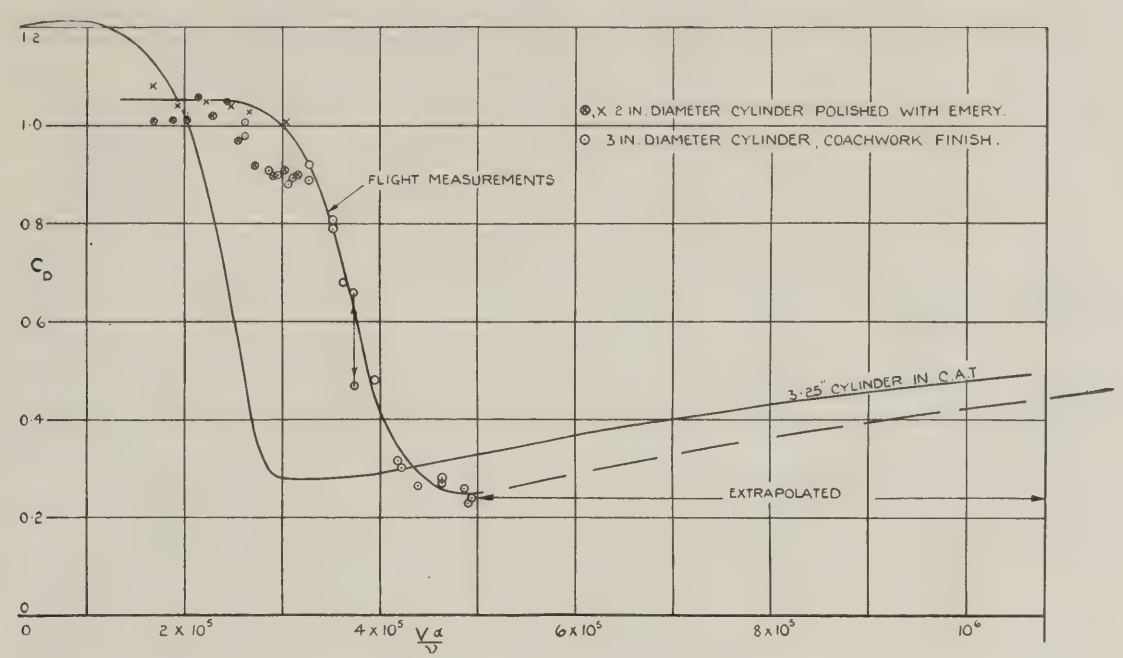


FIG. 2. Drag of smooth cylinders.

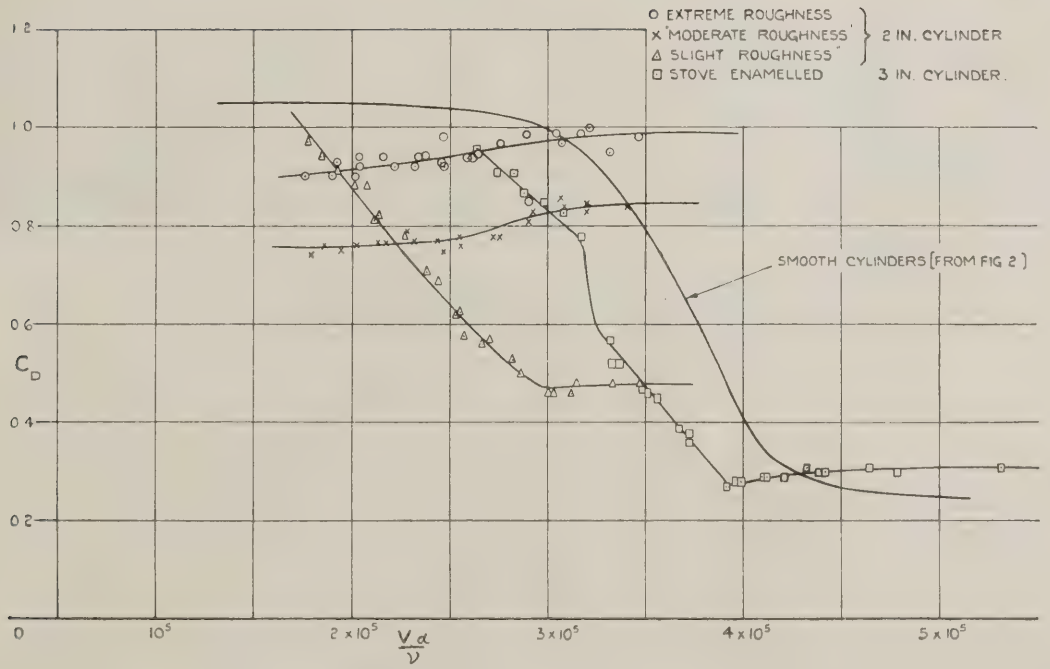


FIG. 3. Drag of rough cylinders.

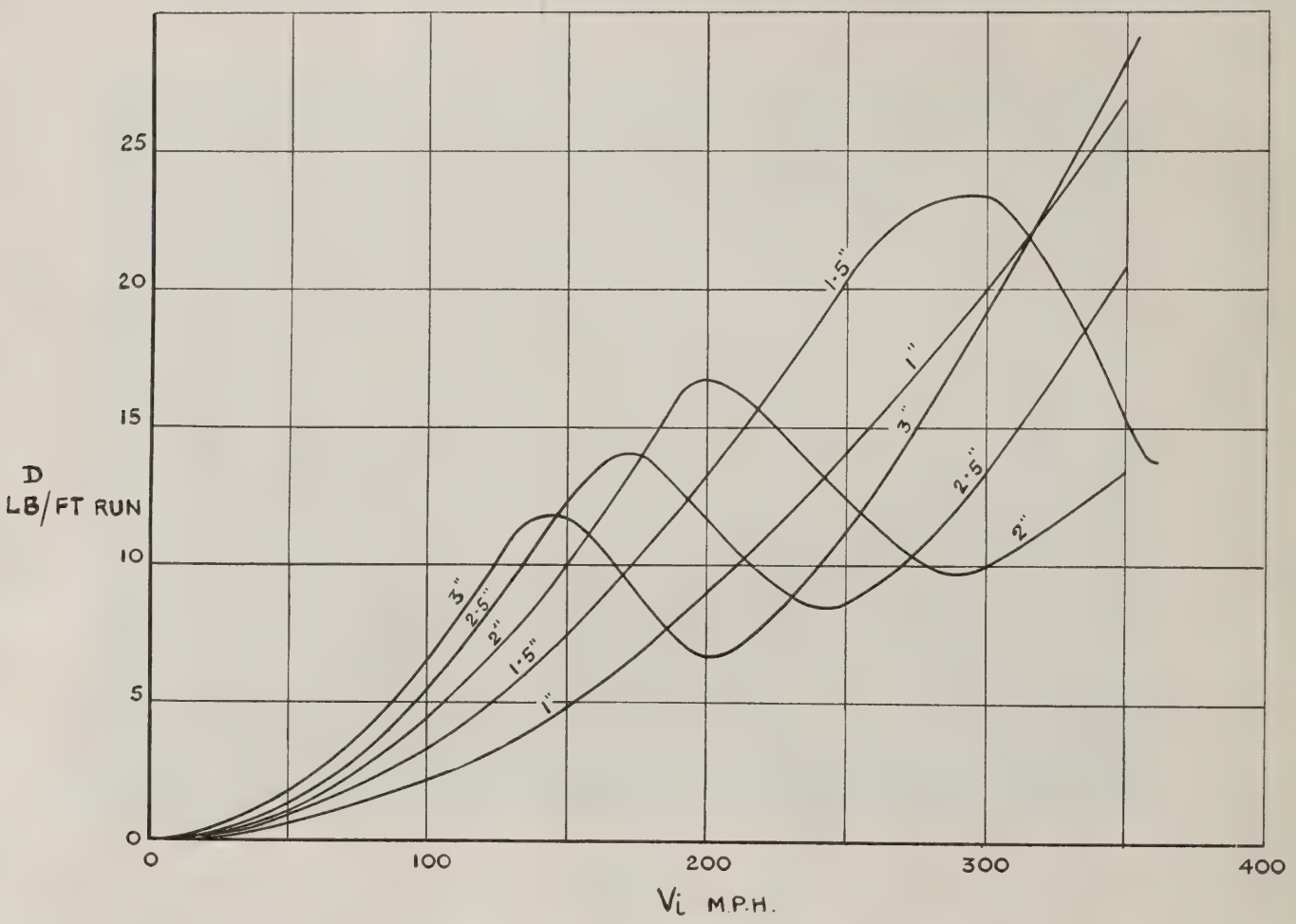


FIG. 4A. Drag of smooth cylinders at sea level.

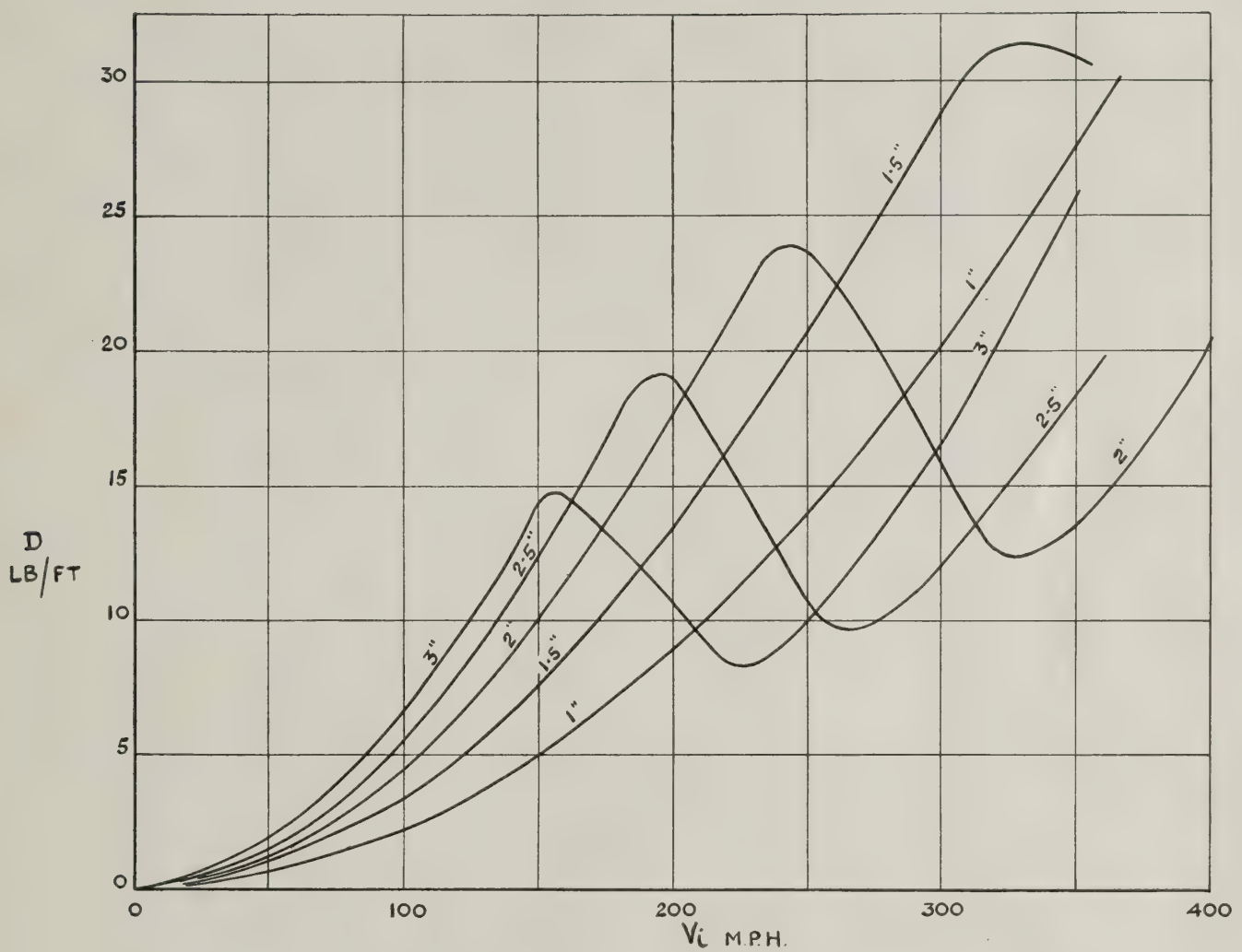


FIG. 4B. Drag of smooth cylinders at 15,000 feet.

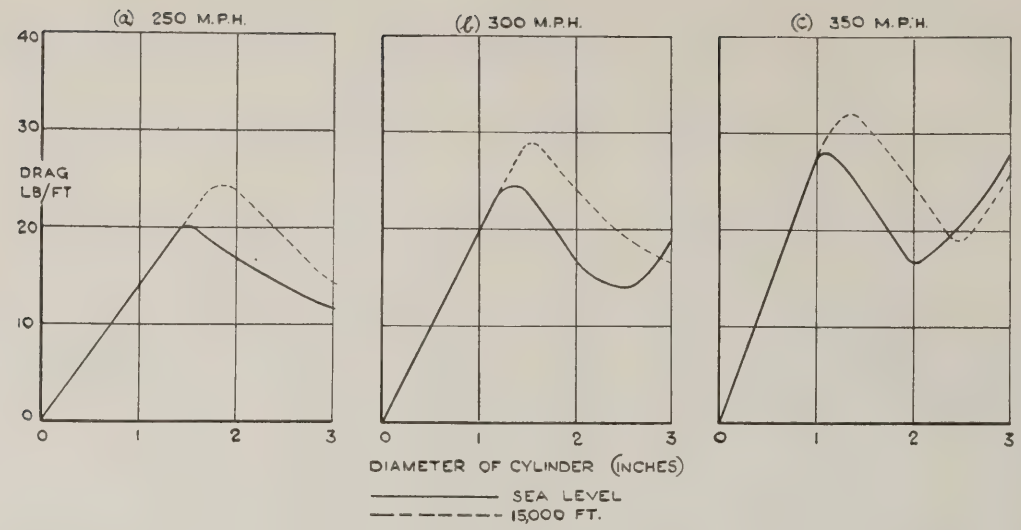


FIG. 5. Effect of diameter on greatest drag of smooth cylinder up to various indicated speeds.

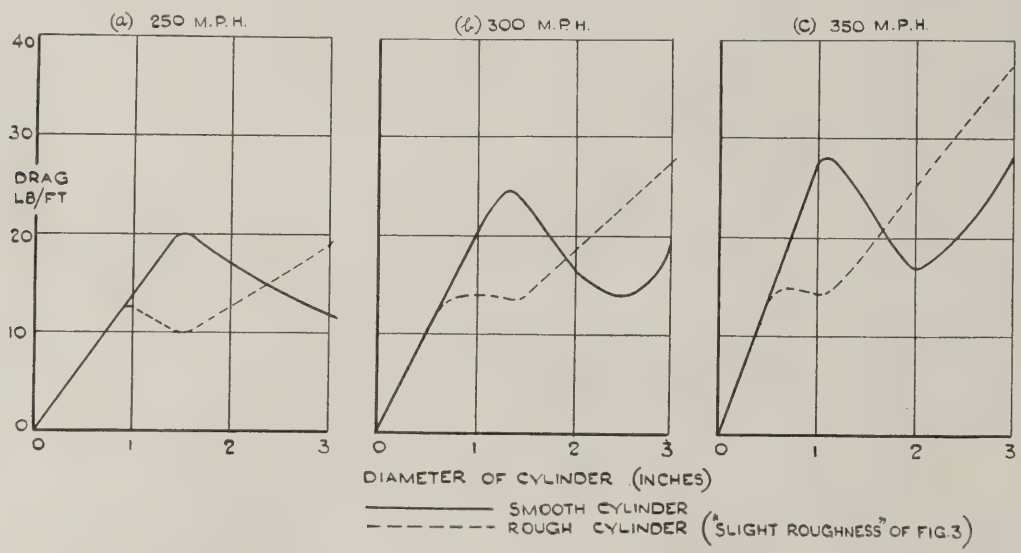


FIG. 6A. Effect of roughness on greatest drag of cylinder up to various speeds at sea level.

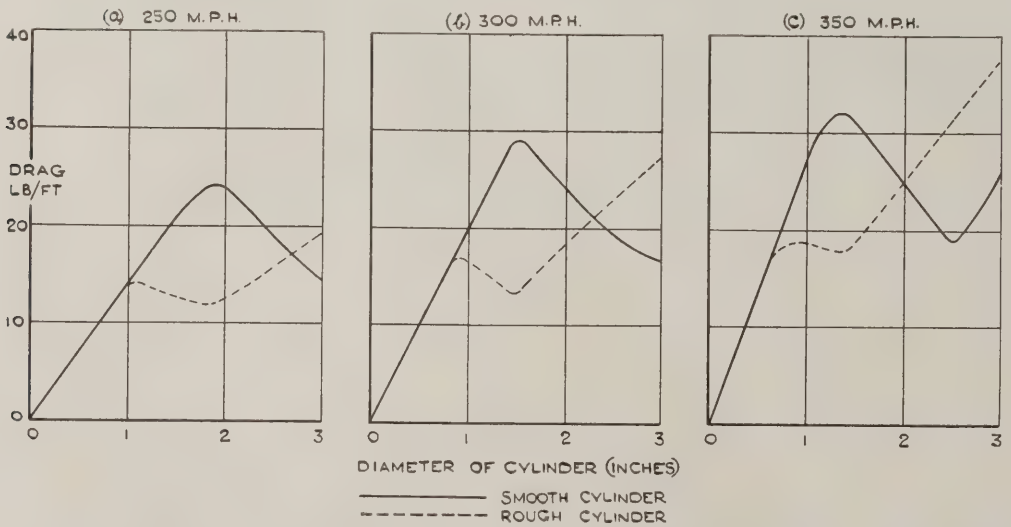


FIG. 6B. Effect of roughness on greatest drag of cylinder up to various indicated speeds at 15,000 feet.

(56096) Wt. 5/536 500 7/41 Hw. 377/1

## SYSTEM OF AXES

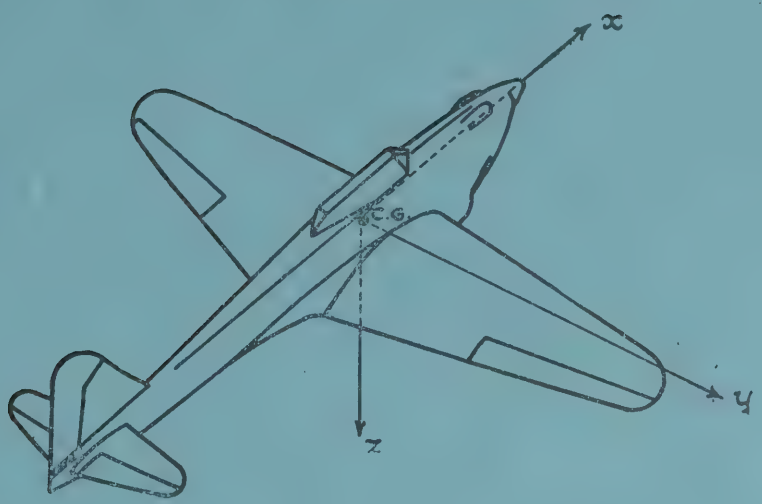


| Axes | Symbol Designation Positive direction | $x$ longitudinal forward | $y$ lateral starboard | $z$ normal downward |
|---|---|---|---|---|
| Force | Symbol | X | Y | Z |
| Moment | Symbol Designation | L rolling | M pitching | N yawing |
| Angle of Rotation | Symbol | $\phi$ | $\theta$ | $\psi$ |
| Velocity | Linear Angular | $u$ $p$ | $v$ $q$ | $w$ $r$ |
| Moment of Inertia | | A | B | C |

Components of linear velocity and force are positive in the positive direction of the corresponding axis.

Components of angular velocity and moment are positive in the cyclic order $y$ to $z$ about the axis of $x$, $z$ to $x$ about the axis of $y$, and $x$ to $y$ about the axis of $z$.

The angular movement of a control surface (elevator or rudder) is governed by the same convention, the elevator angle being positive downwards and the rudder angle positive to port. The aileron angle is positive when the starboard aileron is down and the port aileron is up. A positive control angle normally gives rise to a negative moment about the corresponding axis.

The symbols for the control angles are :—

- $\xi$ aileron angle
- $\eta$ elevator angle
- $\eta_T$ tail setting angle
- $\zeta$ rudder angle

# Publications of the Aeronautical Research Committee

TECHNICAL REPORTS OF THE AERONAUTICAL RESEARCH COMMITTEE—

1933-34 Vol. I. Aerodynamics. £1 5*s*.
Vol. II. Structures, Engines, Instruments, etc. £1 10*s*.

1934-35 Vol. I. Aerodynamics. £2.
Vol. II. Seaplanes, Structures, Engines, Materials, etc. £2.

1935-36 Vol. I. Aerodynamics. £1 10*s*.
Vol. II. Structures, Flutter, Engines, Seaplanes, etc. £1 10*s*.

1936 Vol. I. Aerodynamics General, Performance, Airscrews, Flutter and Spinning. £2.
Vol. II. Stability and Control, Structures, Seaplanes, Engines, etc. £2 10*s*.

ANNUAL REPORTS OF THE AERONAUTICAL RESEARCH COMMITTEE—

1933-34 1*s*. 6*d*.
1934-35 1*s*. 6*d*.
April 1, 1935 to December 31, 1936. 4*s*.
1937 2*s*.

INDEX TO THE TECHNICAL REPORTS OF THE ADVISORY COMMITTEE ON AERONAUTICS—

1909-1919 Reports and Memoranda No. 1600. 8*s*.

NUMERICAL LISTS OF REPORTS AND MEMORANDA published between 1909 and 1936—

Reports and Memoranda Nos. 650 (9*d*.), 750 (6*d*.), 850 (1*d*.), 950 (4*d*.), 1050 (4*d*.), 1150 (4*d*.) (*Out of print*), 1250 (6*d*.) (*Out of print*), 1350 (6*d*.) (*Out of print*), 1450 (6*d*.), 1550 (6*d*.), 1650 (6*d*.), 1750 (1*s*. 3*d*.)

LIST OF PUBLICATIONS ON AERONAUTICS—

Aeronautical Research Committee Publications (classified under subjects). Post free on application

*Prices are net and postage extra.*

## His Majesty's Stationery Office

London W.C.2 : York House, Kingsway

Edinburgh 2 : 120 George Street
Manchester 2 : 39-41 King Street
Cardiff : 1 St. Andrew's Crescent
Belfast : 80 Chichester Street

or through any bookseller.

S.O. Code No. 23-1892

629.13
G79r
no.1893

Engrg.

R. & M. No. 1893
(5127)
A.R.C. Technical Report

MINISTRY OF AIRCRAFT PRODUCTION

REPORTS AND MEMORANDA

# Flow of an Ideal Fluid past a Cascade of Blades (Part II)

*By*

W. MERCHANT, M.A., S.M., of Metropolitan-Vickers Electrical Co., Ltd.
and
A. R. COLLAR, B.A., B.Sc., A.F.R.Ae.S.,
of the Aerodynamics Department, N.P.L.

*Crown Copyright Reserved*

LONDON: HIS MAJESTY'S STATIONERY OFFICE
Price 1*s.* 0*d.* net

# AERODYNAMIC SYMBOLS

## 1. GENERAL

| | |
|---|---|
| $m$ | Mass |
| $t$ | Time |
| V | Resultant linear velocity |
| $\Omega$ | Resultant angular velocity |
| $\rho$ | Density, $\sigma$ relative density |
| $\nu$ | Kinematic coefficient of viscosity |
| R | Reynolds number, $R = lV/\nu$ (where $l$ is a suitable linear dimension) |

Normal temperature and pressure for aeronautical work are 15° C and 760 mm.

For air under these conditions $\left\{\begin{array}{l}\rho = 0{\cdot}002378 \text{ slug/cu. ft.} \\ \nu = 1{\cdot}56 \times 10^{-4} \text{ ft.}^2\text{/sec.}\end{array}\right.$

The slug is taken to be 32·2 lb.-mass.

| | |
|---|---|
| $\alpha$ | Angle of incidence |
| $e$ | Angle of downwash |
| S | Area |
| $b$ | Span |
| $c$ | Chord |
| A | Aspect ratio, $A = b^2/S$ |
| L | Lift, with coefficient $C_L = L/\frac{1}{2}\rho V^2 S$ |
| D | Drag, with coefficient $C_D = D/\frac{1}{2}\rho V^2 S$ |
| $\gamma$ | Gliding angle, $\tan\gamma = D/L$ |
| L | Rolling moment, with coefficient $C_l = L/\frac{1}{2}\rho V^2 bS$ |
| M | Pitching moment, with coefficient $C_m = M/\frac{1}{2}\rho V^2 cS$ |
| N | Yawing moment, with coefficient $C_n = N/\frac{1}{2}\rho V^2 bS$ |

## 2. AIRSCREWS

| | |
|---|---|
| $n$ | Revolutions per second |
| D | Diameter |
| J | $V/nD$ |
| P | Power |
| T | Thrust, with coefficient $k_T = T/\rho n^2 D^4$ |
| Q | Torque, with coefficient $k_Q = Q/\rho n^2 D^5$ |
| $\eta$ | Efficiency, $\eta = TV/P = Jk_T/2\pi k_Q$ |

# Flow of an Ideal Fluid Past a Cascade of Blades (Part II)

*By*

W. Merchant, M.A., S.M., of Metropolitan-Vickers Electrical Co., Ltd.

and A. R. Collar, B.A., B.Sc., A.F.R.Ae.S.,
of the Aerodynamics Department, N.P.L.

Communicated by Dr. H. L. Guy, F.R.S.

*Reports and Memoranda No.* 1893

*26th May*, 1941

*Summary.*—This report gives a method of transforming a cascade of straight blades into a cascade of aerofoils. As the general flow past a cascade of straight blades is known[1, 2] the general flow past the cascade of derived aerofoils can be obtained. An illustrative example is given.

1. *Introduction.*—If any particular flow past a series of oval bodies on an axis of a complex plane is known, a transformation can be found which converts the ovals into a cascade of straight blades, since the corresponding flow past the latter is known. Moreover, by applying the reverse transformation to the general flow round the straight blades, the general flow round the ovals is obtained. The direct transformation can also be applied to an offset series of ovals, which then transform into a cascade of aerofoils : the process corresponds to the usual transformation of a single circle into an aerofoil. This method has been used before by one of the writers[3]. The present report applies the same method to a series of ovals which are in a physical sense much simpler than those previously used and which yield aerofoils approximating more closely to those met with in practice. An illustrative example is given.

2. *Outline of argument.*—The method employed may be briefly summarised as follows :—

(i) The normal flow past a series of doublets on the imaginary axis is known (it has been given by Lamb[4]) and can be interpreted as the normal flow past a series of oval bodies.

(ii) The general flow past a series of laminae lying along the imaginary axis is known ; in particular the normal flow is known, and a transformation can therefore be obtained which converts the laminae into the ovals discussed under (i).

(iii) Application of this transformation to the general flow round the laminae gives the general flow round the ovals.

(iv) A particular case of the general flow round the ovals is that for which the flow at infinity is inclined to the cascade axis, but for which there is no circulation. In this case the ovals can immediately be transformed into a cascade of flat plates parallel to the direction of flow at infinity.

(v) Application of the transformation of (iv) to an offset series of ovals yields a cascade of aerofoils. If the offset ovals pass through the points corresponding to the trailing edges of the inclined flat plates (which are stagnation points in the flow round the transform ovals) the aerofoils will have cusps at their trailing edges.

3. *General Flow past a Cascade of Ovals.*—The flow due to a series of uniform doublets lying along the imaginary axis in the $l$-plane with a period $\pi$ is known to be[4]

$$w = \mathrm{C} \coth l,$$

where C is a parameter defining the strengths of the doublets. If a uniform flow of velocity U parallel to the real axis is added the flow becomes

$$\begin{aligned} w &= \mathrm{U}l + \mathrm{C} \coth l, \\ &= \mathrm{U}\{l + \sinh^2\beta \coth l\}, \quad .. \quad .. \quad .. \quad .. \quad .. \quad .. \quad (1) \end{aligned}$$

where for convenience C is replaced by U $\sinh^2\beta$. Equation (1) gives the velocity potential and and stream function respectively as

$$\phi = \mathrm{U}\left\{m + \frac{\sinh^2\beta \sinh 2m}{\cosh 2m - \cos 2n}\right\},$$

$$\psi = \mathrm{U}\left\{n - \frac{\sinh^2\beta \sin 2n}{\cosh 2m - \cos 2n}\right\}.$$

The streamline $\psi = 0$ evidently consists partly of the axis $n = 0$ and partly of the closed oval

$$\cosh 2m = \cos 2n + \frac{\sinh^2\beta \sin 2n}{n}. \quad .. \quad .. \quad .. \quad .. \quad .. \quad (2)$$

This oval has its centre at the origin, and repeats at intervals of $\pi$ along the imaginary axis. The lengths of the semi-diameters are defined by the equations

$$\begin{aligned} m &= \beta, \\ n \tan n &= \sinh^2\beta. \end{aligned}$$

Equation (1) may therefore be regarded as giving the normal flow past a series of oval bodies, of shape given by (2), immersed in the fluid. The oval corresponding to $\beta = 1{\cdot}0$ is shown in Fig. 1.

Differentiation of equation (1) gives the velocity components of the flow past the ovals in the form

$$\frac{dw}{dl} = \mathrm{U}\left\{1 - \frac{\sinh^2\beta}{\sinh^2 l}\right\}, \quad .. \quad .. \quad .. \quad .. \quad .. \quad .. \quad (3)$$

so that the stagnation points of the flow are given by $l = \pm\beta + ri\pi$ and therefore, as is otherwise obvious, lie at the ends of the major axes of the ovals.

Now consider the flow in the $\zeta$-plane given by

$$w = \mathrm{U} \cosh^{-1}(\sec a \cosh\zeta), \quad .. \quad .. \quad .. \quad .. \quad .. \quad .. \quad (4)$$

or

$$\frac{dw}{d\zeta} = \frac{\mathrm{U} \sinh\zeta}{\sqrt{\sinh^2\zeta + \sin^2 a}}. \quad .. \quad .. \quad .. \quad .. \quad .. \quad .. \quad (5)$$

It represents[1, 2] the flow normal to a series of laminae of length $2a$ distributed along the $\eta$-axis with a period of $\pi$. Equation (5) shows that there are stagnation points when $\sinh\zeta$ vanishes, and that the velocity of flow at infinity is U, as in the case of equation (1). Elimination of $w$ between (1) and (4) therefore yields a transformation which converts the laminae of (4) into the ovals of (1) ; the transformation is

$$\cosh^{-1}(\sec a \cosh\zeta) = l + \sinh^2\beta \coth l. \quad .. \quad .. \quad .. \quad .. \quad .. \quad .. \quad (6)$$

In addition, the stagnation points in the two flows must correspond ; accordingly, we put $\cosh\zeta = 1$, $l = \pm\beta$ in (6), which becomes

$$\sec a = \cosh\{\beta + \sinh^2\beta \coth\beta\}, \quad .. \quad .. \quad .. \quad .. \quad .. \quad (7)$$

a relation which connects the two parameters $a$ and $\beta$. It will be convenient in what follows to employ the two auxiliary quantities

$$\gamma = \beta + \sinh^2\beta \coth \beta, \quad \ldots \quad (8)$$
$$\lambda = l + \sinh^2\beta \coth l. \quad \ldots \quad (9)$$

The transformation (6), connecting the $l$-plane ovals and the $\zeta$-plane laminae, then becomes

$$\cosh \gamma \cosh \zeta = \cosh \lambda. \quad \ldots \quad (10)$$

It may be noted that (7) and (8) show $a$ to be the gudermannian of $\gamma$, so that the circular functions of $a$, if required, are given by

$$\left.\begin{aligned} \sin a &= \tanh \gamma \\ \cos a &= \operatorname{sech} \gamma \\ \tan a &= \sinh \gamma \end{aligned}\right\} \quad \ldots \quad (11)$$

The general flow past the $\zeta$-plane laminae, of which (5) is a particular case, is

$$\frac{dw}{d\zeta} = \frac{\mathrm{U} \sinh \zeta + i\mathrm{W} \cosh \zeta}{\sqrt{\sinh^2 \zeta + \sin^2 a}} - i\mathrm{V}. \quad \ldots \quad (12)$$

Here V is the velocity parallel to the $\eta$-axis, and there is circulation $2\pi$W round each lamina. We now apply the transformation (10) to the flow (12). The laminae transform as before into the $l$-plane ovals, and the general flow round the ovals becomes

$$\frac{dw}{dl} = \left\{ \mathrm{U} + \frac{i\mathrm{W} \cosh \lambda - i\mathrm{V} \sinh \lambda}{\sqrt{\sinh^2 \lambda - \sinh^2 \gamma}} \right\} \left\{ 1 - \frac{\sinh^2 \beta}{\sinh^2 l} \right\}. \quad \ldots \quad (13)$$

When W = V = 0, this agrees with equation (3).

4. *Transformation of the Ovals into Inclined Flat Plates and Aerofoils.*—As a particular case of (13), put W = 0 and V = U tan $\sigma$. The equation then becomes

$$\frac{dw}{dl} = \mathrm{U} \left\{ 1 - \frac{i \tan \sigma \sinh \lambda}{\sqrt{\sinh^2 \lambda - \sinh^2 \gamma}} \right\} \left\{ 1 - \frac{\sinh^2 \beta}{\sinh^2 l} \right\}. \quad \ldots \quad (14)$$

In this case the flow past the ovals is inclined at an angle $\sigma$ to the real axis at large distances on either side of the cascade. Now imagine the flow pattern of (14) to be replotted in the $z$-plane, with the streamlines all straightened out. The flow in the $z$-plane is obviously

$$\frac{dw}{dz} = \mathrm{U}(1 - i \tan \sigma). \quad \ldots \quad (15)$$

Since the flow in the $z$-plane is uniform and rectilinear throughout, it is evident that the ovals have transformed into flat plates lying along the lines of flow.

Elimination of $w$ between (14) and (15) gives the transformation connecting the $l$- and $z$-planes as

$$\frac{dz}{dl} = e^{i\sigma} \left\{ \cos \sigma - \frac{i \sin \sigma \sinh \lambda}{\sqrt{\sinh^2 \lambda - \sinh^2 \gamma}} \right\} \left\{ 1 - \frac{\sinh^2 \beta}{\sinh^2 l} \right\}, \quad \ldots \quad (16)$$

or

$$z = e^{i\sigma} \{ \lambda \cos \sigma - i \sin \sigma \cosh^{-1} (\operatorname{sech} \gamma \cosh \lambda) \} \ldots \quad \ldots \quad (17)$$

At first sight, it would appear that (16) vanishes for $l = \beta$. However, when $l = \beta$, $\lambda = \gamma$ also, and it is found that in this case $dz/dl$ is neither zero nor infinite. Accordingly, the only infinities of (16) are for $\sinh l = 0$; these points are the centres of the ovals. The zeros of (16) are given by

$$\cos \sigma = \frac{i \sin \sigma \sinh \lambda}{\sqrt{\sinh^2 \lambda - \sinh^2 \gamma}},$$

or

$$\sinh \lambda = \pm \cos \sigma \sinh \gamma. \quad \ldots \quad (18)$$

It is evident that when (16) vanishes, (14) also vanishes, and the singularities (18) therefore coincide with the stagnation points in the flow (14). These correspond to the leading and trailing edges of the flat plates in the $z$-plane. By substitution from (18) in (17), these points are given as

$$z = \pm e^{i\sigma}\{\cos\sigma \sinh^{-1}(\cos\sigma \sinh\gamma) + \sin\sigma \sin^{-1}(\sin\sigma \tanh\gamma)\} \quad .. \quad .. \quad (19)$$

Equation (17) is thus a transformation from the $l$-plane to the $z$-plane which converts the cascade of ovals into a cascade of straight blades inclined at an angle $\sigma$ to the real axis. Now, in a manner analogous to the transformation of a circle into Joukowski aerofoils, a cascade of offset ovals can be transformed by (17) into a cascade of curved aerofoils. The process is conveniently illustrated by the example of § 5. It may be noted that, for computational purposes, it is convenient to draw the transformed aerofoil in the Z-plane, where $Z = ze^{-i\sigma}$, since a factor $e^{i\sigma}$ is thereby avoided. The Z-plane axes are rotated through $\sigma$ relative to those of the $z$-plane; and the transformation (17) is simply

$$Z = \lambda\cos\sigma - i\sin\sigma\cosh^{-1}(\text{sech}\,\gamma\cosh\lambda). \quad .. \quad .. \quad .. \quad (20)$$

In the application of the transformation to offset ovals it sometimes happens that the resultant Z-plane contours cross themselves. Usually this is immediately apparent, but occasionally such a cross-over may occur close to a cusp. Care must be taken to determine whether there is a cross-over or not, since it is obviously impossible to associate a fluid flow with a contour which crosses itself.

5. *Illustrative example.*—Take the series of ovals defined by $\beta = 1{\cdot}0$, a member of which is shown in Fig. 1. We shall transform this into a cascade of straight blades at 30° to the real axis, so that $\sigma = \pi/6$. We then have the following data :—

$$\left.\begin{aligned}\beta &= 1{\cdot}0,\\ \sigma &= \pi/6,\end{aligned}\right\} \quad .. \quad .. \quad .. \quad .. \quad .. \quad .. \quad .. \quad .. \quad (21)$$

and substitution in (8) gives

$$\gamma = 2{\cdot}813. \quad .. \quad .. \quad .. \quad .. \quad .. \quad .. \quad .. \quad .. \quad (22)$$

The stagnation points (18) now give

$$\lambda = \pm 2{\cdot}671 \quad .. \quad .. \quad .. \quad .. \quad .. \quad .. \quad .. \quad .. \quad (23)$$

and substitution for $\lambda$ from (9) gives an equation for $l$ of which the solution is found to be*

$$\pm l = 0{\cdot}943 + 0{\cdot}323\,i. \quad .. \quad .. \quad .. \quad .. \quad .. \quad .. \quad (24)$$

Moreover, substitution of the numerical value of $\gamma$ in equation (19), and replacement of $z$ by $Ze^{i\sigma}$, gives the ends of the Z-plane flat plates as

$$Z = 2{\cdot}573. \quad .. \quad .. \quad .. \quad .. \quad .. \quad .. \quad .. \quad .. \quad (25)$$

The Z-plane flat plate is shown in Fig. 2.

Now consider the ovals given by $\beta' = 1{\cdot}1$. If these ovals are offset so that they pass through one of the points (24) (and the corresponding points along the series) and so that they enclose the other zeros and the infinities, they will transform into a cascade of aerofoils with cusps at their trailing edges. In Fig. 1 the oval corresponding to $\beta' = 1{\cdot}1$ has been displaced so that its centre is at the point

$$l = 0{\cdot}139 - 0{\cdot}131\,i, \quad .. \quad .. \quad .. \quad .. \quad .. \quad .. \quad (26)$$

and it then passes through one of the singularities (24), namely

$$l = -0{\cdot}943 - 0{\cdot}323\,i. \quad .. \quad .. \quad .. \quad .. \quad .. \quad .. \quad (27)$$

---

* The solution of this equation may be obtained by finding an approximate value of $l$ and applying Newton's method for a closer approximation. The co-ordinates are of course related by equation (2).

There is no difficulty in the computation of the Z-plane transform ; any point $l$ on the displaced oval is substituted in (9) with $\beta = 1{\cdot}0$ to find $\lambda$, and this is then substituted in (20) to find Z. The Atlas Supplement to Kennelly's Tables of Complex Hyperbolic and Circular Functions[5] was found most convenient for this purpose.

6. *Properties of the Derived Cascade, and Determination of an Equivalent Cascade of Flat Plates.*— The flow at infinity is the same for both the $\beta'$ ovals and the derived aerofoils ; accordingly the properties of the cascade can be determined from those of the ovals. If the Kutta-Joukowski hypothesis is assumed, the velocity of flow at the aerofoil trailing edges is finite ; and therefore there is always a stagnation point at each of the corresponding points on the $\beta'$ ovals.

Now in Fig. 1 we may regard the $\beta'$ oval as being transformed with respect to the $\beta$ oval : the transformation has a singularity at one of the points of intersection of the two ovals, and this is the stagnation point of the flow round the $\beta'$ oval. Suppose we now select a different $\beta$ oval (still with its centre at the origin) and displace the original $\beta'$ oval, and the flow pattern round it, so that the stagnation point on the $\beta'$ oval lies at the new intersection of the two ovals. With this point as a singularity we may transform the $\beta'$ oval with respect to the new $\beta$ oval, and shall obtain a cascade which has the same properties as the $\beta'$ oval and, therefore, as the original cascade. An infinite number of cascades having the same properties may be obtained in this way. In particular, when the $\beta'$ oval coincides with the $\beta$ oval, so that its centre is now at the origin, the process of transformation yields a cascade of flat plates, which may be described as equivalent to the original cascade.

From (26) and (27) the stagnation point, when the $\beta'$ oval is not displaced, is

$$l = -1{\cdot}082 - 0{\cdot}192\,i. \qquad .. \quad .. \quad .. \quad .. \quad .. \quad .. \quad (28)$$

Accordingly, this point and its reflexion in the origin are the singularities of the new transformation ; and they are defined by equation (18). In this equation, $\gamma$ is defined by (8) with $\beta = 1{\cdot}1$ and $\lambda$ by (9) and (28). Accordingly (18) gives $\sigma$, and when these values of $\gamma$, $\lambda$, and $\sigma$ are inserted in (19) the half chords of the flat plates are derived. The results are

$$\left.\begin{aligned} \gamma &= 3{\cdot}329 \\ \lambda &= 3{\cdot}282 \\ \sigma &= 0{\cdot}303 \text{ radian} \\ &= 17{\cdot}4^\circ \\ Z &= 3{\cdot}222 \end{aligned}\right\} \qquad .. \quad .. \quad .. \quad .. \quad .. \quad .. \quad .. \quad (29)$$

The equivalent cascade of flat plates is thus inclined at $17{\cdot}4^\circ$ to the real axis, and has a gap-chord ratio

$$\frac{s}{c} = \frac{\pi}{6{\cdot}444} = 0{\cdot}488. \qquad .. \quad .. \quad .. \quad .. \quad .. \quad .. \quad (30)$$

The properties of cascades of this type are given in Reference 1, and define the properties of the curved aerofoils of Fig. 2. It may be remarked that the angle of the flat plates to the real axis ($17{\cdot}4^\circ$) is the angle of flow for no lift on the cascade of Fig. 2.

7. The writers wish to express their thanks to Messrs. Metropolitan-Vickers Electrical Co., Ltd., and to the Aeronautical Research Committee for permission to publish this paper.

---

## REFERENCES


1. Merchant, W. .. Flow of an Ideal Fluid Past a Cascade of Blades, R. & M. 1890.
2. Collar, A. R. .. Cascade Theory and the Design of Fan Straighteners, R. & M. 1885.
3. Collar, A. R. .. The Flow of a Perfect Fluid through Cascades of Aerofoils, Journal of the Royal Aeronautical Society, May, 1941.
4. Lamb, H. .. .. Hydrodynamics (C.U.P., 5th Edn., p. 68).
5. Kenelly, A. E. .. Tables of Complex Hyperbolic and Circular Functions (Harvard U.P.).

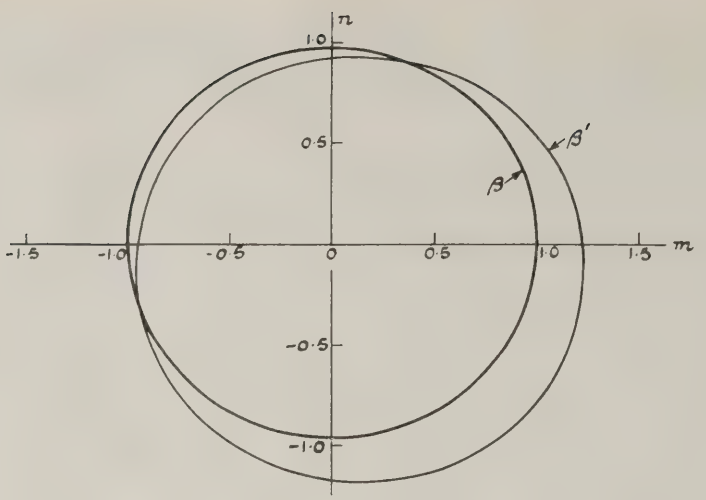


FIG. 1. ζ Plane.

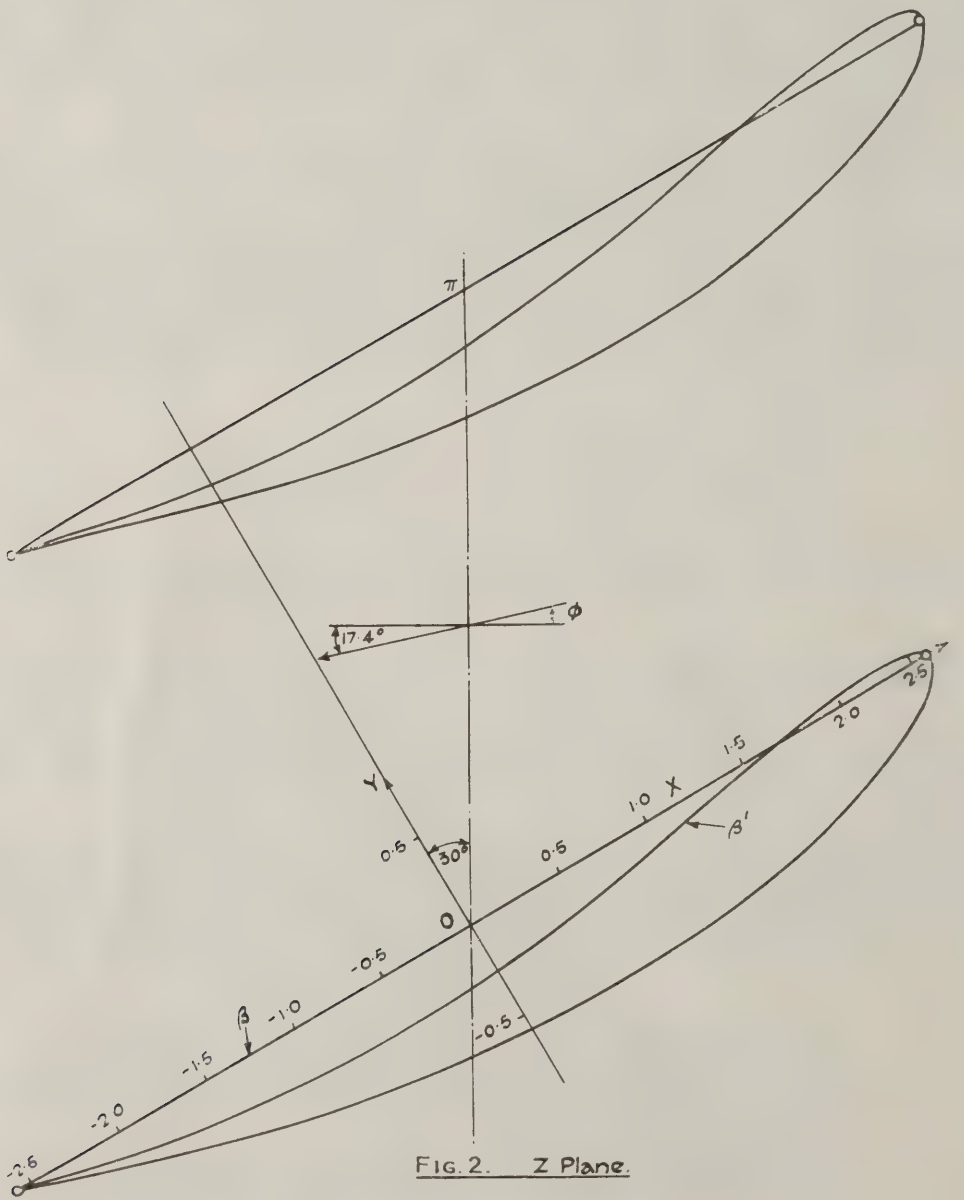


FIG. 2. Z Plane.

(56861) Wt. 5 500 10/41 Hw. G.377/2.

## SYSTEM OF AXES

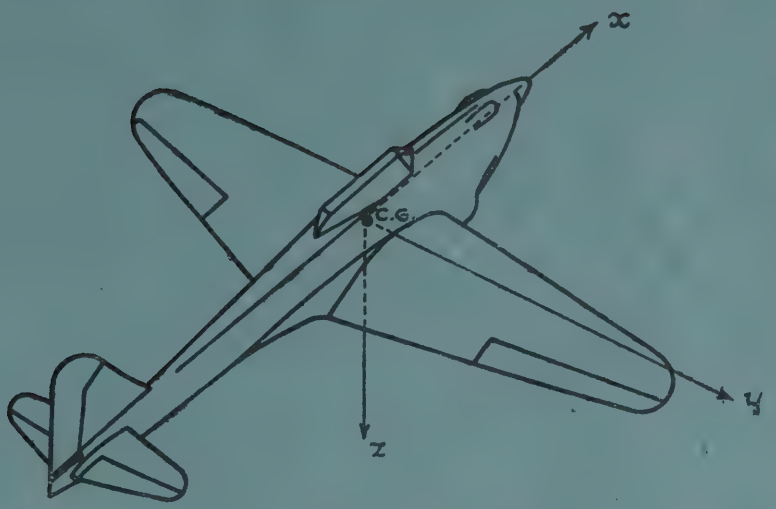


| Axes | Symbol Designation Positive direction | $x$ longitudinal forward | $y$ lateral starboard | $z$ normal downward |
|---|---|---|---|---|
| Force | Symbol | X | Y | Z |
| Moment | Symbol Designation | L rolling | M pitching | N yawing |
| Angle of Rotation | Symbol | $\phi$ | $\theta$ | $\psi$ |
| Velocity | Linear | $u$ | $v$ | $w$ |
| | Angular | $p$ | $q$ | $r$ |
| Moment of Inertia | | A | B | C |

Components of linear velocity and force are positive in the positive direction of the corresponding axis.

Components of angular velocity and moment are positive in the cyclic order $y$ to $z$ about the axis of $x$, $z$ to $x$ about the axis of $y$, and $x$ to $y$ about the axis of $z$.

The angular movement of a control surface (elevator or rudder) is governed by the same convention, the elevator angle being positive downwards and the rudder angle positive to port. The aileron angle is positive when the starboard aileron is down and the port aileron is up. A positive control angle normally gives rise to a negative moment about the corresponding axis.

The symbols for the control angles are :—

$\xi$ aileron angle
$\eta$ elevator angle
$\eta_T$ tail setting angle
$\zeta$ rudder angle

# Publications of the Aeronautical Research Committee

TECHNICAL REPORTS OF THE AERONAUTICAL RESEARCH COMMITTEE—

1933-34 Vol. I. Aerodynamics. £1 5*s*.
Vol. II. Structures, Engines, Instruments, etc. £1 10*s*.
1934-35 Vol. I. Aerodynamics. £2.
Vol. II. Seaplanes, Structures, Engines, Materials, etc. £2.
1935-36 Vol. I. Aerodynamics. £1 10*s*.
Vol. II. Structures, Flutter, Engines, Seaplanes, etc. £1 10*s*.
1936 Vol. I. Aerodynamics General, Performance, Airscrews, Flutter and Spinning. £2.
Vol. II. Stability and Control, Structures, Seaplanes, Engines, etc. £2 10*s*.

ANNUAL REPORTS OF THE AERONAUTICAL RESEARCH COMMITTEE—

1933-34 1*s*. 6*d*.
1934-35 1*s*. 6*d*.
April 1, 1935 to December 31, 1936. 4*s*.
1937 2*s*.

INDEX TO THE TECHNICAL REPORTS OF THE ADVISORY COMMITTEE ON AERONAUTICS—

1909-1919 Reports and Memoranda No. 1600. 8*s*.

NUMERICAL LISTS OF REPORTS AND MEMORANDA published between 1909 and 1936—

Reports and Memoranda Nos. 650 (9*d*.), 750 (6*d*.), 850 (1*d*.), 950 (4*d*.), 1050 (4*d*.), 1150 (4*d*.) (*Out of print*), 1250 (6*d*.) (*Out of print*), 1350 (6*d*.) (*Out of print*), 1450 (6*d*.), 1550 (6*d*.), 1650 (6*d*.), 1750 (1*s*. 3*d*.)

LIST OF PUBLICATIONS ON AERONAUTICS—

Aeronautical Research Committee Publications (classified under subjects). Post free on application.

*Prices are net and postage extra.*

## His Majesty's Stationery Office

London W.C.2 : York House, Kingsway
Edinburgh 2 : 120 George Street — Manchester 2 : 39-41 King Street
Cardiff : 1 St. Andrew's Crescent — Belfast : 80 Chichester Street
or through any bookseller.

S.O. Code No. 23-1893.

Engng.

R. & M. No. 1894
(1576)
A.R.C. Technical Report

629.13
G79r
No.1894

MINISTRY OF AIRCRAFT PRODUCTION

AERONAUTICAL RESEARCH COMMITTEE
REPORTS AND MEMORANDA

# Compression Tests on Curved Plates of Thin Sheet Duralumin

*By*

H. L. Cox, M.A., and W. J. Clenshaw, B.Sc., A.Inst.P.,
of the Engineering Department, N.P.L.

*Crown Copyright Reserved*

LONDON: HIS MAJESTY'S STATIONERY OFFICE
Price 2*s.* 6*d.* net

# AERODYNAMIC SYMBOLS

## 1. GENERAL

$m$ Mass
$t$ Time
V Resultant linear velocity
$\Omega$ Resultant angular velocity
$\rho$ Density, $\sigma$ relative density
$\nu$ Kinematic coefficient of viscosity
R Reynolds number, $R = lV/\nu$ (where $l$ is a suitable linear dimension)

Normal temperature and pressure for aeronautical work are 15° C and 760 mm.

For air under these conditions $\begin{cases} \rho = 0{\cdot}002378 \text{ slug/cu. ft.} \\ \nu = 1{\cdot}56 \times 10^{-4} \text{ ft.}^2\text{/sec.} \end{cases}$

The slug is taken to be 32·2 lb.-mass.

$\alpha$ Angle of incidence
$e$ Angle of downwash
S Area
$b$ Span
$c$ Chord
A Aspect ratio, $A = b^2/S$
L Lift, with coefficient $C_L = L/\frac{1}{2}\rho V^2 S$
D Drag, with coefficient $C_D = D/\frac{1}{2}\rho V^2 S$
$\gamma$ Gliding angle, $\tan\gamma = D/L$
L Rolling moment, with coefficient $C_l = L/\frac{1}{2}\rho V^2 bS$
M Pitching moment, with coefficient $C_m = M/\frac{1}{2}\rho V^2 cS$
N Yawing moment, with coefficient $C_n = N/\frac{1}{2}\rho V^2 bS$

## 2. AIRSCREWS

$n$ Revolutions per second
D Diameter
J $V/nD$
P Power
T Thrust, with coefficient $k_T = T/\rho n^2 D^4$
Q Torque, with coefficient $k_Q = Q/\rho n^2 D^5$
$\eta$ Efficiency, $\eta = TV/P = Jk_T/2\pi k_Q$

629.13
LIBRARY
UNIVERSITY OF ILLINOIS
URBANA

# Compression Tests on Curved Plates of Thin Sheet Duralumin

*By*

H. L. Cox, M.A., and W. J. Clenshaw, B.Sc., A.Inst.P.,
of the Engineering Department, N.P.L.

*Reports and Memoranda No.* 1894
*28th November*, 1941*

*Summary*—(*a*) *Purpose of investigation.*—The results of compression tests previously carried out on flat plates showed[1] that the stress-strain relationship of such plates could be represented approximately by two straight lines. The present tests were undertaken in order to investigate the stress-strain relationship for curved plates and to determine whether in this case a similar simplification of the stress-strain relationship was permissible.

(*b*) *Range of investigation.*—Tests have been made on plates of duralumin having the following dimensions :—

| | | |
|---|---|---|
| 0·067 in. thick<br>0·038 ,,<br>0·030 ,,<br>0·024 ,,<br>0·017 ,, | curved to 18 in. radius | 4, 6, 8, 10 and 12 in. wide (circumferentially). |
| 0·067 ,,<br>0·038 ,, | curved to 36 in. radius | |

All the plates were 24 in. in length parallel to the axis of curvature and all the edges were so held that they could be considered clamped. Compressive loads were applied to the curved edges of the plates (parallel to the length) and the loading conditions were such that the planes containing these curved edges were maintained parallel. The displacements in the direction of the load were measured over the whole plate (including the end fixings) and an amplified record was obtained by means of a hydraulic and mechanical transmission. The use of this transmission in conjunction with the automatic load recorder fitted to the testing machine enabled load-deformation curves to be drawn autographically.

(*c*) *Conclusions.*—Curved plates subjected to compression parallel to the axis of curvature deform in a similar manner to flat plates. Below the buckling load the plate behaves as a solid test piece, the compressive stress being uniform over the whole plate. After buckling the central part of the plate is stressed less heavily than the edges (which are constrained to remain straight) and, since the strain is proportional to the stress in the edges, the stiffness (rate of increase of load/rate of increase of strain) of the plate is reduced.

In contrast to flat plates, buckling of curved plates may result not only in a reduction of stiffness but also in an actual reduction of load. The reduction is greatest in thick, wide plates curved to a small radius ; but the dimensions of plates for which the effect is serious probably lie outside the range of normal aircraft engineering. The elastic behaviour of the thinner, narrower plates may be represented fairly closely by two straight lines. The buckling stress of a curved plate is greater than that of an equivalent flat plate ; but the reduction of stiffness after buckling is also greater.

No theoretical analysis of the buckling and behaviour after buckling of curved plates with clamped edges is available ; but on the basis of the experimental results, empirical formulae for the buckling stress and for the reduction of stiffness after buckling have been developed. In choosing these formulae, use has been made of all the theoretical results available [1, 2].

*Introduction.*—In R. & M. 1554 an approximate theory was developed describing the buckling and the behaviour after buckling† of a flat rectangular plate of thin sheet material subjected to compression parallel to its longer edges. It was shown that, owing to the formation of waves at buckling and the consequent reduction of stress in the centre of the sheet, the effective stiffness

* This work was carried out during 1934.

† The edges of the plate being supported, buckling need not lead at once to complete collapse.

of the plate after buckling should be reduced ; that the ratio of the stiffness immediately after buckling to the stiffness before buckling should be $\frac{1}{3}$ if the edges of the plate were simply supported and about $\frac{1}{2}$ if the edges were clamped ; that a further decrease in stiffness should occur as the load was increased above the buckling load ; and that, if total collapse occurred at some definite value of the strain (i.e., edge stress), the ultimate load carried $P_m$ should be given by the equation

$$P_m = t\,(At + Bd),$$

A and B being constants for any given material with given edge conditions, and the term $At$ being considerably larger than the term $Bd$. The results of tests carried out in America[3] on plates with simply supported edges were shown to agree reasonably well with the theoretical conclusions, and the results of a series of tests carried out at the N.P.L.[1] on plates with clamped edges also confirmed the main theoretical conclusions.

Although for some purposes, formulae giving the ultimate load a plate can carry may be sufficient, such formulae require the specification of the value of the limiting edge stress. If the value of this stress is in doubt, it may be more convenient to refer directly to the stress-strain relationship of the plate. Thus methods can be developed for determining from a simplified stress-strain diagram for the plate in compression the behaviour of stiffened tubes and quadrants in bending.[4] Treatment by this method has the advantage that the theoretical prediction of the behaviour can be compared with the experimental results not only with regard to the value of the collapsing load but also with regard to the deformation at lower loads.

The applicability of this method depends, of course, upon the accuracy with which the stress-strain relationship of the plate can be represented by a simple diagram ; but since in any practical construction the stiffeners will carry the major portion of the load, considerable inaccuracy in the representation of the behaviour of the plate may cause relatively little error in the estimate of the behaviour of the complete structure. Thus, for flat plates the simplified stress-strain diagram consisting of two straight lines is probably sufficiently accurate for all practical purposes ; but, before a similar diagram could be assumed to represent the behaviour of curved plates it became necessary to investigate whether for these plates this assumption was justified.

*Theoretical Considerations.*—The only available theory relating directly to the behaviour of curved plates in compression is the calculation by the Ritz energy method of the buckling stress of a plate with simply supported edges.[2] In addition as limiting cases we have the approximate results of R. & M. 1554 for the buckling (and the behaviour after buckling) of flat plates and the exact calculation of the buckling stress of a complete circular tube in compression given by Professor Southwell's general theory of elastic stability.[5] This latter result is incorporated as a limiting case in the results of reference 2.

In practical stiffened constructions, the edge conditions of the individual plates approximate more closely to clamping than to simple support. Since the limiting condition of the complete tube is presumably independent of edge conditions, it would be reasonable to assume that the buckling of a plate with clamped edges might be defined by the formula of reference 2 with the term $\frac{\pi^2\gamma^2}{b^2}$ replaced by $1{\cdot}82\,\frac{\pi^2\gamma^2}{b^2}$ both as the additive term and under the radical. Comparison of the experimental results with this amended formula is made below.

With regard to the behaviour after buckling, it might be anticipated that, since the development of the buckled form must to a large extent destroy the essential curvature of the plate, this curvature should have relatively little effect. This does not imply that the reduction of stiffness after buckling should be independent of curvature ; but rather that the reduction should be slightly greater for curved than for flat plates, so that, in conjunction with the higher buckling stress for curved plates, the mean stress/maximum stress ratio at maximum stresses well above the buckling stress should be effectively the same for curved as for flat plates.

From the description of the experimental results below it will be apparent that the buckling of curved plates is rather different in type from the buckling of flat plates. The effect of this difference on the effective description of the behaviour of curved plates by simplified stress-strain diagrams will be discussed after description of the experimental results.

SCHRUEPPEL MAY 1 2 1942

*Description of Apparatus.*—The apparatus used for supporting the panels in the present tests is shown in Fig. 1. The top and bottom (curved) edges of the plate to be tested were clamped by curved cover plates to the curved faces of angle pieces bolted to the top and bottom plattens. The longer (straight) edges of the plate were guided in slots $\frac{3}{8}$ in. deep, cut in the edges of a series of strips supported upon two pairs of pillars. These strips were of 16 S.W.G. duralumin and were spaced along the supporting pillars by rubber washers $\frac{1}{4}$ in. thick. The whole " comb " of strips on a pair of supporting pillars formed one unit which could be turned back to front or end for end. Two slots of different widths were cut in each edge of each strip slightly off the centre line, so that the four possible positions of the " combs " brought four different widths of slot into alignment with the top and bottom angles. The lower ends of the supporting pillars of the combs were supported in cylindrical cups fixed to the upper face of the lower platten, and their upper ends were braced laterally by bars connecting one pillar of each pair to the corresponding pillar of the other comb. A number of different positions for the cups supporting the pillars were provided to allow plates 4, 6, 8, 10 and 12 in. in width to be tested.

All the tests were carried out in the 25-ton Denison testing machine installed in the Engineering Department of the National Physical Laboratory. In this machine the upper and lower straining heads are constrained to remain parallel, any provision for axial loading being made independently. In the present tests the plate apparatus was supported on the lower head of the testing machine and the load was applied to the upper platten through a cylindrical seating, 3 in. in diameter, of which the axis was perpendicular to the plane of the centre of the plate. This seating accommodated any lack of parallelism between the upper platten and the upper head of the testing machine in the lateral direction, while the slight flexibility of the upper platten on the plate accommodated any difference in the perpendicular direction. So soon as any appreciable load was applied both these adjustments became inoperative and the plate was subjected to uniform compressive strain.

The apparatus used for recording the strain of the plates is shown in Figs. 1 and 2. To the lower head of the testing machine, at the four corners of the lower platten of the plate apparatus, were fixed four cylinders containing oil, each cylinder being $\frac{3}{4}$ in. in diameter. These cylinders were closed by pistons, to which the motion of the top platten of the plate apparatus was transmitted by ball ended rods bearing against conical depressions in the tops of the pistons and in the under side of the upper platten. All four cylinders were connected by stout copper pipes to a single recording cylinder, about $\frac{1}{4}$ in. in diameter, the bore of this cylinder being straight and true for a length of 4 in. The motion of the piston closing this cylinder was thus about 40 times the relative motion of the top and bottom plattens of the plate apparatus.

The Denison testing machine used in the present tests is fitted with an autographic recorder. The load is weighed through a multiple-lever system by a spring, two springs, one of 25 tons and the other 5 tons capacity, being provided. The motion of the beam to which the spring is attached, rotates, by means of a system of pulleys and wires, a drum upon which a piece of graduated paper is fixed. A bar carrying a pencil is traversed axially over this drum on two pulleys, one of which is actuated by the strain recording mechanism. In the present tests, the pulley moving the pencil was rotated by a wire connected at one end to the piston of the recording cylinder, passing round the pulley and carrying a weight of about one pound at the free end, a mechanical magnification of $2\frac{1}{2}$ to 1 being obtained. The motion of the pencil was therefore about 100 times the relative motion of the upper and lower plattens of the plate apparatus.

The method of supporting the plate* proved very satisfactory throughout the tests. The support afforded to the edges of the plate was sufficient to prevent buckling at the edge, even of plates 0·018 in. in thickness stressed to 12 tons/sq. in. In most cases the plates slipped quite freely through the slots in the strips of the comb ; but, even where, owing to severe local buckling, the plate seized in the slots, the rubber spacing washers prevented any considerable variation of stress being set up. On the other hand, the appearance of the buckled plates showed quite clearly that the edge support was sufficient to maintain the edges of even the thickest plates (16 S.W.G.) in the original form.

The strain recording apparatus also worked satisfactorily. The lost motion was almost negligible and there was no other source of appreciable hysteresis. No particular provision had been made for preventing oil from leaking past the pistons ; in fact, although the pistons all fitted the cylinders fairly closely, reliance was placed upon the leakage (under the pressure of about 20 lb./sq. in.) to maintain effective lubrication. Owing to this leakage there was a slow movement of the strain recorder with time ; but this movement was far too slow to have any measurable effect in the period of a normal test.

The load recording device unfortunately did not work so satisfactorily. For the thicker plates, for which loads as high as 5 tons were in certain cases required, it was possible to use either the 5-ton spring of the recorder with a low mechanical magnification or the 25-ton spring with a correspondingly higher mechanical magnification—either system giving a good positive drive to the recording drum ; but, for the thinner plates, for which much smaller loads were required, it was necessary, in order to obtain a record of reasonable size, to use both the light spring and a high magnification. In such cases the actuating torque on the recording drum was very small and great care had to be exercised to reduce the effect of friction in retarding the motion of the drum. In spite of all precautions, however, the lost motion due to friction was in some cases an appreciable part of the total motion. The accuracy of the results of tests given below is for this reason lower for thin plates than for thick ones.

*Materials Tested.*—Part of the material used in the present tests was the remainder of the duralumin sheet (GQK) previously used in the tests on flat plates described in reference 1. A further supply of duralumin sheet (HKZ) was subsequently obtained. The surface of the material HKZ was anodically treated, that of the material GQK was untreated.

*Method of Test.*—Preliminary tests on fairly thick wide plates showed that the behaviour of a plate on first loading might be appreciably different from its behaviour after it had once been buckled. For this reason, except for the first few plates, each plate was loaded and unloaded three times. In the first test the plate was loaded until it buckled, in the second and third it was loaded up to an edge stress of about 10-12 tons/sq. in. The load was in most cases applied at a rate of about 2–3 tons/sq. in. edge stress per minute, a complete test on one plate taking about 45 minutes.

*Results of Tests.*—For each plate tested a complete record of total load against overall strain was obtained autographically. Unfortunately, it is impracticable to reproduce all these diagrams ; but typical diagrams together with sketches of the buckled forms are shown in Figs. 3–14.

Fig. 3 shows the results of tests on the plate GQK1CB1. On first loading this plate buckled with considerable noise into one central wave at a load of 5·5 tons (stress 7·6 tons/sq. in.). (So violent an oscillation of the recorder was set up that the drum slipped ; but the amount of slip was subsequently determined from the final position of the drum after the plate had been unloaded.) Immediately upon buckling, the strain increased to that corresponding to a load in the unbuckled state of 6·7 tons (stress 9·3 tons/sq. in.), while the actual load carried fell to 2·8 tons. On unloading, the load decreased to just over 1 ton at a strain corresponding to

* The method is a slight modification of that developed at the R.A.E. by the late Mr. Gerard for supporting the edges of a semi-circular tube when compressed parallel to its axis.

a load in the unbuckled state of 2·5 tons ; then the buckle suddenly disappeared, the load *increasing* to about 1·8 tons. During the remainder of the unloading the plate behaved as a solid test piece. On reloading the buckle began to develop at a load of 2·1 tons (stress 2·9 tons/sq. in.) ; but did not assume its final form until the edge stress was about 4·5 tons/sq. in. Then the load, which had remained practically constant since buckling began, fell suddenly to about 1·5 tons. Upon further loading the mean stress increased at about half the rate of the edge stress (the strain). Upon unloading an increase of load from 0·5 to 1·0 ton as the plate returned to the unbuckled form was again observed. The behaviour of the plate in the third loading was very similar to its behaviour in the second loading. Buckling began at a slightly lower load (1·8 tons) but again the buckle took some time to develop. Once again, an increase of load as the buckle disappeared was observed.

The behaviour of the plate GQK1CB1 has been described in some detail because it is typical of the behaviour of many other plates of similar dimensions. As a contrast to this type of record, Fig. 4 shows the results of tests on the plate GQK1CE1. In this narrow plate, the process of buckling was similar to that of a flat plate. The reduction of stiffness at buckling was well-marked ; but there was no actual reduction of load, and the reduction of buckling load on reloading was relatively small. In general, the sudden changes of load became less marked as the width of plate was decreased, as the thickness was decreased or as the radius of curvature was increased ; but the variation of the magnitude of the changes with width was much greater for thick than for thin plates.

For comparison, in particular with Fig. 3, Fig. 5 shows the results of the tests on the plate HKZ2CB1. In this diagram the points chiefly to be remarked are the sudden fall of load (due to a new buckle) that occurred at an edge stress of about 12 tons/sq. in. and the nature of the buckled form finally developed. For plates of which the " bulge " was appreciable this form of buckling appeared to be the normal one. Narrower plates usually buckled into one or more central waves in the manner of flat plates ; but the occurrence of central waves in wide plates (as for instance in GQK1CB1, Fig. 3) may be regarded as abnormal. Another fairly good example of the " side wave " method of buckling is shown in Fig. 6 (HKZ2CC2).

A diagram obtained in tests on the plate HKZ3CB1 is shown in Fig. 7. This thickness of material (0·030 in.) was fitted into the slots used for the thicker materials HKZ2 and GQK2 (0·038 in. thick). In consequence, the edge support was not so good as in the other tests and there was a tendency (indicated in Fig. 7) for the edges of the plate to buckle. This effect probably to some extent reduced all the loads carried by the plates of this thickness.

Typical diagrams for still thinner plates are shown in Fig. 8 (GQK3CB1), Fig. 9 (GQK4CB1) and Fig. 10 (GQK4CD1). As might be expected, plates curved to a larger radius behaved more nearly like flat plates. Examples are shown in Fig. 11 (HKZ2DB1) and Fig. 12 (HKZ1DC1).

*Analysis of Results.*—From the diagrams, Figs. 3–12, it will be apparent that theoretical description of the behaviour of the plates is likely to be difficult. The fact that the buckled form is developed suddenly with simultaneous increase of strain and decrease of load suggests that the unbuckled state may be in unstable equilibrium at loads well below that which actually causes the plate to buckle. Moreover, in the thicker plates, the sudden deflections due to buckling are very large and may well cause permanent deformation ; so that, in subsequent tests, the behaviour of the plate may be affected by damage done in the first loading.

The only figure therefore that is likely to have any real theoretical significance is the value of the primary buckling stress on first loading. The values of this stress deduced from the experimental results are given in the sixth column of Table 1 and in the fifth column are given the values calculated from the formulae :—

$$\text{Buckling Stress} = E' \left\{ 3 \frac{t^2}{b^2} + \sqrt{9 \frac{t^4}{b^4} + \frac{1 - \sigma^2}{3} \frac{t^2}{r^2}} \right\} \qquad (1)$$

where $E' = \dfrac{E}{1 - \sigma^2}$

$E$ = Young's modulus, $\sigma$ = Poisson's ratio } for the material

$t$ = thickness, $b$ = width (circumferentially), $r$ = radius of curvature } of the plate.

Apart from the comparison of the values of the primary buckling stresses, there remains the practical problem whether it be possible to devise empirical formulae that shall describe the behaviour of the plates with accuracy sufficient for the ordinary purposes of design.

The first question that arises in this problem is whether attention should be concentrated upon first loading or upon some subsequent loading. In some cases (*cf.*, for instance Figs. 4, 8 and 9) the choice makes but little difference ; but in others (*cf.*, for instance Figs. 3 and 5) the difference is considerable. This question should be decided by consideration of the severity of the loading condition which, in practical constructions, would cause the constituent plates to buckle. If this loading were so severe that it was never likely to occur in practice, then first loading might be adopted. If it represented ordinarily severe service conditions then perhaps second loading might be used ; whilst, if normal conditions carried the plates well past buckling, third or some subsequent loading might be more suitable.

It may be said at once that, if it is required to represent the behaviour of a plate after an indefinite number of fairly severe loadings (up to 10 tons/sq. in. edge stress, say), the best course is to assume simply that the load is proportional to the strain, the stiffness being, of course, only a fraction of the elastic stiffness. This assumption is equivalent to that made by Sechler and others that the plate is reducible to an " equivalent width " ; but it does not necessitate Sechler's second assumption that the equivalent width is independent of the actual width.

On the other hand, edge stresses of the order of 10 tons/sq. in. are not likely to be set up frequently under working conditions, and, if plates are designed on the " chord stiffness " from zero to 10 tons/sq. in. edge stress, the strength at lower edge stresses may in many cases be seriously underestimated. Figs. 13 and 14 show load-deformation curves obtained in repeated loading firstly up to about 5 tons/sq. in. edge stress (curves marked 1, 2 and 3) secondly, up to 10 tons/sq. in. (curves marked 4 and 5), and thirdly up to about 13 tons/sq. in. (curves marked 6 and 7). It will be seen that the repetition over each range is fairly good and that the behaviour at values of the edge stress in the neighbourhood of 5 tons/sq. in. is represented better by the empirical formula than by the " reduced stiffness " line.

It is suggested therefore that second loading is in general the best criterion. This indicates the behaviour of a plate that has been buckled but which has not been stressed very far above buckling.

Figs. 3–14 show that the behaviour of many plates may be represented fairly accurately by two straight lines, i.e., by the elastic line up to the (nominal) buckling stress $f_b$ and thereafter by a line of which the slope (stress/strain) is $1/n$th of the slope of the elastic line. Results such as those shown in Figs. 3 and 5 do not, of course, conform very closely to this simplified diagram ; but this type of diagram is obtained only from plates lying somewhat outside the range of normal practice in aircraft construction.

After trial of several different expressions for $f_b$ and $n$, the following were adopted :—

$$f_b = E' \left\{ 6 \frac{t^2}{b^2} + 0{\cdot}21 \frac{t}{r} \right\} \quad \ldots \quad (2)$$

$$n = 1{\cdot}3 + 0{\cdot}01 \frac{b}{t} \left( 1 + 2{\cdot}4 \frac{b}{r} \right) \quad \ldots \quad (3)$$

Although, in the choice of these formulae, some attention has been paid to theoretical considerations, the formulae should be regarded as founded entirely on the experimental results. They represent the behaviour of plates of the dimensions normally employed in aircraft construction with reasonable accuracy ; but outside that range they are not applicable. With regard to the formula for $f_b$ greater accuracy over a wider range could be obtained by substituting for (2) an expression similar to (1) with a lower coefficient of $t/r$ (this adjustment might perhaps be regarded as an allowance for the effect of initial waves or waves formed in first loading) ; but the gain in accuracy in the practical range is considered to be outweighed by the greater complexity of the formula.

The expression for $n$ has an even less rational basis ; $n$ certainly increases with the ratio $b/t$, and the increase is greater, the smaller the value of $r$. Otherwise the sole justification for this expression is that it enables the experimental results to be reproduced with reasonable accuracy. The form of the expression for $n$ suggests that $n$ can be less than 2, a result at variance with the conclusions of reference 1. It will be found, however, that the values of $b/t$ that make $n < 2$, also make $f_b >$ about 6 tons/sq. in., so that the exact slope of the line above $f_b$ makes very little difference to the total load at reasonable values of the edge stress.

The simplified diagrams obtained by using the values of $f_b$ and $n$ given by (2) and (3) are shown on Figs. 3–14, and in Table 1 the experimental values of the mean stresses at buckling and at 5 tons/sq. in. and 10 tons/sq. in. edge stress are compared with the values given by the simplified diagram for all the plates tested. The mean stresses quoted in Table 1 are the mean stresses in the free width of plate, the load carried by the $\frac{3}{8}$-in. widths of panel actually supported by the combs having been subtracted. The loads recorded on Figs. 3–14 are, of course, the total loads.

The range over which the formulae (2) and (3) may be regarded as valid is rather difficult to define, since it includes both flat plates and plates for which the first term of (2) is negligible in comparison with the second. On the whole, it appears reasonable to limit the application of the formulae to plates for which the value of $f_b$ given by (2) is less than 5 tons/sq. in. It is improbable that any practical form of construction would have a higher value of $f_b$, and Figs. 3–14 and Table 1 show that with this limitation the agreement between the estimated and the actual stresses is reasonably close.

TABLE 1

*Comparison of Experimental Results with Empirical Formula*

| Reference mark of panel | Dimensions of panel (in.) | | | Primary buckling stress (tons/sq. in.) | | Empirical formula | | Mean stress (tons/sq. in.) at 5 tons/sq. in. edge stress | | Mean stress (tons/sq. in.) at 10 tons/sq. in. edge stress | | Ratio of effective width to thickness at 10 tons/sq. in. edge stress | |
|---|---|---|---|---|---|---|---|---|---|---|---|---|---|
| | Radius $r$ | Thickness $t$ | Width $b$ | Theory* | Exp. | $f_b$** (tons/sq. in.) | $n$† ratio | Theory | Exp. | Theory | Exp. | Theory | Exp. |
| GQK1CA1 | 18 | 0·067 | 12 | 10·36 | 7·99 | 4·68 | 6·0 | 4·73 | 2·58 | 5·56 | 4·33 | 100 | 78 |
| HKZ1CA2 | 18 | 0·067 | 12 | 10·36 | 6·42 | 4·68 | 6·0 | 4·73 | 2·80 | 5·56 | 4·23 | 100 | 76 |
| GQK1CB1 | 18 | 0·067 | 10 | 10·58 | 7·65 | 5·08 | 4·8 | 5 | 2·12 | 6·10 | 4·03 | 91 | 60 |
| HKZ1CB2 | 18 | 0·067 | 10 | 10·58 | 7·83 | 5·08 | 4·8 | 5 | 2·10 | 6·10 | 4·00 | 91 | 60 |
| GQK1CC1 | 18 | 0·067 | 8 | 10·98 | 6·11 | 5·81 | 3·8 | 5 | 3·20 | 6·91 | 5·35 | 82 | 64 |
| HKZ1CC2 | 18 | 0·067 | 8 | 10·98 | 7·48 | 5·81 | 3·8 | 5 | 2·34 | 6·91 | 4·55 | 82 | 54 |
| GQK1CD1 | 18 | 0·067 | 6 | 11·87 | 6·23 | 7·39 | 2·9 | 5 | 4·44 | 8·29 | 6·90 | 74 | 62 |
| HKZ1CD2 | 18 | 0·067 | 6 | 11·87 | 6·10 | 7·39 | 2·9 | 5 | 4·48 | 8·29 | 6·77 | 74 | 61 |
| GQK1CE1 | 18 | 0·067 | 4 | 14·78 | 7·36 | 11·92 | 2·2 | 5 | 5 | 10 | 8·14 | 60 | 48 |
| HKZ1CE2 | 18 | 0·067 | 4 | 14·78 | 7·24 | 11·92 | 2·2 | 5 | 5 | 10 | 8·22 | 60 | 49 |
| GQK2CA1 | 18 | 0·038 | 12 | 5·76 | 3·20 | 2·43 | 9·5 | 2·70 | 1·85 | 3·23 | 2·60 | 102 | 82 |
| GQK2CA2 | 18 | 0·038 | 12 | 5·76 | — | 2·43 | 9·5 | 2·70 | 2·95 | 3·23 | 2·77 | 102 | 87 |
| GQK2CA3 | 18 | 0·038 | 12 | 5·76 | 4·13 | 2·43 | 9·5 | 2·70 | 2·13 | 3·23 | 2·64 | 102 | 83 |
| HKZ2CA4 | 18 | 0·038 | 12 | 5·76 | 4·40 | 2·43 | 9·5 | 2·70 | 3·70 | 3·23 | 3·28 | 102 | 104 |
| HKZ2CB1 | 18 | 0·038 | 10 | 5·83 | 3·70 | 2·56 | 7·4 | 2·89 | 2·71 | 3·56 | 3·26 | 94 | 86 |
| HKZ2CB2 | 18 | 0·038 | 10 | 5·83 | 4·15 | 2·56 | 7·4 | 2·89 | 3·76 | 3·56 | 3·84 | 94 | 101 |
| HKZ2CC2 | 18 | 0·038 | 8 | 5·95 | 4·88 | 2·80 | 5·7 | 3·19 | 3·92 | 4·06 | 5·00 | 85 | 105 |
| HKZ2CD1 | 18 | 0·038 | 6 | 6·23 | 5·24 | 3·31 | 4·1 | 3·72 | 3·72 | 4·94 | 5·70 | 78 | 90 |
| HKZ2CD2 | 18 | 0·038 | 6 | 6·23 | 5·43 | 3·31 | 4·1 | 3·72 | 3·72 | 4·94 | 4·92 | 78 | 78 |
| HKZ2CE1 | 18 | 0·038 | 4 | 7·07 | 3·78 | 4·76 | 2·9 | 4·84 | 4·50 | 6·57 | 4·00 | 69 | 42 |
| HKZ2CE2 | 18 | 0·038 | 4 | 7·07 | 4·61 | 4·76 | 2·9 | 4·84 | 4·76 | 6·57 | 6·40 | 69 | 67 |
| HKZ3CA1 | 18 | 0·030 | 12 | 4·52 | — | 1·87 | 11·7 | 2·14 | 1·86 | 2·56 | 1·78 | 102 | 71 |
| HKZ3CB1 | 18 | 0·030 | 10 | 4·56 | 2·48 | 1·95 | 9·1 | 2·28 | 2·16 | 2·83 | 2·56 | 94 | 85 |
| HKZ3CC1 | 18 | 0·030 | 8 | 4·64 | 2·44 | 2·10 | 6·8 | 2·53 | 2·04 | 3·26 | 2·70 | 87 | 72 |
| HKZ3CD1 | 18 | 0·030 | 6 | 4·81 | 2·92 | 2·42 | 4·9 | 2·95 | 3·00 | 3·97 | 3·61 | 79 | 72 |
| HKZ3CE1 | 18 | 0·030 | 4 | 5·33 | 1·13 | 3·32 | 3·3 | 3·83 | 3·25 | 5·34 | 4·34 | 71 | 58 |
| GQK3CA1 | 18 | 0·024 | 12 | 3·61 | 1·83 | 1·47 | 14·3 | 1·72 | 1·60 | 2·07 | 1·91 | 103 | 96 |
| GQK3CB1 | 18 | 0·024 | 10 | 3·63 | 2·02 | 1·52 | 11·0 | 1·84 | 1·79 | 2·29 | 2·12 | 95 | 88 |
| GQK3CC1 | 18 | 0·024 | 8 | 3·68 | 2·19 | 1·62 | 8·2 | 2·03 | 2·66 | 2·64 | 3·02 | 88 | 101 |
| GQK3CD1 | 18 | 0·024 | 6 | 3·78 | 3·21 | 1·82 | 5·8 | 2·37 | 2·64 | 3·23 | 3·75 | 81 | 94 |
| GQK3CE1 | 18 | 0·024 | 4 | 4·10 | 2·24 | 2·40 | 3·9 | 3·07 | 3·33 | 4·35 | 5·52 | 72 | 92 |

| | | | | | | | | | | | | | |
|---|---|---|---|---|---|---|---|---|---|---|---|---|---|
| GQK4CA1 | 18 | 0·018 | 12 | 2·69 | 0·74 | 1·08 | 18·6 | 1·29 | 1·16 | 1·56 | 1·48 | 104 | 99 |
| GQK4CB1 | 18 | 0·018 | 10 | 2·71 | 0·82 | 1·11 | 14·3 | 1·38 | 1·22 | 1·73 | 1·72 | 96 | 96 |
| GQK4CC1 | 18 | 0·018 | 8 | 2·73 | 0·89 | 1·16 | 10·5 | 1·53 | 1·46 | 2·00 | 1·46 | 89 | 65 |
| GQK4CD1 | 18 | 0·018 | 6 | 2·79 | 1·24 | 1·27 | 7·3 | 1·78 | 2·04 | 2·47 | 2·87 | 82 | 96 |
| GQK4CE1 | 18 | 0·018 | 4 | 2·97 | — | 1·60 | 4·7 | 2·32 | 2·64 | 3·39 | 3·20 | 75 | 71 |
| HKZ1DA1 | 36 | 0·067 | 12 | 5·42 | 2·29 | 2·79 | 4·5 | 3·28 | 2·45 | 4·39 | 2·96 | 79 | 53 |
| HKZ1DB1 | 36 | 0·067 | 10 | 5·64 | 2·39 | 3·19 | 3·8 | 3·67 | 2·63 | 4·98 | 3·86 | 74 | 58 |
| HKZ1DC1 | 36 | 0·067 | 8 | 6·08 | 2·75 | 3·92 | 3·1 | 4·27 | 3·74 | 5·88 | 5·57 | 70 | 66 |
| HKZ1DD1 | 36 | 0·067 | 6 | 7·08 | 3·94 | 5·51 | 2·5 | 5 | 4·21 | 7·27 | 6·42 | 65 | 57 |
| HKZ1DE1 | 36 | 0·067 | 4 | 10·48 | 5·60 | 10·03 | 2·1 | 5 | 5 | 10 | 7·95 | 60 | 47 |
| HKZ2DA1 | 36 | 0·038 | 12 | 2·96 | 1·12 | 1·36 | 7·0 | 1·88 | 1·56 | 2·60 | 2·31 | 82 | 73 |
| HKZ2DA2 | 36 | 0·038 | 12 | 2·96 | 1·81 | 1·36 | 7·0 | 1·88 | 1·89 | 2·60 | 2·63 | 82 | 83 |
| HKZ2DB1 | 36 | 0·038 | 10 | 3·03 | 1·20 | 1·49 | 5·7 | 2·11 | 2·26 | 2·98 | 2·90 | 78 | 76 |
| HKZ2DC1 | 36 | 0·038 | 8 | 3·16 | 0·69 | 1·72 | 4·5 | 2·45 | 2·60 | 3·57 | 3·22 | 75 | 68 |
| HKZ2DD1 | 36 | 0·038 | 6 | 3·45 | 2·15 | 2·23 | 3·5 | 3·02 | 3·07 | 4·45 | 4·38 | 70 | 69 |
| HKZ2DD2 | 36 | 0·038 | 6 | 3·45 | 1·78 | 2·23 | 3·5 | 3·02 | 2·72 | 4·45 | 4·12 | 70 | 65 |
| HKZ2DE1 | 36 | 0·038 | 4 | 4·40 | 3·22 | 3·69 | 2·6 | 4·19 | 4·21 | 6·12 | 6·05 | 65 | 64 |
| HKZ2DE2 | 36 | 0·038 | 4 | 4·40 | 2·94 | 3·69 | 2·6 | 4·19 | 4·66 | 6·12 | 6·65 | 65 | 70 |
| GQK1A1 | ∞ | 0·067 | 12·4 | 0·85 | 0·85 | 0·85 | 3·2 | 2·15 | 2·36 | 3·71 | 3·22 | 69 | 60 |
| GQK1B1 | ∞ | 0·067 | 10·6 | 1·16 | 1·09 | 1·16 | 2·9 | 2·48 | 2·36 | 4·21 | 3·42 | 67 | 54 |
| GQK1C1 | ∞ | 0·067 | 8·6 | 1·76 | 1·64 | 1·76 | 2·6 | 3·01 | 3·38 | 4·93 | 5·10 | 63 | 65 |
| GQK1D1 | ∞ | 0·067 | 6·8 | 2·82 | 2·62 | 2·82 | 2·3 | 3·76 | 3·78 | 5·94 | 5·43 | 60 | 55 |
| GQK1D2 | ∞ | 0·067 | 6·8 | 2·82 | 2·52 | 2·82 | 2·3 | 3·76 | 3·84 | 5·94 | 5·54 | 60 | 56 |
| GQK1E1 | ∞ | 0·067 | 5 | 5·20 | 5·48 | 5·20 | 2·1 | 5 | 5 | 7·49 | 7·32 | 56 | 54 |
| GQK1E2 | ∞ | 0·067 | 5 | 5·20 | 4·98 | 5·20 | 2·1 | 5 | 4·99 | — | 7·02 | 56 | 52 |
| GQK2A1 | ∞ | 0·038 | 12 | 0·29 | 0·27 | 0·29 | 4·5 | 1·34 | 1·54 | 2·45 | 2·28 | 77 | 72 |
| GQK2A2 | ∞ | 0·038 | 12 | 0·29 | 0·34 | 0·29 | 4·5 | 1·34 | 1·38 | 2·45 | — | 77 | — |
| GQK2A3 | ∞ | 0·038 | 12 | 0·29 | 0·23 | 0·29 | 4·5 | 1·34 | 1·58 | 2·45 | 1·80 | 77 | 57 |
| GQK2B1 | ∞ | 0·038 | 10 | 0·42 | 0·42 | 0·42 | 3·9 | 1·59 | 1·50 | 2·88 | 2·29 | 76 | 60 |
| GQK2C1 | ∞ | 0·038 | 8 | 0·65 | 0·73 | 0·65 | 3·4 | 1·93 | 2·30 | 3·40 | 3·42 | 72 | 72 |
| GQK2D1 | ∞ | 0·038 | 6 | 1·16 | 1·08 | 1·16 | 2·9 | 2·48 | 2·63 | 4·21 | 3·60 | 66 | 57 |
| GQK2E1 | ∞ | 0·038 | 4·4 | 2·16 | 2·06 | 2·16 | 2·5 | 3·30 | 3·72 | 5·30 | 5·33 | 61 | 62 |

*Buckling stress $= E' \left\{ 3\frac{t^2}{b^2} + \sqrt{9\frac{t^4}{b^4} + \frac{1-\sigma^2 t^2}{3 \quad r^2}} \right\}$.

**$f_b = E' \left( 6\frac{t^2}{b^2} + 0{\cdot}21\frac{t}{r} \right)$.

† $n = 1{\cdot}3 + 0{\cdot}01\frac{b}{t}\left(1 + 2{\cdot}4\frac{b}{r}\right)$.

*Application of Results.*—The empirical formulae (2) and (3) for $f_b$ and $n$ respectively are suggested for use in analysis on the lines indicated in reference 4. It may, however, be considered that the assumption that the load carried by the panel is proportional merely to $t^2$ $\left(\text{equivalent to the assumptions } f_b = 0,\ n \propto \frac{b}{t}\right)$ is easier to apply and is equally well justified by the experimental results. In the last two columns of Table 1 are listed the ratios of the effective widths of the panels to their thicknesses at 10 tons/sq. in. edge stress according to both the theoretical and experimental results. According to the empirical formulae (2) and (3) there should be a slight increase in this ratio with increasing free width of panel ; the experimental evidence for this variation with width is very slight. On the other hand the formulae (2) and (3) indicate a slight increase in the effective width with increasing curvature, and in this respect the experimental results agree better with the empirical formula than with the assumption that the free width is proportional merely to the thickness.

So far as the values of effective width at 10 tons/sq. in. are concerned, therefore, there appears to be little to choose between the two assumptions. At lower values of the edge stress, the empirical formulae (2) and (3) will normally give better results. It may be suggested that this superiority is of little importance, on the grounds that the conditions at failure are alone of interest ; but it must be remembered that in many cases, e.g. tubes tested in bending, the limiting stress is developed only locally. In such cases, underestimate of the load carried at lower stresses will lead to underestimate of the collapsing load.

Lastly, it is necessary to consider whether the method of reference 4 or the " reduced effective width " method is easier to apply to practical structures. The chief difficulty of the second method consists in determining which parts of the structure are subjected to compression. Thus in estimating the strength of tubes in bending, it is necessary to find the neutral axis by a trial and error method. This difficulty is avoided by the method of reference 4. In fact, in the case of tubes of circular section if the values of $f_b$ and $n$ and of the ratio of the weight of the stringers to the weight of the sheet be given, the analysis of reference 4 enables the bending moment corresponding to any value of the limiting edge stress to be written down at once. Similar analysis could, of course, be worked out for other cross sections under other types of loading. Finally, it may be remarked that the method of reference 4 may be used in conjunction with the " reduced effective width " assumption merely by inserting the values $f_b = 0,\ n = C\frac{b}{t}$ where C is a constant.

---

REFERENCES.

1. The Buckling of Thin Plates in Compression.—H. L. Cox. R. & M. 1554.

2. Elastic Stability of a Curved Plate under Axial Thrust. S. C. Redshaw. J.R.Ae.S., Vol. 42, p. 536.

3. N.A.C.A. Report No. 356.

4. Stress Analysis of Thin Metal Construction.—H. L. Cox. J.R.Ae.S., Vol. 44, pp. 237–243.

5. Phil. Trans. A., Vol. 213, p. 187.

COMPRESSION TESTS ON CURVED PANELS.

Apparatus for supporting panels.

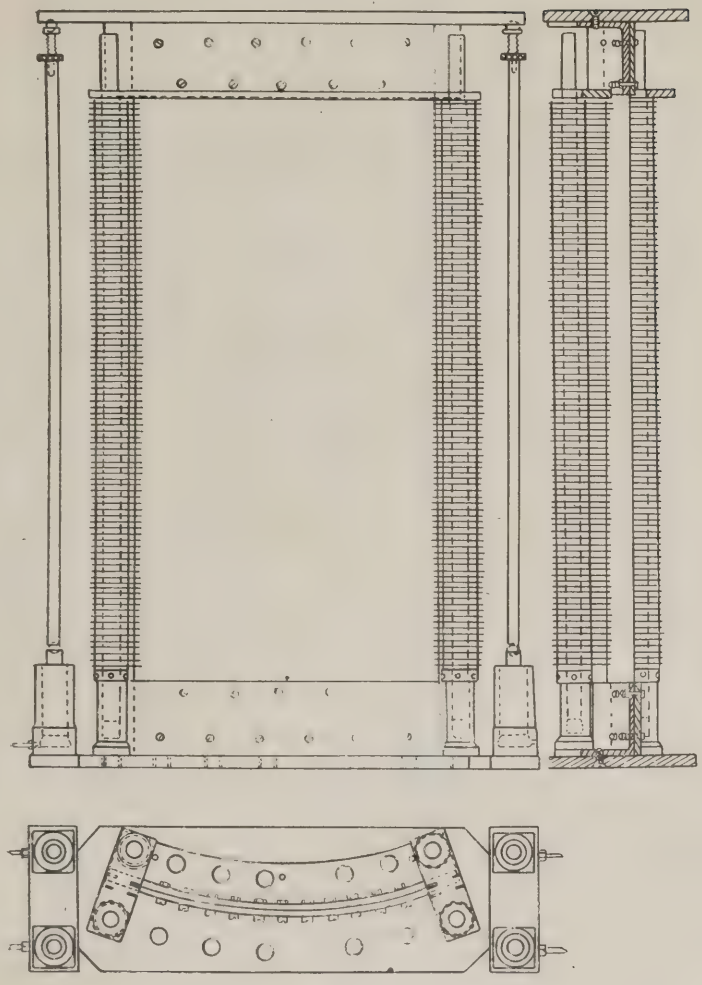

FIG. 1.

COMPRESSION TESTS ON CURVED PANELS

Schematic diagram of Strain Recording Apparatus

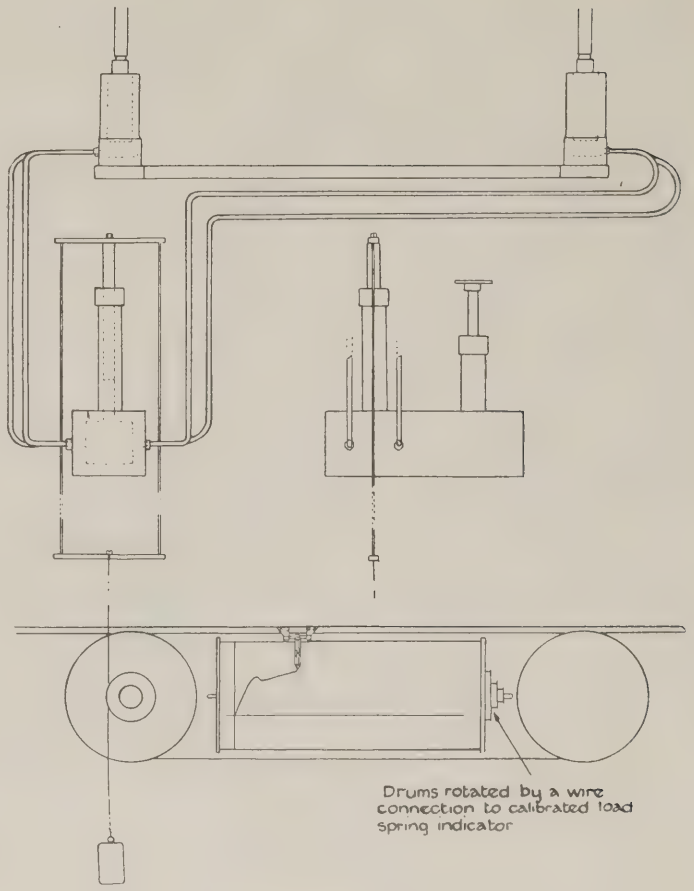


FIG. 2.

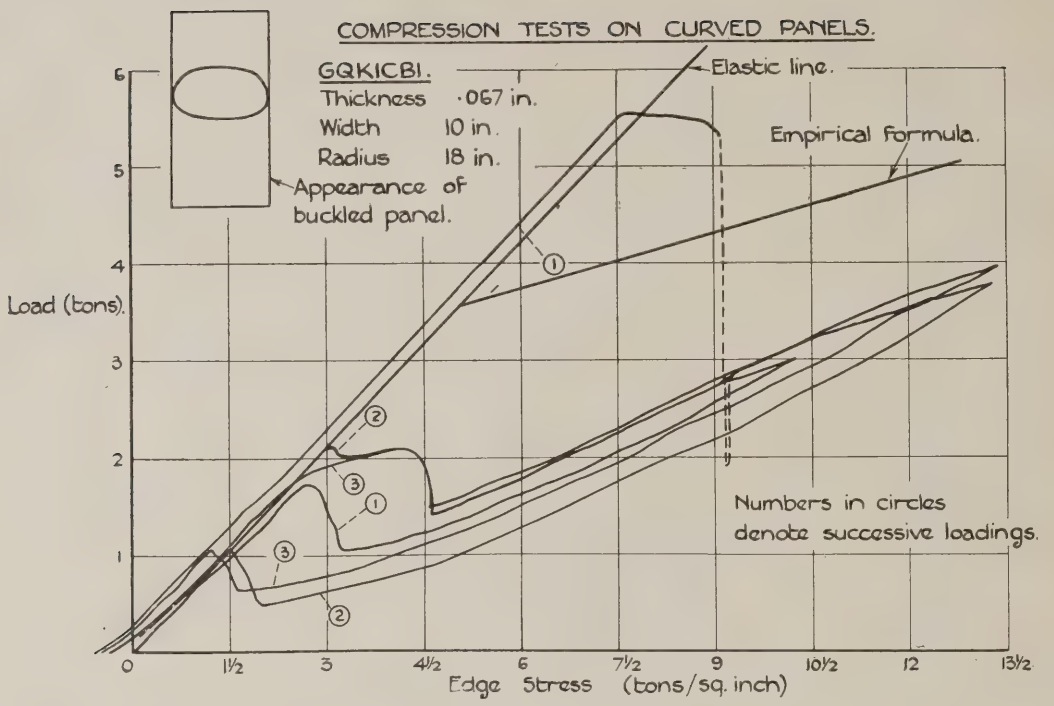
COMPRESSION TESTS ON CURVED PANELS.
GQKICBI.
Thickness ·067 in.
Width 10 in.
Radius 18 in.
Appearance of buckled panel.
Elastic line.
Empirical formula.
Numbers in circles denote successive loadings.
Load (tons).
Edge Stress (tons/sq. inch)
0
1½
3
4½
6
7½
9
10½
12
13½
1
2
3
4
5
6

FIG. 3.

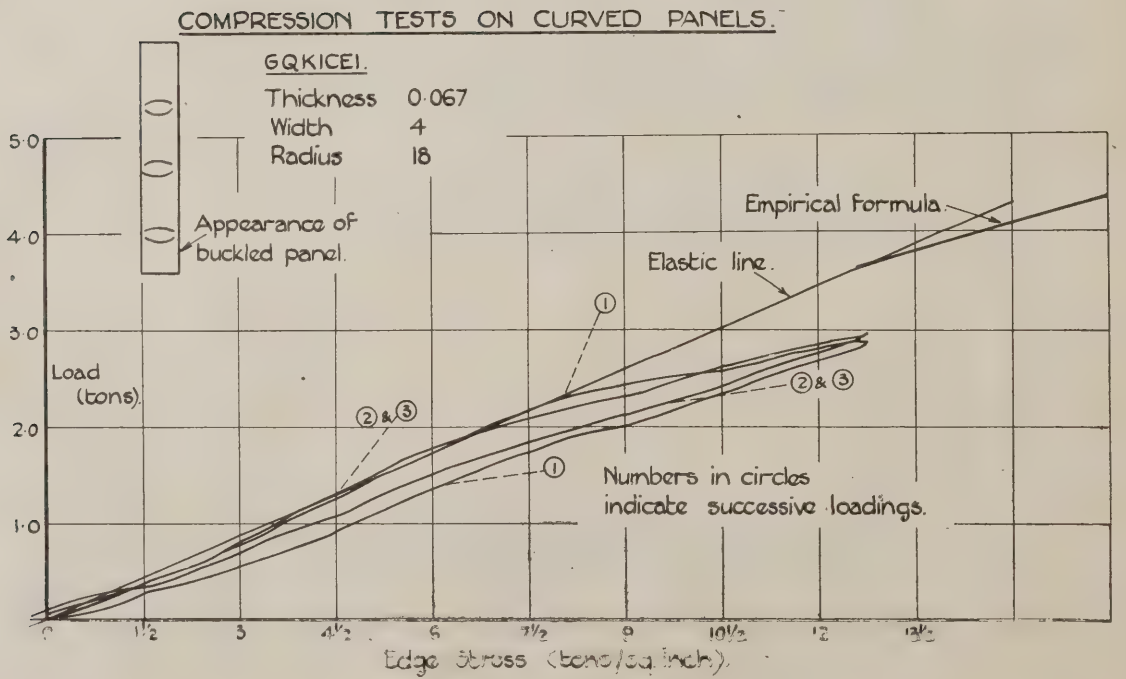
COMPRESSION TESTS ON CURVED PANELS.
GQKICEI.
Thickness 0·067
Width 4
Radius 18
Appearance of buckled panel.
Empirical formula.
Elastic line.
Numbers in circles indicate successive loadings.
Load (tons).
Edge Stress (tons/sq. inch).
1·0
2·0
3·0
4·0
5·0

FIG. 4.

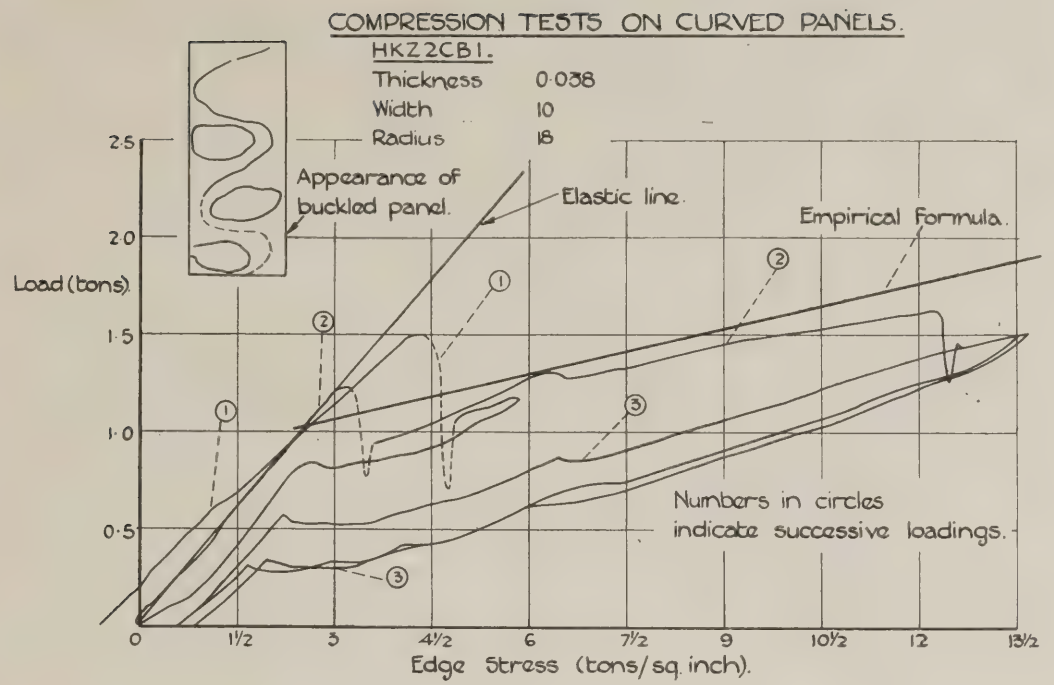
COMPRESSION TESTS ON CURVED PANELS.
HKZ2CB1.
Thickness 0·038
Width 10
Radius 18
Appearance of buckled panel.
Elastic line.
Empirical formula.
Load (tons).
2·5
2·0
1·5
1·0
0·5
Numbers in circles indicate successive loadings.
0
1½
3
4½
6
7½
9
10½
12
13½
Edge Stress (tons/sq. inch).

FIG. 5.

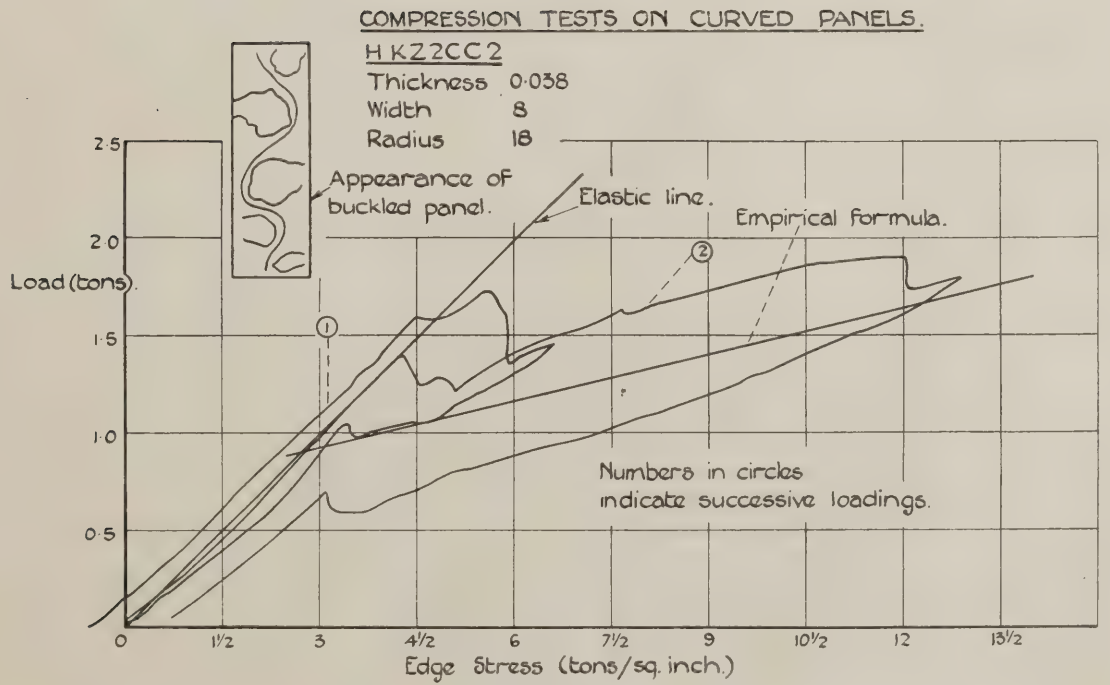
COMPRESSION TESTS ON CURVED PANELS.
HKZ2CC2
Thickness 0·038
Width 8
Radius 18
Appearance of buckled panel.
Elastic line.
Empirical formula.
Load (tons).
2·5
2·0
1·5
1·0
0·5
Numbers in circles indicate successive loadings.
0
1½
3
4½
6
7½
9
10½
12
13½
Edge Stress (tons/sq. inch.)

FIG. 6.

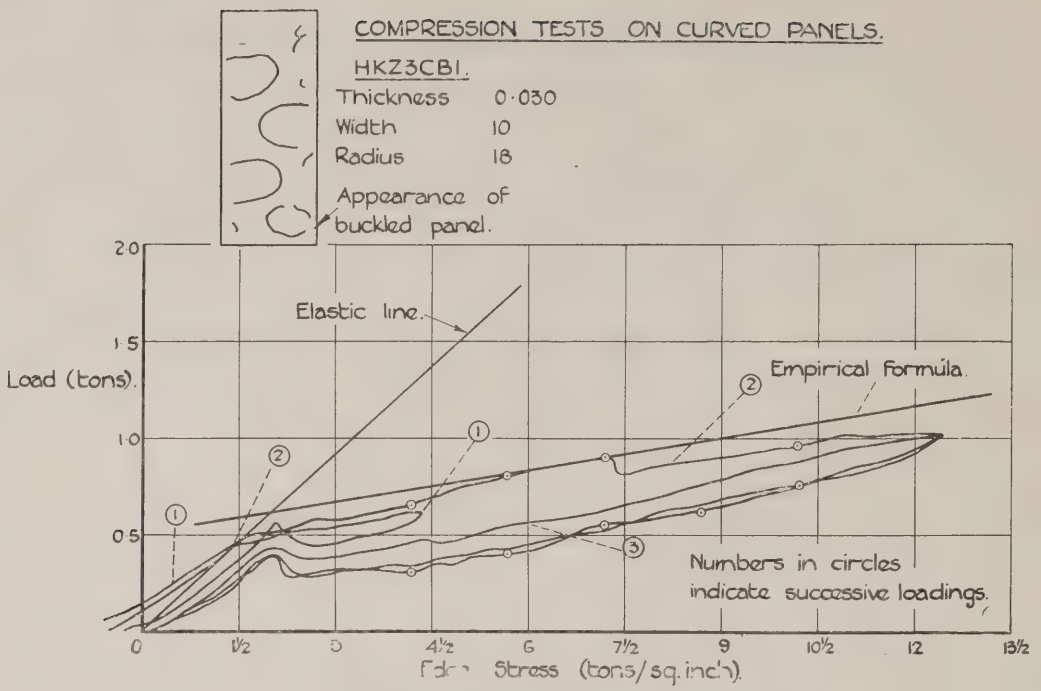
COMPRESSION TESTS ON CURVED PANELS.
HKZ3CB1.
Thickness 0·030
Width 10
Radius 18
Appearance of buckled panel.
Elastic line.
Empirical formula.
Numbers in circles indicate successive loadings.
Load (tons).
Edge Stress (tons/sq.inch).
2·0
1·5
1·0
0·5
0
1½
3
4½
6
7½
9
10½
12
13½

FIG. 7.

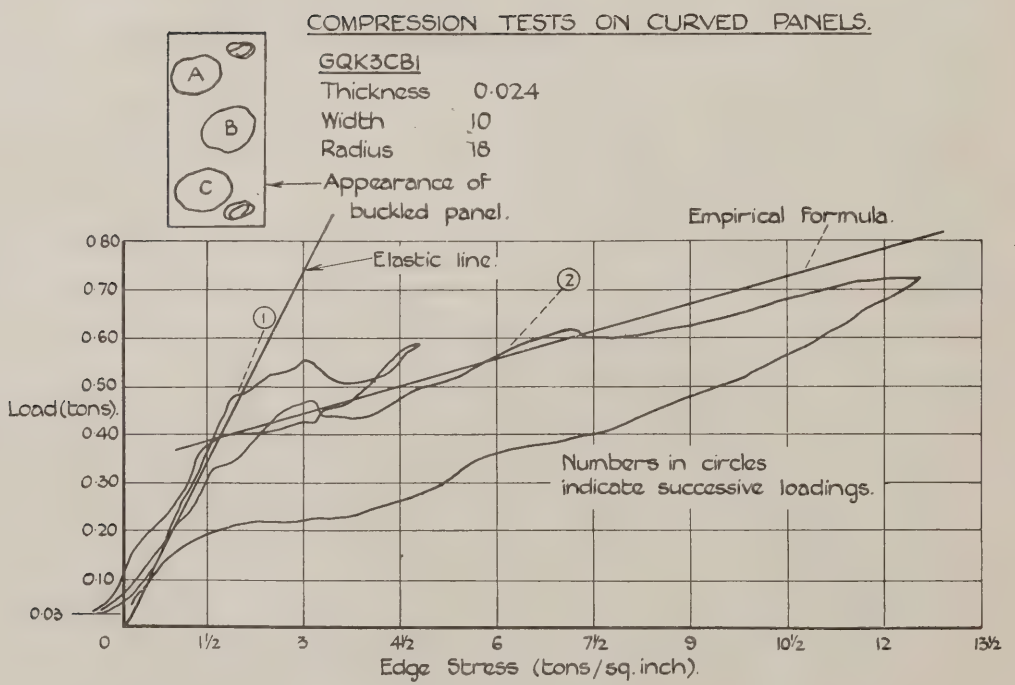
COMPRESSION TESTS ON CURVED PANELS.
GQK3CB1
Thickness 0·024
Width 10
Radius 18
A
B
C
Appearance of buckled panel.
Empirical formula.
Elastic line.
Numbers in circles indicate successive loadings.
Load (tons).
Edge Stress (tons/sq.inch).
0·80
0·70
0·60
0·50
0·40
0·30
0·20
0·10
0·03
0
1½
3
4½
6
7½
9
10½
12
13½

FIG. 8.

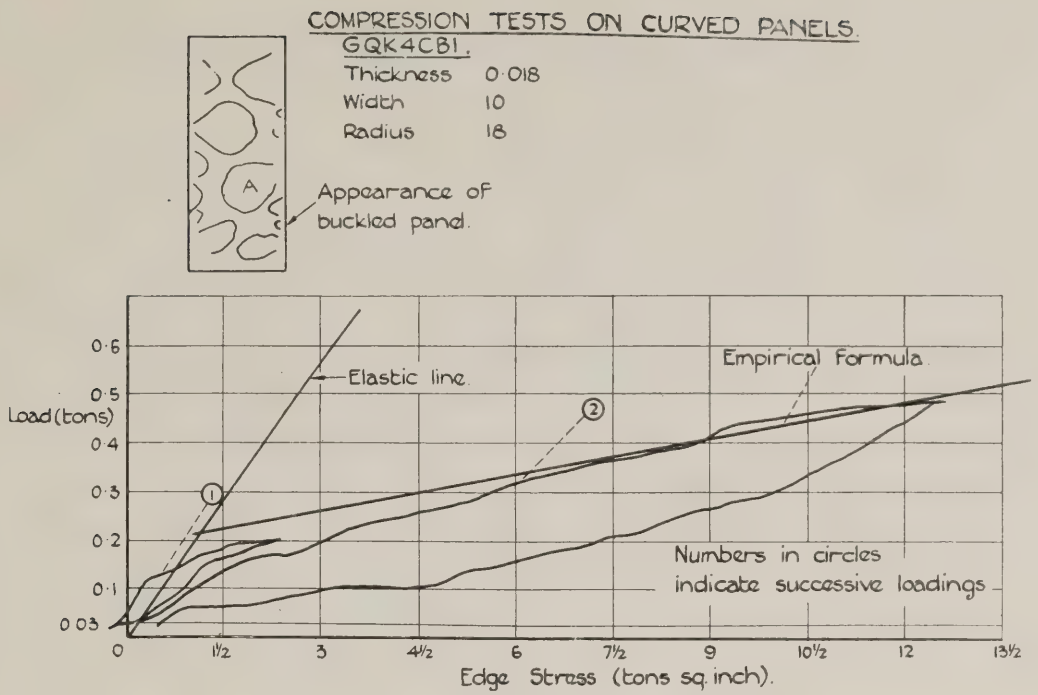
COMPRESSION TESTS ON CURVED PANELS.
GQK4CB1.
Thickness 0·018
Width 10
Radius 18
A
Appearance of buckled panel.
Elastic line.
Empirical Formula.
Load (tons)
0·6
0·5
0·4
0·3
0·2
0·1
0·03
0
1½
3
4½
6
7½
9
10½
12
13½
Numbers in circles indicate successive loadings
Edge Stress (tons sq. inch).

FIG. 9.

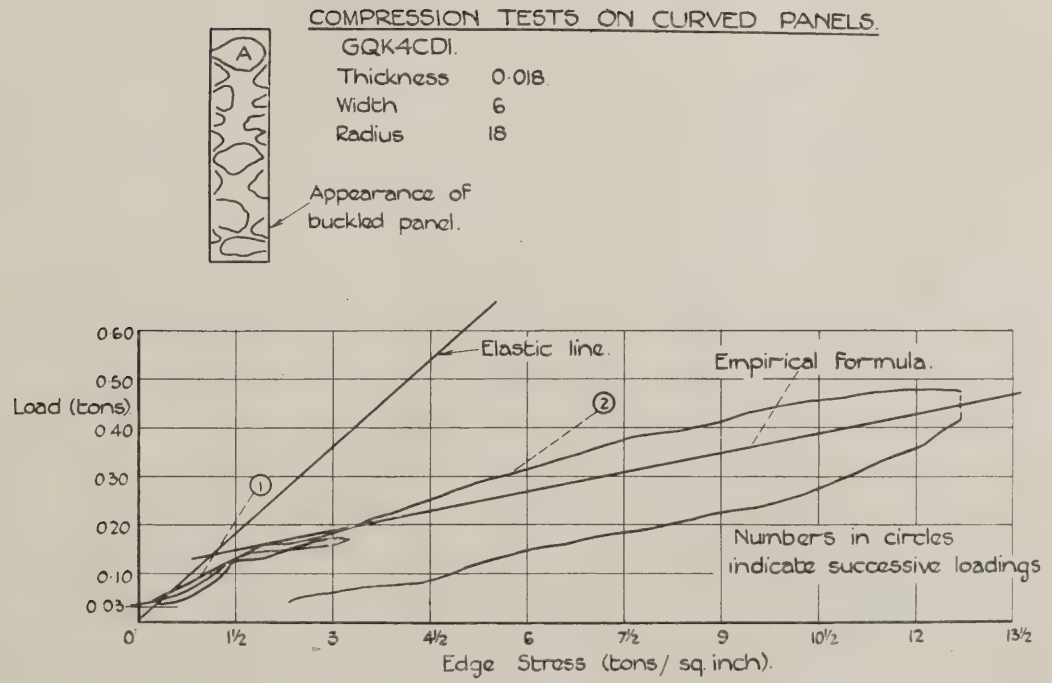
COMPRESSION TESTS ON CURVED PANELS.
GQK4CD1.
Thickness 0·018
Width 6
Radius 18
A
Appearance of buckled panel.
Elastic line.
Empirical Formula.
Load (tons)
0·60
0·50
0·40
0·30
0·20
0·10
0·03
0
1½
3
4½
6
7½
9
10½
12
13½
Numbers in circles indicate successive loadings
Edge Stress (tons/ sq. inch).

FIG. 10.

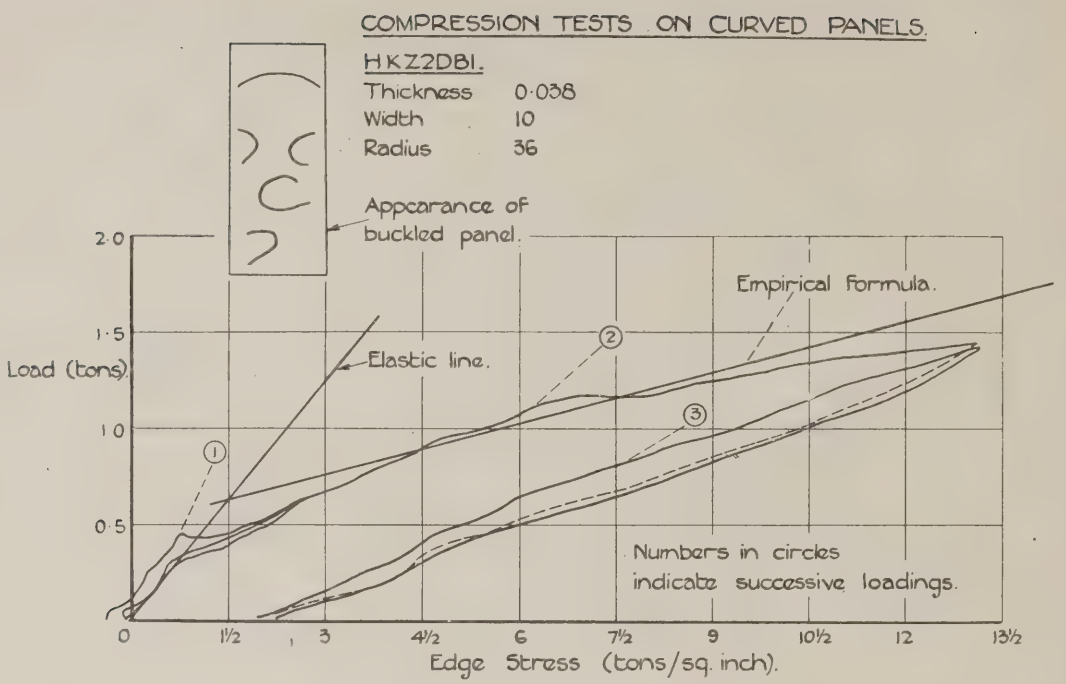
COMPRESSION TESTS ON CURVED PANELS.
HKZ2DB1.
Thickness 0·038
Width 10
Radius 36
Appearance of buckled panel.
Empirical formula.
Elastic line.
Load (tons).
2·0
1·5
1·0
0·5
Numbers in circles indicate successive loadings.
0
1½
3
4½
6
7½
9
10½
12
13½
Edge Stress (tons/sq. inch).

FIG. 11.

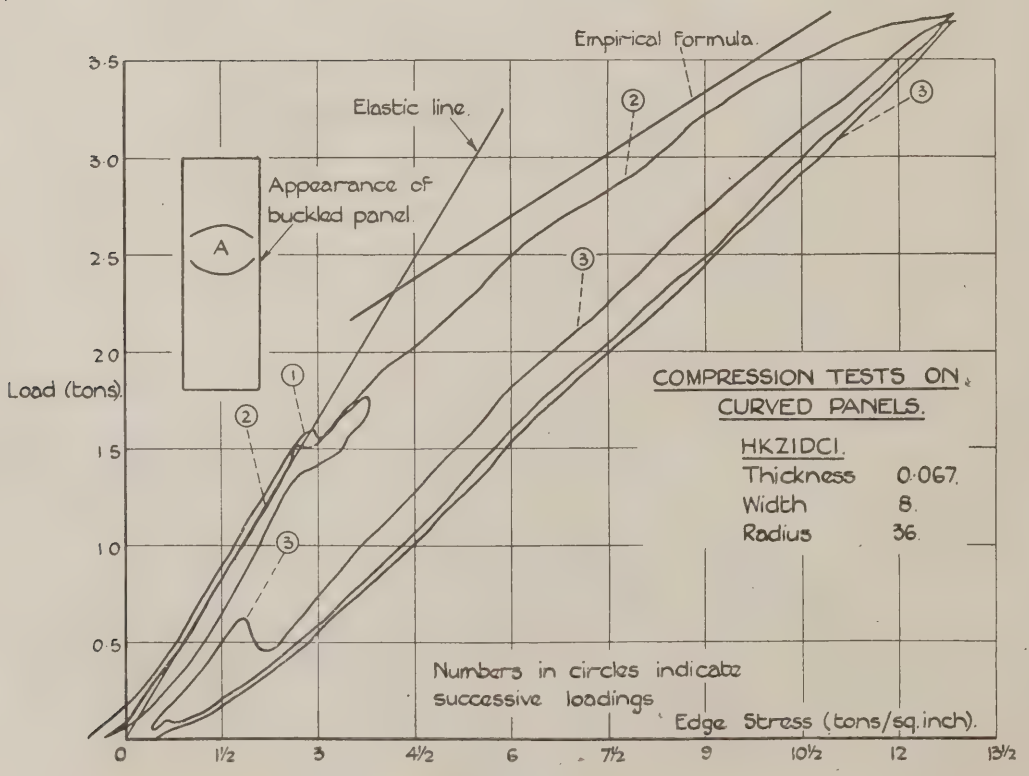
Empirical formula.
Elastic line.
Appearance of buckled panel.
A
Load (tons).
3·5
3·0
2·5
2·0
1·5
1·0
0·5
COMPRESSION TESTS ON CURVED PANELS.
HKZ1DC1.
Thickness 0·067.
Width 8.
Radius 36.
Numbers in circles indicate successive loadings.
0
1½
3
4½
6
7½
9
10½
12
13½
Edge Stress (tons/sq. inch).

FIG. 12.

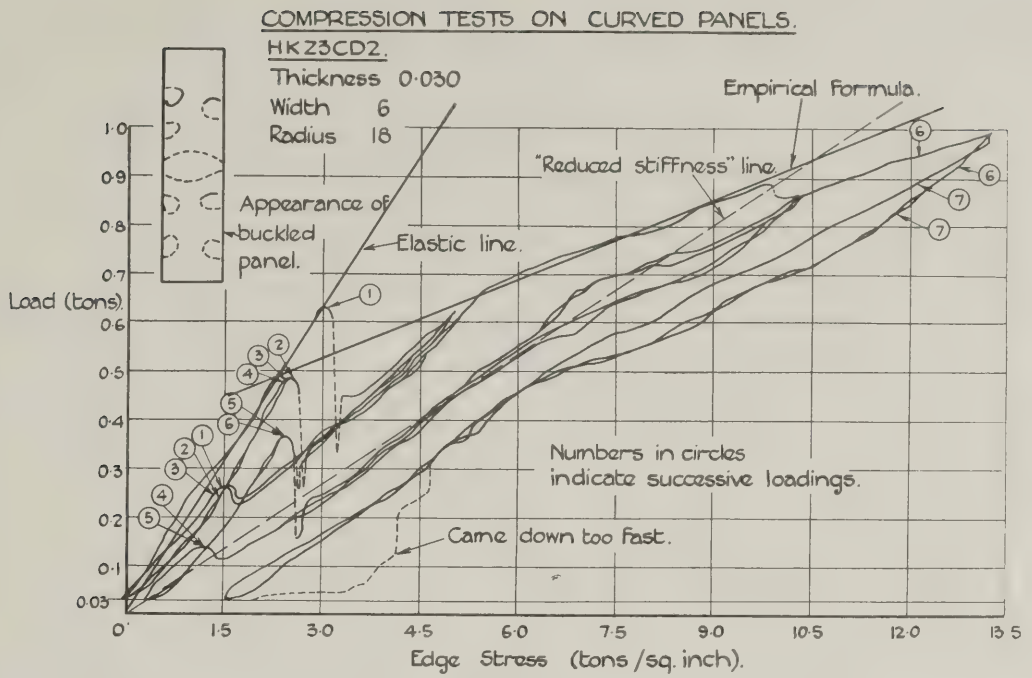


FIG. 13.

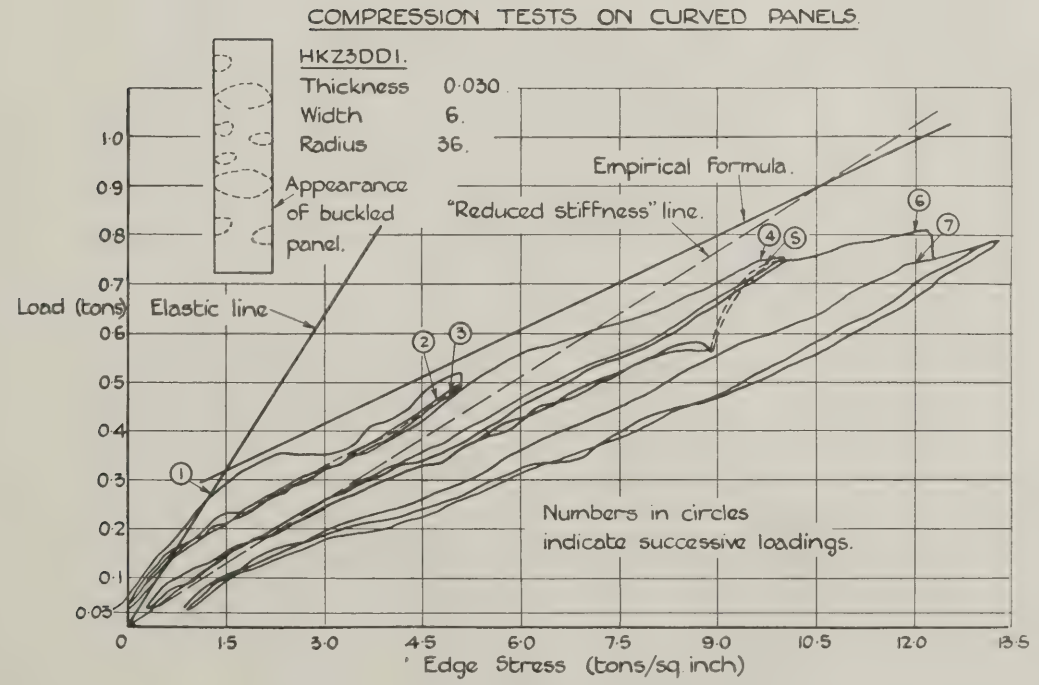


Fig. 14.

(58126) Wt. 5/536 500 2/42 Hw. G.277/1

LIBRARY
UNIVERSITY OF ILLINOIS
URBANA

## SYSTEM OF AXES

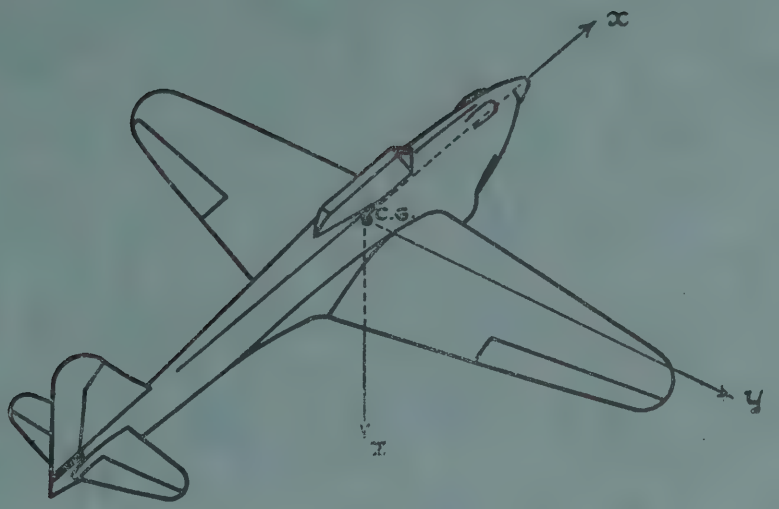


| Axes | Symbol Designation Positive direction | $x$ longitudinal forward | $y$ lateral starboard | $z$ normal downward |
|---|---|---|---|---|
| Force | Symbol | X | Y | Z |
| Moment | Symbol Designation | L rolling | M pitching | N yawing |
| Angle of Rotation | Symbol | $\phi$ | $\theta$ | $\psi$ |
| Velocity | Linear<br>Angular | $u$<br>$p$ | $v$<br>$q$ | $w$<br>$r$ |
| Moment of Inertia | | A | B | C |

Components of linear velocity and force are positive in the positive direction of the corresponding axis.

Components of angular velocity and moment are positive in the cyclic order $y$ to $z$ about the axis of $x$, $z$ to $x$ about the axis of $y$, and $x$ to $y$ about the axis of $z$.

The angular movement of a control surface (elevator or rudder) is governed by the same convention, the elevator angle being positive downwards and the rudder angle positive to port. The aileron angle is positive when the starboard aileron is down and the port aileron is up. A positive control angle normally gives rise to a negative moment about the corresponding axis.

The symbols for the control angles are :—

$\xi$ aileron angle
$\eta$ elevator angle
$\eta_T$ tail setting angle
$\zeta$ rudder angle

# Publications of the Aeronautical Research Committee

TECHNICAL REPORTS OF THE AERONAUTICAL RESEARCH COMMITTEE—

1933-34 Vol. I. Aerodynamics. £1 5s.

Vol. II. Structures, Engines, Instruments, etc. £1 10s.

1934-35 Vol. I. Aerodynamics. £2.

Vol. II. Seaplanes, Structures, Engines, Materials, etc. £2.

1935-36 Vol. I. Aerodynamics. £1 10s.

Vol. II. Structures, Flutter, Engines, Seaplanes, etc. £1 10s.

1936 Vol. I. Aerodynamics General, Performance, Airscrews, Flutter and Spinning. £2.

Vol. II. Stability and Control, Structures, Seaplanes, Engines, etc. £2 10s.

ANNUAL REPORTS OF THE AERONAUTICAL RESEARCH COMMITTEE—

1933-34 1s. 6d.

1934-35 1s. 6d.

April 1, 1935 to December 31, 1936. 4s.

1937 2s.

1938 1s. 6d.

INDEX TO THE TECHNICAL REPORTS OF THE ADVISORY COMMITTEE ON AERONAUTICS—

1909-1919 Reports and Memoranda No. 1600. 8s.

*Prices are net and postage extra.*


## His Majesty's Stationery Office

London W.C.2 : York House, Kingsway

Edinburgh 2 : 120 George Street — Manchester 2 : 39-41 King Street

Cardiff : 1 St. Andrew's Crescent — Belfast : 80 Chichester Street

or through any bookseller.

S.O. Code No. 23-1894

UNIVERSITY OF ILLINOIS

R. & M. No. 1896
(5572)
A.R.C. Technical Report

629.13
G79r
no.1896

MINISTRY OF AIRCRAFT PRODUCTION

AERONAUTICAL RESEARCH COMMITTEE
REPORTS AND MEMORANDA

# Transition in the Boundary Layer Caused by Turbulence

*By*

A. FAGE, F.R.S.,
of the Aerodynamics Department, N.P.L.

*Crown Copyright Reserved*

LONDON: HIS MAJESTY'S STATIONERY OFFICE
Price 2s. 0d. net

# AERODYNAMIC SYMBOLS

## 1. GENERAL

| | |
|---|---|
| $m$ | Mass |
| $t$ | Time |
| V | Resultant linear velocity |
| $\Omega$ | Resultant angular velocity |
| $\rho$ | Density, $\sigma$ relative density |
| $\nu$ | Kinematic coefficient of viscosity |
| R | Reynolds number, $R = lV/\nu$ (where $l$ is a suitable linear dimension) |

Normal temperature and pressure for aeronautical work are 15° C and 760 mm.

For air under these conditions $\begin{cases} \rho = 0{\cdot}002378 \text{ slug/cu. ft.} \\ \nu = 1{\cdot}56 \times 10^{-4} \text{ ft.}^2\text{/sec.} \end{cases}$

The slug is taken to be 32·2 lb.-mass.

| | |
|---|---|
| $\alpha$ | Angle of incidence |
| $e$ | Angle of downwash |
| S | Area |
| $b$ | Span |
| $c$ | Chord |
| A | Aspect ratio, $A = b^2/S$ |
| L | Lift, with coefficient $C_L = L/\frac{1}{2}\rho V^2 S$ |
| D | Drag, with coefficient $C_D = D/\frac{1}{2}\rho V^2 S$ |
| $\gamma$ | Gliding angle, $\tan\gamma = D/L$ |
| L | Rolling moment, with coefficient $C_l = L/\frac{1}{2}\rho V^2 bS$ |
| M | Pitching moment, with coefficient $C_m = M/\frac{1}{2}\rho V^2 cS$ |
| N | Yawing moment, with coefficient $C_n = N/\frac{1}{2}\rho V^2 bS$ |

## 2. AIRSCREWS

| | |
|---|---|
| $n$ | Revolutions per second |
| D | Diameter |
| J | $V/nD$ |
| P | Power |
| T | Thrust, with coefficient $k_T = T/\rho n^2 D^4$ |
| Q | Torque, with coefficient $k_Q = Q/\rho n^2 D^5$ |
| $\eta$ | Efficiency, $\eta = TV/P = Jk_T/2\pi k_Q$ |

# Transition in the Boundary Layer Caused by Turbulence

*By*

A. Fage, F.R.S.,

of the Aerodynamics Department, N.P.L.

*Reports and Memoranda No.* 1896

13*th January*, 1942

*Summary.*—The paper deals with transition from laminar to turbulent flow in the boundary layer of a body caused by turbulence in the free stream. A non-dimensional number representative of the conditions in the boundary layer at transition is derived, and it is shown that this number should tend to have a definite value when the transition is caused solely by isotropic turbulence. This number, denoted by $\xi_L$, is

$$3{\cdot}35\left[\left(\frac{\upsilon\sqrt{\overline{u_t^2}}}{\nu}\right)\left(\frac{\upsilon}{L}\right)^{\frac{1}{5}}\left(\frac{\nu}{u_1\upsilon}\right)^{\frac{2}{5}}\right],$$

where $\upsilon$ is the momentum thickness of the boundary layer,

$\sqrt{\overline{u_t^2}}$ is the root-mean-square value of the downstream component of the turbulent velocity $u_t$,

$\nu$ is the kinematic viscosity,

L is the Taylor scale of turbulence given by $\int_0^\alpha R_t dl$, where $R_t$ is the correlation coefficient for $u$-velocity fluctuations at two points separated by a lateral distance $l$,

and $u_1$ is the mean tangential velocity at the outer edge of the boundary layer.

Values of $\xi_L$ are calculated from the results of experiments made on flat plates, an elliptic cylinder and a long streamline body of revolution in isotropic turbulent streams behind square-mesh grids. The average value of $\xi_L$ obtained is 0·985, and of the six values calculated, four differ from the average value by amounts within $\pm$ 6 per cent., one is 28 per cent. greater and the other is 29 per cent. smaller.

Calculations of $\xi_L$ are also made for two flat plates and thirteen aerofoils in wind-tunnel streams. The conditions of flow in these streams are diverse and differ from those taken in the derivation of $\xi_L$. A representative value of $\xi_L$ for these models appears to be 0.49.

1. *Theory.*—It has been suggested by Professor Taylor[1,18] that the way in which turbulence is most likely to effect a laminar boundary layer is through the action of local pressure gradients which necessarily accompany turbulent flow, and that these gradients when sufficiently great and directed against the flow will cause a reversal of flow and a separation from the surface : and also that pressure gradients smaller than those necessary for the separation of a laminar boundary layer in a steady stream may be capable of causing the boundary layer to become turbulent.

The relation for the root-mean-square value of the fluctuating pressure gradients in the downstream direction $\sqrt{\overline{(\partial p/\partial x)^2}}$, obtained by Professor Taylor[1] for isotropic turbulence produced by passing a stream through a rectangular grid of Mesh M is

$$\frac{\sqrt{2}\lambda\rho\overline{u_t^2}}{\lambda_\eta \mathrm{AM}}\left(\frac{\mathrm{M}\sqrt{\overline{u_t^2}}}{\nu}\right)^{\frac{1}{2}},$$

where

$$\frac{\mathrm{M}\sqrt{\overline{u_t^2}}}{\nu} > 60,$$

$\lambda$ is a length which determines the scale of the eddies responsible for dissipation of energy by viscous forces,

$\lambda_\eta$ is a length which can be determined from diffusion experiments,

$\sqrt{\overline{u_t^2}}$ is the root-mean-square value of the downstream component of turbulent velocity $u_t$,

$$\mathrm{A}^2 = 5\left[\frac{d\left(\frac{\mathrm{U}_0}{\sqrt{\overline{u_t^2}}}\right)}{d\left(\frac{x}{\mathrm{M}}\right)}\right]^{-1},$$

$\mathrm{U}_0$ is the mean velocity in the free stream

and $x$ is the downstream distance behind the grid.

Professor Taylor then proceeds to consider the effect of $\sqrt{\overline{(\partial p/\partial x)^2}}$ on separation for the laminar boundary layer of a flat plate and that for a sphere, and, on the assumption that $\lambda/\lambda_\eta$ and A are constants, obtains a relation for the condition that the boundary layer on a flat plate will become turbulent, and the well-known relation

$$\mathrm{R}_{\mathrm{crit.}} = f\left[\frac{\sqrt{\overline{u_t^2}}}{\mathrm{U}_0}\left(\frac{\mathrm{D}}{\mathrm{M}}\right)^{\frac{1}{5}}\right]$$

for the critical Reynolds number of a sphere.

2. In a recent paper[2] the writer and Dr. Preston adopted the idea that transition can be caused by a separation due to the adverse pressure gradients associated with turbulence in the free stream, and obtained a non-dimensional number whose value at the point of transition in the boundary layer of a body of any form in an isotropic turbulent stream should tend to be constant, when the transition is caused solely by turbulence in the free stream. According to the Kármán-Pohlhausen theory it is to be expected that the instantaneous distribution of velocity in a cross-section of the boundary layer would depend on the local value of $-\frac{\delta^2}{\mu u_1}\frac{\partial p}{\partial s}$, and that the non-dimensional number $-\frac{\delta^2}{\mu u_1}\sqrt{\overline{\left(\frac{\partial p}{\partial s}\right)^2}}$ should tend to have a definite value at transition, where $\delta$ is the boundary layer thickness, $u_1$ is the mean tangential velocity at the outer edge of

the layer, $\nu$ is the viscosity, $p$ is the instantaneous pressure, and $s$ is the distance along the surface. On substitution of the relation

$$\sqrt{\overline{\left(\frac{\partial p}{\partial s}\right)^2} = \frac{\sqrt{2}\lambda\rho\overline{u_t^2}}{\lambda_\eta \mathrm{AM}} \left(\frac{\mathrm{M}\sqrt{\overline{u_t^2}}}{\nu}\right)^{\frac{1}{2}},$$

the number $-\frac{\delta^2}{\mu u_1}\sqrt{\overline{\left(\frac{\partial p}{\partial s}\right)^2}}$ becomes

$$\frac{\sqrt{2}\lambda}{\mathrm{A}\lambda_\eta}\left(\frac{\delta\sqrt{\overline{u_t^2}}}{\nu}\right)^{\frac{5}{2}}\left(\frac{\delta}{\mathrm{M}}\right)^{\frac{1}{2}}\left(\frac{\nu}{\delta u_1}\right),$$

which was written, in the earlier paper[2], in the form

$$\left(\frac{\sqrt{2}\lambda}{\mathrm{A}\lambda_\eta}\right)\left(\frac{\delta}{\upsilon}\right)^2\left(\frac{\sqrt{\overline{u_t^2}}}{u_\mathrm{T}}\right)^{\frac{5}{2}}\left(\frac{\upsilon u_\mathrm{T}}{\nu}\right)^{\frac{5}{2}}\left(\frac{\upsilon}{\mathrm{M}}\right)^{\frac{1}{2}}\left(\frac{\nu}{\upsilon u_1}\right),$$

where $u_\mathrm{T}$ is the maximum value of $u_t$,

$\nu$ is the kinematic viscosity,

$\upsilon$ is the momentum thickness,

given by $\int_0^\delta \left(\frac{u}{u_1}\right)\left(1-\frac{u}{u_1}\right)dy$,

and $u$ is the mean tangential component of the velocity in the boundary layer at a normal distance $y$ from the surface.

The number was then reduced to the simpler form

$$\left(\frac{\upsilon u_\mathrm{T}}{\nu}\right)\left(\frac{\upsilon}{\mathrm{M}}\right)^{\frac{1}{5}}\left(\frac{\nu}{u_1\upsilon}\right)^{\frac{2}{5}},$$

obtained by taking the $(\frac{2}{5})^{\text{th}}$ root, and ignoring the factor

$$\left[\left(\frac{\sqrt{2}\lambda}{\mathrm{A}\lambda_\eta}\right)\left(\frac{\delta}{\upsilon}\right)^2\left(\frac{\sqrt{\overline{u_t^2}}}{u_\mathrm{T}}\right)^{\frac{5}{2}}\right]^{\frac{2}{5}},$$

which was taken to be constant.

It was shown that values of $(\upsilon u_\mathrm{T}/\nu)\ (\upsilon/\mathrm{M})^{\frac{1}{5}}\ (\nu/u_1\upsilon)^{\frac{2}{5}}$ at transition, calculated from measurements taken for a long streamline body of revolution in water streams behind square-mesh grids and also for a flat plate in isotropic turbulent streams, from measurements made by Hall and Hislop[3], had the same order of magnitude.

3. It is convenient in the present paper to introduce the Taylor scale of turbulence, L, where $\mathrm{L} = \int_0^\alpha \mathrm{R}_l dl$, and $\mathrm{R}_l$ is the correlation coefficient for $u$-velocity fluctuations at two points separated by a lateral distance $l$. The number whose value should, on the assumptions made, be constant at transition can then be written in the form

$$\left[\frac{\sqrt{2}}{\mathrm{A}}\ \frac{\lambda}{\lambda_\eta}\left(\frac{\delta}{\upsilon}\right)^2\left(\frac{\mathrm{L}}{\mathrm{M}}\right)^{\frac{1}{2}}\right]^{\frac{2}{5}}\quad\left[\left(\frac{\upsilon\sqrt{\overline{u_t^2}}}{\nu}\right)\left(\frac{\upsilon}{\mathrm{L}}\right)^{\frac{1}{5}}\left(\frac{\nu}{\upsilon u_1}\right)^{\frac{2}{5}}\right]$$

The condition that transition is caused solely by turbulence holds when the value of $\Lambda$, that is $(\delta^2/\nu)\ du_1/ds$, is zero. The value of $\delta/\upsilon$ calculated from a solution of the laminar boundary layer equations for a known pressure distribution is therefore constant. The value given by the Kármán-Pohlhausen theory is 8·51. A representative relation for L/M obtained by Dryden and others [14] (Table III) from measurements made in the turbulent streams behind square-mesh grids, M = 0·25, 0·5, 1·0 and 3·25 in., is $L/M = 0{\cdot}147 + 0{\cdot}0025\ (x/M)$. The relation for A obtained by Taylor [17] (p. 441) is

$$-\frac{U_0}{(\sqrt{\overline{u_i^2}})^3}\ \frac{d\ (\overline{u_i^2})}{dx} = \frac{10}{MA^2},$$

which can be written

$$\frac{d\left(\frac{U_0}{\sqrt{\overline{u_i^2}}}\right)}{d\ (x/M)} = \frac{5}{A^2}.$$

Measurements of $U_0/\sqrt{\overline{u_i^2}}$ obtained from the experiments of Dryden and others[14] (Table IV), are plotted against $x/M$ in Fig. 1. Included in the figure is a curve given by the relation

$$\frac{d\left(\frac{U_0}{\sqrt{\overline{u_i^2}}}\right)}{(d/x\mathrm{M})} = \frac{5}{A^2} = \frac{0{\cdot}20}{[0{\cdot}147 + 0{\cdot}0025\ x/M]}.$$

The measurements lie close to this curve so that $A = 5\ [0{\cdot}147 + 0{\cdot}0025\ x/M]^{\frac{1}{2}}$. The value of $(L/M)^{\frac{1}{2}}/A$ is therefore 0·2. Experimental values of $\lambda_\eta/\lambda$ obtained for turbulent flows behind square-mesh grids are 0·5 (Taylor[17], p. 478) and 1·6 (Hall[3], p. 13), and theoretical values obtained for definite eddy systems are 0·7 (Taylor[3], p. 13) and 0·8 to 1 (Green[3], p. 12). Another experimental value, which lies between Green's theoretical values, 0·8, and 1·0, has been obtained by Hall, since the publication of his paper[3]. It is a matter of some difficulty to obtain a good value for $\lambda_\eta/\lambda$, and no experiments have been made to determine its dependence on the turbulence number $L\frac{\sqrt{\overline{u_i^2}}}{\nu}$. Taking a representative value $\lambda_\eta/\lambda = 1$, and substituting $(\delta/\upsilon)^2 = 72{\cdot}5$ and $(L/M)^{\frac{1}{2}}/A = 0{\cdot}2$, we get

$$\left[\frac{\sqrt{2}}{A}\frac{\lambda}{\lambda_\eta}\left(\frac{\delta}{\upsilon}\right)^2\left(\frac{L}{M}\right)^{\frac{1}{2}}\right]^{\frac{2}{5}} = 3{\cdot}35$$

The analysis therefore leads to the conclusion that the value of

$$3{\cdot}35\left[\left(\frac{\upsilon\sqrt{\overline{u_i^2}}}{\nu}\right)\left(\frac{\upsilon}{L}\right)^{\frac{1}{5}}\left(\frac{\nu}{u_1\upsilon}\right)^{\frac{2}{5}}\right],$$

denoted by $\xi_L$ (*see* footnote), should tend to have a constant value at the point of transition in the boundary layer of a body in a turbulent stream behind a square-mesh grid, when the transition is caused solely by turbulence.

---

The symbol $\xi_L$ was used for the non-dimensional number $\left(\frac{u_T\upsilon}{\nu}\right)\left(\frac{\upsilon}{L}\right)^{\frac{1}{5}}\left(\frac{\nu}{u_1}\right)^{\frac{2}{5}}$ in the earlier paper[2].

4. The Taylor relation

$$\sqrt{\overline{\left(\frac{\partial p}{\partial x}\right)^2}} = \frac{\sqrt{2}\ \lambda\ \rho\ \overline{u_t^2}}{\lambda_\eta\ \mathrm{AM}} \left(\frac{\mathrm{M}\sqrt{\overline{u_t^2}}}{\nu}\right)^{\frac{1}{2}}$$

was obtained by the substitution of

$$\frac{\lambda}{\mathrm{M}} = \mathrm{A}\left[\frac{\nu}{\mathrm{M}\sqrt{\overline{u_t^2}}}\right]^{\frac{1}{2}}$$

in the relation

$$\sqrt{\overline{\left(\frac{\partial p}{\partial x}\right)^2}} = \sqrt{2}\rho\,\frac{\overline{u_t^2}}{\lambda_\eta}$$

(*see* Ref. 17, p. 440). From Dryden's experiments we have obtained the relation $\mathrm{A} = 5(\mathrm{L}/\mathrm{M})^{\frac{1}{2}}$, and on substitution in the relation

$$\frac{\lambda}{\mathrm{M}} = \mathrm{A}\left[\frac{\nu}{\mathrm{M}\sqrt{\overline{u_t^2}}}\right]^{\frac{1}{2}}$$

we obtain

$$\frac{\lambda}{\mathrm{L}} = 5\left[\frac{\nu}{\mathrm{L}\sqrt{\overline{u_t^2}}}\right]^{\frac{1}{2}}.$$

A relation of this form can be obtained from considerations of similarity (*see* Taylor, Ref. 18, p. 299). For similar flow systems the Reynolds stresses are proportional to $\rho\,\overline{u_t^2}$ ($u_t$ = typical velocity), and the rate of dissipation per unit volume is proportional to $\rho\left(\sqrt{\overline{u^2}}\right)^3/\mathrm{L}$ (L = typical length). For isotropic turbulence the rate of dissipation due to viscosity is $15\,\mu\,\overline{u_t^2}/\lambda^2$. The two ways of regarding dissipation are consistent if

$$\rho\,\frac{\left(\sqrt{\overline{u_t^2}}\right)^3}{\mathrm{L}} = 15\,\mu\,\frac{\overline{u_t^2}}{\lambda^2},$$

that is, if

$$\frac{\lambda}{\mathrm{L}} = \mathrm{B}\left[\frac{\nu}{\mathrm{L}\sqrt{\overline{u_t^2}}}\right]^{\frac{1}{2}},$$

where B is a constant. It should be noted that the values of $\mathrm{U}_0/\sqrt{\overline{u_t^2}}$ measured by Dryden at a given value of $x/\mathrm{M}$ behind a grid were independent of $\mathrm{U}_0$ but they were not independent of M. The conditions for similarity were therefore not fully satisfied. The relation $\mathrm{A} = 5(\mathrm{L}/\mathrm{M})^{\frac{1}{2}}$ given in section 3 was obtained for mean curves of $\mathrm{U}_0/\sqrt{\overline{u_t^2}}$ and L/M against $x/\mathrm{M}$, from Dryden's results for $\mathrm{M} = 0{\cdot}25$, $0{\cdot}5$, $1{\cdot}0$ and $3{\cdot}25$ in.

5. Values of $\xi_\mathrm{L}$ at transition ($\Lambda = 0$) calculated for a large number of models of different size and shape and tested in turbulent streams for which the values of $\sqrt{\overline{u_t^2}}$ and of L differ appreciably are given in Tables 1 and 2. The experiments analysed fall into two groups: I, those made on models in streams behind square-mesh grids, and II, those made on models in wind-tunnel streams. The conditions of the experiments of Group II do not satisfy those assumed in the derivation of $\xi_\mathrm{L}$, but the calculations were considered to be worth while since they show the probable variation in $\xi_\mathrm{L}$ to be expected and whether a reasonably representative value of $\xi_\mathrm{L}$ can be obtained.

The results of twenty experiments have been analysed, five in Group I and fifteen in Group II. Descriptions of the models tested and relevant details of the experiments made on them are given below.

*Group I. Models in Streams Behind Square-Mesh Grids.* (1) *Two Flat Plates. Cambridge*[3].—One plate was of smooth plate glass, three-eighths of an inch in thickness, and had an elliptical leading edge. The other plate was of rolled duralumin of thickness one-eighth of an inch, and had a sharp leading edge. Both plates had excellent surfaces. M = 0·5 and 1 in. Position of transition point obtained from surface-tube observations.

(2) *Flat Plate. National Bureau of Standards, U.S.A.*[4].—Polished aluminium plate, 0·125 in. thick, with sharp bevelled leading edge. M = 0·5 and 1 in. Position of transition point obtained from inspection of oscillograph records.

(3) *Elliptic Cylinder. National Bureau of Standards, U.S.A.*[5].—The cylinder was made of wood, and had a smooth polished surface. Major and minor axes 11·78 and 3·98 in., respectively. M = 1 in. Position of transition point deduced from change in shape of velocity distribution in boundary layer.

(4) *Long Streamline Body of Revolution. Small Water Tunnel, N.P.L.*[2].—Brass model with ellipsoidal nose. Polished surface. M = 0·5 in. Position of transition point obtained from behaviour of filament bands in boundary layer.

(5) *Long Streamline Body of Revolution. Water Tunnel, N.P.L.*[2].—Same as (4), except M = 0·25 in.

*Group II. Models in Wind-Tunnel Streams.*—(6) *Flat Plate. National Bureau of Standards, U.S.A.*[4].—Polished aluminium plate, 0·125 in. thick, with sharp bevelled leading edge. Position of transition point obtained from an inspection of oscillograph records.

(7) *Flat Plate. Compressed Air Tunnel*[6].—Aluminium plate 0·125 in. thick having an elliptical leading edge.

(8) *Symmetrical Aerofoil. D.V.L. 5 × 7 Metre Tunnel*[7].—Composite model with a marble surface finish. Chord = 10·5 ft. Maximum thickness = 0·127 chord, 0° incidence.

(9) *Symmetrical Aerofoil. D.V.L. 5 × 7 Metre Tunnel*[7].—Same as (8) except maximum thickness = 0·206 chord.

(10) *Aerofoil N.A.C.A.*23012. *Variable Density Tunnel*[8].—Duralumin model. Chord = 5 in. Maximum thickness = 0·12 chord. Incidence for minimum profile drag.

(11) *Aerofoil N.A.C.A.*0012. *Variable Density Tunnel*[8].—Duralumin model. Symmetrical section. Chord = 5 in. Maximum thickness = 0·12 chord. 0° incidence.

(12) *Aerofoil N.A.C.A.*0012. *Full Scale Wind Tunnel N.A.C.A.*[9].—Model of steel-spar construction with ribs spaced at 12 in. intervals. The covering was $\frac{1}{16}$ in. aluminium sheet. Glossy waxlike finish. Chord 6 ft. Maximum thickness = 0·12 chord.

(13) *Aerofoil N.A.C.A.*0012. *Compressed Air Tunnel*[10].—Steel model chromium plated and hand-finished surface. Chord = 8 in. Maximum thickness = 0·12 chord. 0° incidence.

(14) *Joukowski Aerofoil. Compressed Air Tunnel*[11].—The model was made of cast aluminium and had an aerodynamic smooth surface up to Reynolds number 15 × $10^6$. Chord = 2 ft. Maximum thickness = 0·127 chord. Symmetrical section 0° incidence. Position of the point of transition determined by " wires " method.

(15) *Joukowski Aerofoil. Compressed Air Tunnel*[11].—Same as (14) except maximum thickness = 0·236 chord.

(16) *Aerofoil A. Compressed Air Tunnel*[19].—Hiduminium model, hand finished. Symmetrical section. Chord = 7·84 in. Maximum thickness = 0·12 chord.

(17) *Aerofoil B. Compressed Air Tunnel*[19].—Hiduminium model, with good buffed surface. Chord = 8 in. Maximum thickness = 0·12 chord. Incidence for which profile drag is a minimum.

(18) *Joukowski Aerofoil. No.* 3, 7 *ft. Tunnel, N.P.L.*[12].—Gunmetal model having a smooth polished surface. Chord = 39·7 in. Maximum thickness = 0·1507 chord. Transition point and transition region determined from surface-tube readings.

(19) *Aerofoil C.* 13 *ft.* × 9 *ft. Tunnel, N.P.L.*[19].—Wooden model with hand-polished varnished surface. Chord = 70 in. Maximum thickness = 0·12 chord. Symmetrical section. 0° incidence.

(20) *Aerofoil C.* 13 *ft.* × 9 *ft. Tunnel, N.P.L.*[19].—Same as (19), except chord = 42 in.

6. For models, Nos. 1–6, 14, 15 and 18, the transition point was located experimentally, and for each of the other models (aerofoils) the position taken was that for which the profile drag calculated by the Squire-Young method[13] for the known pressure distribution is equal to the measured drag. The experimental conditions considered are those for transition at or near the point on the surface where $\Lambda = 0$. Calculations of $\upsilon u_1/\nu$ and $\Lambda$ were made bythe Kármán-Pohlhausen method of solution of the laminar boundary layer equations for distributions of $u_1/U_0$ determined either from measured or theoretical pressure coefficients, $(p - p_0)/\frac{1}{2}\rho U_0^2$ (mean values), by the standard relation

$$\frac{u_1}{U_0} = \left[1 - \frac{(p - p_0)}{\frac{1}{2}\rho U_0^2}\right]^{\frac{1}{2}}.$$

Measured values of $\sqrt{\overline{u_t^2}}$ and L were taken in the calculation of $\xi_L$ for models 1, 2 and 3, and measured values of $\sqrt{\overline{u_t^2}}$ (taken to be $(1/3{\cdot}3)^{\text{th}}$ of the value of $u_T$ measured with a fluid-motion microscope) and calculated values of L (from relations in Table 3, Ref. 14) for model 4 (and 5). For each of the other models a value of $\frac{\sqrt{\overline{u_t^2}}}{U_0}\left(\frac{1}{L}\right)^{\frac{1}{5}}$ for the free stream, calculated from the relation $\log_{10}\left[100\left(\frac{\sqrt{\overline{u_t^2}}}{U_0}\right)\left(\frac{D}{L}\right)^{\frac{1}{5}}\right] = 0{\cdot}991 - 2{\cdot}193\ \log_{10}\ [R_{crit.} \times 10^{-5}]$, given in Ref. 15 for the known sphere number, $R_{crit.}$ was taken.

7. *Discussion of Results.*—The results of the calculations made for the models in turbulent streams behind square-mesh grids (Group I) are given in Table 1. Values of $\xi_L$ are plotted against the turbulence number $\frac{L\sqrt{\overline{u_t^2}}}{\nu}$ in Fig. 2. The average value of $\xi_L$ is 0·985. Four of the six values differ from this average value by amounts within ±6 per cent., whilst the value for the flat plate (2*a*) is 28 per cent. greater and that for the long streamline body (5) is 29 per cent. smaller. The values of $\xi_L$ for the flat plate (1) change from 1·07 to 0·90 of its mean value over the range $\upsilon u_1/\nu = 293$ to 559 covered (Table 1). The values of $\xi_L$ for the elliptic cylinder and the long streamline body do not change appreciably with $\Lambda$, over the small ranges covered (Table 1). It will be noticed that the condition $\frac{M\sqrt{\overline{u_t^2}}}{\nu} > 60$, assumed in the derivation of the relation for $\xi_L$, is satisfied for each model.

TABLE 1—GROUP I

| Model and Number | $\frac{vu_1}{\nu}$ | $\Lambda$ | M in. | $\frac{L\sqrt{\overline{u_t^2}}}{\nu}$ | $\frac{M\sqrt{\overline{u_t^2}}}{\nu}$ | $\xi_L$ | $\frac{\sqrt{\overline{u_t^2}}}{U_0}\left(\frac{1}{L}\right)^{\frac{1}{5}}$ L in ft. |
|---|---|---|---|---|---|---|---|
| (1) Flat Plate .. .. .. (Cambridge) | 559 | 0 | 0·5 | 35·1 | 99 | 0·915 | 0·021 |
| | 493 | 0 | 0·5 | 32·6 | 98 | 0·980 | 0·025 |
| | 437 | 0 | 0·5 | 33·9 | 109 | 0·980 | 0·026 |
| | 360 | 0 | 0·5 | 31·4 } 35·7 | 111 | 1·015 } 1·012 | 0·032 |
| | 328 | 0 | 1·0 | 33·9 | 118 | 1·051 | 0·031 |
| | 322 | 0 | 1·0 | 41·7 | 148 | 1·060 | 0·032 |
| | 293 | 0 | 1·0 | 41·0 | 148 | 1·085 | 0·035 |
| (2) Flat Plate .. .. .. National Bureau of Standards | (*a*) 211 | 0 | 0·5 | 186 | 518 | 1·260 | 0·069 |
| | (*b*) 470 | 0 | 1·0 | 115 | 338 | 0·965 | 0·027 |
| (3) Elliptic Cylinder .. .. National Bureau of Standards | 217 | 0·4 | 1·0 | 348 | 1160 | 1·050 | 0·077 |
| | 235 | 0·1 | 1·0 | 327 | 1090 | 1·065 | 0·073 |
| | 242 | 0 | 1·0 | 315 | 1050 | 1·040 | 0·070 |
| | 255 | −0·15 | 1·0 | 294 | 980 | 1·020 | 0·065 |
| (4) Long Streamline Body of Revolution. Water Tunnel (N.P.L.) | 210 } 178 | 0·6 | 0·5 | 32 } 43 | 179 | 0·990 } 0·940 | 0·045 } 0·053 |
| | 146 } | | | 54 } | | 0·890 } | 0·061 } |
| | 168 | 0·3 | 0·5 | 47·1 | 196 | 0·920 | 0·054 |
| Estimated from values given above | 173 | 0 | 0·5 | 45·0 | 187 | 0·930 | 0·054 |
| (5) Long Streamline Body of Revolution | 310 | 0·6 | 0·25 | 28·0 | 76 | 0·700 | 0·028 |
| | 260 | 0·3 | 0·25 | 34·5 | 108 | 0·700 | 0·032 |
| Estimated from values given above | 285 | 0 | 0·25 | 31·3 | 91 | 0·700 | 0·030 |

The results for the models in wind-tunnel streams, Group II, are given in Table 2. Values of $\xi_L$ for these models and those for Group I are plotted against $u_1\upsilon/\nu$ in Fig. 3. The values for Group II are lower than those for Group I. A representative value of $\xi_L$ for the models of Group II, except models 8, 9, 10, 11 and 12, *see* later, is 0·49.

It is hardly to be expected that the values of $\xi_L$ for the models of Group II would lie closely on a smooth curve for they were obtained from experiments made under widely different conditions. It is necessary therefore to consider broadly whether transition on the models (both groups) is affected by conditions other than those due to turbulence, and whether the conditions in the turbulent streams differ from those taken in the derivation of the relation for $\xi_L$. The exactness of location of the transition points and the reliability of the values of $u_1$, $\upsilon$, $\sqrt{\overline{u_t^2}}$ and L taken in the calculation of $\xi_L$ must also be considered.

8. Conditions other than those due to turbulence which affect transition are a gradient in $u_1$, or more explicitly $\Lambda\left(=\frac{\delta^2}{\nu}\frac{du_1}{ds}\right)$, roughness due to small-scale excrescences, and surface waviness. Transition is assisted if $u_1$ falls in the direction of flow for, as is well known, transition may occur in a stream substantially free from turbulence when $\Lambda$ reaches a limiting value, which according to Howarth[16] is about −7·5. The value of $\xi_L$ at transition should therefore be greater for a positive than for a negative value of $\Lambda$. The values of $\xi_L$ plotted in Fig. 3 are for the condition $\Lambda = 0$, that is the condition taken in derivation of the relation for $\xi_L$, except those for models 17, 19 and 20, for which $\Lambda = 0{\cdot}3$, 0·6 and 0·6 respectively. Table 2 shows that for these models $\xi_L$ changes slowly with $\Lambda$ in the region near $\Lambda = 0$.

TABLE 2—GROUP II

| Model and Number | $\frac{\upsilon u_1}{\nu}$ | $\Lambda$ | Sphere | | $\frac{\sqrt{\overline{u_i^2}}}{U_0}\left(\frac{l}{L}\right)^{\frac{1}{5}}$ | $\xi_L$ |
|---|---|---|---|---|---|---|
| | | | $R_{crit.} \times 10^{-5}$ | D in. | L in ft. | |
| (6) Flat Plate. National Bureau of Standards.. .. .. | 697 | 0 | 2·70 | 5 | 0·0132 | 0·560 |
| (7) Flat Plate. (C.A.T.) .. .. .. .. .. | 448 | 0 | 2·24 | 6 | 0·0173 | 0·614 |
| (8) Symmetrical Aerofoil. (D.V.L.) .. .. .. | 1230 | 0 | 3·51* | 6 | 0·0072 | 0·335 |
| (9) Symmetrical Aerofoil. (D.V.L.) .. .. .. | 1300 | 0 | 3·51* | 6 | 0·0072 | 0·305 |
| (10) Aerofoil N.A.C.A.23012. (V.D.T.) .. .. .. | 590 | 0 | 1·5 | 8 | 0·0425 | 0·736 |
| (11) Aerofoil N.A.C.A.0012. (V.D.T.) .. .. .. | 700 | 0 | 1·5 | 8 | 0·0425 | 0·796 |
| (12) Aerofoil N.A.C.A.0012 (F.S.T.) .. .. .. | 1340 | 0 | 3·3 | 8 | 0·0076 | 0·315 |
| (13) Aerofoil N.A.C.A.0012 (C.A.T.) .. .. .. | 780 | 0 | 2·24 | 6 | 0·0173 | 0·371 |
| (14) Joukowski Aerofoil. (C.A.T.) .. .. .. | 980 | 0 | 2·24 | 6 | 0·0173 | 0·512 |
| (15) Joukowski Aerofoil. (C.A.T.) .. .. .. | 1005 | 0 | 2·24 | 6 | 0·0173 | 0·462 |
| (16) Aerofoil A. (C.A.T.) .. .. .. .. .. | 835 | 0 | 2·24 | 6 | 0·0173 | 0·468 |
| (17) Aerofoil B. (C.A.T.) .. .. .. .. .. | 910<br>800 | 0·3<br>0·6 | 2·24 | 6 | 0·0173 | 0·478<br>0·487 |
| (18) Joukowski Aerofoil. (N.P.L.) .. .. .. | 370 | 0 | 2·10 | 6 | 0·0222 | 0·491 |
| (19) Aerofoil C. (N.P.L.) C = 70 in. .. .. .. | 1165<br>1205 | 0·6<br>1·4 | 3·55<br>3·25 | 6<br>3 | 0·0092 | 0·465<br>0·488 |
| (20) Aerofoil C. (N.P.L.) C = 42 in. .. .. .. | 955<br>997 | 0·6<br>1·4 | 3·55<br>3·25 | 6<br>3 | 0·0092 | 0·388<br>0·412 |

* Taken to be 0·91 the atmospheric value 3·85[7].

Fourteen of the models were made of metal, and of the others, models 3, 19 and 20 were made of wood, one of the Cambridge flat plates of glass and models 8 and 9 of marble (*see* section 5). All the models had polished surfaces, and they can be taken to be aerodynamically smooth at the Reynolds numbers of test. Surface waviness is also unlikely to affect the results.

9. The reliability of a calculated value of $\xi_L$ depends primarily on the reliability of the values of $u_1$, $\upsilon$ and $\sqrt{\overline{u_i^2}}$ taken : and the reliability of $u_1$ and $\upsilon$ depends largely on the exactness of location of the transition point. The positions of the transition points for the flat plate 1 and the Joukowski Aerofoil 18 were determined by the surface-tube method, for the flat plate 2 from inspection of oscillograph records, for the Joukowski Aerofoils 14 and 15 by the wires method, for the body of revolution 4 and 5 from the behaviour of filament bands in the boundary layer, and for the elliptic cylinder from the change in the shape of the velocity distribution in the boundary layer (*see* section 5). For the other models (Aerofoils) the transition points were taken to be those for which the profile drag calculated by the Squire-Young method[13] for the known pressure distribution is equal to the measured drag. The relative precision of location obtained by these different methods when applied to bodies of different shape in different turbulent streams is not known : but for the same flow conditions the filament method gives results consistent with those given by the surface-tube method, and the wires method applied to

Joukowski Aerofoils 14 and 15 in the C.A.T. gives results consistent with the Squire-Young method. For an abrupt transition, such as that which occurs on an aeroplane wing in flight, the position of the transition point obtained by the Squire-Young method for a thin wing at a low incidence is in good agreement with that measured by the surface-tube method. Transition on a body in a wind-tunnel stream having a high degree of turbulence is not however an abrupt process, and the position of the transition point predicted by the Squire-Young method occurs beyond the position given by a surface tube. The values of $\upsilon$ and $\xi_L$ will therefore be over-estimated. Thus, the value of $\xi_L$ obtained for the measured point of transition on Joukowski Aerofoil 18 in the stream of the N.P.L. No. 3, 7 ft. Tunnel, for which $\frac{\sqrt{\overline{u_t^2}}}{U_0}\left(\frac{1}{L}\right)^{\frac{1}{5}} = 0{\cdot}0222$, is $0{\cdot}491$, whereas the value obtained for the position given by the Squire-Young method is about $0{\cdot}590$. No reliance can therefore be placed on the values of $\xi_L$ obtained for Aerofoils 10 and 11 in the very turbulent stream of the V.D.T. $\frac{\sqrt{\overline{u_t^2}}}{U_0}\left(\frac{1}{L}\right)^{\frac{1}{5}} = 0{\cdot}0425$, and they are not plotted in Fig. 3. The values of $\xi_L$ for the Joukowski Aerofoils 14, 15 and 18 for which the transition points were measured, are $0{\cdot}512$, $0{\cdot}462$ and $0{\cdot}491$ respectively, and the mean of these values is $0{\cdot}49$. The line $\xi_L = 0{\cdot}49$ is drawn in Fig. 3, and it is seen that it represents the trend of the values of $\xi_L$ obtained for the Aerofoils 13, 14, 15, 16, 17 and the flat plate 7 in the C.A.T., the flat plate 6 in a Bureau of Standards Tunnel, and the Aerofoils 19 and 20 in the N.P.L. 13 ft. $\times$ 9 ft. Tunnel. The values of $\frac{\sqrt{\overline{u_t^2}}}{U_0}\left(\frac{1}{L}\right)^{\frac{1}{5}}$ for these tunnels are $0{\cdot}0173$, $0{\cdot}0132$ and $0{\cdot}0092$, respectively. The values of $\xi_L$ for Aerofoils 8 and 9 in the D.V.L. 5 $\times$ 7 metre Tunnel and Aerofoil 12 in the Full-Scale Wind Tunnel are however low. (*See* below).

10. As mentioned in section 6, the values of $\frac{\sqrt{\overline{u_t^2}}}{U_0}\left(\frac{1}{L}\right)^{\frac{1}{5}}$ taken in the calculation of $\xi_L$ for the models in the wind-tunnel streams, Group II, were obtained from the relation $\log_{10}\left[100\,\frac{\sqrt{\overline{u_t^2}}}{U_0}\left(\frac{D}{L}\right)^{\frac{1}{5}}\right] = 0{\cdot}991 - 2{\cdot}193\log_{10}[R_{crit.} \times 10^{-5}]$. This relation was obtained from tests on spheres in the turbulent streams behind square-mesh grids made for the range $R_{crit.} = 1{\cdot}1 \times 10^5$ to $2{\cdot}85 \times 10^5$, the corresponding range of $\frac{\sqrt{\overline{u_t^2}}}{U_0}\left(\frac{1}{L}\right)^{\frac{1}{5}}$ for a 6 in. sphere being $0{\cdot}092$ to $0{\cdot}011$. The curve given by this relation represents the trend of the observations over this range (Fig. 4). It is known, however, that a sphere ceases to be a sensitive turbulence indicator as the limiting value $R_{crit.} = 3{\cdot}85 \times 10^5$ is approached, and there is no evidence to show how closely the above relation then holds. The values of $R_{crit.}$ for the N.A.C.A. Full-Scale Tunnel and the D.V.L. 5 $\times$ 7 metre Tunnel, $3{\cdot}3 \times 10^5$ and $3{\cdot}51 \times 10^5$ respectively, are well beyond the values covered in the sphere tests (*see* Fig. 4) and the values of $\frac{\sqrt{\overline{u_t^2}}}{U_0}\left(\frac{1}{L}\right)^{\frac{1}{5}}$ calculated for these tunnels from the above relation may be too low and if so this would account for the lowness of the values of $\xi_L$ for Aerofoils 8, 9 and 12. It is apparent that a sphere test in a wind-tunnel stream gives the value of $\frac{\sqrt{\overline{u_t^2}}}{U_0}\left(\frac{1}{L}\right)^{\frac{1}{5}}$ for a turbulent stream behind a rectangular grid which has an equivalent effect on the boundary layer of a

sphere : but it does not follow that the two streams would have the same effect on other bodies. Further, casual changes in the direction and speed of a wind-tunnel stream may have a greater disturbing effect on some models than on others at a low value of $\frac{\sqrt{\overline{u_t^2}}}{U_0}\left(\frac{1}{L}\right)^{\frac{1}{5}}$.

11. The conditions in a boundary layer at transition depend on the local turbulence in the free stream and on the cumulative effect of turbulence on the flow in the boundary layer up to the transition point. This cumulative effect depends on the shape and size of a body, on the mean velocity of the stream and on the turbulence in the free stream, and causes a departure from the conditions taken for a purely laminar layer, and, in particular, an increase in thickness. The measurements made on the models do not allow the actual thickness at the point of transition to be taken in the calculation of $\xi_L$, but if this had been possible the consistency in the values of $\xi_L$ might have been greater.

12. Apart from the N.P.L. No. 3–7 ft. Tunnel, the tunnels in which the experiments on the models of Group II were made are of the return circuit type, with a honeycomb, a setting chamber and a contracting entrance nozzle, through which the air flows on its way to the working chamber. The turbulence spectrum for each of these streams differs from that for a turbulent stream behind a grid, and the conditions taken in the derivation of $\xi_L$ are not likely to hold as closely for the models of Group II as for those of Group I. It is therefore not surprising that the representative value of $\xi_L$ for the models in the wind-tunnel streams differs from that for the models in the turbulent streams behind grids : and in view of the diversity of the conditions in the wind-tunnel streams the agreement between the values of $\xi_L$ obtained for the models in them is as close as would be expected.

13. Finally, the analysis leads to the conclusion that when transition is caused solely by turbulence in the free stream, the value of $3{\cdot}35\left[\left(\frac{U\sqrt{\overline{u_t^2}}}{\nu}\right)\left(\frac{U}{L}\right)^{\frac{1}{5}}\left(\frac{\nu}{u_1 U}\right)^{\frac{2}{5}}\right]$, denoted by $\xi_L$, at the transition point in the boundary layer of a model in a turbulent stream behind a square-mesh grid is $0{\cdot}985$. A representative value of $\xi_L$ for a model in a wind-tunnel stream is $0{\cdot}49$. The corresponding values of $\left(\frac{U\sqrt{\overline{u_t^2}}}{\nu}\right)\left(\frac{U}{L}\right)^{\frac{1}{5}}\left(\frac{\nu}{u_1 U}\right)^{\frac{2}{5}}$ are $0{\cdot}294$ and $0{\cdot}146$.

---

REFERENCES


1. G. I. Taylor. Statistical Theory of Turbulence, V. Effect of Turbulence on Boundary Layer. Proc. Roy. Soc. A., Vol. 156, pp. 307–317, 1936.
2. A. Fage and J. H. Preston. Experiments on Transition from Laminar to Turbulent Flow in the Boundary Layer. Proc. Roy. Soc. A., Vol. 178, pp. 201–227, 1941.
3. A. A. Hall and G. S. Hislop. Experiments on the Transition of the Laminar Boundary Layer on a Flat Plate. R. & M. 1843, 1938.
4. H. L. Dryden. Airflow in the Boundary Layer near a Plate. N.A.C.A. Report 562, 1936.
5. G. B. Schubauer. Airflow in the Boundary Layer of an Elliptic Cylinder. N.A.C.A. Report 652, 1939.
6. R. Jones and D. H. Williams. The Profile Drag of Aerofoils at High Reynolds Numbers in the C.A.T. R. & M. 1804, 1937.
7. H. Doetsch and M. Kramer. Systematic Profile Investigation in the Large Tunnel of the D.V.L. Luftfahrtforschung, Vol. 14, No. 10, 1937.
8. Eastman N. Jacobs and A. Sherman. Aerofoil Section Characteristics as affected by Variation of the Reynolds Number. N.A.C.A. Report 586, 1937.
9. H. J. Goett and W. K. Bullivant. Tests of N.A.C.A.0009, 0012 and 0018 Aerofoils in the Full Scale Tunnel. N.A.C.A. Report 647, 1938.

10. R. Jones and D. H. Williams. Effect of Surface Roughness on Characteristics of Aerofoils N.A.C.A.0012 and R.A.F.34. R. & M. 1708, 1936.
11. R. Jones and A. F. Brown. Drag and Transition Experiments on Two Joukowski Aerofoils in the C.A.T. Not yet published.
12. A. Fage. Profile and Skin-Friction Aerofoil Drags. R. & M. 1852, 1938.
13. H. B. Squire and A. D. Young. The Calculation of the Profile Drag of Aerofoils. R. & M. 1838.
14. H. L. Dryden, G. B. Schubauer, W. C. Mock and H. K. Skramstad. Measurement of Intensity and Scale of Wind-Tunnel Turbulence and their Relation to the Critical Reynolds Number of Spheres. N.A.C.A. Report, No. 581, 1937.
15. A. Fage and D. H. Williams. Critical Reynolds Number of Spheres in the C.A.T. R. & M. No. 1832.
16. L. Howarth. On the Solution of the Laminar Boundary Layer Equations. Proc. Roy. Soc. A., Vol. 164, pp. 547–579, 1938.
17. G. I. Taylor. Statistical Theory of Turbulence. Parts I and II. Proc. Roy. Soc. A., Vol. 151, pp. 421–478, 1935.
18. G. I. Taylor. Some Recent Developments in the Study of Turbulence. Fifth International Congress for Applied Mechanics, Cambridge, Massachusetts.
19. Unpublished Results.

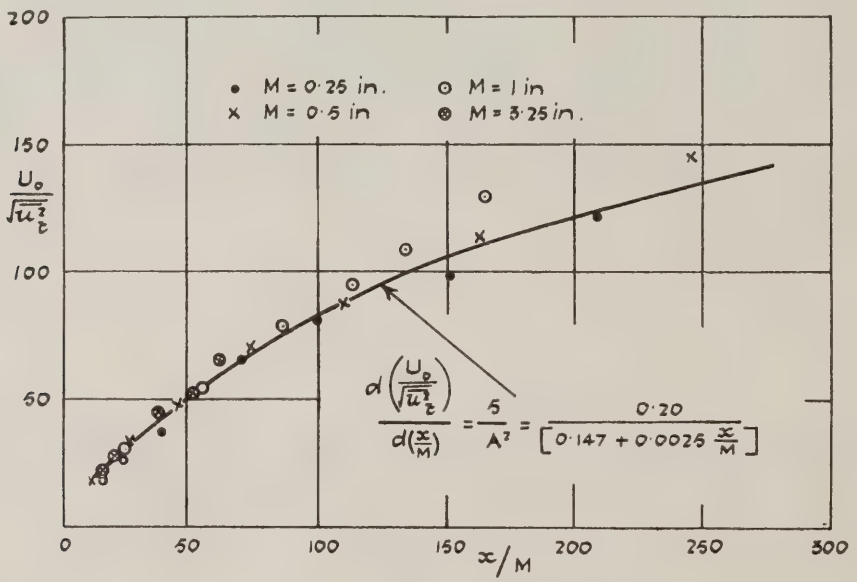


Fig. 1.

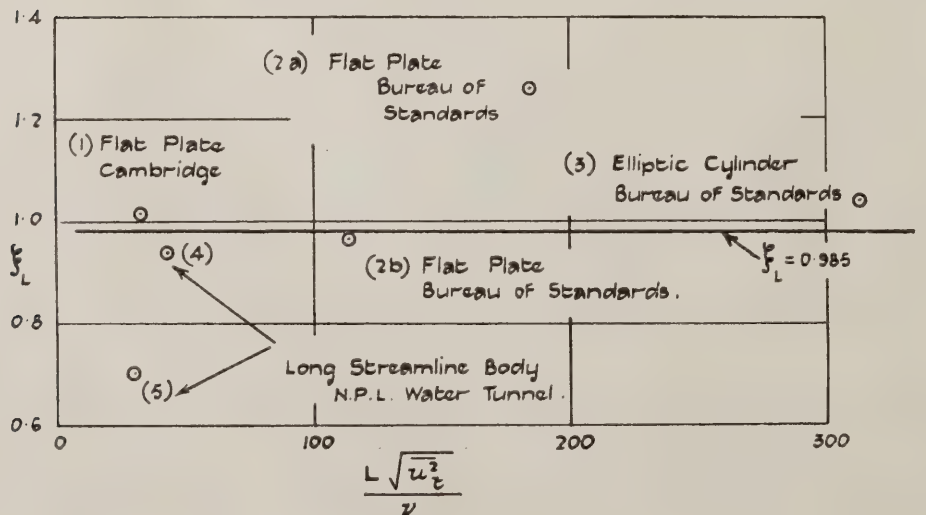


Fig. 2.

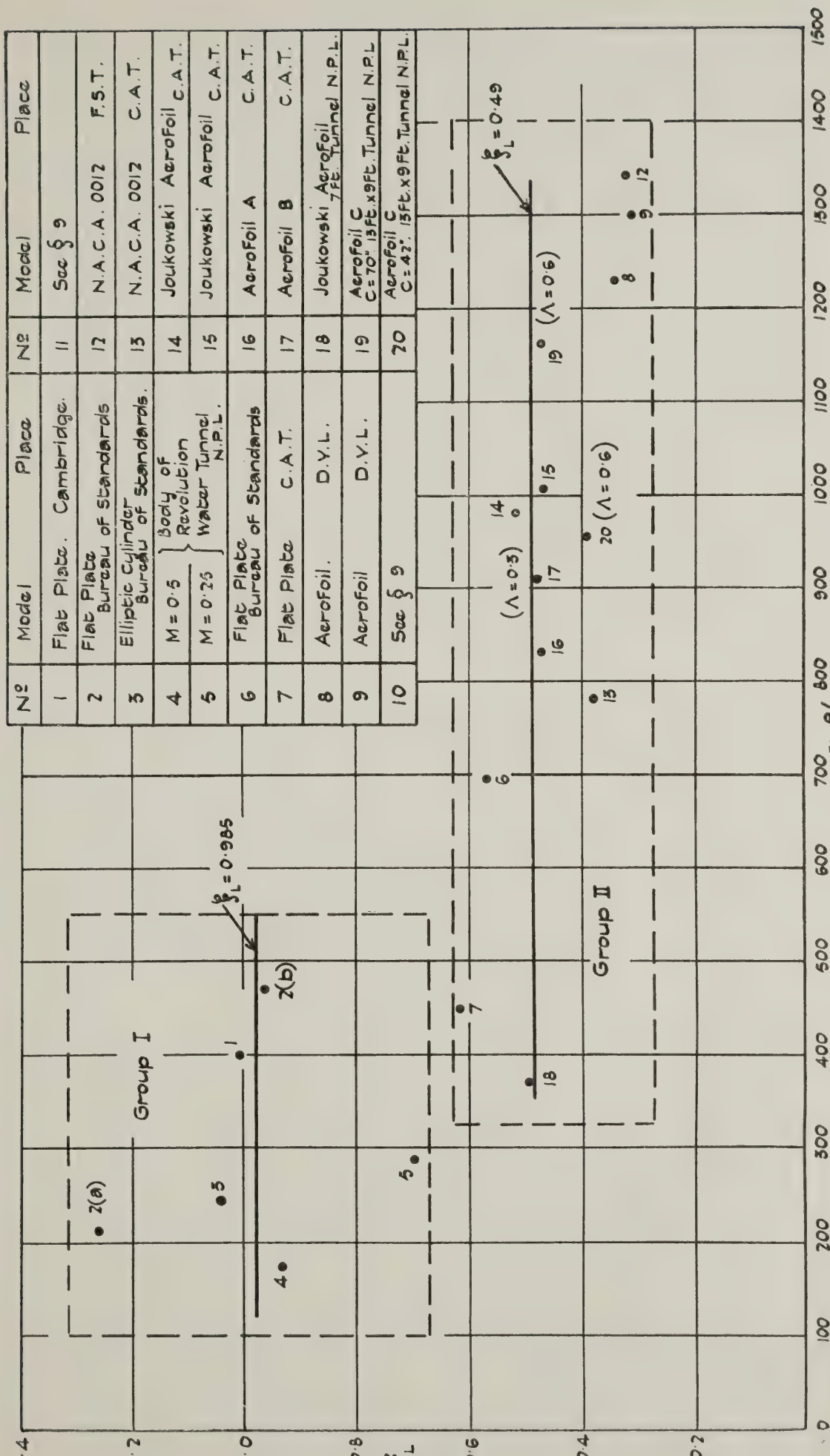


| № | Model | Place | № | Model | Place |
|---|---|---|---|---|---|
| 1 | Flat Plate. | Cambridge. | 11 | Sec § 9 | |
| 2 | Flat Plate | Bureau of Standards | 12 | N.A.C.A. 0012 | F.S.T. |
| 3 | Elliptic Cylinder | Bureau of Standards. | 13 | N.A.C.A. 0012 | C.A.T. |
| 4 | M = 0·5 | Body of Revolution | 14 | Joukowski Aerofoil | C.A.T. |
| 5 | M = 0·25 | Water Tunnel N.P.L. | 15 | Joukowski Aerofoil | C.A.T. |
| 6 | Flat Plate | Bureau of Standards | 16 | Aerofoil A | C.A.T. |
| 7 | Flat Plate | C.A.T. | 17 | Aerofoil B | C.A.T. |
| 8 | Aerofoil. | D.V.L. | 18 | Joukowski Aerofoil 7Ft. Tunnel | N.P.L. |
| 9 | Aerofoil | D.V.L. | 19 | Aerofoil C C=70° 13Ft.x9Ft. Tunnel | N.P.L. |
| 10 | Sec § 9 | | 20 | Aerofoil C C=42°. 15Ft.x9Ft. Tunnel | N.P.L. |

Fig. 3.

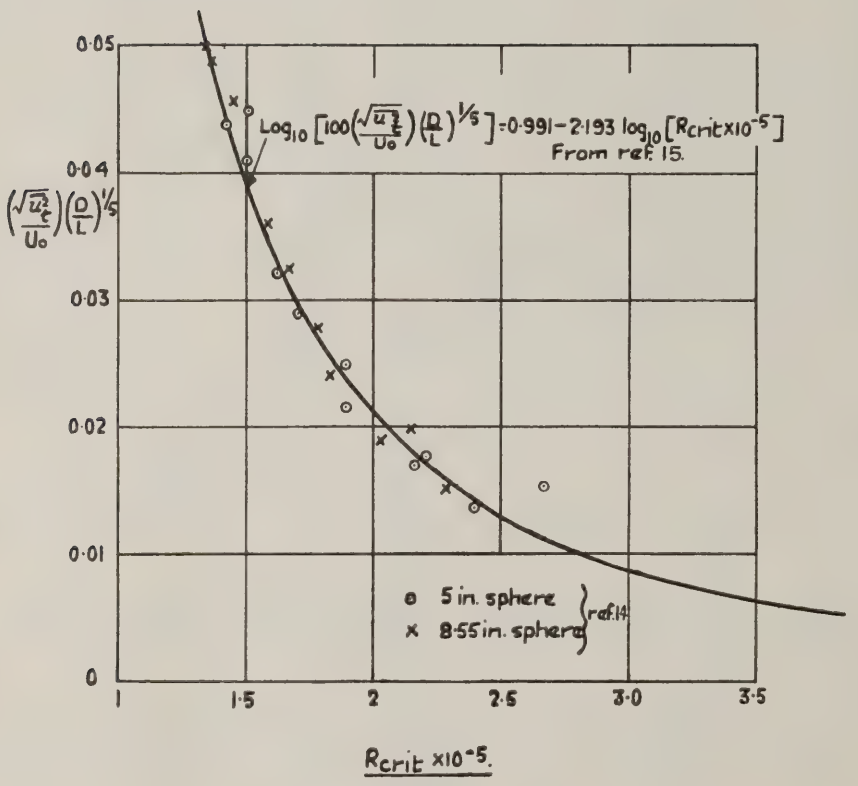


Fig. 4.

(59467) Wt. 6 375 6/42 Hw. G.377/1

## SYSTEM OF AXES

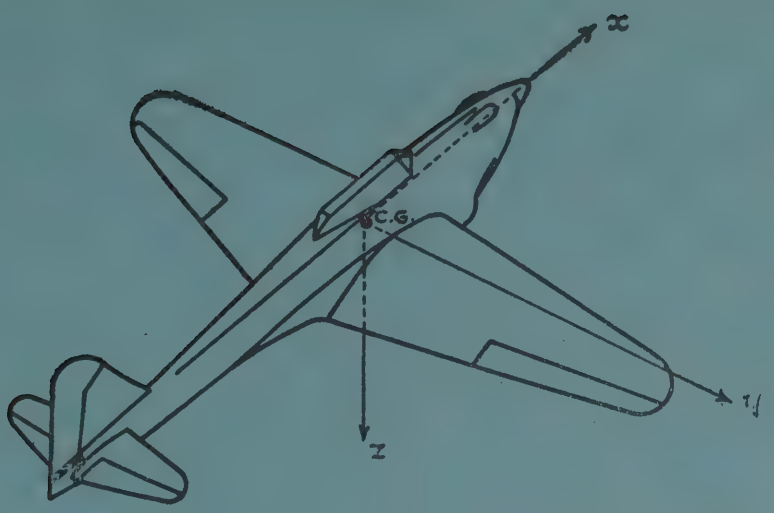


| Axes | Symbol Designation Positive direction | $x$ longitudinal forward | $y$ lateral starboard | $z$ normal downward |
|---|---|---|---|---|
| Force | Symbol | X | Y | Z |
| Moment | Symbol Designation | L rolling | M pitching | N yawing |
| Angle of Rotation | Symbol | $\phi$ | $\theta$ | $\psi$ |
| Velocity | Linear<br>Angular | $u$<br>$p$ | $v$<br>$q$ | $w$<br>$r$ |
| Moment of Inertia | | A | B | C |

Components of linear velocity and force are positive in the positive direction of the corresponding axis.

Components of angular velocity and moment are positive in the cyclic order $y$ to $z$ about the axis of $x$, $z$ to $x$ about the axis of $y$, and $x$ to $y$ about the axis of $z$.

The angular movement of a control surface (elevator or rudder) is governed by the same convention, the elevator angle being positive downwards and the rudder angle positive to port. The aileron angle is positive when the starboard aileron is down and the port aileron is up. A positive control angle normally gives rise to a negative moment about the corresponding axis.

The symbols for the control angles are :—

$\xi$ aileron angle
$\eta$ elevator angle
$\eta_T$ tail setting angle
$\zeta$ rudder angle

# Publications of the Aeronautical Research Committee

TECHNICAL REPORTS OF THE AERONAUTICAL RESEARCH COMMITTEE—

1933-34 Vol. I. Aerodynamics. £1 5*s*.

Vol. II. Structures, Engines, Instruments, etc. £1 10*s*.

1934-35 Vol. I. Aerodynamics. £2.

Vol. II. Seaplanes, Structures, Engines, Materials, etc. £2.

1935-36 Vol. I. Aerodynamics. £1 10*s*.

Vol. II. Structures, Flutter, Engines, Seaplanes, etc. £1 10*s*.

1936 Vol. I. Aerodynamics General, Performance, Airscrews, Flutter and Spinning. £2.

Vol. II. Stability and Control, Structures, Seaplanes, Engines, etc. £2 10*s*.

ANNUAL REPORTS OF THE AERONAUTICAL RESEARCH COMMITTEE—

1933-34 1*s*. 6*d*.

1934-35 1*s*. 6*d*.

April 1, 1935 to December 31, 1936. 4*s*.

1937 2*s*.

1938 1*s*. 6*d*.

INDEX TO THE TECHNICAL REPORTS OF THE ADVISORY COMMITTEE ON AERONAUTICS—

1909-1919 Reports and Memoranda No. 1600. 8*s*.

*Prices are net and postage extra.*

## His Majesty's Stationery Office

London W.C.2: York House, Kingsway

Edinburgh 2: 120 George Street — Manchester 2: 39-41 King Street

Cardiff: 1 St. Andrew's Crescent — Belfast: 80 Chichester Street

or through any bookseller.

S.O. Code No. 23-1896

629.13
G79r
no.1897

R. & M. No. 1897
(5080)
A.R.C. Technical Report

MINISTRY OF AIRCRAFT PRODUCTION

AERONAUTICAL RESEARCH COMMITTEE
REPORTS AND MEMORANDA

# An Experimental Investigation of Wind Tunnel Interference in the R.A.E. 5 ft. Open Jet Circular Tunnel

*By*

J. E. ADAMSON, B.A.

*Crown Copyright Reserved*

LONDON: HIS MAJESTY'S STATIONERY OFFICE
Price 1*s.* 6*d.* net

# AERODYNAMIC SYMBOLS

## 1. GENERAL

| | |
|---|---|
| $m$ | Mass |
| $t$ | Time |
| V | Resultant linear velocity |
| $\Omega$ | Resultant angular velocity |
| $\rho$ | Density, $\sigma$ relative density |
| $\nu$ | Kinematic coefficient of viscosity |
| R | Reynolds number, $R = lV/\nu$ (where $l$ is a suitable linear dimension) |

Normal temperature and pressure for aeronautical work are 15° C and 760 mm.

For air under these conditions $\begin{cases} \rho = 0{\cdot}002378 \text{ slug/cu. ft.} \\ \nu = 1{\cdot}56 \times 10^{-4} \text{ ft.}^2\text{/sec.} \end{cases}$

The slug is taken to be 32·2 lb.-mass.

| | |
|---|---|
| $\alpha$ | Angle of incidence |
| $e$ | Angle of downwash |
| S | Area |
| $b$ | Span |
| $c$ | Chord |
| A | Aspect ratio, $A = b^2/S$ |
| L | Lift, with coefficient $C_L = L/\frac{1}{2}\rho V^2 S$ |
| D | Drag, with coefficient $C_D = D/\frac{1}{2}\rho V^2 S$ |
| $\gamma$ | Gliding angle, $\tan\gamma = D/L$ |
| L | Rolling moment, with coefficient $C_l = L/\frac{1}{2}\rho V^2 bS$ |
| M | Pitching moment, with coefficient $C_m = M/\frac{1}{2}\rho V^2 cS$ |
| N | Yawing moment, with coefficient $C_n = N/\frac{1}{2}\rho V^2 bS$ |

## 2. AIRSCREWS

| | |
|---|---|
| $n$ | Revolutions per second |
| D | Diameter |
| J | $V/nD$ |
| P | Power |
| T | Thrust, with coefficient $k_T = T/\rho n^2 D^4$ |
| Q | Torque, with coefficient $k_Q = Q/\rho n^2 D^5$ |
| $\eta$ | Efficiency, $\eta = TV/P = Jk_T/2\pi k_Q$ |

LIBRARY
UNIVERSITY OF ILLINOIS
URBANA

# An Experimental Investigation of Wind Tunnel Interference in the R.A.E. 5 ft. Open Jet Circular Tunnel

*By*

J. E. Adamson, B.A.

Communicated by the Director of Scientific Research, Ministry of Aircraft Production

*Reports and Memoranda No.* 1897

*26th April,* 1941*

*Summary.—Reasons for enquiry.*—Tests were required to check the validity of the theoretical corrections for wind tunnel interference in the 5-ft. open tunnel when the wing is of large span or spans the jet.

*Range of investigation.*—Two wings of 8-in. and 1-ft. chord were tested on a horizontal diametric axis :—

(*a*) Spanning the 5-ft. open jet wind tunnel.

(*b*) Cut down successively to 0·9, 0·8 and 0·6 of the tunnel diameter.

Lift, drag and pitching moment were measured in all cases.

The following symbols are used in the text :—

| | |
|---|---|
| Wing area .. .. .. .. .. .. .. | S |
| Wing chord .. .. .. .. .. .. .. | $c$ |
| Tunnel diameter .. .. .. .. .. .. | D |
| Tunnel cross sectional area .. .. .. .. | C |

*Conclusions.*(*a*) *Wings inside the jet diameter.*—For values of $S/C < 0{\cdot}25$ and $c/D \leqslant 0{\cdot}2$ the standard corrections may be applied. Beyond this limit further systematic tests are required to derive satisfactory empirical corrections. Pending such tests it is better to calculate the slope of the lift curve in free air for the appropriate aspect ratio and use this to deduce the incidence correction.

(*b*) *Wings spanning the jet.*—The corrections given by Glauert apply with a modified value of $N = 1{\cdot}6$ for $c/D \leqslant 0{\cdot}2$. Further tests are required for larger chord/diameter ratios.

1. *Introduction.*—Theoretical estimates of the boundary interference on the characteristics of wings in open jet tunnels are based on simplifying assumptions which may not be justified in tests on comparatively large models. Tests have, therefore, been made in the 5-ft. open jet tunnel at the R.A.E. on two wings to check the validity of the theoretical corrections in the following cases :—

(1) Wing chord/jet diameter $\not> 0{\cdot}2$, span less than tunnel diameter.

(2) Wing chord/jet diameter $> 0{\cdot}2$, wing spanning the jet.

The wind tunnel corrections on these large models are complicated by " shadow effect "[1] and the difficulty of measuring wind speed. In the tests in this report the effect of model on wind speed has been investigated (Appendix).

*R.A.E. Report, February, 1941.

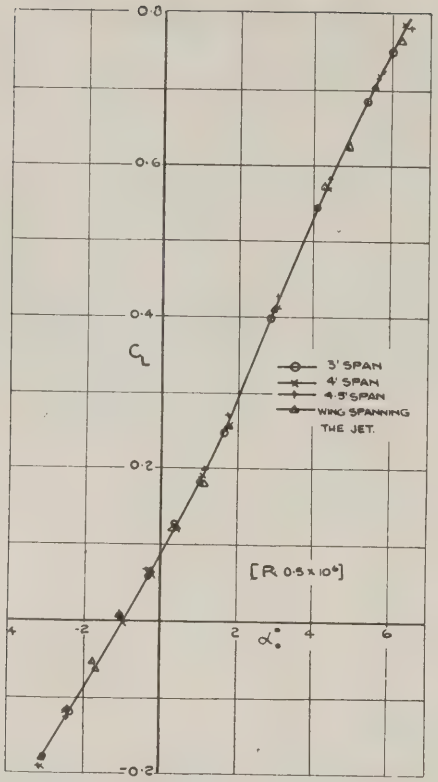


R.A.F.34.

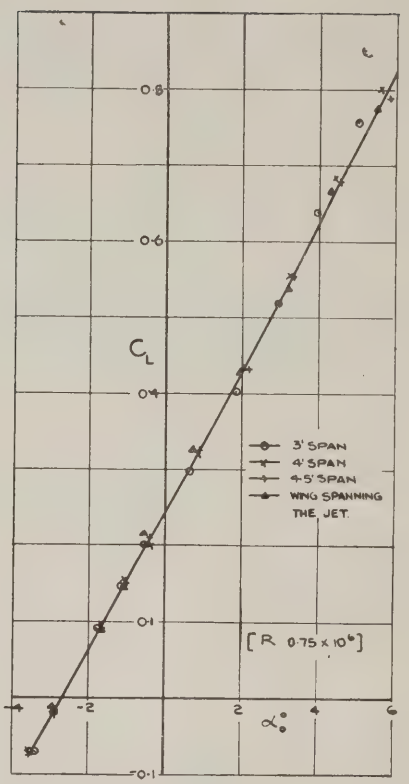


R.A.F.48.

Fig. 1. Lift coefficient ($\alpha_0$ for infinite aspect ratio)

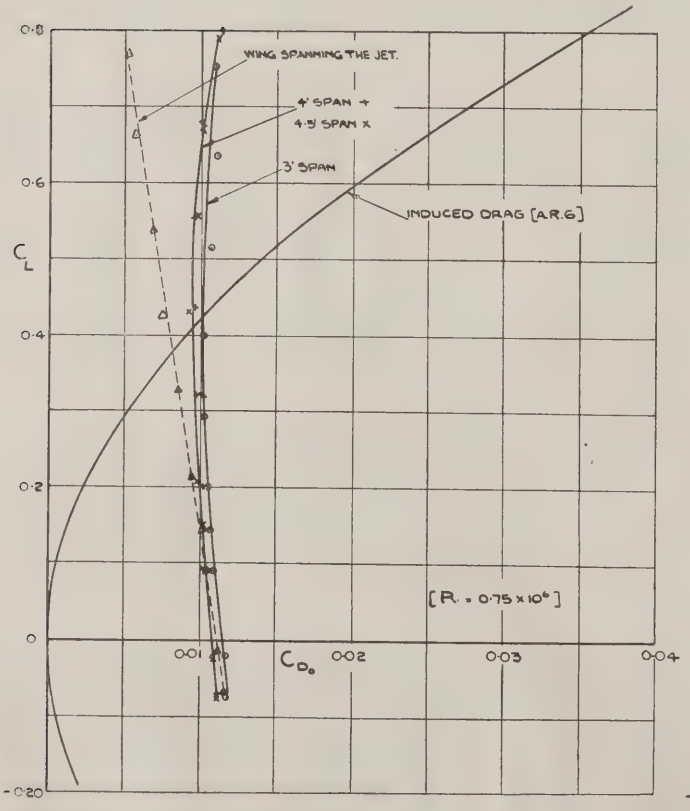


R.A.F.34.

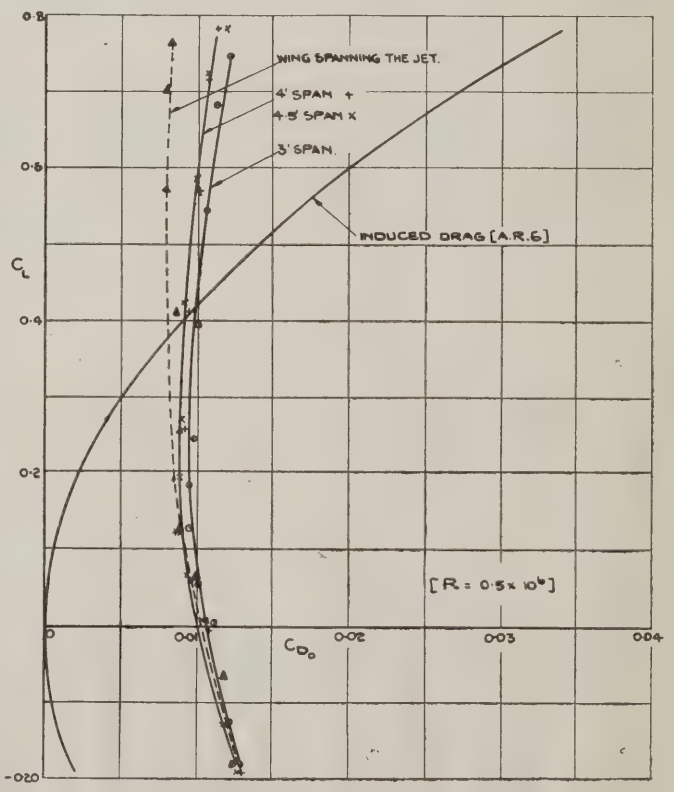


R.A.F.48.

Fig. 2. Profile drag coefficients.

R.A.F.34 (8 in. chord) and R.A.F.48 (1 ft. chord).

3.22 *Profile drag* (*Fig.* 2).—The profile drag curves for the 4·5 ft. and 4 ft. spans are identical, while the profile drag for the 3 ft. span is uniformly greater by about 6 per cent. for both aerofoils. This is probably an end effect[13, 14] since it appears to be a uniform increment for both wings. For the case of the wing spanning the jet, the induced drag is overestimated. Estimated and empirical values are compared below.

TABLE 3

| Condition | Estimated N (Equation 9) | Empirical N |
|---|---|---|
| Wing spanning jet. R.A.F.34 .. .. .. | 1·80 | 1·63 |
| R.A.F.48 .. .. .. | 1·75 | 1·59 |

3.23. *Pitching moments* (*Fig.* 3).—The pitching moment curves shew good agreement for wings inside the jet boundary. For the wing spanning the jet there is a small increment of $\Delta C_M = +0{\cdot}004$ at $C_L = 0{\cdot}6$ for R.A.F.48. This difference may be more important on a thicker wing section.

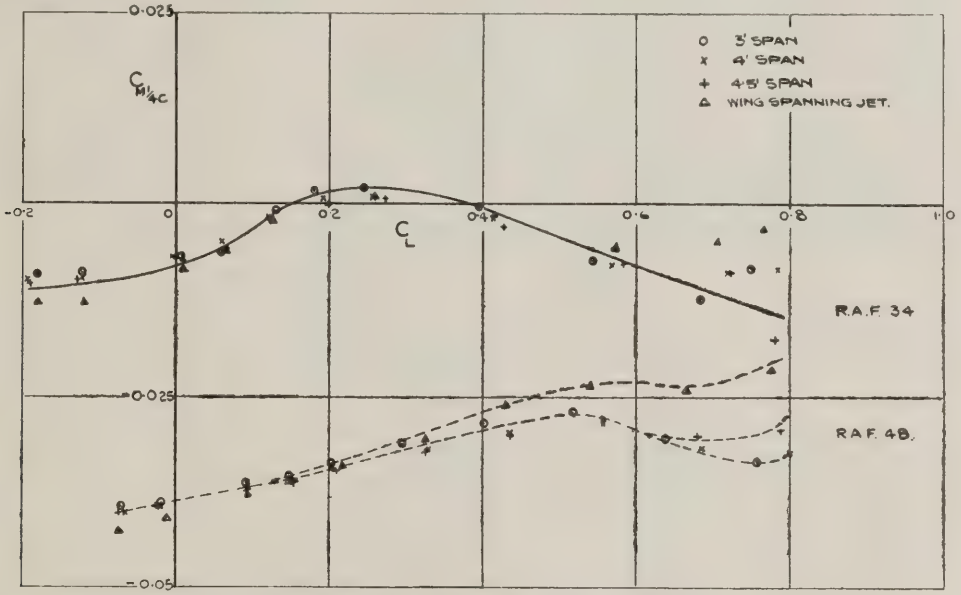


Fig. 3. Pitching moment coefficients.
R.A.F.34 (8 in. chord) and R.A.F.48 (1 ft. chord).

4. *Discussion of results.*—The present tests shew that for wings of spans inside the jet diameter the correction given by equations (4) and (5) gives consistent lift and drag results for wing of varying span and chord for which $S/C \not> 0{\cdot}25$ and the span is not greater than $0{\cdot}9 \times$ tunnel diameter. These conclusions were arrived at by Prandtl[15], Knight and Harris[16], Tani and Taimi[4] for span/diameter ratios up to 0·8. For profile drag measurements the effect of square ends on wings of small aspect ratio may be misleading, but further tests would be necessary before any recommendation, such as rounding the tips, could be made.

For wings spanning the jet the value of M from equation (8) is correct, but the value of N is overestimated.

There is evidence[17] that for wings of chords larger than 0·2D both spanning the jet and with spans inside the jet an additional correction must be applied. This correction is large and is very probably due to the effect of the finite dimensions of the working section. No satisfactory theoretical solution has been found and in the absence of any but scattered data it is hoped to make tests similar to these in this report on wings of 2 ft. and 1·5 ft. chord when an opportunity occurs.

For correcting the lift slope in 5 ft. tunnel tests on large chord wings it has been customary to estimate the value of $\partial C_L/\partial\alpha$ for the wing from other data and correct the measured values of $\alpha$ by an increment of the form $-kC_L$ to give the free air slope. Pending the systematic tests proposed above no better method can be suggested.

Tunnel corrections on a complete model of span greater than the jet diameter are given in a further report.

## APPENDIX

*Experiments to determine the best position of the " hole in the side " of the tunnel with a large wing in the tunnel*

It has been customary in the 5 ft. tunnel to keep the speed steady by an automatic control working on the pressure difference between hole $A_1$ near the top of the tunnel side and atmosphere (see Fig. 4), whereas the calibration of the tunnel was made against three inter-connected holes in the roof. A wing at high lift was found to alter the pressure difference between these holes and atmosphere; vertical traverses were, therefore, made to measure static pressure in the maximum section in the plane of the holes, and velocity before the model. This latter was measured well up the nozzle so as to avoid the velocity field of the wing itself. In Fig. 5 the velocity traverses are shown; and also the static pressure in the maximum section divided by $\frac{1}{2}\rho V^2$ in the centre of the jet for two lift conditions of the wing and the tunnel without wing. It is seen that with the original hole in the side for the automatic (i.e. $A_1$), the pressure is increased by 1·3 per cent. by the presence of a wing at no lift, and by a further 1·7 per cent. when the wing has a lift of 62 lb. at 120 ft./sec. This corresponds to a reduction of speed of 1·5 per cent. in the jet when the pressure is kept constant by this hole. If, however, a lower hole $A_2$ is chosen (Fig. 4) a much more nearly constant result is obtained. A second hole was, therefore, fitted near $A_2$, and these two holes are now used in place of the original roof holes and $A_1$.

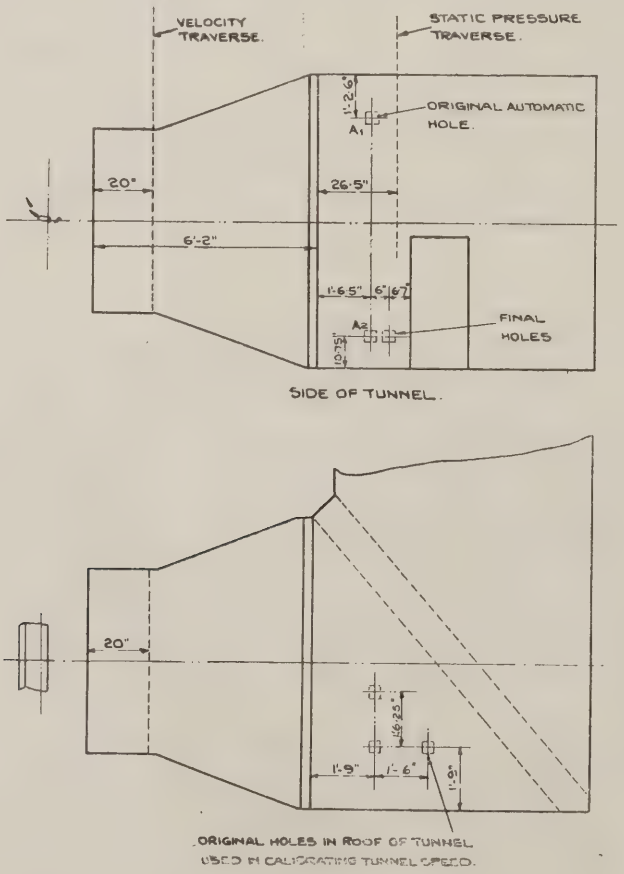


Fig. 4. 5 ft. Tunnel shewing H.I.S. positions.

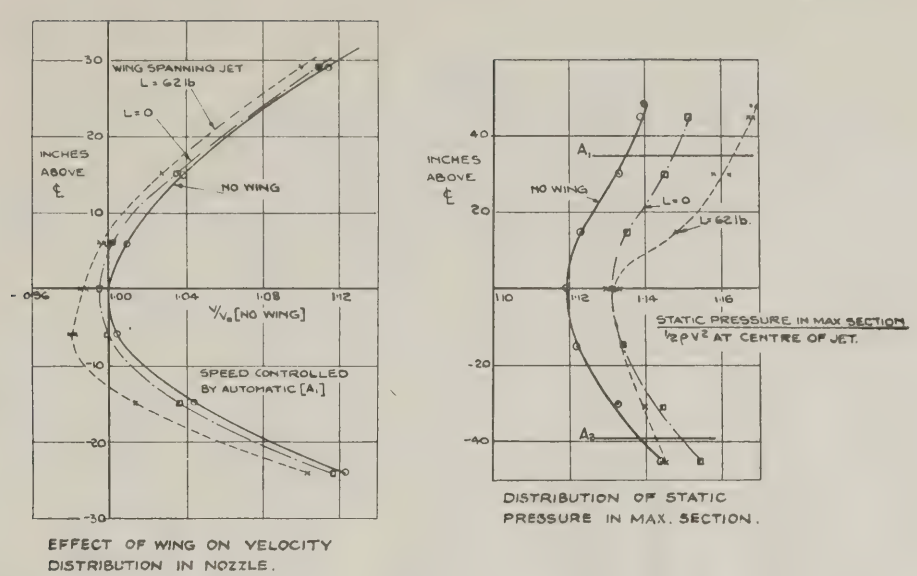


Fig 5. Velocity distribution in nozzle and static pressure in maximum section.

## REFERENCES


| *No.* | *Author.* | *Title, etc.* |
|---|---|---|
| 1 | Perring and Callen .. .. | On the Validity of Large Scale Tests in an Open Jet Tunnel. Tests on a One-fifth Scale Bristol Fighter (7·9 ft. Span) in a 5 ft. Open Jet Tunnel. R. & M. 1348. July, 1930. |
| 2 | Prandtl .. .. .. .. | Tragflügeltheorie. Part 2. |
| 3 | Burgers .. .. .. .. | Aerodynamic Theory, Durand, Vol. 2, Chapter IV. |
| 4 | Tani and Taimi .. .. .. | Two notes on Boundary Influence of Wind Tunnels of Circular Cross-Section. Report No. 121. Aeronautical Research Institute, Tokio Imperial University. |
| 5 | Lotz .. .. .. .. | Correction of Downwash in Wind Tunnels of Circular and Elliptic Sections. Luftfahrtforschung, Vol. 12, No. 8. December, 1935. (Trans. 2626.) |
| 6 | Rosenhead .. .. .. | Effect of Wind Tunnel Interference on the Characteristics of an Aerofoil. Proc. Roy. Soc. A.129 (p. 135). 1930. |
| 7 | Glauert .. .. .. .. | Wind Tunnel Interference on Wings, Bodies and Airscrews. R. & M. 1566. 1933. |
| 8 | Glauert .. .. .. .. | The Interference on the Characteristics of an Aerofoil in a Wind Tunnel of Circular Section. R. & M. 1453. 1931. |
| 9 | Glauert .. .. .. .. | Lift and Drag of a Wing Spanning a Free Jet. R. & M. 1603. 1934. |
| 10 | Stüper .. .. .. .. | Contribution to the Problem of Airfoils spanning a Free Jet. Luftfahrtforschung, Vol. 12. 1935. |
| 11 | Stüper .. .. .. .. | An Aerofoil spanning an Open Jet. "Ingenieur Archiv." 1932, p. 338. (Trans. 2398.) |
| 12 | Squire .. .. .. .. | Lift and Drag of a Rectangular Wing spanning a Free Circular Jet. Phil. Mag., Ser. 7, Vol. XXVII. February, 1939. |
| 13 | Williams, Bell and Brown .. | Tests of Two Joukowski Aerofoils in the Compressed Air Tunnel. R. & M. 1870. 1939. |
| 14 | Doetsch and Kramer .. .. | Profile Drag Measurements in the Large Wind Tunnel at the D.V.L. Luftfahrtforschung, Vol. 14, 4/5. (Trans. Aeroplane. 6th April, 1938). |
| 15 | Prandtl .. .. .. .. | Ergebnisse der Aerodynamischen Versuchanstalt zu Göttingen, Vol. 2, p. 17. 1923. |
| 16 | Knight and Harris .. .. | Experimental Determination of Jet Boundary Correction for Airfoil Tests in Four Wind Tunnels of Different Shapes. N.A.C.A. Report No. 361. 1930. |
| 17 | Diprose .. .. .. .. | Drag Tests on a Fabric Covered, and a Polished Plywood, Wing in the 24 ft. Tunnel. R. & M. 1813. 1937. |

## TABLE 4

*R.A.F.*34, (8 *in. chord*), $\frac{1}{4}$ *chord point* 15 *in. from the nozzle*

| Condition | Measured values | | | | Wind tunnel correction | Corrected to A.R.∞ | | |
|---|---|---|---|---|---|---|---|---|
| | $\alpha^\circ$ | $C_L$ | $C_D$ | $C_{M_{\frac{1}{4}c}}$ | | $\alpha^\circ_0$ | $C_L$ | $C_{D0}$ |
| Wing spanning the jet | −4 | −0·180 | 0·0149 | −0·0131 | Corrected by Glauert and Squire formulae equations (6)–(9) | −3·10 | −0·180 | 0·0124 |
| | −3 | −0·118 | 0·0130 | −0·0128 | | −2·41 | −0·118 | 0·0119 |
| | −2 | −0·063 | 0·0118 | — | | −1·69 | −0·063 | 0·0118 |
| | −1 | 0·010 | 0·0106 | −0·0084 | | −1·05 | 0·010 | 0·0106 |
| | 0 | 0·067 | 0·0100 | −0·0058 | | −0·33 | 0·067 | 0·0100 |
| | 1 | 0·125 | 0·0101 | −0·0021 | | 0·38 | 0·125 | 0·0089 |
| | 2 | 0·192 | 0·0118 | — | | 1·04 | 0·192 | 0·0086 |
| | 3 | 0·257 | 0·0138 | 0·0012 | | 1·75 | 0·257 | 0·0088 |
| | 5 | 0·413 | 0·0209 | −0·0012 | | 3·00 | 0·413 | 0·0080 |
| | 7 | 0·573 | 0·0327 | −0·0056 | | 4·22 | 0·573 | 0·0079 |
| | 8 | 0·625 | — | — | | 4·97 | 0·625 | — |
| | 9 | 0·706 | 0·0455 | −0·0050 | | 5·58 | 0·706 | 0·0080 |
| | 10 | 0·766 | 0·0524 | −0·0031 | | 6·29 | 0·766 | 0·0083 |
| Wing of 4·5 ft. span. A.R. = 6·75 | −4 | −0·190 | 0·0145 | −0·0101 | Equation (4) and (5) | −3·14 | −0·190 | 0·0127 |
| | −3 | −0·126 | 0·0125 | −0·0094 | | −2·44 | −0·126 | 0·0117 |
| | −1 | 0·010 | 0·0104 | −0·0072 | | −1·04 | 0·010 | 0·0104 |
| | 0 | 0·069 | 0·0095 | −0·0058 | | −0·32 | 0·069 | 0·0093 |
| | 1 | 0·122 | 0·0096 | −0·0021 | | 0·45 | 0·122 | 0·0089 |
| | 2 | 0·197 | 0·0108 | −0·0001 | | 1·12 | 0·197 | 0·0089 |
| | 3 | 0·271 | 0·0127 | +0·0007 | | 1·79 | 0·271 | 0·0090 |
| | 5 | 0·426 | 0·0182 | −0·0029 | | 3·09 | 0·426 | 0·0091 |
| | 7 | 0·584 | 0·0267 | −0·0078 | | 4·39 | 0·584 | 0·0097 |
| | 9 | 0·723 | 0·0368 | −0·0089 | | 5·76 | 0·723 | 0·0107 |
| | 10 | 0·781 | 0·0424 | −0·0175 | | 6·50 | 0·781 | 0·0119 |
| Wing of 4 ft. span A.R. = 6 | −4 | −0·192 | 0·0150 | −0·0100 | Equation (4) and (5) | −3·10 | −0·192 | 0·0129 |
| | −3 | −0·122 | 0·0126 | −0·0092 | | −2·43 | −0·122 | 0·0118 |
| | −1 | −0·003 | 0·0108 | −0·0069 | | −0·99 | −0·003 | 0·0108 |
| | 0 | 0·061 | 0·0098 | −0·0050 | | −0·29 | 0·061 | 0·0096 |
| | 1 | 0·122 | 0·0096 | −0·0017 | | 0·43 | 0·122 | 0·0087 |
| | 2 | 0·192 | 0·0110 | 0·0008 | | 1·10 | 0·192 | 0·0084 |
| | 3 | 0·258 | 0·0129 | 0·0010 | | 1·80 | 0·258 | 0·0091 |
| | 5 | 0·413 | 0·0189 | −0·0016 | | 3·09 | 0·413 | 0·0094 |
| | 7 | 0·569 | 0·0282 | −0·0078 | | 4·35 | 0·569 | 0·0101 |
| | 9 | 0·718 | 0·0397 | −0·0088 | | 5·66 | 0·718 | 0·0107 |
| | 10 | 0·783 | 0·0457 | −0·0083 | | 6·36 | 0·783 | 0·0113 |
| Wing of 3 ft. span A.R. = 4·5 | −4 | −0·179 | 0·0150 | −0·0090 | Equation (4) and (5) | −3·05 | −0·179 | 0·0127 |
| | −3 | −0·121 | 0·0132 | −0·0088 | | −2·35 | −0·121 | 0·0121 |
| | −1 | 0·006 | 0·0112 | −0·0066 | | −1·03 | 0·006 | 0·0112 |
| | 0 | 0·059 | 0·0104 | −0·0061 | | −0·31 | 0·059 | 0·0101 |
| | 1 | 0·127 | 0·0107 | −0·0006 | | 0·33 | 0·127 | 0·0095 |
| | 2 | 0·182 | 0·0119 | +0·0017 | | 1·02 | 0·182 | 0·0095 |
| | 3 | 0·246 | 0·0142 | 0·0020 | | 1·69 | 0·246 | 0·0098 |
| | 5 | 0·397 | 0·0216 | −0·0004 | | 2·87 | 0·397 | 0·0101 |
| | 7 | 0·544 | 0·0323 | −0·0073 | | 4·09 | 0·544 | 0·0107 |
| | 9 | 0·684 | 0·0454 | −0·0125 | | 5·35 | 0·684 | 0·0113 |
| | 10 | 0·748 | 0·0531 | −0·0083 | | 6·00 | 0·748 | 0·0122 |

## TABLE 5

*R.A.F.*48, (12 *in. chord*), $\frac{1}{4}$ *chord point* 18 *in. from the nozzle*

| Condition | Measured values | | | | Wind tunnel correction | Corrected to A.R. ∞ | | |
|---|---|---|---|---|---|---|---|---|
| | $\alpha^\circ$ | $C_L$ | $C_D$ | $C_{M_{\frac{1}{4}c}}$ | | $\alpha^\circ_0$ | $C_L$ | $C_{D0}$ |
| Wing spanning the jet A.R. = 5 | −4 | −0·073 | 0·0122 | −0·0425 | Corrected by Glauert and Squire formulae. Equation (6)–(9) | −3·49 | −0·073 | 0·0116 |
| | −3 | −0·012 | 0·0112 | −0·0408 | | −2·92 | −0·012 | 0·0111 |
| | −1 | +0·094 | 0·0113 | −0·0377 | | −1·66 | 0·094 | 0·0103 |
| | 0 | 0·147 | 0·0125 | −0·0359 | | −1·03 | 0·147 | 0·0101 |
| | 1 | 0·216 | 0·0146 | −0·0340 | | −0·51 | 0·216 | 0·0094 |
| | 3 | 0·327 | 0·0202 | −0·0301 | | 0·71 | 0·327 | 0·0084 |
| | 5 | 0·429 | 0·0279 | −0·0262 | | 1·99 | 0·429 | 0·0075 |
| | 7 | 0·538 | 0·0389 | −0·0235 | | 3·22 | 0·538 | 0·0068 |
| | 9 | 0·665 | 0·0545 | −0·0241 | | 4·33 | 0·665 | 0·0055 |
| | 11 | 0·773 | 0·0712 | −0·0215 | | 5·56 | 0·773 | 0·0051 |
| Wing span 4·5 ft. A.R. = 4·5 | −4 | −0·074 | 0·0116 | −0·0403 | Equation (4) and (5) | −3·53 | −0·074 | 0·0112 |
| | −3 | −0·024 | 0·0108 | −0·0392 | | −2·84 | −0·024 | 0·0109 |
| | −1 | 0·093 | 0·0109 | −0·0371 | | −1·60 | +0·093 | 0·0103 |
| | 0 | 0·151 | 0·0118 | −0·0363 | | −0·98 | 0·151 | 0·0101 |
| | 1 | 0·209 | 0·0130 | −0·0347 | | −0·37 | 0·209 | 0·0098 |
| | 3 | 0·325 | 0·0170 | −0·0322 | | 0·88 | 0·325 | 0·0100 |
| | 5 | 0·434 | 0·0230 | −0·0298 | | 2·17 | 0·434 | 0·0092 |
| | 7 | 0·558 | 0·0324 | −0·0279 | | 3·34 | 0·558 | 0·0097 |
| | 9 | 0·679 | 0·0436 | −0·0301 | | 4·57 | 0·679 | 0·0099 |
| | 11 | 0·789 | 0·0566 | −0·0294 | | 5·85 | 0·789 | 0·0111 |
| Wing span 4 ft. A.R. = 4 | −4 | −0·069 | 0·0116 | −0·0401 | Equation (4) and (5) | −3·54 | −0·069 | 0·0112 |
| | −3 | −0·016 | 0·0109 | −0·0393 | | −2·89 | −0·016 | 0·0109 |
| | −1 | 0·096 | 0·0110 | −0·0368 | | −1·64 | 0·096 | 0·0102 |
| | 0 | 0·156 | 0·0109 | −0·0358 | | −1·05 | 0·156 | 0·0089 |
| | 1 | 0·202 | 0·0134 | −0·0344 | | −0·35 | 0·202 | 0·0101 |
| | 3 | 0·324 | 0·0183 | −0·0322 | | 0·83 | 0·324 | 0·0097 |
| | 5 | 0·437 | 0·0252 | −0·0296 | | 2·06 | 0·437 | 0·0096 |
| | 7 | 0·556 | 0·0349 | −0·0284 | | 3·26 | 0·556 | 0·0096 |
| | 9 | 0·684 | 0·0484 | −0·0316 | | 4·41 | 0·684 | 0·0100 |
| | 11 | 0·801 | 0·0638 | −0·0324 | | 5·62 | 0·801 | 0·0113 |
| Wing span 3 ft. A.R. = 3 | −4 | −0·072 | 0·0123 | −0·0393 | Equation (4) and (5) | −3·44 | −0·072 | 0·0117 |
| | −3 | −0·018 | 0·0117 | −0·0387 | | −2·86 | −0·018 | 0·0117 |
| | −1 | 0·091 | 0·0118 | −0·0363 | | −1·72 | 0·091 | 0·0109 |
| | 0 | 0·146 | 0·0130 | −0·0355 | | −1·14 | 0·146 | 0·0107 |
| | 1 | 0·202 | 0·0149 | −0·0338 | | −0·58 | 0·202 | 0·0105 |
| | 3 | 0·296 | 0·0196 | −0·0311 | | 0·67 | 0·296 | 0·0101 |
| | 5 | 0·402 | 0·0277 | −0·0285 | | 1·84 | 0·402 | 0·0102 |
| | 7 | 0·519 | 0·0397 | −0·0270 | | 2·92 | 0·519 | 0·0107 |
| | 9 | 0·639 | 0·0552 | −0·0304 | | 3·97 | 0·639 | 0·0110 |
| | 11 | 0·756 | 0·0727 | −0·0335 | | 5·06 | 0·756 | 0·0107 |

## TABLE 6

*Results of traverses in the nozzle and the maximum section*

$$\tfrac{1}{2}\rho V^2 = P - S = \left(\frac{65{\cdot}7}{66{\cdot}12}\right)^2 (P - S') = 0{\cdot}987\ (P - S')$$

$$(S - A)/\tfrac{1}{2}\rho V^2 = 1{\cdot}013\ (S - A)/(P - S')$$

| Tunnel condition | Traverse at J in nozzle | | | | Traverse at M in maximum section | | | |
|---|---|---|---|---|---|---|---|---|
| | In. above C line | H–A | P–S′ | $\frac{1}{2}\rho V^2$ | In. above C line | H–A | S–A | $\frac{S-A}{\frac{1}{2}\rho V^2}$ |
| No wing in tunnel | | | | | 48 | 3·059 | 3·094 | 1·140 |
| | 24 | 3·057 | 3·365 | 3·321 | 45 | 3·058 | 3·093 | 1·139 |
| | 15 | | 2·959 | 2·920 | 30 | 3·058 | 3·076 | 1·133 |
| | 6 | | 2·799 | 2·763 | 15 | 3·058 | 3·048 | 1·123 |
| | 0 | | 2·751 | 2·715 | 0 | 3·059 | 3·038 | 1·110 |
| | − 6 | | 2·774 | 2·738 | −15 | 3·059 | 3·047 | 1·122 |
| | −15 | | 2·995 | 2·956 | −30 | 3·059 | 3·075 | 1·133 |
| | −24 | | 3·422 | 3·378 | −45 | 3·059 | 3·107 | 1·144 |
| 1 ft. chord wing spanning the jet (at no lift) | 24 | 3·056 | 3·354 | 3·310 | 45 | 3·056 | 3·096 | 1·151 |
| | 15 | | 2·943 | 2·905 | 30 | 3·057 | 3·079 | 1·145 |
| | 6 | | 2·762 | 2·726 | 15 | 3·058 | 3·053 | 1·135 |
| | 0 | | 2·725 | 2·690 | 0 | 3·058 | 3·043 | 1·132 |
| | − 6 | | 2·731 | 2·701 | −15 | 3·058 | 3·050 | 1·134 |
| | −15 | | 2·955 | 2·917 | −30 | 3·055 | 3·075 | 1·145 |
| | −24 | | 3·390 | 3·346 | −45 | 3·055 | 3·104 | 1·154 |
| 1 ft. chord wing spanning the jet at $\alpha = 11°$ (L = 62 lb.) | | | | | 48 | 3·010 | 3·081 | 1·169 |
| | 24 | 3·011 | 3·298 | 3·255 | 45 | 3·011 | 3·080 | 1·168 |
| | 15 | 3·011 | 2·888 | 2·850 | 30 | 3·014 | 3·063 | 1·162 |
| | 6 | 3·011 | 2·717 | 2·682 | 15 | 3·014 | 3·026 | 1·148 |
| | 0 | 3·066 | 2·671 | 2·636 | 0 | 3·011 | 2·979 | 1·130 |
| | − 6 | 3·010 | 2·641 | 2·607 | −15 | 3·012 | 2·990 | 1·134 |
| | −15 | 3·004 | 2·808 | 2·771 | −30 | 3·012 | 3·006 | 1·140 |
| | −24 | 3·009 | 3·309 | 3·266 | −45 | 3·011 | 3·017 | 1·145 |

(59862) Wt. 6/R.8 375 8/42 Hw. G.377/1

## SYSTEM OF AXES

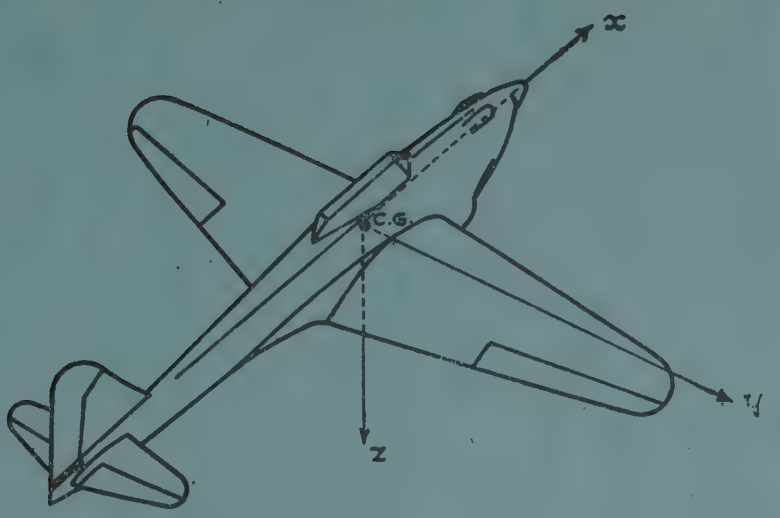


| Axes | Symbol Designation Positive direction | $x$ longitudinal forward | $y$ lateral starboard | $z$ normal downward |
|---|---|---|---|---|
| Force | Symbol | X | Y | Z |
| Moment | Symbol<br>Designation | L<br>rolling | M<br>pitching | N<br>yawing |
| Angle of Rotation | Symbol | $\phi$ | $\theta$ | $\psi$ |
| Velocity | Linear<br>Angular | $u$<br>$p$ | $v$<br>$q$ | $w$<br>$r$ |
| Moment of Inertia | | A | B | C |

Components of linear velocity and force are positive in the positive direction of the corresponding axis.

Components of angular velocity and moment are positive in the cyclic order $y$ to $z$ about the axis of $x$, $z$ to $x$ about the axis of $y$, and $x$ to $y$ about the axis of $z$.

The angular movement of a control surface (elevator or rudder) is governed by the same convention, the elevator angle being positive downwards and the rudder angle positive to port. The aileron angle is positive when the starboard aileron is down and the port aileron is up. A positive control angle normally gives rise to a negative moment about the corresponding axis.

The symbols for the control angles are :—

$\xi$ aileron angle
$\eta$ elevator angle
$\eta_T$ tail setting angle
$\zeta$ rudder angle

# Publications of the Aeronautical Research Committee

TECHNICAL REPORTS OF THE AERONAUTICAL RESEARCH COMMITTEE—

1933-34 Vol. I. Aerodynamics. £1 5s.
Vol. II. Structures, Engines, Instruments, etc. £1 10s.

1934-35 Vol. I. Aerodynamics. £2.
Vol. II. Seaplanes, Structures, Engines, Materials, etc. £2.

1935-36 Vol. I. Aerodynamics. £1 10s.
Vol. II. Structures, Flutter, Engines, Seaplanes, etc. £1 10s.

1936 Vol. I. Aerodynamics General, Performance, Airscrews, Flutter and Spinning. £2.
Vol. II. Stability and Control, Structures, Seaplanes, Engines, etc. £2 10s.

1937 Vol. I. Aerodynamics General, Performance, Airscrews, Flutter and Spinning. £2.
Vol. II. Stability and Control, Structures, Seaplanes, Engines, etc. £3.

ANNUAL REPORTS OF THE AERONAUTICAL RESEARCH COMMITTEE—

1933-34 1s. 6d.
1934-35 1s. 6d.
April 1, 1935 to December 31, 1936. 4s.
1937 2s.
1938 1s. 6d.

INDEX TO THE TECHNICAL REPORTS OF THE ADVISORY COMMITTEE ON AERONAUTICS—

1909-1919 Reports and Memoranda No. 1600. 8s.

*Prices are net and postage extra.*

## His Majesty's Stationery Office

London W.C.2 : York House, Kingsway
Edinburgh 2 : 120 George Street Manchester 2 : 39-41 King Street
Cardiff : 1 St. Andrew's Crescent Belfast : 80 Chichester Street
or through any bookseller.

S.O. Code No. 23-1897

629.13
G79r
no.1898

OF THE
UNIVERSITY OF ILLINOIS

R. & M. No. 1898
(2799)
A.R.C. Technical Report

MINISTRY OF AIRCRAFT PRODUCTION

AERONAUTICAL RESEARCH COMMITTEE
REPORTS AND MEMORANDA

# Tests of Aerofoil N.A.C.A. 23012 in the Compressed Air Tunnel

*By*

D. H. WILLIAMS, B.Sc., A.F.R.Ae.S., A. H. BELL
AND E. SMYTH, B.Sc., A.F.R.Ae.S.

of the Aerodynamics Department, N.P.L.

*Crown Copyright Reserved*

LONDON: HIS MAJESTY'S STATIONERY OFFICE
Price 2*s.* 0*d.* net

# AERODYNAMIC SYMBOLS

## 1. GENERAL

| | |
|---|---|
| $m$ | Mass |
| $t$ | Time |
| V | Resultant linear velocity |
| $\Omega$ | Resultant angular velocity |
| $\rho$ | Density, $\sigma$ relative density |
| $\nu$ | Kinematic coefficient of viscosity |
| R | Reynolds number, $R = lV/\nu$ (where $l$ is a suitable linear dimension) |

Normal temperature and pressure for aeronautical work are 15° C and 760 mm.

For air under these conditions $\begin{cases} \rho = 0{\cdot}002378 \text{ slug/cu. ft.} \\ \nu = 1{\cdot}56 \times 10^{-4} \text{ ft.}^2\text{/sec.} \end{cases}$

The slug is taken to be 32·2 lb.-mass.

| | |
|---|---|
| $\alpha$ | Angle of incidence |
| $e$ | Angle of downwash |
| S | Area |
| $b$ | Span |
| $c$ | Chord |
| A | Aspect ratio, $A = b^2/S$ |
| L | Lift, with coefficient $C_L = L/\frac{1}{2}\rho V^2 S$ |
| D | Drag, with coefficient $C_D = D/\frac{1}{2}\rho V^2 S$ |
| $\gamma$ | Gliding angle, $\tan\gamma = D/L$ |
| L | Rolling moment, with coefficient $C_l = L/\frac{1}{2}\rho V^2 bS$ |
| M | Pitching moment, with coefficient $C_m = M/\frac{1}{2}\rho V^2 cS$ |
| N | Yawing moment, with coefficient $C_n = N/\frac{1}{2}\rho V^2 bS$ |

## 2. AIRSCREWS

| | |
|---|---|
| $n$ | Revolutions per second |
| D | Diameter |
| J | $V/nD$ |
| P | Power |
| T | Thrust, with coefficient $k_T = T/\rho n^2 D^4$ |
| Q | Torque, with coefficient $k_Q = Q/\rho n^2 D^5$ |
| $\eta$ | Efficiency, $\eta = TV/P = Jk_T/2\pi k_Q$ |

Return this book on or before the
**Latest Date** stamped below.

University of Illinois Library

L161—H41

629.13

# Tests of Aerofoil N.A.C.A. 23012 in the Compressed Air Tunnel

*By*

D. H. Williams, B.Sc., A.F.R.Ae.S., A. H. Bell and E. Smyth, B.Sc., A.F.R.Ae.S.
of the Aerodynamics Department, N.P.L.

*Reports and Memoranda No.* 1898
*2nd January*, 1937

*Summary.*—N.A.C.A. 23012 is 12 per cent. thick and has a maximum camber of 2 per cent. at 15 per cent. aft of the leading edge. It is designed to have a very small pitching moment and a high maximum lift. The profile is superior to R.A.F.34 in that the minimum profile drag is lower, occurring at $C_L = 0{\cdot}2$ for N.A.C.A. 23012, whereas it occurs at $C_L = 0$ for R.A.F.34.

The section has also been tested in the Variable Density Tunnel and in the Full Scale Tunnel of the N.A.C.A. Results from the three tunnels are compared. Agreement is good at high Reynolds numbers, taking the "effective" Reynolds number for the Variable Density Tunnel. The very high maximum lift coefficient (1·61) observed in the V.D.T. was not obtained in the C.A.T., where the highest value was 1·49. The maximum lift values obtained in the C.A.T. and F.S.T. are in good agreement.

Later measurements on the aerofoil with a 15 per cent. split flap at 90° have been included.

As an extension of the study of a family of aerofoils in the Variable Density Tunnel, a series was developed having the maximum camber forward of the usual position. The most promising section, N.A.C.A. 23012, was tested[1] over a range of Reynolds numbers in the Variable Density Tunnel (V.D.T.) and in the Full Scale Tunnel (F.S.T.) of the National Advisory Committee for Aeronautics. It is claimed that this section is superior to sections in common use, in that it has a high maximum lift, a low minimum drag and a very small movement of the centre of pressure. In order to test its properties independently, the aerofoil has been tested in the Compressed Air Tunnel (C.A.T.) over the complete range of Reynolds number available. The results are of particular interest, as they afford an opportunity of a direct comparison of results from the Compressed Air Tunnel with those from the two American tunnels at high Reynolds numbers.

The section N.A.C.A. 23012 has a maximum camber of approximately 2 per cent. (actual 1·85 per cent.) situated 15 per cent. aft of the leading edge with the usual N.A.C.A. 12 per cent. thick fairing, the maximum thickness occurring at 0·3c. The centre line is straight from a point just behind the position of maximum camber to the tail. The profile and centre line are shown in Fig. 1 and the ordinates of the section are given in Table 1.

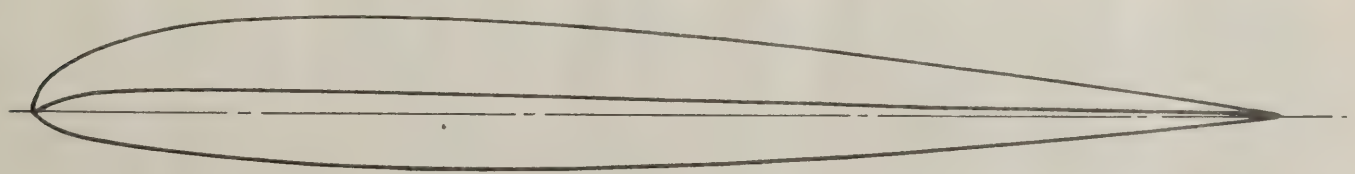

Fig. 1

The model tested in the Compressed Air Tunnel was of hiduminium, with hand-finished surface. It was rectangular, of aspect ratio 6; the chord was 8 in. and the span 48 in.

Lift, drag, pitching moment and centre of pressure coefficients are given in Table 2, corrected for tunnel interference. The profile drag coefficient has been included, calculated from the formula

$$C_D = C_{D_0} + 0{\cdot}0555\ C_L^2.$$

The most important characteristics have been plotted against Reynolds number in the figures, together with the corresponding results from the American wind tunnels.

In general, the results substantiate the claims made for the aerofoil.

Values of lift, drag and pitching moments on the aerofoil with a 15 per cent. split flap at 90°, fixed 0·15c forward of the trailing edge, have been given in Table 3. These measurements were made later than those on the plain wing. The results are taken from Table 7 of A.R.C. report 4191.*

*Comparison with R.A.F.34.*—In N.A.C.A. 23012, a small pitching moment was obtained by placing the maximum camber far forward. In R.A.F.34, the same effect was achieved by giving the aerofoil a reflexed trailing edge. The series of aerofoils tested[2] in the Variable Density Tunnel included some with reflexed trailing edge and having the maximum camber far forward, but it was found that the series without reflexed trailing edge had the smaller minimum profile drag, hence the choice of this particular section for further test.

The following table gives a comparison of certain characteristics of the two aerofoils, obtained[3] in the Compressed Air Tunnel—

| | N.A.C.A. 23012 | R.A.F.34 |
|---|---|---|
| Reynolds number .. .. .. .. | $7{\cdot}05 \times 10^6$ | $7{\cdot}17 \times 10^6$ |
| $C_L$ max. .. .. .. .. .. | 1·49 | 1·41 |
| $C_{D_0}$ min. .. .. .. .. .. | 0·0074 | 0·0080 |
| L/D max. .. .. .. .. .. | 24·4 | 23·4 |
| $C_L$ at L/D max. .. .. .. .. | 0·35 | 0·35 |
| $C_D$ at $C_L = 0$ .. .. .. .. .. | 0·0078 | 0·0080 |
| $dC_L/d\alpha_0$ .. .. .. .. .. | 0·100 | 0·103 |
| $C_L$ max./$C_{D_0}$ min. .. .. .. .. | 191 | 176 |
| $C_{m_0}$ .. .. .. .. .. .. | −0·0093 | −0·0041 |
| C.P. forward position .. .. .. | 0·250 | 0·250 |
| C.P. at 1/4 $C_L$max. .. .. .. .. | 0·275 | 0·251 |

The advantages of N.A.C.A. 23012 over R.A.F.34 are that it has a higher maximum lift, a lower minimum profile drag, a higher maximum L/D and a higher " speed-range index " ($C_L$max./$C_{D_0}$min.). The minimum profile drag occurs at zero lift for R.A.F.34, for the American section it occurs at about $C_L = 0{\cdot}2$. R.A.F.34 is superior in that it has a smaller value of $C_{m_0}$, though this coefficient is small for both aerofoils. R.A.F.34 also has a smaller C.P. movement at low values of $C_L$.

*Comparison with American Tunnels.*—At the outset it is necessary to explain the procedure in recent American reports[1,2] for the presentation of results. Owing to the turbulence in the tunnel, the maximum lift values measured in the Variable Density Tunnel have been much higher than those obtained in less turbulent tunnels and on full scale, so a " turbulence factor " has been introduced. Multiplying the actual Reynolds number of the test by the turbulence factor, an " effective Reynolds number " is obtained, and it is this value of R that is used in the diagrams. The tentative turbulence factor adopted for the Variable Density Tunnel

* Tests in the Compressed Air Tunnel on N.A.C.A.0015 with and without a flap and on other aerofoils with a flap.—R. Jones, A. H. Bell and A. F. Brown. August, 1939. (Unpublished.)

is 2·64, that for the Full Scale Tunnel is 1·1. The lift values have been applied directly at the effective Reynolds number but a correction has been applied to the drag results to allow for the change of Reynolds number. It is assumed that the measured drag coefficients are too high and may be diminished by an amount equal to the decrease in the turbulent skin friction coefficient due to moving from one Reynolds number (test) to a higher Reynolds number (effective). At the highest Reynolds number for the Variable Density Tunnel results, the correction to profile drag coefficient is 0·0011.

The results for the Full Scale Tunnel are given in Tables in the American report, but the Variable Density Tunnel results are given only in small diagrams, except for isolated data for comparison with other results. In all the American diagrams, points are plotted at the effective Reynolds number.

Maximum lift has been plotted in Fig. 2. The Compressed Air Tunnel values have been plotted at the actual Reynolds number, the Full Scale Tunnel results at the effective Reynolds number—the points should be moved slightly to the left for the actual Reynolds number—and the Variable Density Tunnel values have been plotted at both test and effective Reynolds number. There is good agreement between the results from the Compressed Air Tunnel and the Full Scale Tunnel, the results from the Variable Density Tunnel agree with these when plotted at the effective Reynolds number, except for high values of R, when the V.D.T. results are considerably higher than those of the C.A.T. The highest values obtained in the three tunnels are: 1·61 at $R = 8{\cdot}05 \times 10^6$ (effective) in the V.D.T., 1·49 at $R = 7{\cdot}05 \times 10^6$ in the C.A.T., and 1·46 at $R = 4{\cdot}0 \times 10^6$ and $R = 4{\cdot}5 \times 10^6$ in the F.S.T. There is no similarity between the results on maximum lift from the Compressed Air Tunnel and the Variable Density Tunnel when the results from the latter are plotted at the test Reynolds number.

The drag coefficient at zero lift is shown in Fig. 3. The values for the V.D.T. at actual Reynolds number have been obtained by estimating the corrections applied and adding them to the values given at the effective Reynolds numbers. The information given is sufficient for determining the position of only one of the four points accurately, but any errors in the positions of the other three points must be small. For the highest Reynolds numbers, the results agree for all three tunnels, taking the corrected values for the V.D.T. at the effective Reynolds number. The C.A.T. results are surprisingly low at low values of Reynolds number.

Three other quantities are given in Fig. 4, for as many points from the three tunnels as are available. They are minimum profile drag, moment coefficient at zero lift and the slope of the lift curve at zero lift ($dC_L/d\alpha_0$ at $C_L = 0$).

Finally, the following table gives a comparison of data from the three tunnels.

N.A.C.A. 23012

| Test R.N. | C.A.T. | | F.S.T. | | V.D.T. | |
|---|---|---|---|---|---|---|
| | $4{\cdot}47 \times 10^6$ | $3{\cdot}1 \times 10^6$* | $4{\cdot}50 \times 10^6$ | $3{\cdot}09 \times 10^6$† | $3{\cdot}09 \times 10^6$‡ | $1{\cdot}29 \times 10^6$† |
| $C_L$max. | 1·44 | 1·40 | 1·50§ | 1·40 | 1·61 | 1·43 |
| $\alpha_{L_0}$ degrees | −1·0 | −1·0 | −1·2 | −1·2 | −1·2 | −1·2 |
| $dC_L/d\alpha_0$ | 0·100 | 0·098 | 0·101 | 0·099 | 0·104 | 0·102 |
| $C_{D_0}$min. | 0·0072 | 0·0074 | 0·0069 | 0·0072 | 0·0074 | 0·0084 |
| $C_{m_0}$ | −0·0100 | −0·0100 | −0·0087 | −0·0053 | −0·0075 | −0·0065 |
| $C_L$max./$C_{D_0}$min. | 200 | 189 | 208‖ | 195 | 217 | 170 |
| $C_D$min. | 0·0077 | 0·0077 | 0·0078 | 0·0081 | 0·0077 | 0·0086 |
| L/D max. | 24·1 | 22·8 | 25·0‖ | 24·1 | 23·8 | 22·5 |
| $C_L$ at L/D max. | 0·35 | 0·35 | 0·3 | 0·30 | 0·36 | 0·40 |
| C.P. forward pos. | 0·249 | 0·248 | 0·250 | 0·250 | 0·256 | — |
| C.P. at $C_L = 0{\cdot}3$ | 0·264 | 0·262 | 0·260 | 0·250 | — | — |

* Results interpolated from those at $R = 2{\cdot}36 \times 10^6$ and $R = 4{\cdot}47 \times 10^6$. † Effective R.N. of $3{\cdot}40 \times 10^6$.
‡ Effective R.N. of $8{\cdot}16 \times 10^6$. § Highest value given in Tables is 1·46. ‖ As given.

The values given for the Variable Density results at the test Reynolds number of $3{\cdot}09 \times 10^6$ are taken from the American report[1] giving results from the V.D.T. and the F.S.T. An American Technical Note[4] giving results on a series based on N.A.C.A. 23012 with various thickness ratios gives a higher value of maximum lift coefficient (1·68) and a lower minimum drag coefficient (0·0072) at an effective Reynolds number of $8{\cdot}37 \times 10^6$. These values have, however, had corrections applied for turbulence and for tip effect, the latter correction increases maximum lift by 3 per cent.

---

## REFERENCES


1. Jacobs and Clay.—Characteristics of the N.A.C.A. 23012 airfoil from tests in the Full-Scale and Variable-Density Tunnels. T.R. 530, N.A.C.A. March, 1935.
2. Jacobs and Pinkerton.—Tests in the Variable-Density Wind Tunnel of related airfoils having the maximum camber unusually far forward. T.R. 537, N.A.C.A. May, 1935.
3. Jones and Williams.—The effect of surface roughness on the characteristics of the aerofoils N.A.C.A. 0012 and R.A.F.34. R. & M. 1708. Feb. 1936.
4. Jacobs and Pinkerton.—Tests of N.A.C.A. airfoils in the Variable-Density Wind Tunnel. Series 230. T.N.567, N.A.C.A. May, 1936.


---

## TABLE 1

*N.A.C.A. 23012*

*Dimensions in Terms of Chord*

| Distance from Leading Edge | Distance above Chord | Distance below Chord |
|---|---|---|
| 0 | 0 | 0 |
| 0·0125 | 0·0267 | 0·0123 |
| 0·025 | 0·0361 | 0·0171 |
| 0·050 | 0·0491 | 0·0226 |
| 0·075 | 0·0580 | 0·0261 |
| 0·10 | 0·0643 | 0·0292 |
| 0·15 | 0·0719 | 0·0350 |
| 0·20 | 0·0750 | 0·0397 |
| 0·25 | 0·0760 | 0·0428 |
| 0·30 | 0·0755 | 0·0446 |
| 0·40 | 0·0714 | 0·0448 |
| 0·50 | 0·0641 | 0·0417 |
| 0·60 | 0·0547 | 0·0367 |
| 0·70 | 0·0436 | 0·0300 |
| 0·80 | 0·0308 | 0·0216 |
| 0·90 | 0·0168 | 0·0123 |
| 0·95 | 0·0092 | 0·0070 |
| 1·00 | 0 | 0 |

L.E. Rad.: 0·0158

## TABLE 2

*Aerofoil N.A.C.A. 23012. Aspect Ratio 6*

$R = 0{\cdot}315 \times 10^6$, P = 1 atmos., $\frac{1}{2}\rho V^2 = 6{\cdot}62_5$, V = 74·9 f./s.

| $\alpha^\circ$ | $C_L$ | $C_D$ | $C_{D0}$ | $C_m(c/4)$ | C.P. |
|---|---|---|---|---|---|
| $-\ 4{\cdot}5_5$ | −0·233 | 0·0176 | 0·0146 | −0·0211 | 0·160 |
| $-\ 2{\cdot}4_5$ | $-0{\cdot}084_5$ | 0·0124 | 0·0120 | −0·0156 | +0·066 |
| $-\ 1{\cdot}4$ | −0·022 | 0·0106 | 0·0106 | −0·0108 | −0·236 |
| $-\ 0{\cdot}3_5$ | $+0{\cdot}042_5$ | 0·0101 | 0·0100 | −0·0069 | +0·412 |
| $+\ 0{\cdot}6_5$ | 0·113 | 0·0104 | 0·0097 | −0·0030 | 0·276 |
| 1·7 | $0{\cdot}188_5$ | 0·0126 | 0·0106 | −0·0008 | 0·254 |
| $3{\cdot}7_5$ | 0·366 | 0·0197 | 0·0123 | −0·0066 | 0·268 |
| $6{\cdot}8_5$ | 0·617 | 0·0351 | 0·0140 | −0·0123 | 0·270 |
| $9{\cdot}9_5$ | 0·812 | 0·0532 | 0·0166 | −0·0059 | 0·257 |
| 13·0 | 1·000 | 0·0770 | 0·0215 | +0·0021 | 0·248 |
| $15{\cdot}0_5$ | 1·086 | 0·0951 | 0·0297 | 0·0080 | 0·243 |
| 16·1 | 1·104 | 0·106 | 0·038 | +0·0079 | 0·243 |
| 16·3* | 0·893 | — | — | −0·0408 | — |
| $17{\cdot}1_5$ | 1·080 | 0·131 | 0·066 | −0·0075 | 0·257 |
| $17{\cdot}3_5$* | 0·793 | 0·227 | 0·192 | −0·0711 | 0·336 |
| $18{\cdot}2_5$ | 1·058 | 0·154 | 0·092 | −0·0208 | 0·270 |
| 18·4* | 0·744 | 0·249 | 0·218 | −0·0769 | 0·348 |
| $20{\cdot}5_5$ | 0·657 | 0·280 | 0·256 | −0·0805 | 0·362 |
| $23{\cdot}7_5$ | 0·642 | 0·326 | 0·323 | −0·0850 | 0·368 |

* Decreasing incidence.
Stalling angle 16·0°

$R = 0{\cdot}802 \times 10^6$, P = 2·9 atmos., $\frac{1}{2}\rho V^2 = 15{\cdot}1$, V = 66·6 f./s.

| | | | | | |
|---|---|---|---|---|---|
| $-\ 4{\cdot}6$ | −0·241 | 0·0131 | 0·0099 | −0·0189 | 0·172 |
| $-\ 2{\cdot}4_5$ | −0·095 | 0·0096 | 0·0091 | −0·0139 | +0·103 |
| $-\ 1{\cdot}4$ | −0·021 | 0·0088 | 0·0088 | −0·0115 | −0·293 |
| $-\ 0{\cdot}3_5$ | +0·044 | 0·0077 | 0·0076 | −0·0077 | +0·425 |
| $+\ 0{\cdot}6_5$ | 0·113 | 0·0078 | 0·0071 | −0·0045 | 0·290 |
| 1·7 | $0{\cdot}186_5$ | 0·0094 | 0·0075 | −0·0017 | 0·259 |
| 3·8 | 0·334 | 0·0141 | 0·0079 | +0·0015 | 0·246 |
| $6{\cdot}8_5$ | 0·576 | 0·0277 | 0·0093 | −0·0008 | 0·251 |
| 10·0 | 0·795 | 0·0477 | 0·0126 | +0·0006 | 0·249 |
| 12·0 | 0·932 | 0·0620 | 0·0138 | 0·0033 | 0·246 |
| $14{\cdot}1_5$ | 1·065 | 0·0800 | 0·0170 | 0·0058 | 0·244 |
| $15{\cdot}1_5$ | 1·111 | 0·0908 | 0·0224 | 0·0070 | 0·243 |
| $16{\cdot}1_5$ | 1·162 | 0·101 | 0·026 | +0·0091 | 0·242 |
| $17{\cdot}2_5$ | 1·115 | 0·134 | 0·065 | −0·0148 | 0·263 |
| $19{\cdot}3_5$ | 1·059 | 0·176 | 0·114 | −0·0344 | 0·282 |
| $21{\cdot}4_5$ | 1·005 | 0·225 | 0·169 | −0·0548 | 0·304 |

TABLE 2—*continued*

$R = 1{\cdot}26 \times 10^6$, P = 4·28 atmos., $\frac{1}{2}\rho V^2 = 25{\cdot}4$, V = 71·0 f./s.

| $\alpha°$ | $C_L$ | $C_D$ | $C_{D0}$ | $C_m(c/4)$ | C.P. |
|---|---|---|---|---|---|
| − 4·6 | −0·249 | 0·0123 | 0·0089 | −0·0172 | 0·181 |
| − 2·5 | −0·100 | 0·0091 | 0·0085 | −0·0130 | +0·120 |
| − 1·4 | −0·022 | 0·0082 | 0·0082 | −0·0112 | −0·255 |
| − $0{\cdot}3_5$ | +$0{\cdot}049_5$ | 0·0080 | 0·0079 | −0·0089 | +0·430 |
| + $0{\cdot}6_5$ | 0·121 | 0·0078 | 0·0070 | −0·0057 | 0·297 |
| $1{\cdot}7_5$ | 0·191 | 0·0089 | 0·0069 | −0·0034 | 0·268 |
| 3·8 | 0·344 | 0·0137 | 0·0071 | −0·0007 | 0·252 |
| 6·9 | 0·576 | 0·0261 | 0·0077 | +0·0018 | 0·247 |
| $10{\cdot}0_5$ | 0·799 | 0·0461 | 0·0107 | 0·0036 | 0·245 |
| 12·1 | 0·943 | 0·0618 | 0·0125 | 0·0044 | 0·245 |
| $14{\cdot}1_5$ | 1·073 | 0·0804 | 0·0165 | 0·0050 | 0·245 |
| $16{\cdot}2_5$ | 1·193 | 0·101 | 0·022 | 0·0063 | 0·245 |
| $17{\cdot}2_5$ | 1·244 | 0·113 | 0·027 | +0·0065 | 0·245 |
| $18{\cdot}3_5$ | 1·130 | 0·158 | 0·087 | −0·0223 | 0·270 |
| $20{\cdot}4_5$ | 1·045 | 0·202 | 0·141 | −0·0465 | 0·294 |
| $22{\cdot}6_5$ | 0·968 | 0·251 | 0·199 | −0·0639 | 0·314 |

Stalling angle 18·0°

$R = 2{\cdot}36 \times 10^6$, P = 7·84 atmos., $\frac{1}{2}\rho V^2 = 54{\cdot}1_5$, V = 78·6 f./s.

| | | | | | |
|---|---|---|---|---|---|
| − $1{\cdot}4_5$ | −0·032 | 0·0080 | 0·0079 | −0·0108 | −0·086 |
| − $0{\cdot}3_5$ | +$0{\cdot}041_5$ | 0·0076 | 0·0075 | −0·0090 | +0·467 |
| + 0·7 | 0·118 | 0·0084 | 0·0076 | −0·0071 | 0·310 |
| $1{\cdot}7_5$ | 0·192 | 0·0099 | 0·0079 | −0·0052 | 0·277 |
| 3·9 | 0·345 | 0·0157 | 0·0091 | −0·0024 | 0·257 |
| $7{\cdot}0_5$ | 0·583 | 0·0280 | 0·0091 | +0·0001 | 0·250 |
| $10{\cdot}2_5$ | 0·801 | 0·0478 | 0·0122 | 0·0019 | 0·248 |
| 12·3 | 0·959 | 0·0650 | 0·0140 | 0·0024 | 0·248 |
| $14{\cdot}4_5$ | 1·102 | 0·0844 | 0·0171 | 0·0019 | 0·248 |
| 16·5 | 1·242 | 0·106 | 0·020 | 0·0014 | 0·249 |
| $17{\cdot}5_5$ | 1·295 | 0·118 | 0·025 | 0·0013 | 0·249 |
| 18·6 | 1·347 | 0·130 | 0·029 | +0·0010 | 0·249 |
| 18·6* | 1·148 | 0·165 | 0·092 | −0·0308 | 0·277 |
| 19·6 | 1·083 | 0·195 | 0·130 | −0·0509 | 0·297 |
| $20{\cdot}6_5$ | 1·043 | 0·215 | 0·155 | −0·0566 | 0·304 |
| $22{\cdot}7_5$ | 0·931 | 0·258 | 0·210 | −0·0736 | 0·327 |

* Decreasing incidence.
Stalling angle 19·4°

TABLE 2—*continued*

$R = 4{\cdot}47 \times 10^6$, P = 14·83 atmos., $\frac{1}{2}\rho V^2 = 102{\cdot}5$, V = 78·7 f./s.

| $\alpha°$ | $C_L$ | $C_D$ | $C_{D0}$ | $C_m(c/4)$ | C.P. |
|---|---|---|---|---|---|
| $-\ 1{\cdot}4_5$ | $-0{\cdot}034$ | 0·0079 | 0·0078 | $-0{\cdot}0108$ | $-0{\cdot}066$ |
| $-\ 0{\cdot}3_5$ | $+0{\cdot}046$ | 0·0077 | 0·0076 | $-0{\cdot}0090$ | $+0{\cdot}446$ |
| $+\ 0{\cdot}7_5$ | 0·128 | 0·0081 | 0·0072 | $-0{\cdot}0073$ | 0·307 |
| 1·8 | 0·212 | 0·0098 | 0·0073 | $-0{\cdot}0057$ | 0·277 |
| $4{\cdot}0_5$ | 0·374 | 0·0156 | 0·0078 | $-0{\cdot}0029$ | 0·258 |
| 7·3 | 0·616 | 0·0295 | 0·0084 | $+0{\cdot}0002$ | 0·250 |
| 10·6 | 0·852 | 0·0508 | 0·0106 | 0·0009 | 0·249 |
| $12{\cdot}6_5$ | 1·007 | 0·0684 | 0·0122 | $+0{\cdot}0004$ | 0·250 |
| $14{\cdot}8_5$ | 1·156 | 0·0891 | 0·0150 | $-0{\cdot}0003$ | 0·250 |
| 17·0 | 1·291 | 0·115 | 0·022 | $-0{\cdot}0017$ | 0·251 |
| $18{\cdot}0_5$ | 1·352 | 0·124 | 0·023 | $-0{\cdot}0023$ | 0·252 |
| 19·1 | 1·410 | 0·137 | 0·027 | $-0{\cdot}0031$ | 0·252 |
| $18{\cdot}9_5$* | 1·140 | 0·178 | 0·106 | $-0{\cdot}0380$ | 0·283 |
| 19·9* | 1·052 | 0·207 | 0·146 | $-0{\cdot}0558$ | 0·302 |
| 20·9 | 1·005 | 0·228 | 0·173 | $-0{\cdot}0626$ | 0·311 |
| 23·0 | 0·898 | 0·274 | 0·219 | $-0{\cdot}0803$ | 0·336 |

* Decreasing incidence.
Stalling angle 20·1°

$R = 5{\cdot}50 \times 10^6$, P = 18·1 atmos., $\frac{1}{2}\rho V^2 = 125{\cdot}2_5$, V = 78·2 f./s.

| | | | | | |
|---|---|---|---|---|---|
| $-\ 1{\cdot}5$ | $-0{\cdot}035_5$ | 0·0077 | 0·0076 | $-0{\cdot}0105$ | $-0{\cdot}044$ |
| $-\ 0{\cdot}3_5$ | $+0{\cdot}046_5$ | 0·0078 | 0·0077 | $-0{\cdot}0086$ | $+0{\cdot}435$ |
| $+\ 0{\cdot}7_5$ | 0·131 | 0·0086 | 0·0076 | $-0{\cdot}0071$ | 0·304 |
| 1·9 | $0{\cdot}214_5$ | 0·0103 | 0·0077 | $-0{\cdot}0055$ | 0·276 |
| 4·1 | 0·382 | 0·0158 | 0·0077 | $-0{\cdot}0030$ | 0·258 |
| 7·4 | 0·620 | 0·0301 | 0·0088 | $+0{\cdot}0001$ | 0·250 |
| 10·7 | 0·865 | 0·0516 | 0·0101 | $+0{\cdot}0002$ | 0·250 |
| 12·9 | 1·026 | 0·0690 | 0·0107 | $-0{\cdot}0006$ | 0·251 |
| $15{\cdot}0_5$ | 1·165 | 0·0913 | 0·0161 | $-0{\cdot}0021$ | 0·252 |
| $17{\cdot}2_5$ | 1·311 | 0·113 | 0·018 | $-0{\cdot}0039$ | 0·253 |
| $18{\cdot}3_5$ | 1·370 | 0·128 | 0·024 | $-0{\cdot}0041$ | 0·253 |
| 19·4 | 1·426 | 0·141 | 0·028 | $-0{\cdot}0045$ | 0·253 |
| $19{\cdot}0_5$* | 1·084 | 0·187 | 0·122 | $-0{\cdot}0420$ | 0·289 |
| 20·1 | 1·024 | 0·211 | 0·153 | $-0{\cdot}0557$ | 0·304 |
| $21{\cdot}0_5$ | 0·991 | 0·232 | 0·177 | $-0{\cdot}0620$ | 0·311 |
| $23{\cdot}0_5$ | 0·890 | 0·275 | 0·231 | $-0{\cdot}0806$ | 0·337 |

* Decreasing incidence.
Stalling angle 20·1°

TABLE 2—*continued*

$R = 7{\cdot}05 \times 10^6$, P = 22·6 atmos., $\frac{1}{2}\rho V^2 = 160{\cdot}5$, V = 78·7 f./s.

| $\alpha°$ | $C_L$ | $C_D$ | $C_{D0}$ | $C_m(c/4)$ | C.P. |
|---|---|---|---|---|---|
| − 1·5 | $-0{\cdot}036_5$ | 0·0080 | 0·0079 | −0·0101 | −0·022 |
| − $0{\cdot}3_5$ | $+0{\cdot}047_5$ | 0·0077 | 0·0076 | −0·0083 | +0·426 |
| + 0·8 | $0{\cdot}133_5$ | 0·0084 | 0·0074 | −0·0067 | 0·300 |
| $1{\cdot}9_5$ | 0·220 | 0·0101 | 0·0074 | −0·0051 | 0·273 |
| $4{\cdot}2_5$ | 0·389 | 0·0161 | 0·0083 | −0·0023 | 0·256 |
| $7{\cdot}5_5$ | 0·638 | 0·0309 | 0·0083 | −0·0002 | 0·250 |
| 11·0 | 0·884 | 0·0545 | 0·0112 | −0·0005 | 0·251 |
| 13·2 | 1·048 | 0·0737 | 0·0127 | −0·0020 | 0·252 |
| $15{\cdot}4_5$ | 1·198 | 0·0969 | 0·0172 | −0·0036 | 0·253 |
| 17·6 | 1·343 | 0·119 | 0·019 | −0·0054 | 0·254 |
| 18·7 | 1·398 | 0·134 | 0·025 | −0·0060 | 0·255 |
| $19{\cdot}7_5$ | 1·460 | 0·147 | 0·029 | −0·0065 | 0·255 |
| $20{\cdot}2_5$ | 1·485 | — | — | — | — |
| $20{\cdot}5_5$ | 1·024 | 0·219 | 0·161 | −0·0599 | 0·308 |
| $21{\cdot}5_5$ | 0·980 | 0·236 | 0·183 | −0·0647 | 0·315 |
| $23{\cdot}4_5$ | 0·875 | 0·285 | 0·242 | −0·0786 | 0·337 |

Stalling angle $20{\cdot}2_5°$

TABLE 3

*N.A.C.A. 23012 with 0·15c split flap at 90°, fixed at 0·15c from trailing edge*
*Aspect Ratio 6*

$R = 0{\cdot}315 \times 10^6$, P = 1 atmos., $\frac{1}{2}\rho V^2 = 6{\cdot}72$
V = 76·1 f./s.

| $\alpha°$ | $C_L$ | $C_D$ | $C_m$ |
|---|---|---|---|
| $-6{\cdot}9_5$ | 0·449 | 0·168 | −0·166 |
| −5·1 | 0·616 | 0·182 | −0·180 |
| $-1{\cdot}1_5$ | 0·897 | 0·212 | −0·183 |
| $+2{\cdot}9_5$ | 1·149 | 0·244 | −0·180 |
| $7{\cdot}1_5$ | 1·402 | 0·283 | −0·174 |
| $10{\cdot}1_5$ | 1·602 | 0·319 | −0·174 |
| 12·2 | 1·713 | 0·344 | −0·176 |
| $12{\cdot}4_5$* | 1·262 | 0·447 | −0·235 |
| 13·3 | 1·772 | 0·359 | −0·177 |
| 13·7* | 1·136 | 0·475 | −0·234 |
| 14·3 | 1·838 | 0·368 | −0·180 |
| $14{\cdot}7_5$ | 1·086 | 0·501 | −0·237 |
| $15{\cdot}8_5$ | 1·058 | 0·523 | −0·237 |
| $17{\cdot}9_5$ | 1·069 | 0·587 | −0·249 |

* Decreasing incidence.
Stalling angle 14·7°

$R = 0{\cdot}81 \times 10^6$, P = 3·0 atmos., $\frac{1}{2}\rho V^2 = 15{\cdot}1$
V = 65·6 f./s.

| $\alpha°$ | $C_L$ | $C_D$ | $C_m$ |
|---|---|---|---|
| −7·0 | 0·447 | 0·164 | −0·163 |
| −5·1 | 0·606 | 0·179 | −0·174 |
| $-1{\cdot}1_5$ | 0·923 | 0·212 | −0·186 |
| +3·0 | 1·202 | 0·245 | −0·185 |
| $7{\cdot}1_5$ | 1·471 | 0·283 | −0·181 |
| 10·2 | 1·656 | 0·320 | −0·179 |
| 12·2 | 1·769 | 0·346 | −0·178 |
| $13{\cdot}3_5$ | 1·839 | 0·361 | −0·179 |
| $14{\cdot}3_5$ | 1·898 | 0·376 | −0·181 |
| 15·4 | 1·957 | 0·388 | −0·180 |
| 15·7* | 1·366 | 0·507 | −0·232 |
| 16·4 | 2·018 | 0·405 | −0·183 |
| $16{\cdot}7_5$* | 1·248 | 0·670 | −0·229 |
| 17·4 | 2·072 | 0·417 | −0·186 |
| $17{\cdot}8_5$ | 1·162 | 0·592 | −0·247 |
| 19·0 | 1·146 | 0·633 | −0·256 |
| 20·0 | 1·156 | 0·666 | −0·262 |
| $22{\cdot}1_5$ | 1·152 | 0·722 | −0·269 |

* Decreasing incidence
Stalling angle 17·8°

TABLE 3—*continued*

$R = 1{\cdot}27 \times 10^6$, P = 4·4 atmos., $\frac{1}{2}\rho V^2 = 25{\cdot}3$, V = 70·1 f./s.

| $\alpha^\circ$ | $C_L$ | $C_D$ | $C_m$ |
|---|---|---|---|
| −7·0 | 0·445 | 0·168 | −0·166 |
| −5·1 | 0·602 | 0·181 | −0·173 |
| −1·1$_5$ | 0·929 | 0·214 | −0·187 |
| +3·0$_5$ | 1·206 | 0·248 | −0·186 |
| 7·2 | 1·468 | 0·290 | −0·184 |
| 10·2$_5$ | 1·665 | 0·325 | −0·182 |
| 12·3 | 1·785 | 0·351 | −0·181 |
| 14·4 | 1·910 | 0·378 | −0·181 |
| 15·5 | 1·961 | 0·395 | −0·182 |
| 15·6* | 1·628 | 0·423 | −0·204 |
| 16·5 | 2·037 | 0·406 | −0·183 |
| 16·7* | 1·494 | 0·454 | −0·211 |
| 17·5 | 2·098 | 0·421 | −0·184 |
| 17·8* | 1·360 | 0·580 | −0·249 |
| 18·5$_5$ | 2·153 | 0·439 | −0·187 |
| 18·9$_5$* | 1·115 | 0·604 | −0·245 |
| 19·9$_5$ | 1·242 | 0·645 | −0·251 |
| 22·1 | 1·235 | 0·705 | −0·258 |

* Decreasing incidence
Stalling angle 18·9°

$R = 2{\cdot}47 \times 10^6$, P = 8·0 atmos., $\frac{1}{2}\rho V^2 = 53{\cdot}9$, V = 76·7 f./s.

| $\alpha^\circ$ | $C_L$ | $C_D$ | $C_m$ |
|---|---|---|---|
| −7·0$_5$ | 0·438 | 0·167 | −0·166 |
| −5·1$_5$ | 0·591 | 0·179 | −0·170 |
| −1·1 | 0·909 | 0·212 | −0·179 |
| +3·1 | 1·203 | 0·248 | −0·181 |
| 7·3$_5$ | 1·479 | 0·291 | −0·180 |
| 10·4$_5$ | 1·675 | 0·327 | −0·180 |
| 12·5$_5$ | 1·797 | 0·352 | −0·178 |
| 14·7 | 1·923 | 0·384 | −0·179 |
| 15·7 | 1·984 | 0·395 | −0·179 |
| 16·7$_5$ | 2·045 | 0·411 | −0·180 |
| 16·8* | 1·552 | 0·458 | −0·214 |
| 17·8 | 2·094 | 0·425 | −0·179 |
| 17·8$_5$* | 1·432 | 0·483 | −0·223 |
| 18·9 | 2·175 | 0·440 | −0·182 |
| 18·9$_5$* | 1·299 | 0·515 | −0·224 |
| 19·9 | 2·215 | 0·456 | −0·184 |
| 20·0$_5$* | 1·258 | 0·545 | −0·235 |
| 21·1$_5$ | 1·217 | 0·577 | −0·238 |
| 22·1 | 1·226 | 0·637 | −0·256 |
| 23·1$_5$ | 1·246 | 0·697 | −0·272 |

* Decreasing incidence
Stalling angle 20·4°

$R = 4{\cdot}47 \times 10^6$, P = 14·6 atmos., $\frac{1}{2}\rho V^2 = 101{\cdot}7$, V = 78·8 f./s.

| $\alpha^\circ$ | $C_L$ | $C_D$ | $C_m$ |
|---|---|---|---|
| −7·1$_5$ | 0·450 | 0·169 | −0·169 |
| −5·2 | 0·600 | 0·181 | −0·174 |
| −1·0$_5$ | 0·909 | 0·209 | −0·177 |
| +3·3 | 1·211 | 0·245 | −0·178 |
| 7·6 | 1·489 | 0·289 | −0·177 |
| 10·7$_5$ | 1·688 | 0·327 | −0·177 |
| 12·9$_5$ | 1·814 | 0·355 | −0·177 |
| 15·1 | 1·933 | 0·383 | −0·177 |
| 17·2$_5$ | 2·067 | 0·414 | −0·180 |
| 17·0* | 1·536 | 0·471 | −0·215 |
| 18·3 | 2·134 | 0·430 | −0·181 |
| 18·0* | 1·469 | 0·520 | −0·230 |
| 19·4 | 2·192 | 0·446 | −0·183 |
| 19·0$_5$* | 1·322 | 0·535 | −0·235 |
| 20·4$_5$ | 2·244 | 0·465 | −0·184 |
| 20·1* | 1·262 | 0·556 | −0·234 |
| 21·1$_5$* | 1·218 | 0·585 | −0·242 |
| 23·1$_5$ | 1·212 | 0·712 | −0·268 |

* Decreasing incidence
Stalling angle 21·4°

$R = 5{\cdot}43 \times 10^6$, P = 18·1 atmos., $\frac{1}{2}\rho V^2 = 124$, V = 78·4 f./s.

| $\alpha^\circ$ | $C_L$ | $C_D$ | $C_m$ |
|---|---|---|---|
| −7·2 | 0·453 | 0·171 | −0·171 |
| −5·2 | 0·599 | 0·180 | −0·173 |
| −1·0 | 0·917 | 0·210 | −0·178 |
| +3·4 | 1·221 | 0·245 | −0·178 |
| 7·7$_5$ | 1·501 | 0·290 | −0·178 |
| 10·9$_5$ | 1·705 | 0·329 | −0·177 |
| 13·0$_5$ | 1·834 | 0·358 | −0·177 |
| 15·3 | 1·967 | 0·387 | −0·178 |
| 17·4$_5$ | 2·076 | 0·419 | −0·180 |
| 17·0$_5$* | 1·522 | — | — |
| 18·5 | 2·137 | 0·436 | −0·182 |
| 18·0$_5$* | 1·477 | 0·511 | −0·229 |
| 19·6$_5$ | 2·210 | 0·453 | −0·185 |
| 19·1* | 1·329 | 0·545 | −0·236 |
| 20·7 | 2·263 | 0·467 | −0·185 |
| 20·1* | 1·258 | 0·563 | −0·234 |
| 21·1$_5$* | 1·204 | 0·600 | −0·245 |
| 22·1$_5$ | 1·216 | 0·656 | −0·259 |
| 24·0$_5$ | 1·232 | 0·750 | −0·284 |

* Decreasing incidence
Stalling angle 21·7°

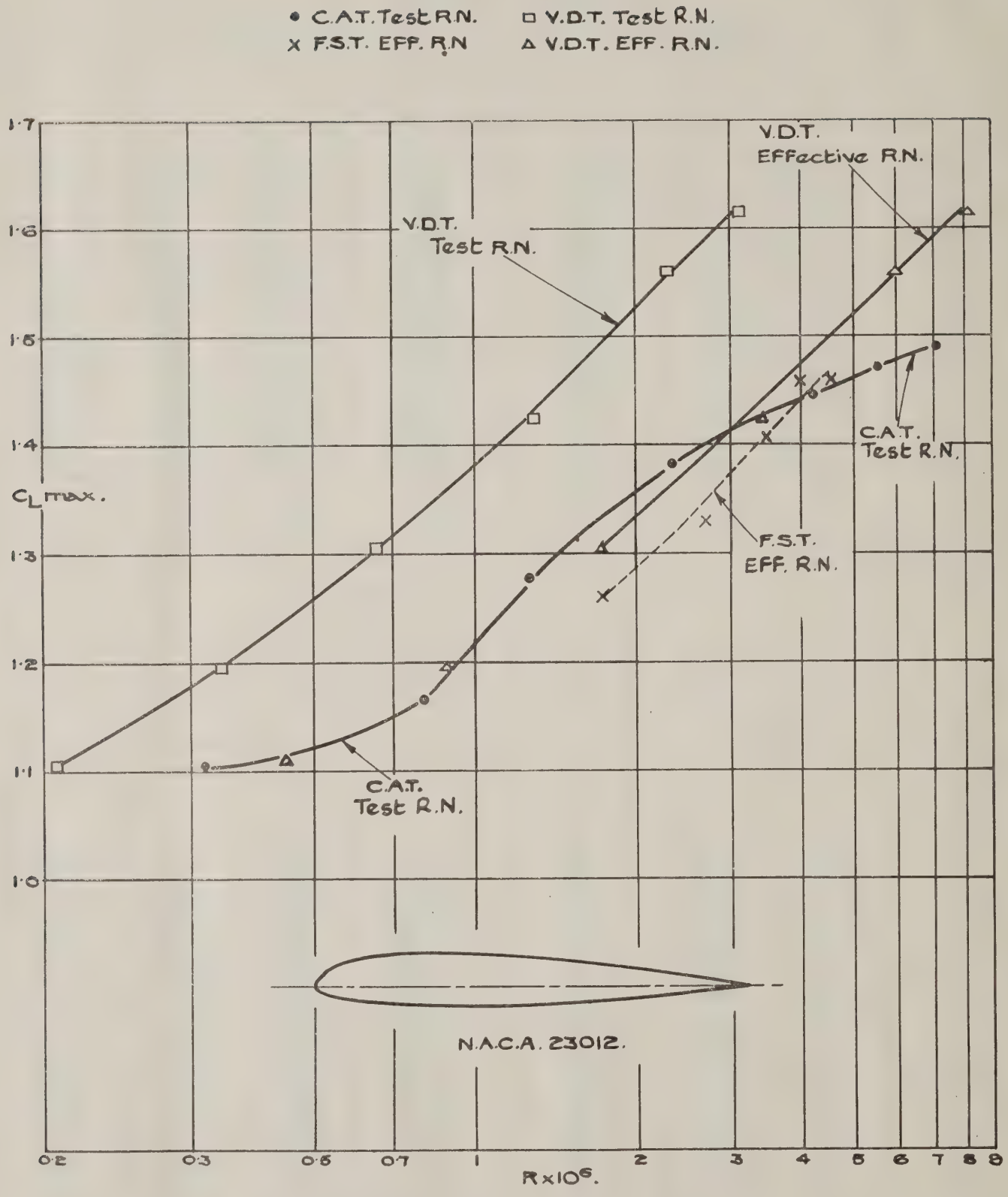


MAXIMUM LIFT AGAINST REYNOLDS NUMBER

FIG. 2

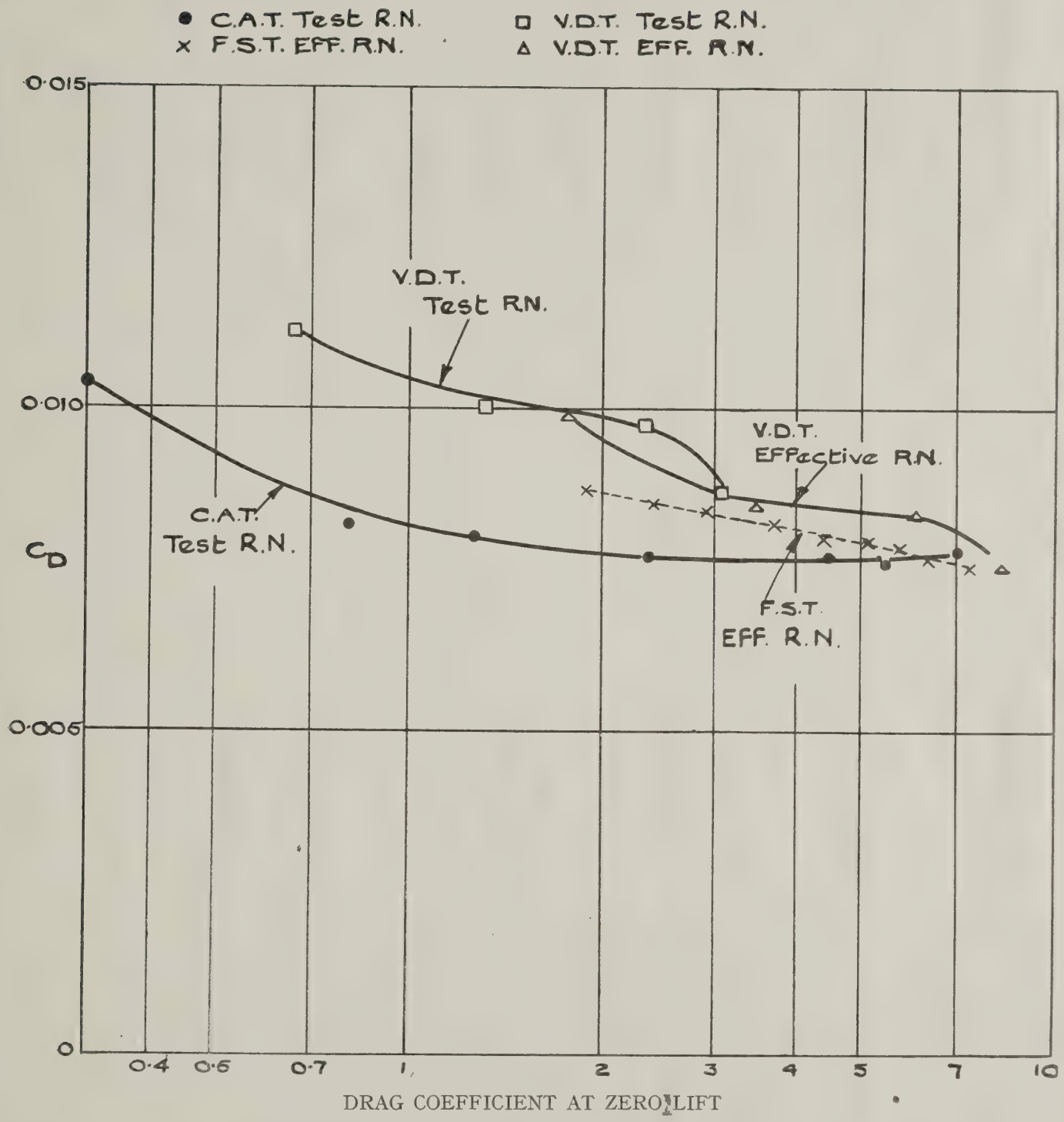
● C.A.T. Test R.N.
× F.S.T. EFF. R.N.
□ V.D.T. Test R.N.
△ V.D.T. EFF. R.N.
0·015
0·010
0·005
0
$C_D$
V.D.T.
Test R.N.
V.D.T.
Effective R.N.
C.A.T.
Test R.N.
F.S.T.
EFF. R.N.
0·4
0·6
0·7
1
2
3
4
5
7
10
DRAG COEFFICIENT AT ZERO LIFT

FIG. 3

COMPARISON OF $C_{D_0}$ min., $C_{m_0}$ AND $(dC_L/d\alpha_0)$ IN C.A.T. AND AMERICAN WIND TUNNELS.

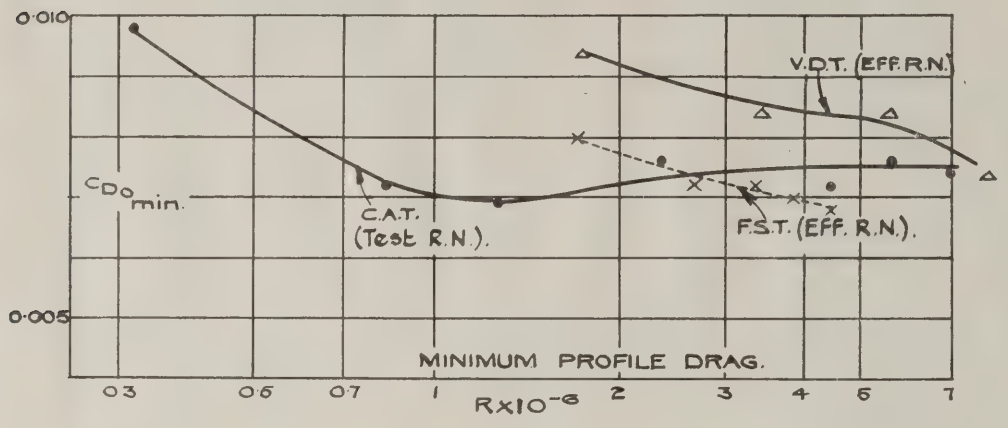


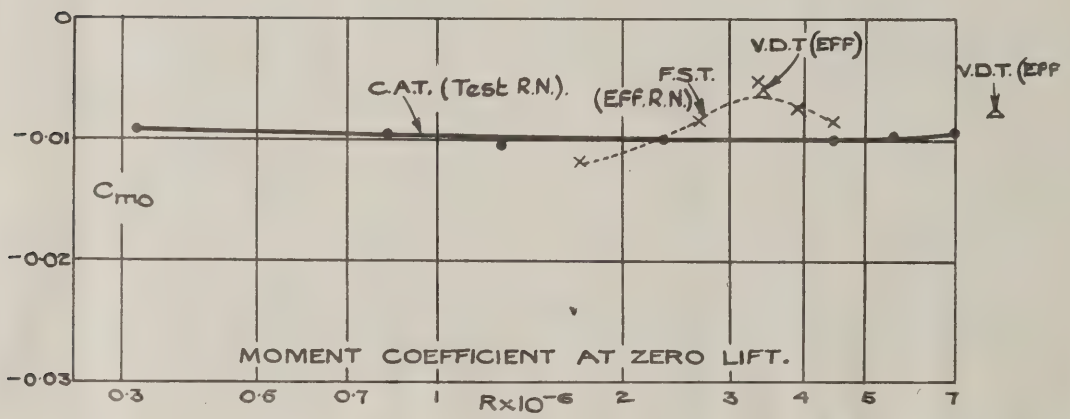


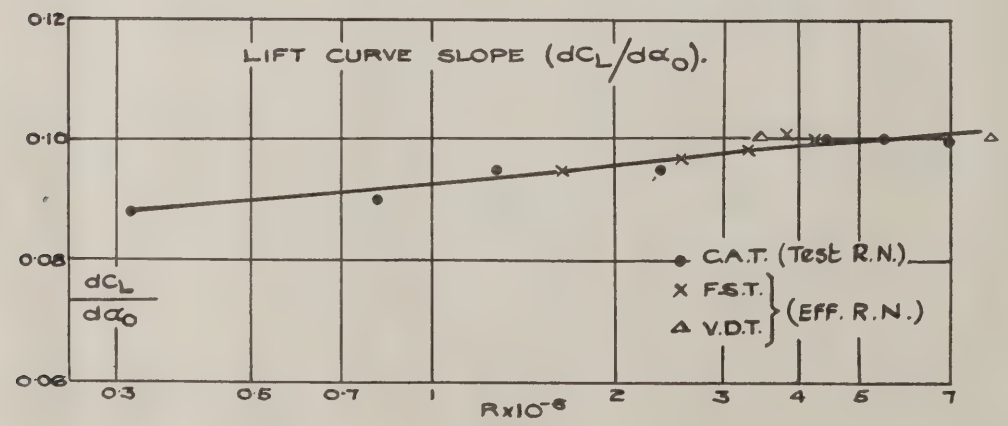


FIG. 4

(60168) Wt. 6/R8 375 8/42 Hw. G.377/1

## SYSTEM OF AXES

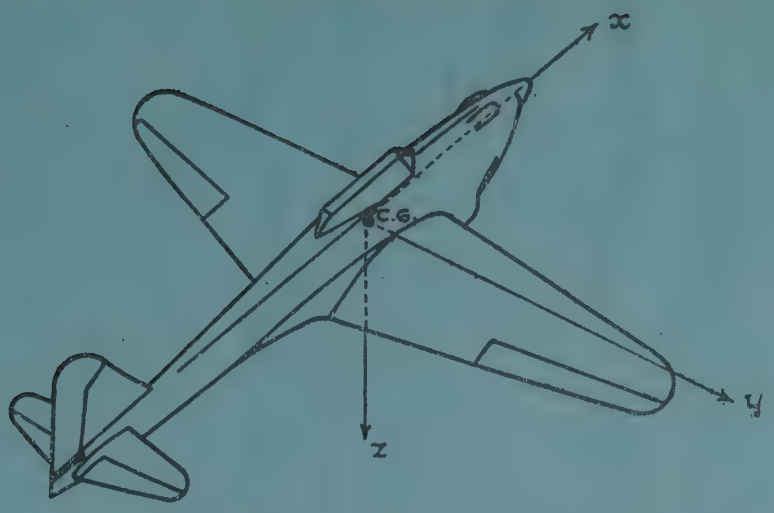


| Axes | Symbol Designation Positive direction | $x$ longitudinal forward | $y$ lateral starboard | $z$ normal downward |
|---|---|---|---|---|
| Force | Symbol | X | Y | Z |
| Moment | Symbol Designation | L rolling | M pitching | N yawing |
| Angle of Rotation | Symbol | $\phi$ | $\theta$ | $\psi$ |
| Velocity | Linear Angular | $u$ $p$ | $v$ $q$ | $w$ $r$ |
| Moment of Inertia | | A | B | C |

Components of linear velocity and force are positive in the positive direction of the corresponding axis.

Components of angular velocity and moment are positive in the cyclic order $y$ to $z$ about the axis of $x$, $z$ to $x$ about the axis of $y$, and $x$ to $y$ about the axis of $z$.

The angular movement of a control surface (elevator or rudder) is governed by the same convention, the elevator angle being positive downwards and the rudder angle positive to port. The aileron angle is positive when the starboard aileron is down and the port aileron is up. A positive control angle normally gives rise to a negative moment about the corresponding axis.

The symbols for the control angles are :—

$\xi$ aileron angle
$\eta$ elevator angle
$\eta_T$ tail setting angle
$\zeta$ rudder angle

# Publications of the Aeronautical Research Committee

TECHNICAL REPORTS OF THE AERONAUTICAL RESEARCH COMMITTEE—

1933-34 Vol. I. Aerodynamics. £1 5*s*.
Vol. II. Structures, Engines, Instruments, etc. £1 10*s*.

1934-35 Vol. I. Aerodynamics. £2.
Vol. II. Seaplanes, Structures, Engines, Materials, etc. £2.

1935-36 Vol. I. Aerodynamics. £1 10*s*.
Vol. II. Structures, Flutter, Engines, Seaplanes, etc. £1 10*s*.

1936 Vol. I. Aerodynamics General, Performance, Airscrews, Flutter and Spinning. £2.
Vol. II. Stability and Control, Structures, Seaplanes, Engines, etc. £2 10*s*.

1937 Vol. I. Aerodynamics General, Performance, Airscrews, Flutter and Spinning. £2.
Vol. II. Stability and Control, Structures, Seaplanes, Engines, etc. £3.

ANNUAL REPORTS OF THE AERONAUTICAL RESEARCH COMMITTEE—

1933-34 1*s*. 6*d*.
1934-35 1*s*. 6*d*.
April 1, 1935 to December 31, 1936. 4*s*.
1937 2*s*.
1938 1*s*. 6*d*.

INDEX TO THE TECHNICAL REPORTS OF THE ADVISORY COMMITTEE ON AERONAUTICS—

1909-1919 Reports and Memoranda No. 1600. 8*s*.

*Prices are net and postage extra.*

## His Majesty's Stationery Office

London W.C.2: York House, Kingsway
Edinburgh 2: 120 George Street Manchester 2: 39-41 King Street
Cardiff: 1 St. Andrew's Crescent Belfast: 80 Chichester Street
or through any bookseller.

S.O. Code No. 23-1898

UNIVERSITY OF ILLINOIS-URBANA
3 0112 124406759